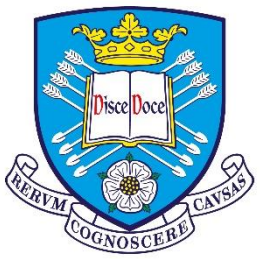

The University Of Sheffield.

Defining the differential effects of Zoledronic acid under pre and post-menopausal concentrations of oestradiol on anti-cancer immunity

Christopher George

Registration No: 180155017

A thesis submitted in partial fulfilment of the requirements for the degree of Doctor of Philosophy

The University of Sheffield

Faculty of Medicine Dentistry and Health

Department of Oncology and Metabolism

March 2022

Declaration

All work in this thesis is my own unless otherwise stated; large data set statistical analysis was performed by Dr Lewis Quayle and technical help was provided throughout by Diane Lefley, Jennifer Down and Alyson Evans. I, the author, confirm that the Thesis is my own work. I am aware of the University's Guidance on the Use of Unfair Means. This work has not previously been presented for an award at this, or any other, university.

Acknowledgements

Throughout my PhD I have received a great deal of support from both within and outside the University of Sheffield. Firstly, I would like to thank my supervisor Dr Penelope Ottewell for her unwavering support, patience and kindness to me during my studies. Under her guidance, I have been able to grow as a researcher and find my voice to share ideas, have confidence in my work and present my findings. I would like to thank my funding body Western Park Cancer Charity for their support during my studies. I am grateful for both the monetary support they provided for my project alongside the important work they do across the community for cancer treatment.

I would like to thank all the members of my group and beyond who have supported me during this time. I would like to thank Diane Lefley for supporting me through my project with her expertise in all my practical work. I would like to thank Dr Munitta Muthana, my second supervisor, for her support and guidance. I am sincerely grateful to Alyson Evans for helping me with my histology work. I greatly appreciate the help of Jennifer Down for my ex-vivo studies. I have conducted a large amount of flow cytometry experiments throughout my studies, and these would not have been possible without the support and guidance of Sue Clarke. I am most grateful to Dr Lewis Quayle for his help with large data set analysis.

I would like to thank all the members of my group who have created a kind and supportive environment to work in, and for entertaining me during long incubation times: Victor Canuas, Jiabao Zhou, Claudia Tulotta, Margherita Puppo, Veli Aydin. I am glad I was able to be part of such a friendly community and I thank you for making my time in Sheffield so great.

Throughout my studies, I have had the pleasure to supervise and teach a number of masters and undergraduate students who have all contributed to the final publication of this project. Thank you to Hannah Corness, Jessica Cantwell, Elena Assiotou, Andre Alves for your contributions to this project, and for putting your faith and trust in me.

Finally, I would like to thank my family for supporting me throughout my long studies, with particular thanks to my partner Alessandro. I could not have completed this marathon project without the support I was given, and I am truly thankful.

Contents

List of figures

List of tables

List of abbreviations

µCT	Microcomputed tomography
µl	Microlitre
ABCSG	Austrian Breast Cancer Study Group
AI	Aromatase inhibitor
AZURE	Does Adjuvant Zoledronate redUce REcurrence in early breast cancer?
BRCA1	BReast CAncer gene 1
BSA	Bovine serum albumin
BV/TV%	Percentage trabecular bone volume over tissue volume
BV	Bone volume
CCR4	C-C chemokine receptor type 4
CDK4/6	Cyclin-dependent kinase 4 and 6
CO2	Carbon dioxide
CTLA4	Cytotoxic T-lymphocyte-associated protein
CXCL	C-X-C Motif Chemokine Ligand
CXCR	C-X-C chemokine receptor
DFS	Disease free survival
DKK-1	Dickkopf WNT signaling pathway inhibitor 1
DMSO	Dimethyl sulfoxide
DNTP	Deoxyribose nucleotide triphosphate
DTCs	Disseminated tumour cells
DTT	Dithiothreitol
ECM	Extracellular matrix
EDTA	Ethylenediamine tetraacetic acid
EMT	Epithelial to mesenchymal transition
ER	Oestrogen receptor
FBS	Foetal bovine serum
FFP	Farnesyl diphosphate synthase
FMO	Fluorescence minus one
Foxp3	Forkhead box P3
FSH	Follicle stimulating hormone

GFP	Green fluorescent protein
GGPP	Geranyl Geranyl diphosphate synthase
GnRH	Gonadotropin hormone-releasing hormone
GPER1	G protein-coupled estrogen receptor 1
H&E	Haematoxylin Eosin Staining
H2O2	Hydrogen peroxide
HER2	Human epidermal growth factor receptor 2
HLA	Human leukocyte antigen
HR	Hormone receptor
HRP	Horseradish peroxidase
HSC	Hematopoietic stem cell
IC50	Half-maximal inhibitory concentration
iDFS	Invasive disease free survival
IFNγ	Interferon gamma
IGF	Insulin-like growth factor
IgG	Immunoglobulin G
IgM	Immunoglobulin M
IL…	Interleukin
IPP	Isopentenyl pyrophosphate
iTreg	Induced T regulatory cells
IVIS	In vivo imaging system
KO	Knock out
LUC	Luciferase
Luciferin	D-Luciferin-Potassium Salt
LY6G	Lymphocyte antigen 6 complex locus G6D
M-CSF	Macrophage colony-stimulating factor
MDSC	Myeloid derived suppressor cell
MHC	Major histocompatibility complex
Ml	Millilitre
MMPs	Matrix metalloproteinases
MRC1	Mannose Receptor, C type 1
NGS	Nottingham grading system

NK cells	Natural killer cells
NKG2D	Natural Killer Group 2D
nTreg	Natural T regulatory cells
OPG	Osteoprotegerin
ORR	Overall response rate
OS	Overall survival
OVX	Ovariectomy
P1NP	Procollagen type 1 N-terminal propeptide
PARP	Poly adenosine diphosphate-ribose polymerase
PBMCs	Peripheral blood mononuclear cells
PD-1	Programmed cell death protein 1
PD-L1	Programmed death-ligand 1
PI-9	Proteinase Inhibitor 9
PTEN	Phosphatase and tensin homolog
PTH	Parathyroid hormone
PTHrP	Parathyroid hormone-related protein
qPCR	Quantitate reverse transcription polymerase chain reaction
RANKL	Receptor activator of nuclear factor kappa-B ligand
SREs	Skeletal related events
TAMs	Tumour associated macrophages
TCR	T cell receptor
TGF-β	Transforming growth factor beta
TNBC	Triple negative breast cancer
TNF-α	Tumour necrosis factor alpha
TNM	Tumour, Node, Metastasis
TRAP	Tartrate-resistant acid phosphatase 5b
Treg	T regulatory cells
uRap1A	Unprenylated ras-proximate-1
VEGF	Vascular endothelial growth factor
Wnt	Wingless-related integration site
Zol	Zoledronic acid

Abstract

Background: Late-stage breast cancer often recurs in bone. Neoadjuvant Zoledronic Acid (Zol) combined with standard of care can reduce bone metastases in pre- and post- menopausal women while prolonging life in post-menopausal women. However, pre-menopausal women experience worse iDFS and increased soft tissue tumour recurrence. Zol and oestrogen can both affect bone homeostasis and immune cells. Therefore, we hypothesise that oestrogen may inhibit anti-tumour activities of Zol in pre-menopausal women through immune regulatory pathways, and that combination therapy with Avelumab and Zol could improve treatment efficacy.

Methods: Menopausal conditions were modelled in mice by ovariectomy followed by 10 pM/L, 84 pM/L and 300pM/L oestradiol. Metastases were induced by intracardiac injection of mouse mammary cancer E0771 and 4T1 cells before treatment with 100ug/kg/week Zol or control. Effects on tumours, bone, immune cells and hormones were assessed by IVIS imaging, uCT, flowcytometry, NanoString and ELISA. In same model, mice were treated with 400µg/kg every 2-days Avelumab in combination with Zol.

Finding: Ovariectomy followed by oestrogen administration (n=15 per group) reliably recreated pre-peri and post- menopausal serum concentrations, while trabecular bone volume was significantly decreased under postmenopausal oestradiol ($p<0.0001$). Non-bone metastasis in pre-menopausal mice increased following Zol treatment, mirroring clinical findings. Data from flowcytometry and Nanostring analysis suggest that Zol and oestradiol exert deferential effects on immune populations, with oestrogen increasing M2 macrophage populations while decreasing B cells ($P= 0.0091$), and Zol increasing M1 ($P=0.0374$) populations, increasing T cells and decreasing PD-1 expression in the bone. Combination therapy with Avelumab and Zol significantly reduced metastasis to bone ($P=0.0011$) and lung ($P=0.0004$), irrespective of oestradiol concentrations, while increasing T cell activity.

Conclusions: Oestradiol inhibits the anti-metastatic effect of Zol by inducing a pro-tumour immune microenvironment. Novel combination therapy with the anti PD-L1 Avelumab removes this inhibition and prevents bone and soft tissue metastasis.

Chapter 1: Introduction

1.1 Background

Breast cancer is the most common form of cancer in women, resulting in 11,563 deaths in the UK alone in 2016 (Cancer Research UK). Furthermore, in 2011 the national audit office estimated the NHS annually spent over £6.7 billion on the treatment of cancer, with the economic cost from patient deaths and loss of productivity bringing this figure up to a staggering £18.3 billion (Creighton et al., 2015). This highlights the need for new treatments for breast cancer patients to increase patient survival, decrease suffering, and reduce economic burden. It is rarely the primary tumour in breast cancer that causes fatalities, but its dissemination and growth in distal organs forming secondary incurable tumours around the body, resulting in mortality (Jin and Mu, 2015).

Metastasis occurs independently of the breast cancer subtype. Oestrogen Receptor (ER)+ve breast cancers preferentially metastasise to bone and ER-ve preferentially metastasise to lung and although lung metastases often occur soon after removal of the primary tumour, recurrence in bone is commonly not detected until many years after removal of the primary tumour. However, recurrence in any metastatic site can occur at any time point with recent data showing increased incidence of recurrence associated with increased time post primary tumour removal (Colzani et al., 2014). Once secondary tumours have formed, breast cancer is considered incurable with few effective treatments available. Breast cancers metastasise to bone, lung, liver and brain, with the bone being the most common site (Roodman, 2004). Therefore, finding new drugs or repurposing old drugs to prevent bone metastasis is important for reducing mortality in breast cancer patients. Bisphosphonates, a class of bone targeting agents used to treat osteoporosis and prevent bone loss, have shown promise at preventing bone metastasis in both the lab and the clinic.

1.2 Breast cancer

Breast cancers are graded and characterised using three different classification systems. One system assesses tumours for aggressiveness using the tumour, node, metastasis (TNM) stage system which factors in: Tumour size and location, lymph node involvement and distant metastasis (Table 1.1). This clinical classification can be accompanied by classification according to receptor expression, most notably oestrogen and progesterone hormone receptors (HR), the proliferation marker Ki-67, as well as HER2 expression (Sorlie et al., 2003). Expression of these markers are not only important for informing treatment options (Braunstein et al., 2015), but can also predict likely recurrence and metastatic sites and are used to determine which subtype a breast cancer is classified into (Table 1.2).

Stage	Description
0	**(T)** No tumour evident, **(N)** Spread to lymph, **(M)** No spread of tumour,
Ia	**(T)** Tumours are <2cm, **(N)** No lymph node involvement and, **(M)** there is no metastatic spread from the primary.
Ib	**(T)** Breast has no tumour **(N)** microscopic metastatic spread to auxiliary lymph nodes **OR** **(T)** Primary breast tumour <2cm **(N)** Lymph nodes involved
IIa	**(T)** No primary breast tumour, **(N)** Macroscopic auxiliary node tumour in 1-3 nodes (0.2-2mm), **(M)** No Metastasis **OR** **(T)** Primary tumour <2cm with, **(N)** Spread to auxiliary nodes, **(M)** no metastasis **OR** **(T)** Primary tumour 2-5cm, **(N)** no lymph node spread **(M)** no metastasis
IIb	**(M)** Primary tumour 2-5 cm, **(N)** Spread to 1-3 auxiliary lymph nodes, **(M)** no metastasis **OR** **(T)** Primary tumour >5 cm, **(N)** Not present in lymph, **(M)** no metastasis
IIIa	**(T)** No primary tumour found in breast **(N)** Spread to 4-9 auxiliary lymph nodes or internal mammary nodes **(M)** No Metastasis **OR** **(T)** Primary tumour > 5cm **(N)** Axillary and internal mammary node spread **(M)** no metastasis
IIIb	**(T)** Primary tumour any size spread to skin of breast or chest wall **(N)** Axillary and internal mammary node spread
IIIc	**(T)** Primary tumour any size, **(N)** spread to >10 axillary lymph nodes **OR** **(N)** Lymphatic spread to supraclavicular nodes **OR** **(N)** Spread to internal mammary nodes and axillary lymph nodes
IV	**(M)** Metastatic spread to distal organs around the body

Table 1.1: Tumour, Node, Metastasis staging for breast cancer classification

A third grading system is also used to predict the outcome of breast cancers, the Nottingham grading system (NGS). This is a histological grading system based on the evaluation of three morphological features in the tumours: the degree of tubule or gland formation, the nuclear pleomorphism and the mitotic count (Elston and Ellis, 1991). Studies have shown that NGS has prognostic value equal to that of lymph node status and above simple tumour size grading (Sundquist et al., 1999). Therefore, in the clinic, NGS is often used in combination with lymph node status and tumour size to determine the tumour grade. Furthermore, NGS is an inexpensive and simple grading system that does not require access to expensive new technologies. Studies suggest that molecular characterisation of tumours should become the gold standard of breast cancer grading, with NGS receiving criticism due to the subjective nature of histological grading (Peppercorn et al., 2008). However, evidence suggests that newer molecular tests should be used to compliment the histological grading, not replace it, providing optimal predictive behaviours to ensure the best therapy for patients (Rakha et al., 2010).

Subtype	Molecular Characteristics	Phenotype	Metastasis	Treatment
Luminal A	HR **+** HER2 – Low Ki-67	Slow growing, Low lymph node involvement, Good Prognosis,	Bone = 58.52 % Lung = 21.70 % Liver = 15.48 % Brain = 4.30 %	Endocrine therapy (Tamoxifen), Aromatase inhibitors,
Luminal B	HR **+** HER2 +/- High Ki-67	Faster growing, High lymph node involvement, Worse prognosis	Bone = 47.28 % Liver = 25.65 % Lung = 21.17 % Brain = 5.89 %	Endocrine therapy, Chemotherapy,
Triple Negative/ Basal-like	HR – HER2 – High Ki-67	Highest death rate, Aggressive	Bone = 36.39 % Lung = 32.09 % Liver = 22.40 % Brain = 9.12 %	Chemotherapy (Doxorubicin/ cyclophosphamide) Platinum based Chemotherapy (cisplatin)
HER2- enriched	HR – HER2 + Med-high Ki-67	High recurrence rate, Poor prognosis	Bone = 34.49 % Liver = 31.72 % Lung = 25.48 % Brain = 8.31 %	HER2 targeted treatment (Trastuzumab), Chemotherapy

Table 1.2: Breast cancer molecular and hormone receptor classification showing expression of hormone receptors, HER2 and KI-67, and predicting growth characteristics and metastatic tendencies

1.3 Metastasis

Due to an increase in screening and more successful treatments for primary breast cancer patients, the breast cancer survival rate has almost doubled over the last 40 years (Cancer Research UK). However, treatments have not improved significantly for breast cancers that have spread and consequently most breast cancer related deaths are due to metastasis, which is often resistant to therapies and difficult to remove by surgery (Langley and Fidler, 2007). In order to metastasise, tumour cells must undergo a series of transformations in the primary site, named the epithelial to

mesenchymal transition (EMT) (Thiery, 2003) (Figure 1.1). This process is vital to enable tumour cells to leave the primary site and disseminate into the blood/lymph (Figure 1.1).

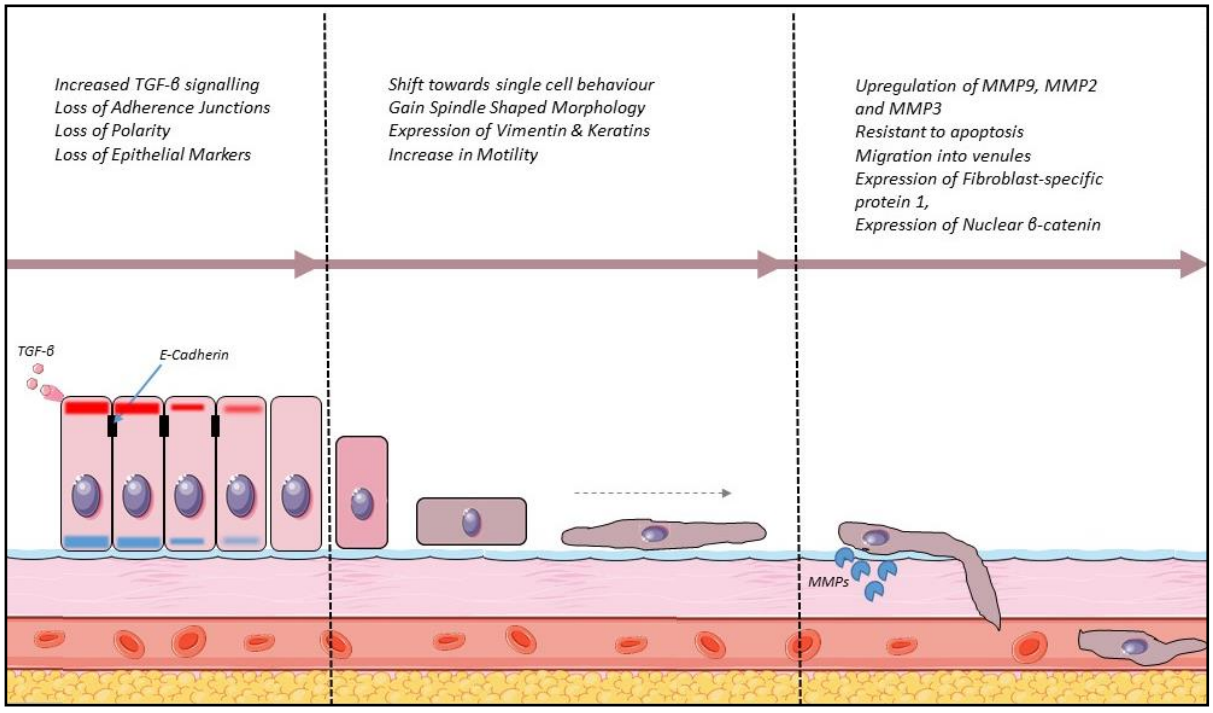

Figure 1.1: Epithelial Mesenchymal Transition (EMT) where epithelial derived tumour cells lose adherence junctions via down regulation of E-Cadherin, polarity, epithelial markers and undergo a morphological switch towards a spindle shape allowing greater motility. Cells upregulate expression of fibroblast-specific protein 1 and nuclear β-catenin to promote tumour metastasis, as well as secreting numerous proteinases such as matrix metalloproteinase (MMP) 9, 2 and 3 to allow invasion of the basement membrane and connective tissue and facilitate entry into circulation.

From the circulation tumour cells home to a metastatic niche within a distant organ before undergoing the reverse process of mesenchymal to epithelial transition enabling subsequent proliferation and formation of a secondary tumour. Throughout all these processes tumour cells must evade clearance by the immune system. Therefore, unsurprisingly, metastasis is an inefficient process with *in vivo* studies showing that only 0.01% of injected tumour cells successfully form secondary tumours (Fidler, 1970).

Cancer metastasis is not a random process. In 1889, it was first proposed that different cancers have preferential sites of metastasis (Paget, 1989). Furthermore, different classes of breast cancer also have preferential sites of metastasis (Table 1.2). Over time, cancer cells acquire a series of alterations to facilitate metastasis and survival at a metastatic site, as made evident in laboratory experiments from multiple research groups: Repeated passaging of human, MDA-MB-231 breast cancer cells through mouse bones or lungs produces distinct clones that subsequently metastasise

specifically to these organs (Kang et al., 2003; Nutter et al., 2014). Importantly, all of these studies identified molecular changes in the organ homed cells that were also observed in primary tumours from breast cancer patients that subsequently developed metastases in these organs (Nutter et al., 2014; Westbrook et al., 2016; Tulotta and Ottewell, 2018). For example, metastatic tumour cells upregulate expression of CXCR4, enabling interaction with CXCL12 found on osteoblasts and mesenchymal stem cells allowing efficient tumour homing to the bone (explored in section 1.6). The homing of tumours to preferred metastatic sites opens the possibility for a treatment that alters microenvironments preferential for metastatic outgrowth, such as the bone, to form an inhospitable environment for tumour cells, therefore preventing metastasis.

1.4 Pharmacological treatment of primary tumours

Breast cancer is normally removed from the primary site by surgery as a first line treatment before other pharmacological interventions are pursued (Heil et al., 2012). Breast cancer therapies are tailored to the molecular tumour type and aim to target the growth and survival of cancer cells. Hormone treatments are often utilised as a first line in ER^+ cancer prior to cytotoxic chemotherapy if visceral metastasis has not been identified (Salkeni and Hall, 2017). HR positive tumours are treated with goserelin to inhibit the GnRH pathway and prevent ovarian release of oestrogen. In pre-menopausal women, ovarian suppression reduces the mortality rate and recurrence by 25% and is more common than adjuvant therapy alone (Bui et al, 2020). The beneficial use of goserelin is limited to premenopausal women with ER^+ tumours, since circulating oestrogen is low in postmenopausal women (Puhalla et al., 2012). Furthermore, when patients with ER^- tumours were treated with goserelin it was found to be less effective than chemotherapy standard of care (Kaufmann et al.). Tamoxifen is also commonly used in ER+ve breast cancer. Tamoxifen is a selective oestrogen receptor modulator, which blocks the effect of oestrogen on ER and stops proliferation of breast cancer ductal cells leading to a 31% reduced mortality rate (Abe et al., 2005). Furthermore, this drug has favourable effects on bone metabolism since it does not abolish systemic oestrogen, allowing normal bone turnover and has even been shown to increase bone health in post-menopausal women. Both goserelin and tamoxifen are regularly used drugs in the clinic, and are often used together as an alternative to chemotherapeutic agents in ER+ve breast cancer, as shown in the ABCSG 05 (Austrian Breast Cancer Study Group) trial (Jakesz et al., 2002).

Hormonal treatments for post-menopausal women target local oestrogen synthesis since local oestrogen concentrations in tissues can be much higher than systemic concentrations (Simpson et al., 2000). Aromatase, the hormone that normally converts androgens to oestrogen in organs

including bone, vascular endothelium and liver (Schneider et al., 2011), is overexpressed in adipose tissue of breast cancer patients and is the target for treatment in these women (Bulun et al., 2007). Therefore, aromatase inhibitors (AIs) block conversation of androgen to oestrogen and reduce circulating oestrogens. In premenopausal women, AIs as a single treatment can lead to an increase in secretion of gonadotropins and raised systemic oestrogen, therefore they must be used alongside GnRH inhibitors (Pistelli et al., 2018). In the TARGET clinical trial of 668 post-menopausal women receiving either anastrozole 1 mg once daily relative to tamoxifen 20 mg once daily, following subgroup analysis of women with ER^+ breast cancer, anastrozole (an AI) gave a longer disease free progression when compared to tamoxifen (Nabholtz and Arimidex Study, 2003). However, guidelines for use have still not changed much, with both drugs still in regular clinical use in postmenopausal women.

Triple negative breast cancer (TNBC), representing about 15% of all breast cancer (Dent et al., 2007), does not respond well to hormone treatment, instead standard of care for these patients is anthracycline/ taxane–based doxorubicin and cyclophosphamide chemotherapy drugs. Although TNBC response is good, the chance of relapse is still very high after 3-4 years, but decreases following 8-10 years (Criscitiello et al., 2012). In addition, the platinum based chemotherapeutic agent cisplatin has been shown both clinically and pre- clinically to be effective against BRCA1 mutated breast cancers with a 56% response rate compared to 25% overall response rate (Isakoff et al., 2015). These agents work by causing excessive DNA damage, leading to tumour cell apoptosis.

Alongside these older treatments, there are now newer targeted treatments available to patients as standard of care. PARP inhibitors are a targeted therapy licenced for use against BRCA1/2+ breast cancer and work by interfering with DNA damage repair (Zeman and Cimprich, 2014) to sensitise cancer cells to chemotherapy or radiation. HER2 inhibitors are routinely used in the treatment of HER2-positive breast cancers. Drugs including pertuzumab, along with trastuzumab are monoclonal antibodies against HER2/3 to block proliferation and survival signalling (Swain et al., 2015). Cyclin-dependent kinase 4 and 6 (CDK4/6) are also cancer treatment targets, with palbociclib being a selective inhibitor for CDK4/6 for use in HR positive HER2 negative patients leading to improved progression free survival in these patients (Kim and Scott, 2017).

1.5 Targeting the immune system

Newer treatments for breast cancer aim to target the immune system to stimulate immune cell clearance of tumour cells by unmasking cells and allowing immune detection and killing.

Treatments targeting the immune system are common in cancers such as lymphoma, melanoma and lung, but are less common for breast cancer due to poor response rates. Breast cancer is often categorised as immunologically silent depending on their subtype, with low rates of infiltrating immune cells making immune based therapies a challenge for ER^+ tumours (Julia et al., 2018). However, bioinformatic analysis of neoepitope frequency found that the less common TNBC has significantly more somatic mutations with a median of 63 mutations when compared to ER+ tumours with a median of 32 mutations (Narang et al., 2019). This led to a higher frequency of neoantigens detected when compared to other subtypes, increasing its immunogenicity. Therefore, therapies for TNBC have aimed to improve tumour targeting by unmasking tumour cells to make them more amenable to clearance by T cells and prevent T cell exhaustion. One such class are checkpoint inhibitors. Under normal physiological conditions, CD8+ T cell responses are mediated through antigen recognition by the T cell receptor (TCR), which is regulated by co-stimulatory and inhibitory signals known as immune checkpoints. This normally helps maintain self-tolerance; however, tumour cells can overexpress inhibitory signals to evade immune detection. Therefore, agents that are either agonists for co-stimulatory signals or antagonists for inhibitory signals are exciting targets in the clinic. The PD-1/PD-L1 inhibitory pathway is a promising strategy for therapy, and the drug atezolizumab (FDA approved) shows promise in the clinic for triple negative breast cancer with a 53% response rate verses 33% for placebo. Avelumab is another checkpoint inhibitor, an antibody inhibiting PD-L1. Interestingly, in pre-clinical studies avelumab has been shown to induce antibody dependent cell mediated cytotoxicity of tumour cells, an additional mechanism of action. For breast cancer, avelumab has been studied in the phase 1b JAVELIN Solid Tumour study clinical trial (Dirix et al., 2018a). 168 patients with metastatic breast cancer who had already received extensive treatment were studied and the best overall response rate was observed in patients with PD-L1+ tumour associated immune cells (16.7% vs 1.6% for $PD\text{-}L1^-$). TNBC patients also had a benefit from avelumab treatment.

Immune based treatments represent an exciting new chapter in breast cancer therapy, forming the fourth pillar of standard care for patients. Although more work needs to be done to improve response rates and understand the mechanisms behind tumour immune suppression, these new treatments are paving the way for future combination therapies to target virulent tumours.

1.6 Bone metastasis

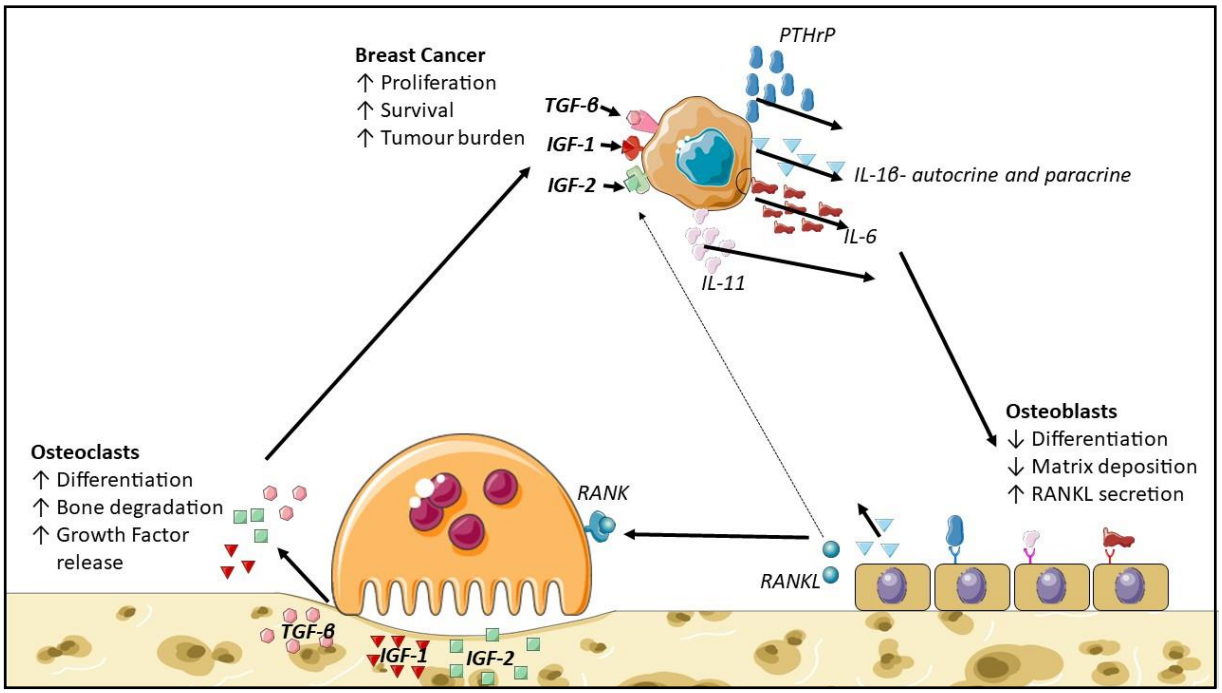

Figure 1.2: The vicious cycle of breast cancer induced bone degradation. The growth factors TGF-β, IGF-1 and IGF-2, normally trapped in the bone, are released when osteoclasts degrade the bone. These act on tumour cells to stimulate proliferation and survival of the cells, therefore increasing tumour burden. The tumour cells release molecules such as PTHrP, IL-6 and IL-11 which act on osteoblasts to downregulate differentiation and anabolic activity whilst upregulating release of RANKL (Mancino et al., 2001). RANKL acts on both the osteoclasts to increase their differentiation, survival and activity, and on the tumour cells directly to promote proliferation (Tan et al., 2011). This leads to a vicious cycle of bone degradation and excessive bone loss.

70% of patients with late stage breast cancer develop bone metastases resulting in painful lesions, hypercalcemia and an increased risk of fractures (Roodman, 2004), leading to 10% survival rate of just 5 years after diagnosis (Svensson et al., 2017). It is thought that tumour cells are attracted to bone through biochemical and physical signals provided by cells within the bone microenvironment. Osteoblasts and peri-vascular cells within the bone express high levels of CXCL12 which binds to its receptor CXCR4, often expressed on breast cancer cells (Muller et al., 2001). This plays a vital role in tumour homing to the bone, and overexpression of CXCR4 on breast cancer cells increases their metastatic capabilities (Kang et al., 2003). The physiological process of bone remodelling, through osteoclast degradation of the bone and subsequent osteoblast deposition of bone matrix, releases growth factors and cytokines (Pfeilschifter and Mundy, 1987) stimulating tumour growth and survival (Pfeilschifter and Mundy, 1987). Moreover, the disseminating tumour cells secrete PTHrP, IL-6 and IL-11, leading to increased bone degradation via stimulation of RANKL in osteoblasts, which subsequently stimulates osteoclastogenesis causing a vicious cycle of tumour growth and osteolysis (Figure 1.2). Tumour cells within the bone metastasis can inhibit osteoblast differentiation by secreting factors into

the microenvironment such as activin A, sclerostin, DKK-1 and noggin (Krzeszinski and Wan, 2015). Further to the classical model of the vicious cycle, tumour derived Jagged 1 can bind to Notch receptors on osteoblasts, increasing expression of osteoblast derived IL-6 in the bone/ tumour microenvironment (Sethi et al., 2011) stimulating tumour growth (Dethlefsen et al., 2013) and osteoclast differentiation (Bussard et al., 2010). In order to break this vicious cycle, there have been efforts to treat bone metastasis with therapies targeted to reducing osteoclast activity (bisphosphonates and demosumab), however this strategy has not been as effective as originally hoped. (Figure 1.2).

1.7 Dormancy

Breast cancer micro metastasis can be found in the skeleton at early stages of the disease. These cells are often maintained in a quiescent or dormant state by the bone niches for long periods of time, before "re awakening" and proliferating into overt metastases. Meta-analysis of 9 studies including 4703 patients with stage I, II or III breast cancer found that 30-40% of breast cancer patients have disseminated tumour cells (DTCs) in their bone marrow, with DTCs contributing to poor overall survival and disease free survival (Braun et al., 2005). Indeed, approximately 20% of recovered breast cancer patients relapse in the bone up to 15 years later (Demicheli et al., 1996), and these cells can transit through the bone to form metastasis in other organs (Capulli et al., 2012). Circulating tumour cells are thought to home to specific niches within the bone thought to contribute to both the maintenance of dormancy and the subsequent re-activation and proliferation of cells.

The endosteal niche is primarily made up of osteoblasts, with mouse models of breast cancer showing that tumour cells home to areas of high osteoblast activity. Furthermore, changing bone activity with drugs such as zoledronic acid (Zol) results in relocation of tumour cells to other osteoblast rich areas (Haider et al., 2014). Furthermore, it is within the endosteal niche that the CXCR4/CXCL12 interaction from osteoblasts is most prevalent in homing the tumour cells to the bone (Wang et al., 2014). Evidence also suggests that osteoblasts are able to maintain tumour cells in a dormant state in the endosteal niche through the interactions of CXCR4 and CXCL12, similar to how osteoblasts maintain hematopoietic stem cell (HSC) dormancy (Wang et al., 2014).

The HSC niche is one that is also rich in CXCL12, so it also attracts the CXCR4 positive tumour cells to the site. On arrival, the tumour cells must compete with HSCs for site colonisation, and the eventual outgrowth of tumour cells in the niche is thought to be supported by the proliferation of HSCs (Pedersen et al., 2012).

The importance of the vascular niche is supported by evidence that once tumour cells have completed extravasation, they remain closely associated with the capillaries, supported by CXCL12/CXCR4 interactions with vascular cells (Carbonell et al., 2009). Furthermore, vascular E-selectin can bind directly to disseminated tumour cells to promote bone metastasis by inducing epithelial-mesenchymal transition and Wnt signalling (Esposito et al., 2019). Their proliferation leads to engulfment of the capillary and eventual remodelling of the capillary network, as reviewed in (Kusumbe, 2016). Taken together, the data suggests that it is the endosteal niche that is important in maintaining tumour cell quiescence, whereas the vascular and HSC niches are more involved in tumour outgrowth in the bone, as reviewed in George *et al.* (2020).

The immune system also plays an important role in tumour dormancy and outgrowth within the bone. Dormancy is primarily maintained by the adaptive immune system where proliferation of tumour cells is balance by immune cell killing, a process that is regulated mainly by T-cells, IL-12 and interferon-γ (Schreiber et al., 2011). Over time, the tumour cells can escape immune recognition in via two mechanisms: developing insensitivity to attach by immune cells or the tumour microenvironment can become immunosuppressed, leading to a lack of immune infiltration (Rooney et al., 2015). These individual yet interconnected niches within the bone highlight the complexity of the bone metastatic process and the difficulty of finding effective treatments.

1.8 Treatment of bone metastasis

Treatment of metastatic tumours of the bone often involve bone targeted agents, with the aim of breaking the vicious cycle and reducing skeletal related events (SREs) such as fracture. Bisphosphonates have been used in these treatments for several decades alongside standard of care, with intravenous pamidronate and Zol showing the highest efficacy for the prevention of SREs (Rosen et al., 2003). A retrospective analysis of Zol in a phase III clinical trial showed Zol corelated with an improved survival for breast cancer patients with reduced risk of death by 48% (Lipton et al., 2008). However, it is unclear whether this was due to direct anti-cancer effects or the benefit of prevention of fracture and its associated morbidity. Denosumab, the monoclonal antibody against RANKL, is a newer drug given alongside standard of care (neo/adjuvant chemotherapy and/or endocrine therapy). Both these drugs are successful at preventing SREs, with denosumab showing increased efficacy against fracture risk (Stopeck et al., 2010).

Interestingly, pre-clinical data suggested that Zol may have effects on primary tumour growth and early events associated with bone metastasis with in vivo experiments showing Zol had efficacy

against disseminated dormant tumour cells in the bone, and increased efficacy in ovariectomised mice compared to sham operated mice (Ottewell et al., 2014b). This reflects clinical observations from ABCSG-12 and AZURE trials (described later). For denosumab, the effects on early bone metastasis development are dependent on the dose. The DCARE study was of 4509 pre- and post-menopausal patients randomised to receive neo/adjuvant therapy +/- high dose denosumab (120mg) monthly for 6 months, then 3 monthly up to 5 years (Coleman et al., 2018b). There were no benefits in bone metastasis free survival in either the overall population or the post-menopausal subgroup, although there was clear benefit in fracture risk. On the other hand, in the ABCSG-18 study, where 167 pre-menopausal women were treated with low dose denosumab (60mg every 6 months) vs 203 receiving placebo, there was an 18% reduced risk of recurrence after 4 years with denosumab (Gnant et al., 2015b). However, this study was unblinded and patients received active treatment following 4 years, so long-term follow-up data is not available. This inconsistency in results suggests that bone metastasis is regulated by more than the bone microenvironment and that RANKL inhibition is not sufficient to prevent metastasis.

1.9 Zoledronic acid – Structure and mechanism of action

Bisphosphonates specifically target the bone to reduce osteoclast activity and are commonly used to treat breast cancer induced bone metastases. There are two classes of these drugs: nitrogen containing bisphosphonates and non-nitrogen containing bisphosphonates.

Zol is an intravenously administered bisphosphonate and is licenced to treat skeletal related events caused by breast cancer bone metastases, reducing hypercalcemia and the risk of fractures in patients, offering an improved quality of life (Wilson et al., 2018). Zol is a member of the nitrogen containing bisphosphonate class with a structure similar to other bisphosphonates, with a phosphorus-carbon-phosphorus core as well as a hydroxyl group at the R1 terminus (Li and Davis, 2003). The structure that distinguishes Zol from the other bisphosphonates is the heterocyclic imidazole group found attached to the R2 position (Figure 1.3) (Schech et al., 2013). Zol has a high affinity for mineralised bone, binding to calcium phosphate bone mineral hydroxyapatite at sites of high bone turnover (Räkel et al., 2011). Indeed, Zol is the most potent bisphosphonate, having the highest affinity for hydroxyapatite when compared to the other bisphosphonate drugs, binding to bone matrix within 4 hours of administration.

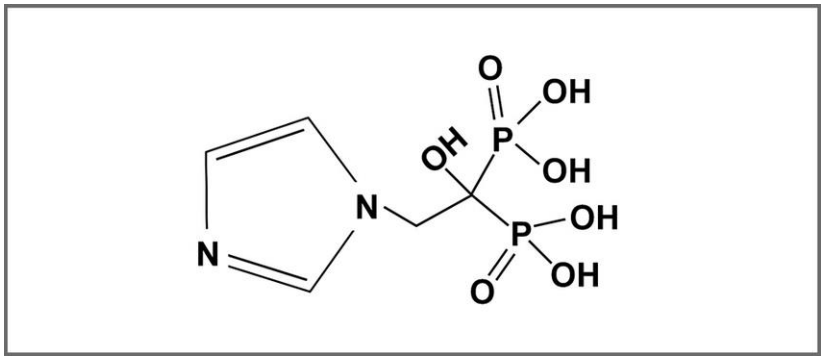

Figure 1.3: The molecular structure of Zoledronic acid

When bone is resorbed, Zol is internalised by the osteoclasts through endocytosis and interferes with osteoclast activity, preventing formation of the ruffled boarder causing osteoclasts to dethatch from bone, inhibiting differentiation and inducing apoptosis. These inhibitory mechanisms are the result of Zol induced inhibition of farnesyl pyrophosphate synthase in osteoclasts, preventing the synthesis of FPP and geranylgeranyl diphosphate and then leading to reduced post-translational modification of GTPases, which are necessary for osteoclast function and survival (Luckman et al., 1998) (Figure 1.4).

The mevalonate pathway is ubiquitous to all cells leading to speculation that Zol can have direct killing effects on cell types other than osteoclasts. Indeed, there is a wealth of data showing that Zol can kill tumour cells *in vitro* (Jagdev et al., 2001; Zekri et al., 2014). However, the ability to directly kill tumour cells when administered alone, *in vivo,* are less convincing and it has been hypothesised that the short time that Zol is retained in the circulation ~2.5h means that not enough of this drug reaches the tumour for it to exert maximum effects. Interestingly, evidence from the laboratory and clinic suggest that early treatment (combining chemotherapy with Zol before evidence of metastases) may reduce breast cancer relapse in bone (Ottewell et al. 2008; Ottewell and Wilson, 2019). Therefore, Zol has anti-cancer effects further than just preventing bone loss, a property that is extremely desirable because once overt tumours form in the bone, they are incurable.

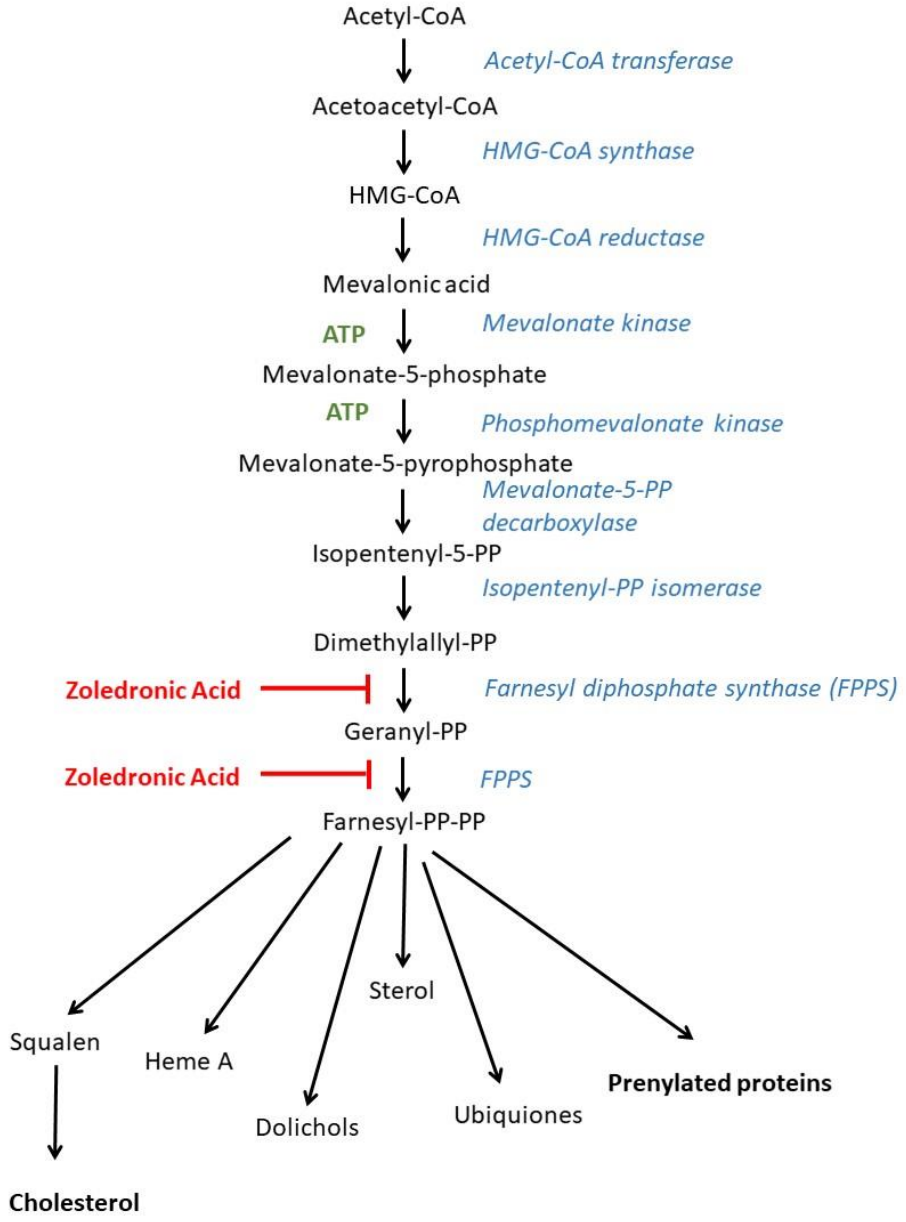

Figure 1.4: The mevalonate pathway showing intermediates, enzymes responsible and the site of Zol action

1.10 Anti-tumour effects of Zol in adjuvant/neoadjuvant settings

Zol has been shown to have effects further than just protecting the bone from resorption, it has been shown to have direct anti-cancer effects. As previously discussed, DTCs in the bone marrow present a problem because they increase the risk of developing overt bone metastasis. Furthermore, DTCs can be seen in the bone marrow of early-stage breast cancer patients, with DTCs observed in 30-

40% of patients, and can be observed in the bone long after the primary tumour has been removed (Braun et al., 2005). Therefore, clinical trials have been carried out to determine if early intervention with Zol could reduce numbers of DTCs in bone and therefore, reduce disease recurrence in this site, with promising results.

Zol was studied in a non-randomised phase 2 clinical trial of 31 women with early breast cancer and persisted DTCs in bone marrow receiving 4mg Zol, 4 times per week for 6 weeks vs 141 control patients. Bone aspirates showed 87% of DTCs eliminated in Zol group vs 73% in control groups (Rack et al., 2010). The negative aspirates were further associated with a better survival. The largest study into the effects of Zol on DTCs assessed bone aspirates from 3141 patients with early breast cancer and found that 803 of them had DTCs (Hartkopf et al., 2014). All patients then received systemic treatment alongside adjuvant Zol, and retrospective analysis found that disease free survival and overall survival was better in patients with detectable DTCs treated with Zol. Subgroup analysis was performed on this data to separate the effects on pre- and post-menopausal women. Interestingly, overall survival was found to be improved only in post-menopausal women with detectable DTCs ($p=0.009$), suggesting an effect of menstrual hormones in changing the effects of Zol.

Zol is now used as an adjuvant anticancer treatment to eliminate micro metastasis, with clinical benefit first described in the Danish collaborative study GAIN, the Austrian ABCSG-12 trial and the multi-centre AZURE trial, reporting menopause dependent results. The ABCSG-12 trial studies 1803 pre-menopausal women with ER^+ breast cancer receiving adjuvant goserelin and endocrine treatment either with or without Zol (4mg every 6 months) (Gnant et al., 2015a). Results from this study showed that relative risk of disease progression was reduced in women receiving Zol. However, the women in this study had low circulating oestrogens due to endocrine therapy and all tumours were ER+, limiting the analysis.

In the AZURE trial (Figure 1.5), 3360 women were randomised to receive standard adjuvant systemic treatment, with or without Zol (4 mg every 3–4 weeks for six doses, then every 3 months for eight doses, followed by every 6 months for five doses, for a total period of 5 years). Although initial analysis showed that overall survival (OS) and disease-free survival (DFS) were similar for both control and Zol treated women, sub-group analysis of menopausal status showed differences. Women who were 5 years or more into the menopause showed benefit with invasive disease-free survival (iDFS) of 78.2% compared to control 71% (95% CI, P=0.02) and OS of 84.6% compared to control 78.7% after 5 years (95% CI, P=0.04) (Coleman et al., 2011). On the other hand, while pre-menopausal women had reduced skeletal metastasis, this was accompanied by an increased risk of extra skeletal recurrence (Coleman et al., 2014b). This result was mirrored in the large meta-analysis of 26 randomised trials on

adjuvant Zol in early breast cancer, encompassing 18,766 women (J. Bergh *et al.*, 2015). Sub-group analysis showed that Zol had the most significant effects on bone recurrence, overall recurrence, distant recurrence, and mortality in post-menopausal women.

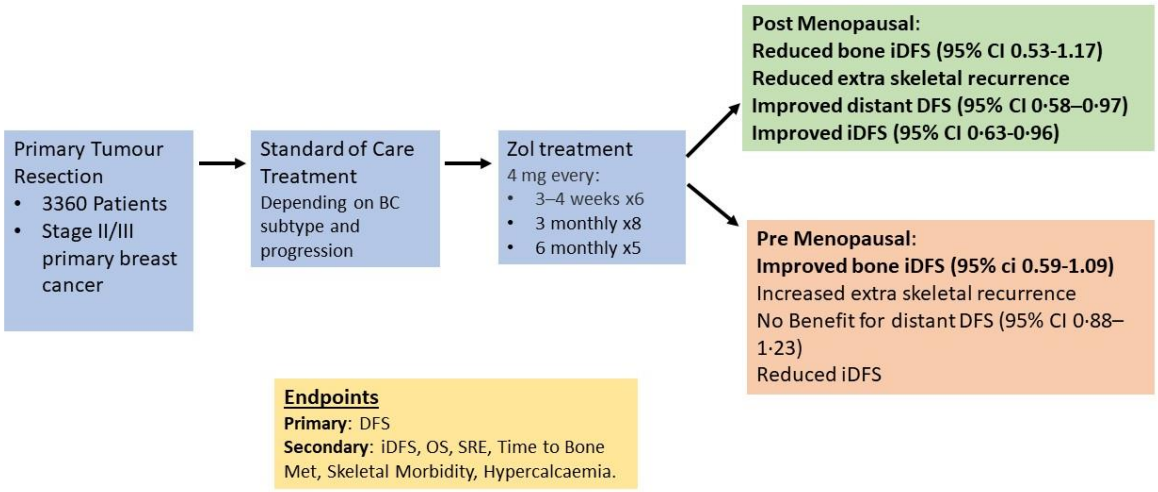

Figure 1.5 The AZURE trial treatment methods and outcome according to menopausal status.

The AZURE trial investigated the use of Zol in primary breast cancer patients to prevent bone and extra skeletal recurrence. Figure summarises patient recruitment, patient treatment, experimental endpoints and study outcomes according to menopausal subgroups.

Reproductive hormone levels were analysed from the serum of patients in the AZURE trial, studying levels of inhibin A, FSH and oestradiol with the aim to understand the role of these hormones in the context of the AZURE trial (Wilson et al., 2016b). This analysis found that post-menopausal levels of oestrogen alone corelated with significantly shorter iDFS (CI: 1.05-1.78, p=0.022). On the other hand, oestrogen and FSH levels representing post-menopausal conditions lead to improved iDFS with addition of Zol (CI: 0.54-1.22) and a trend towards decreased non bone metastasis, highlighting the benefit of adjuvant Zol in post-menopausal women when compared to pre-menopausal women.

1.11 Oestrogen and the menopause

The menopausal transition marks a shift in the endocrine landscape and function in women and occurs at a median age of 51.4 (McKinlay et al., 1992). On average, women spend 4 years in menopausal transition (peri-menopause) before the final menstrual period which marks the end of the transition (post-menopause), but there is a large variability in length between individuals. Therefore, the menopausal state of a woman can only accurately be determined by measuring ovarian hormone concentrations. (McKinlay et al., 1992).

During the normal menstrual cycle FSH is secreted from the anterior pituitary gland and is regulated through negative feedback by inhibin B and oestrogen produced in ovarian follicles. As the number of ovarian follicles decreases with age, accelerating towards the menopausal transition, so does inhibin B, leading to a decrease in negative feedback and an increase in FSH secretion (Su and Freeman, 2009). Inhibin B decline is one of the earliest markers of the menopausal transition. Oestrogen levels tend to remain fairly stable in the early menopausal transition and can even be seen to rise during the early follicular phase of the cycle (Burger et al., 1999). However, nearer the end of the menopausal transition, oestrogen rapidly declines and is considered the final biomarker of the final menstrual period (the last point of the menopausal transition).

The action of oestrogen is mediated through two distinct receptor proteins encoded from separate genes on different chromosomes, ERα and ERβ. These receptors comprise of six structural domains with the C and E domains carrying a high degree of homology between ERα and ERβ. The other four sections are divergent and are involved in transcription activation and ligand dependent activation or inactivation (Hamilton et al., 2014). The expression profiles of each receptor differ in each tissue and cell type, but expression is widespread. In the classical mechanism of action, oestrogen binds ER and the complex directly binds to oestrogen response elements to influence transcription (Katzenellenbogen et al., 2000). Oestrogen can also act through a tethered mechanism whereby ER does not directly bind to DNA but binds to transcription factors such as c-Jun to form a transcription activation complex (Jakacka et al., 2001). Furthermore, ERs have also been shown to be involved in extracellular non genomic signal transduction, binding to receptors such as GPER1 on the cell membrane (Madak-Erdogan et al., 2008).

Oestrogen has wider effects than just those on ovarian regulation and the menstrual cycle. ERs are found in many tissues around the body. One of these is bone where oestrogen is vital in maintaining normal bone remodelling by regulating the expression of RANKL in osteoblasts, affecting osteoclast mediated bone resorption (Streicher et al., 2017). This interaction is important in the regulation of osteoclasts, as shown in the menopause where the reduced concentration of circulating oestrogen leads to increased osteoclast activity and reduced bone volume (Ji and Yu, 2015). ERs have also been found on numerous immune cells, and have been shown to regulate the immune landscape, perhaps contributing to the differences observed in immune response between men and women (Irelli et al., 2020). Furthermore, ERs have a major role in tumour progression, with ~80% of breast cancers expressing ER, through which ER/oestrogen interactions contribute to tumour proliferation and survival.

1.12 Effects of Zol and oestradiol on bone metastasis and bone resident cells

Zol, the third-generation nitrogen containing bisphosphonate, excerpts its primary method of action by inhibiting osteoclast maturation and stimulating apoptosis of these cells via inhibition of the mevalonate pathway (Figure 1.4) (Holen and Coleman, 2010). Because osteoclast and osteoblast activity is closely linked via feedback mechanisms, Zol also reduces osteoblast activity, stopping the expansion of the endosteal niche. Moreover, through the inhibition of the mevalonate pathway within endothelial cells in the bone, Zol can inhibit the sprouting of new blood vessels, therefore inhibiting the vascular niche (Lang et al., 2016). These effects on bone niche expansion act to inhibit tumour growth within the bone, but preclinical studies have shown that Zol has optimal anti-tumour effects only under post-menopausal concentrations of oestradiol. Mimicking the menopause by ovariectomy (OVX) was shown to increase bone resorption and trigger tumour outgrowth in bone. Treatment with Zol prevented the OVX induced bone resorption while also preventing growth of disseminated tumour cells, an effect that was not observed in sham operated mice (Ottewell et al., 2014b). Initially, this mechanism was proposed to be mediated by altered osteoclast activity by menopausal related hormones. Indeed, deprivation of menopausal related hormones was shown to increase RANKL expression in the bone, a molecule that is essential for osteoclast differentiation, activity and survival, with disruption to this pathway reducing osteoclast bone resorption and reducing tumour outgrowth (Ottewell et al., 2015). However, clinical treatment with the anti-RANKL antibody Denosumab, had no effect on tumour recurrence irrespective of menopausal status, suggesting that other cell types are responsible (Stopeck et al., 2010). Indeed, oestradiol can affect the activity of a plethora of cells within the bone, while also affecting expression of inflammatory molecules such as TNF-α, IL-6 and IL-1, suggesting a more complex mechanism for oestradiol and Zol on bone metastasis (Weitzmann and Pacifici, 2006).

1.12.1 Effect of Zol on bone resident cells

In the bone, Zol acts on a number of cells and niches, such as the vascular niche which regulates bone cell progenitor maturation and supports cell growth, while being closely linked to tumour dormancy and outgrowth. The number of vascular endothelial cells has been shown to be decreased by Zol treatment in a dose dependent manner *in vitro* (Lang et al., 2016). Furthermore, Zol treatment decreased the activity and migration of vascular endothelial cells while changing their morphology (Lang et al., 2016). However, these results were not observed *in vivo,* with no differences in vessel number in Zol treated and untreated mice. Interestingly, when younger (4 week old), immunocompetent mice (with low circulating oestradiol) were treated with Zol, it increased vessel

numbers, a change that was not observed in older (4 month) mice (Soki et al., 2013). In human patients, Zol has been shown to decrease serum concentrations of VEGF, an important factor for blood vessel development and function, which would suggest a decrease in blood vessel number, but studies to confirm this or the effects of oestradiol have not yet been carried out (Santini et al., 2003).

The haematopoietic and mesenchymal niches in bone are also directly affected by Zol. Indeed, haematopoietic stem cell numbers are significantly increased by Zol in *in vivo* immunocompetent mouse models, but motility and re-localisation patterns are unchanged (Soki et al., 2013). It was previously assumed that haematopoietic niche mobilisation was dependent on osteoclast activity, suggesting that Zol induced reductions in osteoclast activity would reduce haematopoietic cell motility (Miyamoto et al., 2011; Miyamoto, 2013). Therefore, this data suggests that other mechanisms may also be at play. In the mesenchymal niche, Zol treatment deceased the number of osteoprogenitors (Hughes et al., 2019) while also reducing numbers and activity of osteoblasts within the bone (Brown et al., 2012; Ottewell et al., 2014b). However, this decrease in osteoblasts appears to be a simplification, with numbers of osteoblasts increasing in areas of high bone turnover, and numbers decreasing in regions of low remodelling (Haider et al., 2014; Hughes et al., 2019). These dramatic effects on bone affect processes thought to reduce the ability of tumour cells to colonise and grow in bone. Furthermore, oestradiol may have opposing effects through its anabolic action on the bone.

1.12.2 Effect of oestradiol on bone resident cells

Osteoclasts, osteoblasts and a plethora of bone resident cells are able to respond to oestradiol through the ERα and ERβ receptors which are expressed widely through the bone microenvironment. Cell types within the bone respond differently to oestradiol stimulation depending on ER type, cell type or downstream signalling.

Osteoblasts, derived from the mesenchymal lineage, differentiate from early osteoblast progenitor cells which respond to oestradiol signalling to alter their self-renewal mechanisms. Under pre-menopausal concentrations of oestrogen, osteoblast progenitors are stimulated to commit to differentiation into osteoblasts. Furthermore, pre-menopausal concentrations of oestradiol increase expression of adhesion molecules such as N-cadherin, increasing motility for migration to the sites of resorption (Di Gregorio et al., 2001; Mödder et al., 2011). Low oestradiol concentrations impair this. Mature osteoblasts can also respond to oestradiol signalling, with pre-menopausal concentrations of oestradiol preventing cells from apoptosis by inhibiting Caspase-3/7 activation (Bradford et al., 2010).

Osteoclasts are profoundly influenced by oestradiol signalling in the bone, having an influence over osteoclast maturation, activation and life span. ERα knock out (KO) in the haematopoietic cells of mice led to a significant increase in osteoclasts and osteoclast progenitors (Martin-Millan et al., 2010). High concentrations of oestradiol have been shown to supress osteoclastogenesis and bone resorption, partially because of an oestradiol dependent change in secretion of, IL-6, TNFα, IL-1 and M-CSF (Weitzmann and Pacifici, 2006). Indeed, post-menopausal concentrations of oestradiol increase production of IL-1 and RANK-L, resulting in increased numbers and activity of osteoclasts (Streicher et al., 2017; Weitzmann and Pacifici, 2006). Oestradiol can directly act on active osteoclasts, inducing apoptosis via a TGF-β dependent manner (Hughes et al., 1995). This mechanism was shown *in vivo* to be important in the regulation of osteoclasts in the trabecular bone area, an area where Zol has its most potent anti resorptive effects (Martin-Millan et al., 2010).

Oestradiol and Zol both have profound effects on bone resident cells and tumour growth but acting through different mechanisms. Zol acts by actively killing osteoclasts whereas oestradiol has anabolic effects on osteoblasts while decreasing the lifespan of osteoclasts. This difference may account for Zol being less effective at reducing resorption and the vicious cycle of bone metastasis in pre-menopausal oestradiol. This goes some way to explaining the differential effects of Zol and oestrogen on bone metastasis, however, clinical trials showed that the most striking negative effects of Zol treatment in pre-menopausal women was seen outside of the bone, with an increase in soft tissue metastasis and a decrease in iDFS (Coleman et al., 2014b). Therefore, it is likely that Zol and oestradiol are having systemic actions, possibly acting through immune cells.

1.13 Immune landscape of breast cancer and bone metastasis

In cancer cells, genetic and epigenetic modifications lead to expression of cancer associated antigens that can be recognised by complement proteins of the immune system. In order to survive, proliferate and metastasise to form secondary tumours in the bone, breast cancer must evade immune recognition and destruction. Furthermore, the immune cells within the bone microenvironment are in proximity and communicate with osteoclasts and osteoblasts, affecting both bone turnover and immune cells present within the bone. For example, CD4+ T cells can regulate osteoclast activity by regulating RANKL and OPG release to increase osteolytic lesions (Teng et al., 2000). Conversely, CD4+ T cells can have the opposite effect by releasing IFNγ to inhibit the activity of osteoclasts (Xu et al., 2009). This suggests that it is the balance between pro tumorigenic and anti-tumorigenic immune cells within the bone that can influence metastasis. Breast cancer cells express immune modulatory molecules, such as PD-L1, an inhibitory molecule allowing tumour cells to escape

T-cell toxicity. Furthermore, the PD-L1 allows expansion of the immunosuppressive T regulatory cells (Treg) cells in the tumour microenvironment, causing a suppression of CD8+ T cell activity. The presence of Tregs in the tumour microenvironment predicts a poor prognosis for patients (Bates et al., 2006) and that expression is significantly increased in prostate cancer patients with bone metastasis (Zhao et al., 2012). Natural Killer (NK) cells are important for immune mediated tumour killing, recognising the down regulation of major histocompatibility complex (MHC) proteins on tumour cells usually employed to avoid T cell recognition. NK dysfunction is often observed in the tumour microenvironment, partly mediated through release of tumour derived immunosuppressive cytokines such as IL-10 and TGF-β (Lee et al., 2004). Macrophages can be broadly classed into tumour supressing macrophages and tumour associated macrophages (TAMs), with higher levels of TAMs being associated with a poor prognosis (Zabuawala et al., 2010). This is because TAMs have been shown to secrete high levels of IL-10 and TGF-β, decreasing CD4+ and CD8+ T cell activation as well as NK cells (Biswas and Mantovani, 2010a).

Tumours can profoundly alter the immune cell populations in the microenvironment; therefore, the presence of specific immune cell subsets can act as a predicter for cancer prognosis. The presence of eosinophils, B lymphocytes, neutrophils and CD4+ or CD8+ T cells in the tumour microenvironment are indicative of good prognosis. On the other hand, presence of TAMs, Tregs and activated mast cells in the microenvironment can be a marker of poor prognosis and predispose tumour cells to metastasise (Xiang and Gilkes, 2019).

1.14 Effect of Zol on immune response to breast cancer

Zol has profound effects on the immune system due, in part, to immune cells expressing the mevalonate pathway enzymes. More specifically, Zol influences Treg cell activation and infiltration, NK cell activity, macrophage polarisation in the tumour microenvironment, Gamma delta T cells (γδ T cells) activation and PD-L1 expression and subsequent effector T cell activity (Figure 1.5). Understanding the action of Zol on the immune cell subsets in the context of breast cancer may help explain the mechanisms whereby adjuvant Zol prevents bone metastasis in post-menopausal women.

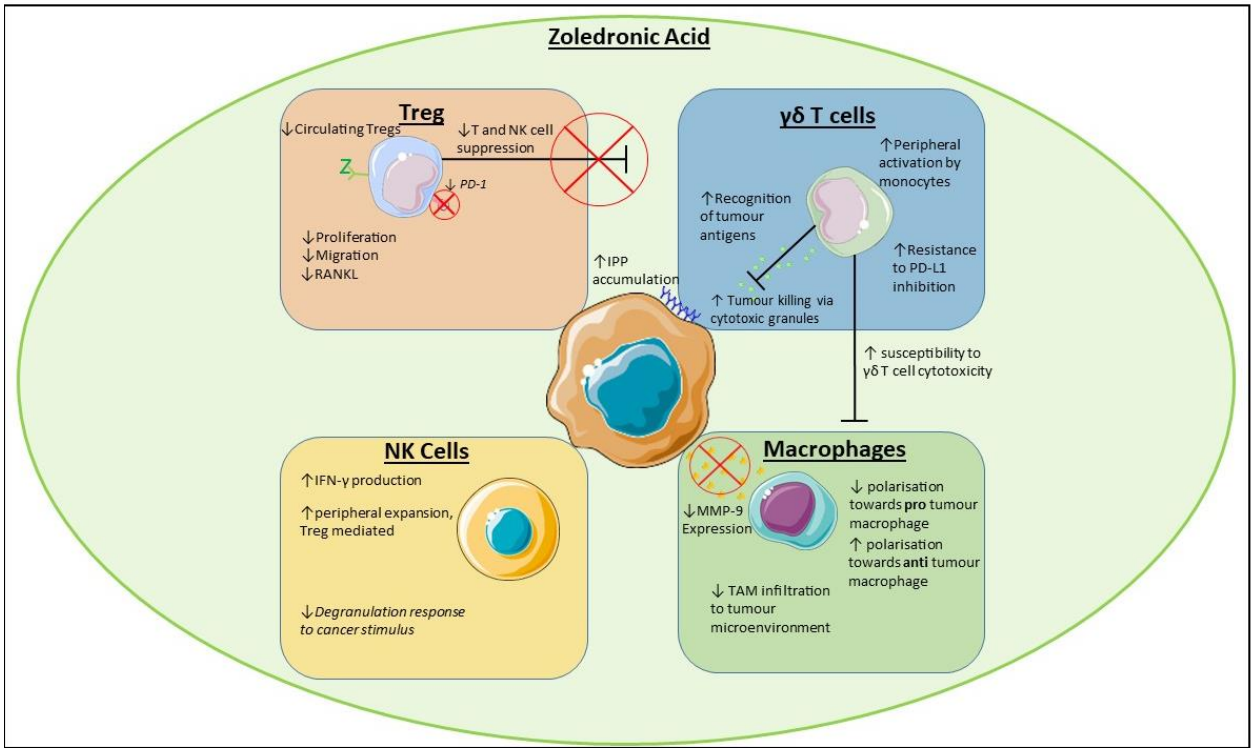

Figure 1.6: The immune modulatory effects of Zol in the context of breast cancer.

Overall, Zol results in an immune stimulatory effect by acting on a number of immune cell types. Zol decreases Treg cell proliferation and action within the tumour microenvironment, therefore reducing T cell and NK cell suppression. Macrophage polarisation favours an anti-tumour phenotype following Zol treatment while acting of γδ T cells to increase activation and recognition of tumour antigens. Zol increases IPP accumulation in tumour cells to increase targeting by the immune system, overall having an immune stimulatory effect.

1.14.1 Gamma delta T cells

γδ T cells enable response to microbes and tumours by detection of self-prenyl pyrophosphate metabolites. Most of these cells express the Vγ9Vδ2 T cell receptor and can respond to potential pathogens without dependence on expression of MHC class proteins, which are often downregulated in breast cancer cells. γδ T cells respond instead to the immunoglobulin family protein butyrophilin 3A1 which is expressed on all human cells (Sandstrom et al., 2014). Therefore, any healthy or tumour cell can present antigens to γδ T cells, releasing the dependence on MHC proteins that is characteristic of other T cell responses. γδ T cells respond to the accumulation of isopentenyl pyrophosphate (IPP), which is produced as part of the mevalonate pathway (Figure 1.4) and often accumulates in unregulated tumour cells. Furthermore, Zol can inhibit the mevalonate pathway enzyme farnesyl pyrophosphatase which is downstream of IPP production, leading the accumulation of IPP and subsequent γδ T cell activation and tumour cell targeted apoptosis (Kondo et al., 2011). The administration of Zol to peripheral blood mononuclear cells *in vitro* resulted in a significant expansion

of γδ T cells. Interestingly, γδ T cells have been shown to be activated in circulation with Zol able to stimulate the accumulation of IPP in circulating monocytes (Roelofs et al., 2009). This led to increased immunostimulatory effects and tumour targeting by degranulation of γδ T cells in the tumour microenvironment causing apoptosis by cytotoxic granule release. On the other hand, it has been shown that peripherally activated γδ T cells lack the ability to migrate into the tumour microenvironment suggesting that the Zol mediated anti-tumour effect of γδ T cells is from direct contact with tumour cell IPP (Fowler et al., 2014).

PD-1 is expressed by γδ T cells, and expression is upregulated when cells are co-cultured with tumour cells (Fleming et al., 2017). Interestingly, γδ T cells from tumour bearing mice respond to mitogen poorly when compared to the healthy mice which proliferate readily, and treatment with an anti-PD-1 monoclonal antibody rescues the proliferation in mitogen treated cells (Lopez et al., 2012). Incubating γδ T cells, expressing PD-1, with PD-L1 expressing tumour cells pre-treated with Zol causes an increase in γδ T cell activation when compared to untreated control tumour cells, suggesting that Zol can overcome PD-L1 inhibition through inhibition of IPP signalling. (Iwasaki et al., 2011).

1.14.2 Treg cells

Treg cells are immune suppressor cells that supress T effector and NK cell activity to maintain peripheral tolerance. The most widely studied are the $CD4^+$, $Foxp3^+$ Tregs which are categorised as either induced (iTreg), which are naïve $CD4^+$ cells converted into mature cells in the periphery under the influence of IL-2 and TGFβ, or natural (nTreg) which are committed cells from the thymus (Francisco et al., 2009; Jacobs et al., 2009). PD-1 and PD-L1, expressed on Treg cells, directly affect Treg cell generation; mouse models studying the conversion and maintenance of iTreg found that it was dependent on PD-L1 via the inhibition of mTOR/AKT pathway (Francisco et al., 2009). Therefore, it is unsurprising that Tregs play an important role in tumour immune evasion by supressing $CD4^+$, $CD25^-$, $CD8^+$ T cells. Indeed, Tregs are upregulated in mouse and human tumours (Nishikawa and Sakaguchi, 2010), with infiltration characteristic of more invasive tumours and a predictor of diminished survival.

Zol has been shown to have an immunomodulatory action on Treg cells, with levels of $CD4^+$, $CD8^+$, $Foxp3^+$ Tregs significantly decreased in mice following treatment with Zol (Kikuiri et al., 2010). Further to the immune inhibitory action, Tregs directly stimulate tumour growth by secreting RANKL (Tan et al., 2011). The effect of Zol on the immunosuppressive activity of Tregs and the progression of breast cancer has been demonstrated in a series of *in vitro* experiments (Liu et al., 2019; Liu et al.,

2016). Treatment of Treg cells with 10μM Zol for 12 days significantly inhibited proliferation by 12% and induced cytoplasmic vacuoles indicating cell stress, while having no effect on isolated lymphocytes. In trans-well assays, Zol significantly inhibited migration of Treg cells in response to MDA-MB-231 conditioned medium. Furthermore, treatment with Zol significantly decreased expression of CCR4, important for Treg recruitment to tumours, suggesting Zol could reduce Treg infiltration. Expression of CTLA4 and PD-1, molecules important in conveying inhibitory signals to effector T cells, were also found to be significantly decreased following Zol treatment showing a change in the phenotypic inhibitory function of Treg cells with Zol. Indeed, when Tregs pre-treated with Zol were co cultured with peripheral blood mononuclear cells (PBMCs), the expression of CD69 (an early activation marker for T cells) was found to be significantly increased, both in the presence and absence of tumour cells (Liu et al., 2016). In breast cancer, Tregs have been shown to increase the migratory capacity of tumour cells. Interestingly, when tumour cells were co-cultured with Tregs pre-treated with Zol, there was a significant and dose dependent decrease in migration in wound healing assays compared to control. Moreover, this was shown to be regulated by RANKL, with Zol decreasing Treg RANKL expression in a dose dependent manner. These findings were expanded in further studies, showing that treatment of Tregs with Zol reduced expression of CD25, TGFβ and STAT5 leading to a reduced capacity for Tregs to supress NK and effector T cells (Sarhan et al., 2017).

1.14.3 Macrophages

Macrophages are mononuclear cells from the myeloid lineage which are derived from monocytes in the bone marrow and are part of the innate immune system. Once monocytes leave the bone marrow, they differentiate into macrophages and have varied effects depending on the stimulation they receive. Macrophages collaborate with T and B cells and are important regulators of T cell recruitment, both promoting and inhibiting recruitment depending on their polarisation (Nilsson and Carlsten, 1994). Macrophages can differentiate into two broad classes depending on local cytokine stimulation acting on precursors. Pro-inflammatory, anti-tumour macrophages secrete IL-1, IL-6, IL-12 and IFN-γ and are important in recruiting T cells into the microenvironment, eliminating tumour cells (Xiang and Gilkes, 2019). TAMs are immune suppressive and are important regulators of tumour progression and bone metastasis (Lo and Lynch, 2018). This is because they secrete cytokines such as IL-10 and TGF-β leading to reduced activity and infiltration of $CD4^+$ and $CD8^+$ T cells in the tumour microenvironment (Biswas and Mantovani, 2010b).

Zol has been shown to affect macrophage polarisation and function in the tumour microenvironment. Zol can be actively taken up by macrophages, both *in vitro* and *in vivo*. Treatment

of macrophages with 5μM Zol over 24 hours led to a significant increase in uRap1A, a marker of inhibition of the mevalonate pathway (Rogers et al., 2013). Furthermore, in macrophages isolated from breast cancer xenografts uRap1A was found significantly increased in patients who received 1 dose of Zol (Rogers et al., 2013). Further to being taken up by macrophages, Zol can affect their function. Mice were treated with Zol for 3 weeks before tumours were removed and histologically analysed, finding that mice treated with Zol had reduced TAM infiltration and reduced vascularisation due to a switch in macrophage polarisation towards an anti-tumour phenotype (Coscia et al., 2010).

The interaction between tumour cells and macrophages leads to an increase in matrix metalloproteinase-9 (MMP-9) expression in TAMs. MMP-9 is an enzyme important for vascularisation, invasion and metastasis of breast cancer cells because it assists extracellular matrix (ECM) remodelling by degrading basement membranes (Foda and Zucker, 2001). Furthermore, MMP-9 is required by myeloid derived suppressor cells (MDSCs) in the tumour microenvironment to assist their immune suppressive function (Yang et al., 2004). When mice were treated with Zol, there was a significant decrease in levels of MMP-9 and numbers of TAMs, followed by a reduced expansion of MDSC. This was due, in part, to decreased bone marrow progenitor derived MMP-9 (Melani et al., 2007). In a series of *in vitro* experiments to study to interactions of cancer cells and macrophages in the presence or absence of Zol, Zol was found to supress MMP-9 expression in TAMs and change macrophage polarisation to drive the activation and proliferation of γδ T cells (Tsagozis et al., 2008).

Zol can affect the interactions of macrophages and γδ T cells in the tumour microenvironment. In an *in vitro* experiment, human monocytes were isolated and differentiated into either pro or anti-tumour monocytes before treatment with Zol. Zol significantly increased γδ T cell targeting of macrophages in a perforin dependent manner, independently of macrophage polarisation (Fowler et al., 2017). This could represent an important mechanism whereby macrophages are cleared from the tumour microenvironment.

1.14.5 NK Cells

NK cells are part of the innate immune system and are a vital immune cell having cytotoxic effects on breast cancer cells, targeting stress induced markers (Diefenbach et al., 2001). Research into the effects of Zol on NK cells in the context of breast cancer are limited and often show conflicting results between different studies, highlighting the need for further research into this area. In one study in which NK cells and dendritic antigen presenting cells were co cultured with or without the addition of Zol reported that Zol stimulated IFN-γ expression in NK cells. This was found to be due to

NK cell interactions with dendritic cells, where Zol caused depletion of endogenous prenyl pyrophosphatases in dendritic cells, stimulating the secretion of IL-18 and IL-1β which in turn led to caspase 1 dependent NK cell activation (Nussbaumer et al., 2011). As described previously, treatment with Zol reduces Treg cell infiltration, but also significantly increases NK cell proliferation in peripheral blood (Sarhan et al., 2017). This was demonstrated to be mediated via Treg signalling, where Treg treated with Zol had a reduced capacity to inhibit NK cell proliferation. In contrast, an *in vitro* study has shown opposing data. When NK cells were isolated from healthy patients and from patients with Ewing sarcoma and treated with Zol, Zol impaired both NK cell expansion and degranulation in response to Ewing sarcoma stimulus (Mueller et al., 2013).

NK cells are an attractive target for immune therapy for cancer because of their MHC independent, non-tumour antigen specific killing of tumour cells. Therefore, it is unsurprising that new clinical approaches are being developed to boost NK cell activity in response to cancer. One such treatment is the adoptive transfer of NK cells, and another is to block mechanisms that dampen NK cell responses to allow an uninhibited NK cell action on tumours (Lorenzo-Herrero et al., 2018). These new treatments highlight the need for further understanding of the effects of Zol on the anti-tumour activity of NK cells.

1.14.6 Immune stimulatory effects of Zol summery

Zol has a significant effect on the immune response to cancer, leading to improved immune infiltrate and tumour cell killing. Zol acts to decrease Treg cell activation and infiltration in the tumour microenvironment, leading to an increase in $CD4^+$ and $CD8^+$ T cells, NK cell infiltration and cytotoxic action. Furthermore, Zol can shift macrophage polarisation towards an anti-tumour phenotype, counteracting the immune-inhibitory environment in the tumours. As shown in the ABCSG-12 (Gnant et al., 2011) and AZURE trials (Coleman et al., 2014b), post-menopausal breast cancer patients treated with Zol had a survival benefit and decreased bone metastasis. These immune effects could represent a bone resident cell independent mechanism whereby Zol mediated anti-tumour activity. However, the AZURE trial showed that the same benefit was not observed in pre-menopausal patients, who had increases soft tissue metastasis and decreased iDFS, raising the question of the effect of oestrogen on the immune action of Zol.

1.15 The effect of oestrogen on the cancer associated immune responses

Oestrogen is immunogenic, affecting the activity and survival of a plethora of immune cells. ER is expressed on dendritic cells, mast cells, macrophages, neutrophils, NK cells, B cells, $CD4^+$ T cells,

$CD8^+$ T cells and Tregs, highlighting oestrogens potential to modulate the immune system. However, not all these cells are directly involved in anti-tumour responses highlighting the complexity of oestrogens involvement in the anti-tumour immune response (Figure 1.6).

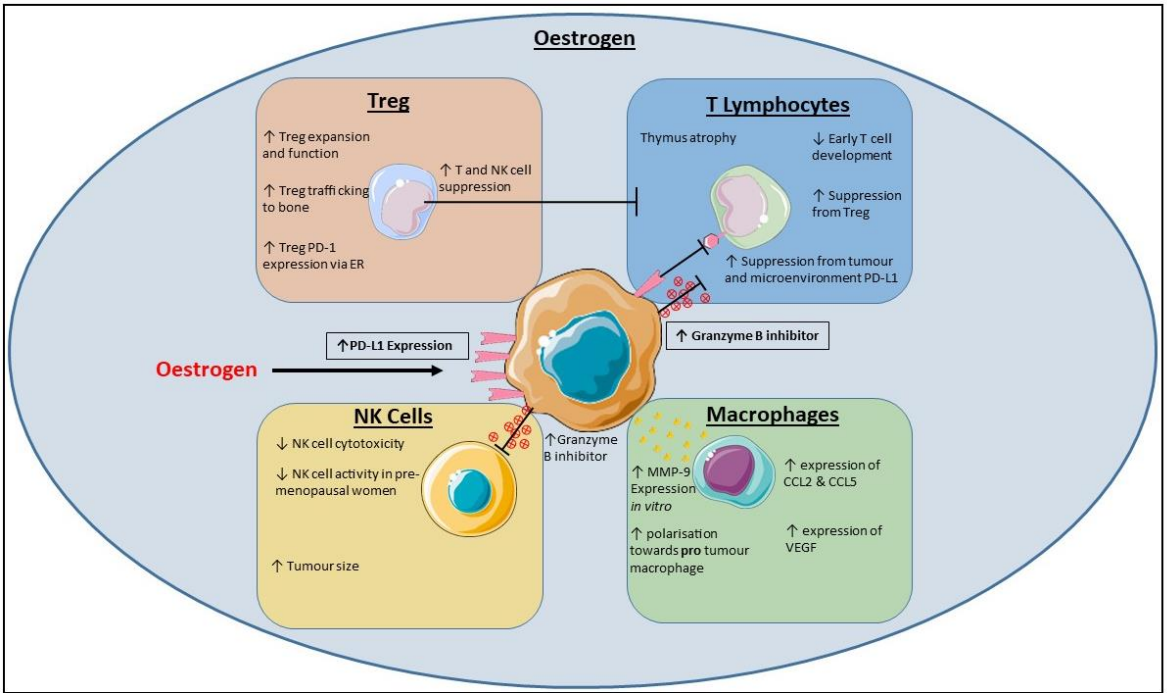

Figure 1.7: The immune modulatory effects of oestradiol in the context of breast cancer.

Overall, oestradiol results in an immune inhibitory effect by acting on a number of immune cell types. Oestradiol increases Treg cell expansion, function and trafficking into the tumour microenvironment**,** therefore increasing T cell and NK cell suppression. Macrophage polarisation favours a pro-tumour phenotype under high oestradiol concentrations while acting on T cells to decrease early development. Zol increases granzyme B inhibitor expression, PD-L1 expression while decreasing NK cell cytotoxicity, overall leading to an immune inhibitory effect.

1.16 Pre-clinical effects of oestrogen on immune response to breast cancer

A series of *in vitro* experiments utilising ER^+ breast cancer cells and immune cells have shown that PD-L1 expression is responsive to oestrogen (Yang et al., 2017). When the ER+ MCF7 breast cancer cell line is cultured with oestradiol, PD-L1 protein expression is significantly increased, via activation of the AKT/PI3K pathway. This effect was found to be due to increased mRNA stability and not increased transcription; since blocking transcription had little effect on PD-L1 protein expression. When MCF7 cells and isolated T cells were co cultured in the presence and absence of oestradiol, the treatment with oestrogen was found to increase PD-L1 expression and decrease T cell function, as

shown by decreased T cell derived IFN-γ and IL-2 indicating T cell exhaustion. Moreover, this effect was found to be independent of oestradiol's direct action on T cells (Yang et al., 2017). However, an oestradiol concentration of 10 nM was used for these experiments which is significantly higher than physiologically relevant concentrations, which are normally in the range of 30-400 pM.

This increased expression of PD-L1, driven by oestrogen, may explain the reduced anti-tumour effect of Zol in pre-menopausal women, because Zol acts to increase the activation of T cells in the tumour microenvironment. Oestrogen could prevent this by causing T cell exhaustion in the microenvironment to prevent anti-tumour activity.

1.16.1 Treg cells

The immune suppressive T lymphocytes, have been shown to express ERs, which enhance their function and enable expansion of the Treg cell compartment (Polanczyk et al., 2004). In one study, OVX mice were administered pre-menopausal physiological concentrations of oestradiol, and it was observed that there was increased conversion of $CD4^+$ $CD25^-$ cells into $CD4^+$ $CD25^+$ cells. Furthermore, there was increased expression of FoxP3 and IL-10, which are important Treg cell markers (Tai et al., 2008). The increased Treg cell conversion was accompanied by increased suppression of mixed lymphocytes both *in vitro* and *in vivo*. Interestingly, Tregs can interact with osteoclasts and have been shown to modify their bone degradation function, with oestrogen enhancing this effect. When freshly isolated human bone marrow and human Tregs were co cultured in the presence or absence of oestradiol, osteoclast differentiation was supressed better with oestradiol, which was shown to be regulated by Treg derived IL-10 and TGF-β (Luo et al., 2011).

As described previously, oestradiol can increase PD-L1 expression in the tumour microenvironment. This can augment Treg immunosuppression further because the PD-1/ PD-L1 axis increases iTreg conversion, enhances Treg function and maintains Treg phenotype by stabilising FoxP3 expression (Cai et al., 2019). This has important implications for bone metastasis patients where an increase in Treg cells is observed, with signalling through the CXCR4/ CXCL12 axis mediating Treg trafficking to the bone, stimulation local iTreg conversion via local PD-L1 and suggesting the bone as a preferential site for functional Tregs (Zou et al., 2004). The presence of Treg in the bone is indicative of adverse effects for breast cancer patients, as their activity promotes metastasis.

Further to increasing PD-L1 expression in the microenvironment, oestrogen can influence Treg differentiation and suppressive activity by regulating PD-1 expression. Intracellular PD-1 expression in Treg is oestrogen sensitive and has been shown to be moderated by ER signalling. When comparing

the effect of oestrogen on Treg cells and Treg cells with ER KO, estrogen was found to increase PD-1 expression in normal Treg cells but have no effect on ER KO Tregs (Polanczyk et al., 2007). Furthermore, when PD-1 was KO from Treg cells, they lost their functional suppressive activity, highlighting the importance of the oestrogen and PD-1/ PD-L1 axis for Treg immune suppression.

Tregs are a major source of RANKL in the tumour microenvironment and in the bone, expressing up to four-fold more RANKL then $CD4^+$ $CD25^-$ T cells (Tan et al., 2011). Therefore, Treg cells are important for maintaining RANKL expression in the tumour microenvironment of metastatic breast cancer. Tregs increase the metastatic potential of breast cancer, and these adverse effects were found to be replaceable with exogenous RANKL, suggesting it is through RANKL signalling that Tregs have their predominant pro-metastatic effects (Tan et al., 2011).

Zol has contrasting effects to oestrogen on Treg activity and PD-1 expression on Treg cells. Zol decreases PD-1 expression on T reg cells, leading to decreased iTreg conversion and a decreased ability for Tregs to functionally supress T effector cells in the tumour microenvironment. Zol also inhibits the proliferation and migration of Treg cells, potentially leading to a reduced capacity for Tregs to infiltrate the tumour microenvironment in bone metastasis. Oestrogen has the opposite effect, leading to increased Treg infiltration through CXCR4/ CXCL12 signalling to create a more immune suppressive tumour environment. This represents one potential mechanism for the differential effects of Zol in the pre- and post-menopausal setting.

1.15.2 T Lymphocytes

$CD4^+$ and $CD8^+$ T lymphocytes are important players for immune protection from breast cancer metastasis. $CD4^+$ T cells assist B cells in antibody mediated protection, whereas $CD8^+$ T cells exert a direct cellular response to have cytotoxic effects on tumour cells. Indeed, $CD8^+$ T cell infiltration in the tumour microenvironment corelates with improved overall survival (Ali et al., 2014). $CD8^+$ T cells are a vital defence to prevent bone metastasis, with down regulation of MHC signalling on tumour cells leading to an escape from T cell detection, promoting bone metastasis (Bidwell et al., 2012). Alongside downregulation by Treg cells, T cells also express ERα and their activity is profoundly affected by oestrogen signalling. Oestrogen blocks early T cells development in the thymus (Rijhsinghani et al., 1996), leading to reduced thymus derived T cells in mice following oestrogen administration (Okasha et al., 2001). This has been shown to be due to thymic atrophy in response to oestrogen, because of a reduced production of $Flt3^+Sca\text{-}1^+c\text{-}Kit^+$ thymic homing progenitors followed by reduced proliferation of thymocytes, as shown in mouse models (Zoller and Kersh, 2006).

Furthermore, the apoptosis observed in the thymus in response to oestrogen involves signalling via Fas/Fas ligand dependent mechanisms (Yao and Hou, 2004).

Oestrogen can also affect $CD8^+$T cell tumour killing in the tumour microenvironment. $CD8^+$ T cells normally have their cytotoxic effects via granule mediated exocytosis of serein proteases, such as granzyme B, to stimulate caspase induced apoptosis (Lieberman, 2003). Interestingly, when the ER^+ breast cancer cell line MCF7 was treated with oestrogen, it led to an increase in expression of PI-9, a granzyme B inhibitor, conveying protection form the cytotoxic effects of T and NK cells (Jiang et al., 2007).

These studies highlight the overlapping and contrasting effects of Zol and oestrogen regarding anti-tumour immune activity in pre-menopausal patients. In post-menopausal patients, Zol has antitumor effects, in part, by decreasing Treg cell activity, consequently leading to increased $CD8^+$ T cell activity. However, in pre-menopausal conditions, $CD8^+$ T cell function may be further inhibited by granzyme B inhibitors. Therefore, if Zol does decrease Treg activity, the $CD8^+$ T cell could have diminished functions independent of Treg.

1.15.3 Macrophages

TAMs contribute to breast cancer progression and metastasis and are involved in invasion, vascularisation, intravasation, circulating tumour cell survival, extravasation and pre-metastatic niche formation (Lin et al., 2019; Vasiliadou and Holen, 2013). Macrophages are derived from the same lineage as osteoclasts and, like osteoclasts, are able to respond to oestrogen signalling. Indeed, in an OVX mouse asthma model, treatment with oestrogen led to increased expression of IL4 and increased M2 macrophage gene expression, suggesting a mechanism for gender differences in the inflammatory disease progression (Keselman et al., 2017).

Macrophages express ERα and ERβ, with TAMs expressing ERs across a plethora of different cancer types (Kovats, 2015). ER signalling within the tumour microenvironment has been shown to affect macrophage polarisation. For example, in a mouse breast cancer model, using Polyomavirus Middle T ER^+ breast cancer, treated with oestrogen, there was a significant increase in M2 macrophage infiltration compared to untreated controls which had higher M1 macrophage infiltration (Kovats, 2015; Svensson et al., 2015). This effect was found to be mediated via increased expression of CCL2 and CCL5 in macrophages following oestrogen treatment. Furthermore, macrophages treated with oestrogen had higher VEGF secretion, a molecule important for tumour progression and the angiogenic switch (Svensson et al., 2015). Oestrogen was also shown to act on macrophages to

increase expression of MMP-9 *in vitro*, a molecule important for ECM remodelling and therefore tumour invasion (Hwang et al., 2006). These studies show how oestradiol can regulate the non-immune functions of macrophages, assisting tumour progression by regulating angiogenesis, migration and invasion of cancer cells.

These studies show another overlapping effect of Zol and oestrogen and the anti-cancer immune response. MMP-9 expression in macrophages is significantly increased by oestrogen *in vitro* and significantly decreased by treatment with Zol. Decreased MMP-9 would lead to decreased TAM infiltration and decreased tumour invasion and metastasis. The opposing effects on MMP-9 represent another mechanism whereby oestrogen alters the anti-tumour effects of Zol, possibly contributing to the discrepancies seen in anti-tumour actions of Zol on pre- and post-menopausal women in the ABCSG-12 and AZURE trials. Moreover, Zol and oestrogen affect macrophage polarisation in opposite ways, with oestrogen increasing pro tumour macrophage polarisation and infiltration via CCL2 and CCL5 signalling and Zol inhibiting this infiltration and influencing polarisation towards an anti-tumour phenotype.

1.15.4 NK Cells

NK cells, part of the innate immune system, are important for immune protection from breast cancer, and depletion of NK cells in cancer models leads to bone metastasis and uncontrolled proliferation (Bidwell et al., 2012). NK cells recognise stress markers, binding to surface ligands such as NKG2D (Diefenbach et al., 2001), but also recognise and respond to down regulation of MHC molecules on tumour cells, killing the target by granule mediated exocytosis and Fas-Fas ligand interactions (Garrido et al., 2010). Interestingly, tumours can become resistant to NK cell recognition by loss of HLA class 1 molecules, a common mutation in breast cancer cells (Watson et al., 2006).

ERα and ERβ are both expressed on NK cells, having functional effects, with ERβ being first described as the main mechanism for oestrogen effect (Curran et al., 2001). In *in vivo* experiments using a range of castrated mouse strains, oestrogen treatment led to a significant decrease in NK cytotoxicity in a dose dependent manner (Baral et al., 1995; Nilsson and Carlsten, 1994). These *in vivo* results were mirrored in humans, where post-menopausal women were given oestrogen replacement therapy, leading to a significant decrease in NK cell activity when compared to untreated control patients (Albrecht et al., 1996). Moreover, this treatment has been linked to enhanced pulmonary metastasis in melanoma and fibrosarcoma. Indeed, in mouse models of breast cancer, oestrogen treatment significantly decreased NK cell activity and increased tumour size (Curran et al., 2006).

However, it is unclear whether these were the direct effect of oestrogen on NK cells or due to broader effects of oestrogen. These studies show an overlapping effect of oestrogen and Zol on NK cell activity, but they also highlight the need for further research into the field. Immunotherapy by targeting NK cells in the context of breast cancer is getting closer to clinical use and Zol is already an important clinical tool in the treatment of bone metastasis. Therefore, understanding the interactions of Zol and oestrogen on NK cells in cancer is an important research area.

Zol and oestrogen have substantial effects on breast cancer progression and metastasis to the bone, affecting both the tumour directly and the microenvironment. There is a complex interaction of the immune system in the bone metastasis microenvironment with Zol and oestrogen. Zol has been shown to have the potential to induce a favourable environment for immune cell clearance of tumour cells whereas oestrogen signalling can create an immune suppressive environment. Some of the most notable effects of oestrogen and Zol are on Treg cells and PD-L1 expression both *in vitro* and *in vivo*. However, their interactions together in the context of breast cancer bone metastasis has not been studied.

1.16 Project aims

This project hypothesises: Pre-menopausal concentrations of oestradiol inhibit the anti-tumour effects of Zol via PD-L1 induced reduction in T cell activity.

This project aims:

1) To create mouse models of breast cancer metastasis under pre, peri and post-menopausal concentrations of oestradiol representative of clinical trials.
2) To identify how oestradiol and Zol alter growth of disseminated tumour cells in the bone and the soft tissue
3) To understand the effects of Zol and oestrogen on the immune response to cancer
4) To determine if inhibition of PD-L1 signalling can increase anti-tumour effects of Zol under pre-menopausal concentrations of oestradiol.

Chapter 2: Methods

2.1 Cell culture

2.1.1 Cell lines

The cell lines used in this project were triple negative bone homed mouse mammary E0771 (kind gift from Prof Sandra McAllister (Harvard University, Boston USA)) and 4T1 (purchased from the European Cell Culture Collection). Both cell lines were stably transfected to express luciferase (LUC) and Green Fluorescent Protein (GFP) by members of the lab team before I started my project. Both of these cell lines are highly aggressive and fast growing and have been shown to produce both primary tumours and spontaneously metastasise when implanted into the mouse mammary glands (Wright et al, 2016). The E0771 and 4T1-LUC positive cell lines used in this project have been repeatedly passaged through bone to produce variants that preferentially metastasise to bone in C57BL/6 and BALB/c mice respectively.

2.1.2 Cell maintenance

Cells were used between passage 9 and 24 and grown in T75 filter toped tissue culture flasks (corning) in RPMI 1640 medium supplemented with glutamax (GIBCO) and 10% foetal bovine serum (FBS) (Sigma-Aldrich, UK) and incubated in a humid incubator in 5% CO2 at 37^{o}C. Confluence of the monolayer was estimated visually using an Olympus CK2 microscope using a 10 x lens and cells were passaged when 80% confluence was reached.

2.1.3 Cell passaging

Monolayers were grown to 80% confluence, before their medium was removed and discarded and cells subsequently washed 2 x in phosphate buffered saline (PBS) (Sigma-Aldrich, UK). The wash removed any cell debris and dead cells, but it also removed any calcium or phosphate from the flask which inhibits the action of trypsin. 1ml of trypsin (Sigma-Aldrich, UK) was added before cells were incubated at 37 °C for 5 minutes. Trypsin was neutralised following detachment using 9 ml RPMI with 10% FBS and cells were mixed to achieve a single cell suspension, before centrifugation at 800 *g* for 5 minutes and resuspension in 10 ml of fresh growth medium. 1 ml of this suspension was added to a new T75 flask alongside 9 ml of fresh medium to achieve a splitting ratio of 1:10.

2.2 In vitro assays

2.2.1 Growth curve

Cells were detached from the T75 flasks at 80% confluence as described above in section 2.1.3 and the final 10ml of single cell suspension was put in a 15 ml falcon tube. These cells were then counted using a haemocytometer (Neubauer-improved, Depth = 0.10 mm) to determine the number of cells in suspension, cells within the falcon were subsequently centrifuged at 800 *g* for 5 minutes to pellet the cells. Cell density was calculated using the following equation:

Cell Density = (Number of cells counted/number of squares counted) X Volume of cells X 10,000

After centrifugation, the supernatant was removed before re-suspending cells in complete medium to a density of $1X10^6$ cells per ml and then further diluted to 20,000 cells per ml. 1 ml of this was added 12 wells of a 24 well plate to make a final seed density of 20,000 cells per well.

Every 24 hours for a total of 96 hours cells from three individual wells were detached using 500 µl of trypsin and the number of cells was counted using a haemocytometer to determine cell number and growth dynamics of the cell lines.

2.2.2 Determination of IC50 for zoledronic acid

2.2.2.1 Cell counting

Cells were detached from an 80% confluent T75 flask, counted by haemocytometer and re-suspended to 20,000 cells/ml. From this, 500 µl of cells was added to a 48 well plate representing 5 treatment groups in duplicate with 3 time points (n=3) (Figure 2.1 A and B).

Following seeding, E0771 cells were left for 24 hours to grow to confluence before treatment was added. Cells were treated with five concentrations of zoledronic acid ([1-Hydroxy-2- (1H-imidazoledronic acid-1-yl) ethylidene] bisphosphonic acid; Zol) made from a sterile 200µM stock solution (Novartis pharmaceuticals, Switzerland) or PBS control) using the following concentrations: 1% PBS in RPMI with 10 % FBS as control, 5 µM Zol, 10µM, 25µM, 50µM.

4T1-LUC cells were left to proliferate for 24 hours following seeding. Following this incubation period, 4T1-LUC cells were treated with: RPMI containing 10 % FBS, with PBS or 25 µM, 50µM, 100µM, 200µM Zol. Both cell types were counted at 24, 48 and 72 hours following treatment following trypsin detachment and counting with the aid of a haemocytometer.

2.2.2.2 Cell viability

Cell suspensions were made up to 20,000 cells per ml and 100 µl was added to 96 well plates to make 2000 cells per well with 6 technical repeats per group (n=3). Following either 24 hours, Zol treatments were made up as described above and 100 µl of control/treatment was added to appropriate wells using a multichannel pipette after the medium was removed from cells. At each time point, cell viability was assessed via the 3-[4,5-dimethylthiazole-2-yl]-2,5-diphenyltetrazolium bromide (MTT) assay (Sigma-Aldrich, UK).

2.2.3 MTT assays

The MTT assay was used to quantify the number of viable cells in a cell culture. MTT is taken up by mitochondria in living cells where it is reduced by mitochondrial reductases to formazan, which is insoluble, therefore in metabolically active cells formazan precipitates, this can be re-solubilised and detected by absorbance. Therefore, cells must be active with functional mitochondria to be detected by this assay. MTT aliquots were defrosted and diluted 1:6 in pre warmed RPMI with 10 % FBS (37^0C) to make a working stock of 1mg/ml and this was protected from direct light. Immediately prior to analysis, supernatant was removed from cells in 96 well plates by inversion onto tissue before cells were washed once with PBS to remove cell debris. 100 µL of MTT working stock was then added to each well and plates were protected from light and incubated in a humid incubator at 37°C, 5% CO^2 for 3 hours. MTT solution was then removed from each well by gentle pipetting to avoid loss of the formazan crystals produced by mitochondrial reductases in viable cells. The formazan was solubilised by addition of 100 µL Dimethyl sulfoxide (DMSO) (Sigma-Aldrich, UK) to each well and left to dissolve with agitation for 15 minutes before reading the absorbance at 570 nM on SpectraMax M5 plate reader (Molecular Devices).

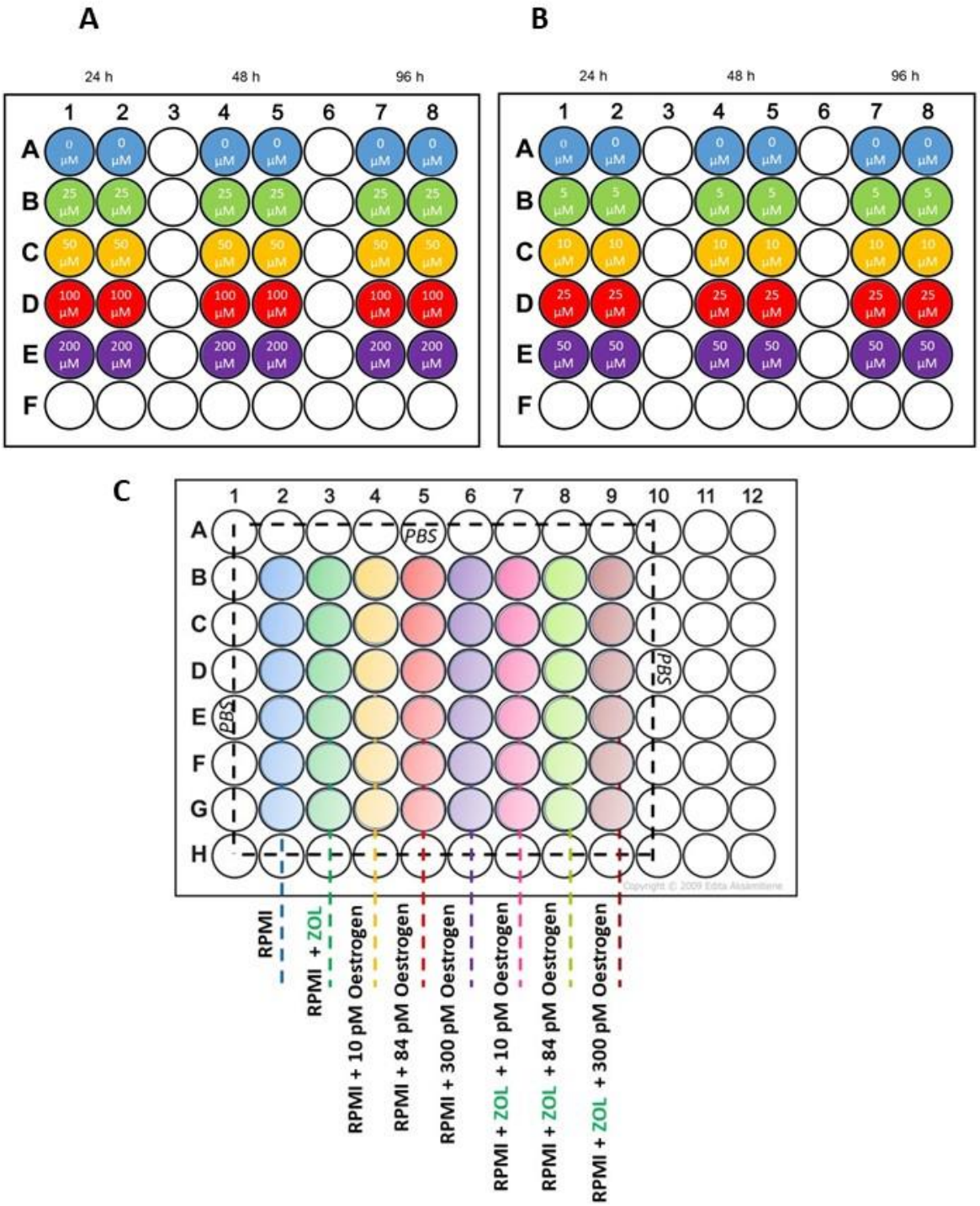

Figure 2.1: Templates of plate layouts for in vitro experiments (A) Plate layout for determination of IC50 for Zol on E0771 cells **(B)** Plate layout Plate layout for determination of IC50 for Zol on 4T1-LUC cells. **(C)** Plate layout to determine the effects of oestradiol on viability of E0771 and 4T1-LUC cells in the presence or absence of Zol

2.2.4 *In vitro* combination experiments with Zol and Oestrogen

Cells were detached from an 80% confluent T75 flask, counted using a haemocytometer and re-suspended to 20,000 cells/ml. From this, 100 µl of cells (2000 cells per well) was added to a 96 well plate representing 8 treatment groups with 6 technical replicates (n=3). The borders of the plate were filled with PBS to prevent excessive evaporation of cell media. E0771 and 4T1-LUC cells were left for 24 hours before treatment. E0771 cells were treated with three different concentrations of oestradiol (Sigma-Aldrich, UK) to mimic post- peri and pre-menopausal concentrations, with or without 25 µM of Zol. Oestradiol was diluted to 10 pM/l, 84 pM/l and 300 pM/L in MEM medium without phenol with 10% charcoal filtered FBS either with or without 25 µM of Zol. The old medium was removed from each well by gentle pipetting before 100 µl of each treatment was added, two treatment groups contained RPMI +10% FBS or RPMI +10% FBS with 25 µl Zol as technical control. Cells were then incubated for 24 h, 48 h or 96 h, after MTT assay was utilised to assess cell viability (Figure 2.1C).

4T1-LUC cells were treated in the same way, except that the Zol concentration used was 40 µM and the final time point was 72 hours due to a faster proliferation time for these cells.

2.2.5 Migration assay

E0771 and 4T1-LUC cells were plated in a 12 well plate at 250,000 cells per well and left for 24 hours to attach in duplicate (n=3). Cells were washed after 24 hours once in sterile PBS before treatment with 10 µg/ml of mitomycin C (Sigma-Aldrich, UK) for 3 hours to prevent cell proliferation. Cells were washed after 3 hours and a scratch was put down the centre of the well using a p200 tip. Cells were washed 3 times in RPMI to clean the scratch before treatments were added to cells. Cells were treated with oestradiol at 10 pM/l, 84 pM/l or 300 pM/l diluted in Phenol free RPMI+10% charcoal stripped FBS, either in the presence or absence of Zol at 15 µM (4T1-LUC) or 7.5 µM (E0771). The scratch was imaged using the EVOS FL Auto (Life Technologies) microscope at 0h, 24h, 48h, and 72h time points (n=3). Analysis of scratch width was performed using the Tscratch software (cselab).

2.2.6 Invasion assay

T75 flasks of E0771 or 4T1-LUC cells were grown to 70% confluence before being treated for 3 hours with 10 µg/ml of mitomycin C (n=3). Meanwhile, matrigel coated cell inserts were rehydrated in RPMI for 3 hours. Following incubation, cell treatments and cell suspensions were made up in phenol free RPMI + 0.1% BSA. 100,000 cells per well insert were combined with 10 pM/ml or 300

pM/ml of oestradiol, +/- 15 µM Zol (4T1-LUC) or 7.5 µM Zol (E0771). The well inserts were submerged in RPMI + 10% FBS as a chemoattractant and incubated at 37°C for 24 hours.

The cell insert membrane was washed to remove cells on the surface before fixing in ethanol and staining with haematoxylin and eosin. The membrane was cut from the insert and mounted on a slide using cryo-m-bed embedding compound (Bright) before imaging on an Olympus BX51 microscope. The number of cells in the matrigel membrane was analysed using image J software colour threshold tool and data was normalised to 10pM/ml samples as control..

2.3 Quantitate reverse transcription polymerase chain reaction (qPCR)

2.3.1 Cell treatment and RNA extraction for qPCR

Before analysis by quantitative polymerase chain reaction (qPCR), E0771 and 4T1-LUC cells were plated in a 6 well plate at 100,000 cells per well and left for 24 hours to attach. Cells were washed after 24 hours in sterile PBS before treatments were added to cells (n=3). Cells were treated with oestradiol at 10 pM/l, 84 pM/l or 300 pM/l diluted in Phenol free RPMI+10% charcoal stripped FBS, either in the presence or absence of Zol at 15 µM (4T1-LUC) or 7.5 µM (E0771). Cells were treated for 48 hours before treatment was washed off with PBS and cells were lysed by cell scraping with of 1ml of Tri Reagent (Sigma-Aldrich, UK). 200 µl of chloroform (Honeywell) was added to lysed cells and shaken for 1 minute before centrifugation at 16,000 *g* for 20 minutes to separate out protein from nucleic acids. The top layer was carefully transferred to a separate 1.5ml tube before 500 µL of isopropanol (Acros Organics) was added to solution to precipitate RNA out of solution. The precipitate was pelleted by centrifugation at 16,000 *g* for 20 minutes before the pellet was washed using 75% ice cold ethanol (Honeywell). The pellet was resuspended in nuclease-free microbiology water and stored at -80°C until needed.

2.3.2 cDNA reverse transcription

Following RNA isolation, reverse transcription was performed using the Superscript III (Invitrogen) kit. A total concentration of 500 ng of RNA was used for the reverse transcription protocol. Firstly, a mix of RNA, H2O (to make up 500 ng) and 0.5 µl random hexamer primers (ThermoFisher) was made for each sample and heated to 65°C for 5 minutes. In the meantime, a master mix of 2 µl first strand buffer (Invitrogen REF: Y02321), 1 µl deoxyribose nucleotide triphosphate (DNTPs) (10mM, Invitrogen, REF:18427-013), 1 µl dithiothreitol (DTT) (0.1M, Invitrogen), 1 µl RNAse Out (Invitrogen

REF:10777-019), 1 µl reverse transcriptase super script III (Invitrogen, REF:18080-044) was made up and mixed with the pre-heated sample. This mix was heated in a thermocycler with the following protocol: 25°C for 5 minutes, 50°C for 60 minutes, 70°C for 15 minutes, 4°C to finish. cDNA was stored at -20°C until needed for qPCR array.

2.3.3 qPCR

qPCR analysis was performed using *Cd274* (Thermo Fisher, cat: 4331182), *Maf* (Thermo Fisher, cat: 4331182) and *Gapdh* (Thermo Fisher, cat: 4331182) Taqman expression probes. For each reaction I used, 10 µl of Taqman universal PCR master mix (Applied Biosystems), 1 µl of primer, 100 ng of cDNA and H20 to make up final volume of 20 µL. Samples were loaded in a 96 well PCR plate in triplicate and run on a MX3000P machine (Stratagene). Amplification analysis was performed using MxPro qPCR software (Stratagene).

2.4 Generating *In vivo* models that mimic human pre- peri- and post- menopausal oestradiol conditions and their effects on breast cancer metastasis.

2.4.1 Mouse models

10-12 week old female C57BL/6 or BALB/c mice were purchased from Charles River, UK and left to acclimatise to new conditions for 7 days prior to use to minimise the effects of traveling stress. Conditions in the room were maintained at regulation levels: Temperature = 19-23 °C; humidity = 45-55 %; illumination at 350 – 400 lux on a 12 hour cycle. Food and water were readily available to mice throughout the experiment. All experiments were carried out with Home Office approval under Project Licence: P99922A2E (Dr Penelope Ottewell) and personal licence (IB24B0AC5) Mr Christopher George.

2.4.2 Modelling menopausal concentrations of oestradiol

On commencement of the experiment, mice were ovariectomised (OVX), to diminish production of ovarian hormones including oestrogen: Mice were placed under the anaesthetic isoflurane and were administered with 120 µg/kg of the analgesic vetergesic (buprenorphine: Vetergesic, CEVA Animal Health) and 10g/kg baytril antibiotic (enrofloxacin: Baytril, Bayer) via subcutaneous injection to minimise pain and chance of infection. The lower back of each mouse was

then shaved using an electric razor and sterilised with iodine before an incision was made into the skin using a sterile scalpel to make a 1cm longitudinal cut through the skin (running along the spine ~0.5cm from below the shoulder blades towards the tail). The skin was then detached from the muscle layer beneath by blunt dissection using blunt ended forceps before the muscle wall was punctured to one side of the spinal cord to access the visceral cavity. The ovaries were then taken out of this hole using blunt ended cat spay forceps and the top of the womb was clamped just below the ovaries, to reduce bleeding, while the ovaries were removed. Following removal of the ovaries on both sides the remaining tissue was replaced into the visceral cavity, the wound was then closed with a simple interrupted suture using polypropylene monofilament suture and a reverse cutting blade. The mice were placed in a 30 °C incubator for recovery and were given a second dose of vetergesic and baytril 24h later to assist recovery and reduce pain.

The mice were split into 3 groups and 2 groups were administered oestradiol via their drinking water. 1 group received 1.375 mg/l (to model peri-menopausal) and 1-group was given 12.5 mg/l (to model premenopausal) concentrations of oestradiol while the third group received no oestradiol to model the postmenopausal state (Figure 2.2). All groups were given a daily 40 µg dose of Goserelin (Sigma-Aldrich, UK) daily via subcutaneous injection to prevent the release of FSH from the pituitary gland, allowing the focus of the experiment to be on oestradiol.

Numbers of animals required to generate statistically significant data were calculated using the following formula:

Z = the z score

E = margin of error

N = the population size

P = the population proportion

Data were based on our extensive previous experience using these in vivo models which show that ~70% of BALB/c mice 4T1 cells and ~80% of C57BL/6 mice injected with E0771 cells via the left cardiac ventricle develop metastasis. Assumptions made were based on a finite population of 20, with confidence levels set at 80% and margin of error set at 10%. Using the above assumptions and preliminary data we calculated that in order to attain data of significant difference:

1. Experiments involving 4T1 cells injected into BALB/c mice will require 10 mice per
2. group.

2. Experiments involving E0771 cells injected into NOS SCID mice will require 9 mice per group.

The mouse numbers used in practice for the project were increased due to lower than expected bone metastasis following intracardiac injection. C57BL/6 mice with E0771 cells had 15 mice per group, while BALBc mice with 4T1 tumours had 12 mice per group.

2.4.3 Intra-cardiac injection of mammary cancer cells

C57BL/6 mice were injected with 100,000 E0771-LUC cancer cells or 50,000 4T1-LUC cells directly into the left ventricle 7 days after OVX: Cells were labelled with the membrane dye DiD at 3µL per million cells and incubated for 10 minutes at 37°C before pelleting cells by centrifugation at 800 x *g* and washing them in PBS 3 times before re-suspending at $1x10^6$ cells/ml (E0771-LUC) or $0.5x10^6$ cells/ml (4T1-LUC) in PBS + 10% FBS. This cell suspension was passed through a 70 µm nylon mesh to prevent cell aggregates then stored on ice prior to injection. Mice were anesthetised with isoflurane/O_2 in an induction chamber, before being placed on a heat pad and being positioned in a straight position with an empty syringe placed behind the back to push up the sternum. A syringe with 27G calibre needle loaded with 100 µL of cell suspension containing 100,000 cells (E0771-LUC)or 50,000 cells (4T1-LUC) was inserted 2mm to the right of the sternum and penetrated to half the length of the needle to reach the left ventricle. The needles' location was confirmed by gentle pull back on the syringe, showing bright red oxygenated blood if the location was correct, before the cells were gently injected. Mice were placed in a 30 °C incubator for recovery and monitored closely over the next 12 hours (Figure 2.2).

After three days, each group of mice (pre- post and peri- menopausal) were divided in half with one half receiving subcutaneous injection of Zol (Novartis) at 100 µg/kg by sub-cutaneous injection and the other half receiving PBS (control) (Figure 2.2). C57BL/6 mice (n=15 per group) and BALBc mice (n=12 per group). Mice were culled 19 days (C57BL/6 with E0771-LUC) or 15 days (BALBc with 4T1-LUC) after OVX by pentobarbital overdose, cervical dislocation and exsanguination. Blood was collected from each mouse from the heart before death. Tibia (fixed in 4 % Paraformaldehyde (PFA) or frozen in FBS + 10% DMSO), femur (frozen in FBS + 10% DMSO or snap frozen), spleen (frozen in FBS + 10% DMSO), lungs (snap frozen or frozen in FBS + 10% DMSO) and liver (snap frozen) were collected post-mortem and imaged by IVIS for tumour burden before storage/downstream analysis. The blood was left at room temperature to clot before being spun at 8000 *g* for 10 minutes to separate serum, which was removed and frozen at -80 °C. A second round of experiments treated mice with 400 µg/kg of Avelumab every two days after cancer injection by intra peritoneal injection.

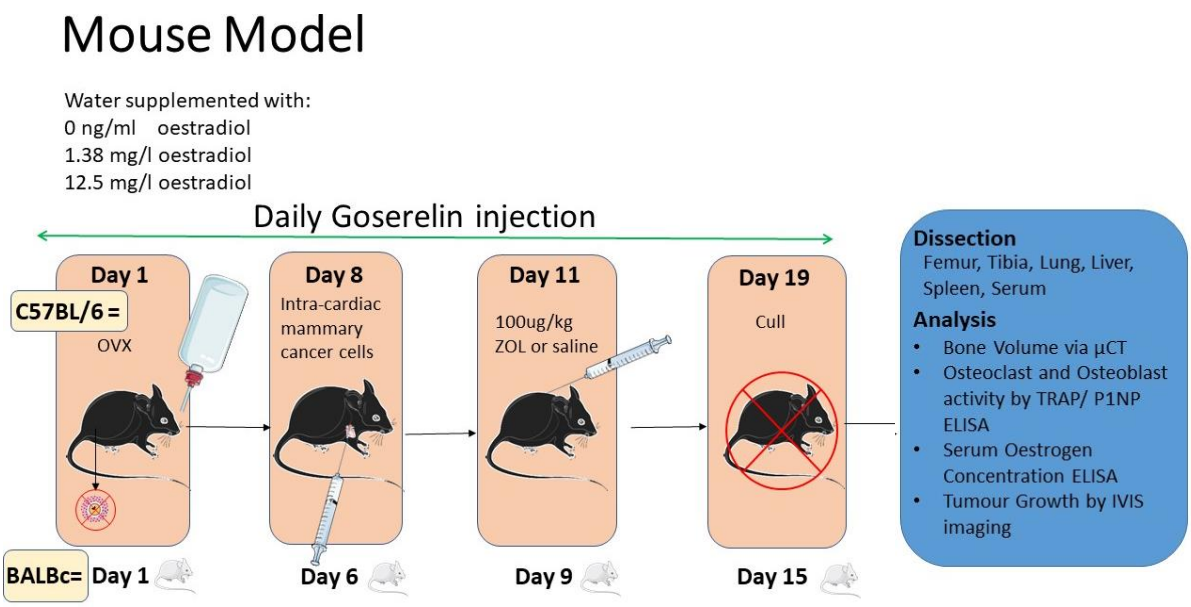

Figure 2.2: Protocol and schedule for in vivo modelling of the effects of oestrogen with or without Zol on C57BL/6 mice(n=15 per group) and BALBc mice (n=12 per group). Menopausal status established by OVX and oestrogen replacement in drinking water. Tumour cells delivered via intracardiac route and Zol administered in one done by subcutaneous injection.

2.4.4 *In vivo* imaging

All cancer cell lines used *in vivo* were transfected with luciferase, an oxidoreductase enzyme that emits a luminescent signal at a wavelength of 562 nm when combined with its consumable substrate luciferin. Luciferin is oxidised by luciferase to an excited state, emitting light as it decays to its ground state. Therefore, mice were injected with luciferin leading to the emission of visible light at the tumour location (Zinn et al, 2008). The emission of the tumours through the metastatic organs was detected by a charged coupled camera, which detects the photons released, using the *in vivo* imaging system (IVIS) LUMINA II (caliper life sciences).

Each treatment group was imaged twice per week following intracardiac injection of tumour cells. Mice were anaesthetised with isofluorane/O_2 before subcutaneous injection of 100 µL of D-Luciferin-Potassium Salt (Luciferin) (30 mg/kg) (Perkin Elmer). The luciferin was left for two minutes to enter circulation before the dorsal followed by the ventral side of the mouse were imaged to determine tumour growth. Visible tumours were measured in photons per second and analysed using the Living Image software 4.1 (Caliper Life Sciences).

2.5 Ex Vivo bone analysis

2.5.1 Microcomputed tomography

Microcomputed tomography (µCT) takes a series of 272 2D X-ray photos, using an X-ray source and a detector, of the bone while it rotates through 180° on a turntable between the source and detector. This series of 2D images is then used to reconstruct a 3D structure of the bone, allowing virtual slices to be taken and the analysis of bone structure. This concept is similar to CT machines used in hospitals, however here the sample moves instead of the camera and the pixel resolution is in the µm range (Boerckel et al, 2014).

Figure 2.3: Representative virtual slice of trabecular bone using Microcomputed tomography imaging. Area in red represents trabecular region of interest analysed.

Tibias were fixed in 4 % PFA for 48 hours and then stored in PBS. The fixed tibias were wrapped in cling film to prevent the bones drying while scanning and maintain stability, before they were scanned at a resolution of 4.3 µm per pixel using a 0.5 mm aluminium filter with the 2016 Camera using a Skyscan 1272 (Bruker, Billerica, Massachusetts, USA). The scans were reconstructed using the NRecon software (Bruker) and then trabecular volume was analysed using the CTan software (Figure 2.3). The region of interest was standardised by setting a 47 pixel offset from end of the growth plate and spongy bone, and analysing a region of trabecular bone 116 pixels deep. Percentage trabecular bone volume to tissue volume was analysed for bones (n=30 for C57BL/6, n=24 for BALBc).

2.5.2 Histology, immunohistochemistry

Bones and lungs were processed for histology. Hard calcified bones need to be decalcified to allow them to be sectioned effectively for histology. Therefore, bones were decalcified in 0.4M of Ethylenediamine tetraacetic acid (EDTA) (Sigma-Aldrich, UK) for 3 weeks, with the EDTA being changed 3 times per week for fresh solution. Lungs and decalcified bones were dehydrated through a series of ethanol baths, displacing the water, which was then replaced with paraffin wax throughout the sample. These samples were then embedded in a block of paraffin wax and bones were specifically positioned with a flat side against the outer portion of the block to allow for effective sectioning through the bone marrow.

Embedded blocks were sectioned using an RM2265 microtome and sliced to 3 µm thick. These slices were placed atop a water bath at 37 °C to float for 20 minutes to allow wrinkles to float out of the samples before being transferred to positively charged slides (Superfrost Plus Slides) and left in a 37 °C dry oven for 24 hours. Following this, sections were ready for staining.

2.5.3 Haematoxylin eosin staining

Haematoxylin Eosin Staining (H&E) is the principal histological stain, staining the nucleus blue and extracellular matrix shades of pink and violet. This stain was used to confirm the presence of disseminated tumour cells in the bone, check bone morphology and confirm the depth of microtome sectioning for further downstream histological analysis.

Sections were first dewaxed through two passages in xylene (Honeywell) before being rehydrated via sequential passaging through decreasing concentrations of ethanol (from 100% - 40%). The sections were then submerged in haematoxylin (Sigma-Aldrich, UK) for 2 minutes followed by a wash in tap water to remove excess haematoxylin stain. Sections were then incubated in eosin (Sigma-Aldrich, UK) for 5 minutes before a further wash in tap water. The sections were then dehydrated through increasing concentrations of ethanol, followed by xylene before being mounted using the DPX mounting medium (MERCK).

2.5.5 Immunohistochemistry

The bone and lung sections on the slides were also stained using the immunohistochemical technique to target specific proteins in the sample (n=3-5). The samples were first dewaxed in xylene before being rehydrated through sequential alcohol concentrations of 100%, 90%, 70% and finishing in water. Following rehydration, slides were incubated in 3% hydrogen peroxide solution (H2O2) (Merck) in methanol for 10 minutes to block endogenous peroxidases before antigen retrieval was performed. Antigen retrieval methodology differed depending on the antigen of interest, summarised in Table 2.1. The slides were then blocked using 1x casein (Sigma-Aldrich UK) in PBS with 0.1% Tween (Sigma-Aldrich UK) for 30 minutes at room temperature prior to incubation with the primary antibody against the antigen of interest diluted into 1x casein in PBS with 0.1% Tween (Table 2.1). Slides were then washed in PBS+0.1% Tween for 5 minutes on an orbital shaker 3 times before incubation with a secondary biotin conjugated antibody for 30 minutes in 1x casein in PBS with 0.1% Tween. Following another washing step, the staining was then amplified using the ABC kit (Vector), containing avidin

and biotin, and incubated for 30 minutes. The slides were developed using the DAB peroxidase substrate kit (Vector) which was added to the slides for 2-10 minutes (depending on the control) until the brown colour appears before being washed thoroughly in water. Following this, slides were counterstained in Gill's haemotoxylin before being dehydrated through ethanol and mounted using DPX mounting medium.

Antigen	Antigen Retrieval	Primary Ab conc.	Secondary Ab conc.
F480	Proteinase K	Bio-Rad (MCA497G)	1:500 Anti-Mouse Jackson (115-066-003)
CD163	70°C Tris Base 1 hour	1:200 Abcam (ab182422)	1:500 Anti-Rabbit
Ly6G	70°C Citrate Buffer 1 hour	1:200 BioLegend (Cat127602)	1:500 Anti Rat Jackson (112-066-003)
Granzyme B	70°C Citrate Buffer 1 hour	1:100 Abcam (ab4059)	1:500 Anti-Rabbit

Table 2.1: IHC protocol information showing antigen retrieval method, primary antibody concentration and make and secondary antibody concentration and make for the antigens F480, CD163, L6G and Granzyme B.

The staining was quantified using the QuPath software. The tumours within the bone and lung were isolated as the region of interest using the selection tool within the program, then the automatic positive cell detection was used, with a standard threshold set between 0.1 and 0.2 depending on the intensity of the staining and the background present. The output of the analysis was the percentage of positive cells compared to all cells in the specified tumour area for the desired marker. IHC staining was performed on two levels per organ, taking the average percentage positive cells per organ.

2.6 Immune cell population determination by flow cytometry

2.6.1 Sample preparation

Organs used were the spleen, the lung and the bone marrow. Following dissection, lungs and spleen were slowly frozen down in FBS with 10% DMSO and stored at -80°C until needed for flowcytometry (n=3-5).

2.6.2 Bone marrow

Following dissection, femur heads were chopped off before placing femurs in a 0.5 ml PCR tube with the bottom removed and spinning this in a centrifuge at 6000 *g* for 5 minutes to remove bone marrow. This marrow was slowly frozen down in FBS with 10% DMSO and stored at -80°C until needed for flowcytometry.

2.6.3 Spleens

Spleens were defrosted quickly in a 37°C water bath before being washed twice in PBS to remove any leftover DMSO in the organ. The organs were then finely chopped using a scalpel before being dissociated in 5µl of Liberase stock (Roche) (Stock= 2mg/ml) and diluting into 995µl RPMI. The dissociation solution was left in a 37°C incubator for 45 minutes with a vortex step every 15 minutes to dissociate tissue to a single cell suspension. Following incubation, the remaining spleen tissue was passed through a 100µm cell strainer using the flat end of a 5ml syringe before being diluted with a further 1ml of RPMI and having 10% FBS added to neutralise the Liberase solution.

2.6.4 Lung dissociation

Lungs were defrosted quickly in a 37°C water bath before being washed twice in PBS to remove any leftover DMSO in the organ. The organs were then finely chopped using a scalpel before being dissociated in Colaginase (0.2mg/ml) (Gibco) & Dispase (2mg/ml) (Gibco) diluted in PBS. The dissociation solution was left in a 37°C incubator for 45 minutes with a vortex step every 15 minutes to dissociate tissue to a single cell suspension. Following incubation, the remaining lung tissue was passed through a 100µm cell strainer using the flat end of a 5ml syringe before being diluted with a further 5ml of PBS and having 10% FBS added to neutralise the enzymes.

2.6.5 Staining

48 h before performing flow cytometry, all antibodies used were aliquoted into the necessary labelled tubes for samples and controls before they were stored at 4°C overnight. The controls used were single stained cells, single stained beads (AbC & ArC compensation beads, Invitrogen) and fluorescence minus one (FMO) containing all antibodies except one. Two panels were run back-to-back on the same samples, a myeloid panel and a lymphoid panel. The antibodies used were all diluted 1:100:

- **Myeloid Panel**: Zombie UV viability Dye (Cat:423107), CD45 (Clone:30-F11), MHCII (Clone: M5/114.1115.2)), CD11b (Clone:M1/70), Ly6G (Clone:1A8), Ly6C (Clone:HK1.4), F4/80 (VBM8), MRC1 (Clone:C068C2), CD11c (Clone:N418)
- **Lymphoid Panel**: Zombie UV viability Dye (Cat:423107), CD45 (Clone:30-F11), CD3 (Clone: 145-2C11), CD4 (Clone:GK1.5), CD8 (Clone:53-6.7), CD19 (Clone:6D5), NK1.1 (Clone:PK136), PD-1 (Clone:J43).

Following dissociation or defrosting, the bone marrow, lung or spleen cell suspensions were then centrifuged at 3400*g* for 5 minutes and the cell pellet was resuspended in 400µL of PBS+ 1% FBS twice as a washing step. A master mix of samples was created with cells from every sample, of which 100µL was pipetted into the control antibody solutions. 100µL of each unmixed sample was also pipetted into the complete sample antibody mixes and all samples were left to incubate on ice, in the dark for 45 minutes with one flick mix after 25 minutes of incubation. 1 ml of PBS was then added to each sample before centrifuging at 3400*g* for 5 minutes to pellet cells. The stained pellet was resuspended and fixed in 1% PFA (Fisher Scientific) diluted in PBS and stored overnight at 4°C in the dark.

2.6.6 Flow cytometry

Flow cytometric analysis was performed on an LSRII (BD) machine using the FACsDIVA software for capture. Flow cytometry utilises a combination of microfluidics, laser diffraction and fluorescence to effectively characterise a population of cells. Cells in a single cell suspension are taken into the machine by the fluidics and organised into a single cell line. The fluidics manipulate the cells to fall through a series of lasers one at a time to determine the cell size and the immunofluorescent staining of each sample. Filters are used to allow individual analysis of the wavelengths of emission to quantify proportional protein expression.

Stained compensation beads were used to set compensation thresholds for overlapping fluorescent signals before controls were run through. 100,000 viable cells, gated by the unstained zombie UV dye population, from samples and controls were recorded during capture. Analysis was performed using the FlowJo software (v10.6.2) and the gating strategy is outlined in Figures 2.4 & 2.5 and Supplementary Figures F, G, H, I.

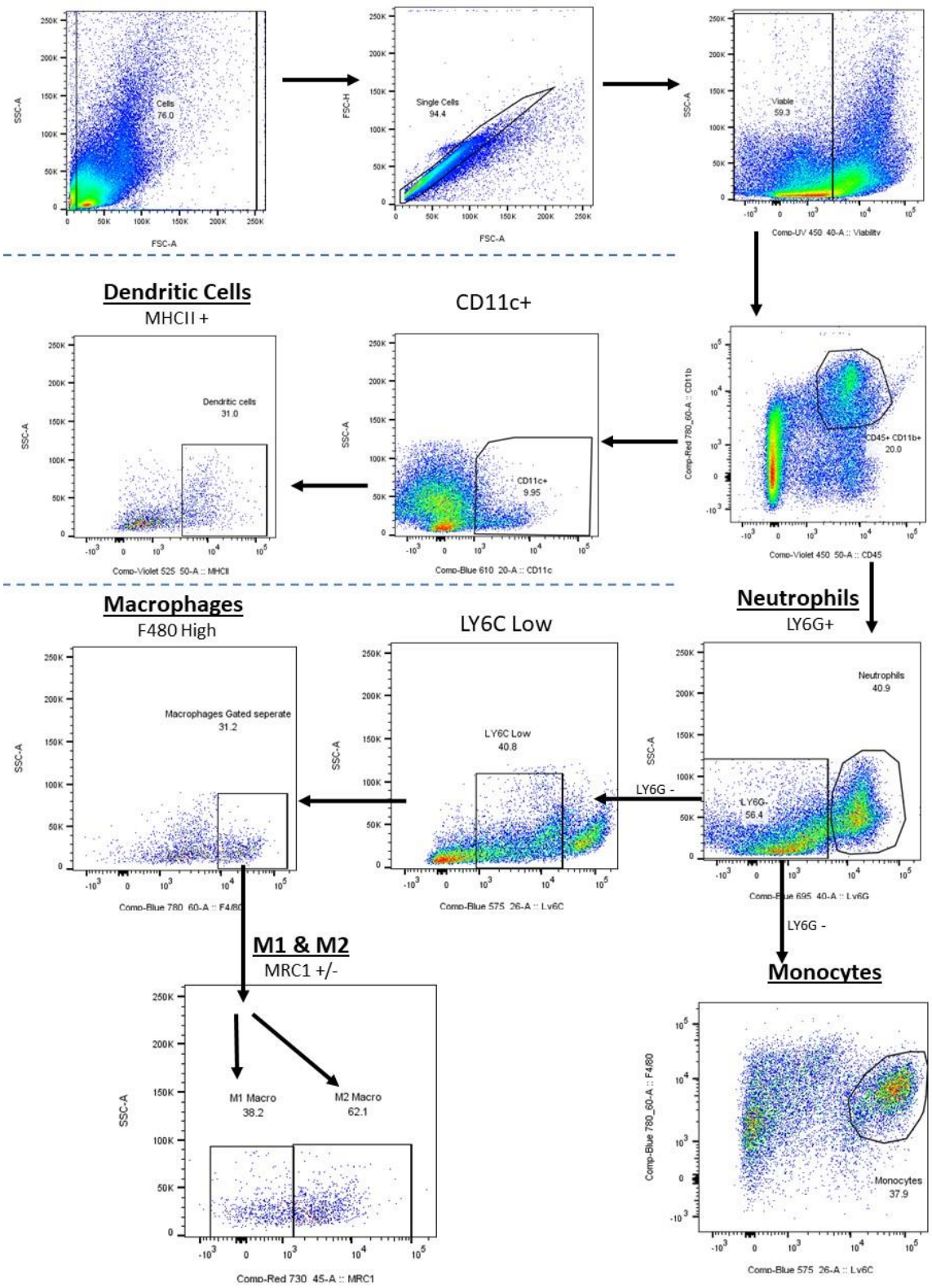

Figure 2.4: Flow cytometry myeloid panel gating strategy for Bone Marrow.

Dendritic cells (CD45+,CD11b+,CD11c+,MHCII+), Neutrophils (CD45+,CD11b+,Ly6G+), Monocytes (CD45+,CD11b+,LY6G-,LY6C+,F480) High, Macrophages (CD45+,CD11b+,LY6G-,LY6C Low, F480 High), M1 Macrophages (Macrophage, MRC1-), M2 Macrophages (Macrophage, MRC1+)

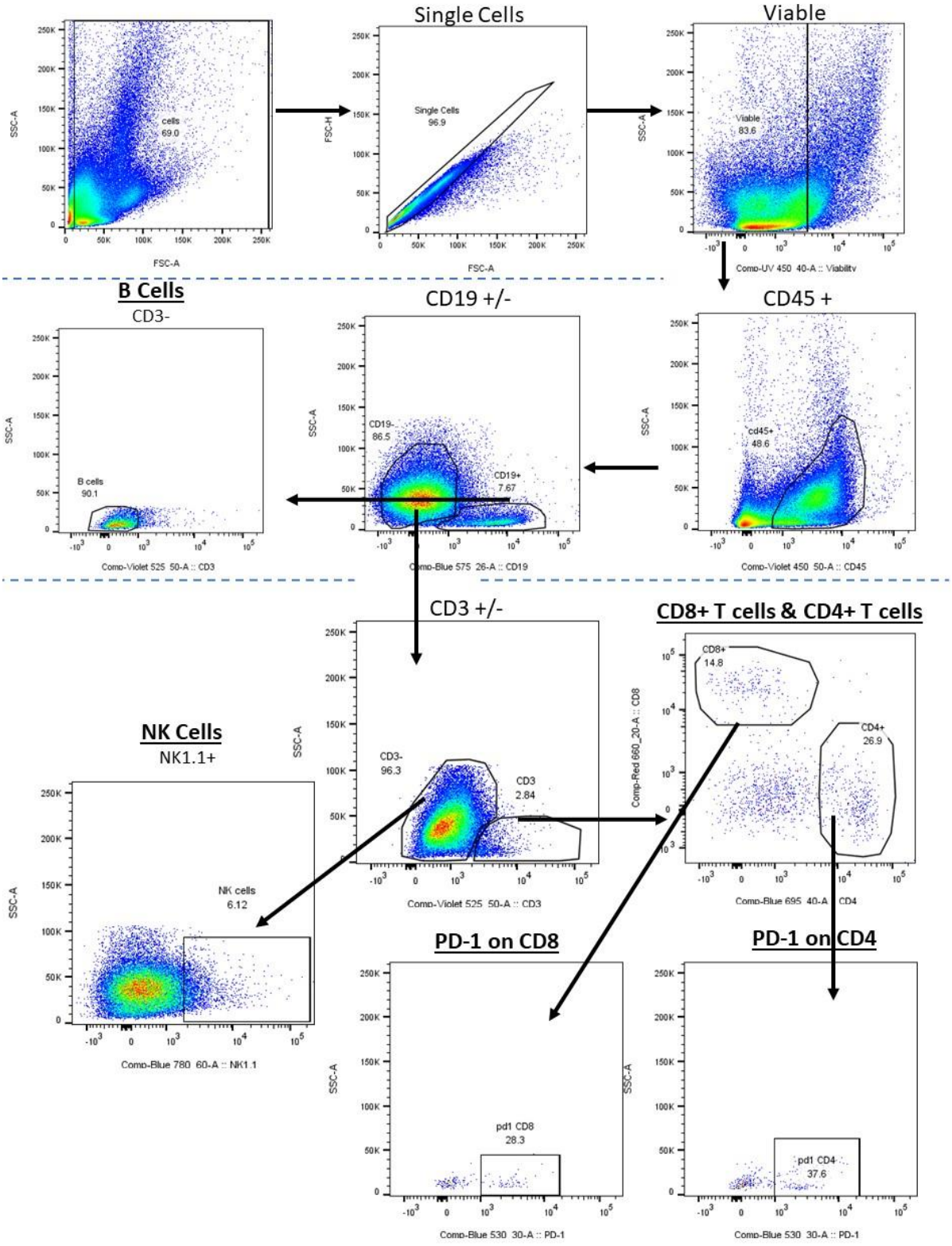

Figure 2.5: Flow cytometry lymphoid panel gating strategy for Bone Marrow.

CD4+ T cells (CD45+,CD19-,CD3+,CD4+), B Cells (CD45+,CD19+,CD3-), CD8+ T cells (CD45+,CD19-, CD3+,CD8+), PD-1 on CD4+ T cells (CD4 T cells, PD-1+), PD-1 on CD8+ T cells (CD8 T cells, PD-1+), NK cells (CD45+,CD19-,CD3-, NK1.1+)

2.7 Immune population gene expression

2.7.1 Nanostring analysis

Flash frozen bones and lungs from BALBc mice containing metastasised 4T1-LUC tumours were lysed and RNA was extracted using the Tri Reagent (Sigma-Aldrich, UK) protocol (n=3). Organs were homogenised in a bead mill (Fisher Brand version 4) with 1ml Tri Reagent for 1 minute before being placed on ice. 200 µl of chloroform was added to homogenised tissue and shaken for 1 minute before centrifugation at 16,000 *g* for 20 minutes to separate out protein from nucleic acids. The top layer was carefully transferred to a separate 1.5ml tube before 500 µL of isopropanol was added to solution to precipitate RNA out of solution. The precipitate was pelleted by centrifugation at 16,000 *g* for 20 minutes before the pellet was washed using 75% ice cold ethanol. The pellet was resuspended in nuclease-free microbiology water and stored at -80°C until needed.

Nanostring analysis was performed by collaborators Prof. Graham Pockley and Dr Jayakumar Vadakekolathu at Nottingham Trent university using the NanoString nCounter™ panCancer Immune profiling panel (NanoString Technologies). 150 ng of RNA was used for analysis in accordance with manufacturer recommendations and analysis was performed using the nSolverTM 4.0 and Advanced Analysis 2.0. Cell type analysis and statistical analysis was performed by Dr. Lewis Quale. Determination of cell types was performed in R, gene expression was mean-centred for all samples before calculation of the raw cell-type signature scores as the average of Log2 expression intensities for genes in each cell type signature. The gene signatures determining each cell type were taken with reference from the Nanostring document LBL-10043-08 (nCounter PanCancer Immune Profiling Panel Gene List.xlsx).

2.7.2 qPCR array cards

RNA was extracted from flash frozen tumour bearing bones and lungs of C57BL/6 mice by the method described above (Section 2.7.1) (n=3). Following RNA isolation, reverse transcription was performed using the Superscript III (Invitrogen) kit and protocol described in section 2.3.2.

To run the qPCR Taqman Low Density Array card (Production number: 000004113924), cDNA was combined with TaqMan Fast Advanced Master Mix (Applied Biosystems) (ref:4444557). cDNA, molecular water and 2x Master Mix were combined to a final cDNA concentration of 3 ng/µl in 110 µl final volume. 100 µl of this was loaded into the card reservoir which was centrifuged for 1 minute at 331*g* a total of two times to enable microfluidic loading of the card from the reservoirs. The card was

then run on a QuantStudio 7 qPCR thermocycler (ThermoFisher). Analysis and statistics were performed by Dr. Lewis Quale. Statistics performed were t-tests (adjusted for multiple testing using FDR method) where there were two groups in a comparison and ANOVA followed by Tukey's post-hoc test where there were more than two groups. Cell-type scores were computed by taking the geometric mean (take log of values, calculate mean, exponentiate result) and cell types were determined using the following gene markers classifications:

B Cells: *Blk, Cd19, Ms4a1, Tnfrsf17,* **CD8 T cells**: *Cd8a, Cd8b1*, **Cytotoxic cells**: *Ctsw, Gzma, Gzmb, Klrb1, ,Klrd1, Klrk1, Prf1,* **Dendritic Cells**: *Ccl2, Cd209e, Hsd11b1*, **Exhausted CD8**: *Cd244, Eomes, Lag3,* **Macrophages**: *Cd163, Cd68, Cd84*, **Mast cells**: *Ms4a2*, **Neutrophils**: *Csf3r, Fcgr4,* **NK cells**: *Il21r, Ncr1, Xcl1,* **T cells**: *Cd3d, Cd3e, Cd3g, Cd6, Sh2d1a*, **TH1**: *Tbx21*, **Treg**: *Foxp3, CD25,* **CD4 T cells**: *CD4*

2.8 Ex Vivo biochemical assays

2.8.1 Human oestrogen ELISA

To detect circulating concentrations of oestradiol in the mouse models, the oestradiol enzyme-linked immunosorbent assay (ELISA) (Calbiotech) was utilised in accordance with the manufacturer's instructions. 25 µL of the standards and samples (n=10-12) were added to each streptavidin coated well in duplicate followed by 50 µL of oestradiol biotin reagent containing the oestradiol antibody. The plate was incubated at room temperature for 45 minutes before 100 µL of enzyme reagent was added to each well and incubated for a further 45 minutes at room temperature whereby a fixed amount of HRP conjugated oestrogen and the samples endogenous oestrogen competes for Ab binding. The wells were then washed 3 times using 300 µL of the washing buffer provided before the TMB reagent was added to the wells to develop a blue colour, a process which was stopped after 20 minutes using the stop solution. The absorbance of the plate was read at 450 nm on a SpectraMax M5 (Molecular Devices) plate reader.

2.8.2 P1NP ELISA

Procollagen type 1 N-terminal propeptide (P1NP) is a marker of osteoblast activity and therefore a marker of bone deposition. Organic bone matrix consists mainly of type 1 collagen which is synthesised in the bone from procollagen (Gelse et al, 2003). During bone catabolism, procollagen is cleaved by proteases from the osteoblast removing the *N* and *C* terminal peptides prior to collagen

assembly into fibres (Gelse et al, 2003). P1NP is the *N* terminal peptide which is released into circulation and the majority of it is up taken by the liver (Melkko et al, 1994). Therefore, serum P1NP acts as a biomarker for bone remodelling, allowing simple quantification of the bone microenvironment status using commercially available immunoassay kits (Koivula et al, 2010).

The ELISA kit used was the rat/mouse P1NP enzyme immunoassay (Immunodiagnostic Systems Limited) which was used according to the manufactures instructions. 50 µL of sample (n=10-12) or standard was added to each well of the polyclonal rabbit anti P1NP coated plate along with biotin as the amplification method before a 1 hour incubation at room temperature. Following this, the wells were washed 3 times using the kit wash buffer before HRP conjugated avidin was added and left to incubate for 30 minutes to bind the biotin/ antibody complex. Excess HRP avidin was washed off with three washes after 30 minutes and the enzyme chromogenic substrate (TMB) was added, left to develop for 30 minutes before the reaction was stopped by the addition of hydrochloric acid. The absorbance of the wells was read using a SmectraMax 5Me plate reader at the wavelength 450 nm and results interpreted from the calibration curve.

2.8.3 TRAcP 5b ELISA

The tartrate-resistant acid phosphatase 5b (TRAP) enzyme is secreted by osteoclasts, dendritic cells, macrophages and a number of other cell types in a variety of organs. Of the two main forms of TRAP, the subtype TRACP 5b is predominantly derived from osteoclasts and can be used as a serum biomarker for osteoclast activity and bone resorption since it is released into the blood stream before being degraded into fragments and removed from blood.

The Mouse TRAP ELISA (Immunodiagnostic System Limited) was used for all experiments following the manufacturer's instructions. The polyclonal Ab against TRACP 5b was added to an anti-rabbit IgG coated 96 well plate and incubated for 60 mins before 100 µL of standard, control and diluted sample (n=10) (25 µL of sample in 75 µL of NaCl) was added to each well. Following a 60 min incubation, the chromogenic substrate was added to each well to develop before sodium hydroxide was used to stop the enzymatic reaction. The final absorbance of the wells was determined using the SmectraMax 5Me plate reader at the wavelength 405 nM.

2.9 Statistics

All values presented represent mean +/- SEM. Statistical analyses were performed using the ANOVA test followed by Tukey's post-hoc test and unpaired student t test using the GraphPad prism 7 software as indicated on individual figures. P values are presented as ** < 0.05, ** < 0.01, *** < 0.001, ****<0.0001.*

Chapter 3: Modelling the effect of Zol treatment under post-, peri-, and pre-menopausal concentrations of oestradiol on breast cancer metastasis

3.1 Introduction

In the AZURE trial and ABCSG12 trial, Zol was shown to be effective at preventing bone metastasis while reducing disease free survival, however the AZURE trial showed that only the post-menopausal cohort of women benefit, with patients with pre-menopausal concentrations of oestradiol having reduced iDFS and increased soft tissue metastasis (Coleman et al., 2018a). The post-menopausal phenotype is characterised by low levels of circulating oestradiol, a decline in inhibin B concentrations alongside increased FSH secretion (Su and Freeman, 2009). A retrospective analysis of patient serum from the AZURE trial showed that oestradiol concentrations of >50 pM/L correlated with improved iDFS following adjuvant Zol. This, along with the strong immunogenic nature of oestradiol and its crucial role in bone homeostasis, led to the hypothesis that this hormone drives differential anti-tumour effects following Zol. Indeed, oestradiol and Zol interact with a plethora of cells around the body and in the tumour microenvironment, including a wide array of immune cells, bone resident cells such as osteoblasts and osteoclasts, and tumour cells themselves depending on ER status (George et al., 2020). Therefore, studying the effects of these two drugs on cancer progression required a whole-body organism.

The menopause has profound effects on bone volume as it progresses, due to oestradiol driven processes. The bone is constantly remodelled to maintain healthy bone mineral density by a balanced process of bone resorption and bone formation. The process of this remodelling is regulated by a number of hormones, including PTH, vitamin D3, calcitonin and oestradiol (Siddiqui and Partridge, 2016). Oestradiol affects bone turnover in a number of ways, including: lowering PTH sensitivity, increasing calcium absorption in the intestine, increasing calcitonin production, and acting directly on osteoclasts to decrease their activity and promote apoptosis (Bhattarai et al., 2020). Therefore, oestradiol deficiency during the menopause disrupts this normal bone turnover favouring increased osteoclast activity and decreased osteoblast activity leading to a reduction in bone volume and bone mineral density (Lerner, 2006). This loss is predominantly in the trabecular bone volume during the first 4-8 years of menopause and is directly related to oestradiol loss.

Mouse models of breast cancer bone metastasis are an invaluable tool to assess the efficacy of new treatments and to effectively model and recreate clinical conditions in a controlled environment. The use of animal models in my project allowed the analysis of the complex immune oncology interactions across different metastatic sites, the sights of tumour dissemination and the expression changes happening at multiple metastatic locations. Specifically, the conditions modelled were human menopausal oestradiol concentrations, disseminated breast cancer cells and zoledronic acid treatment.

Menopausal concentrations of oestradiol can be modelled via a number of different techniques and normally involve removing the mouses ability to produce ovarian hormones before administering hormone replacement to control systemic levels. Unlike humans, mice have an oestrous cycle rather than a menstrual cycle that occurs every four to five days, however the hormone fluctuations present in this cycle are similar to the human menstrual cycle (Caligioni, 2009). Furthermore, mice do not undergo menopause in the same way as humans do, instead experiencing irregular oestrus cycles around the age of 9-12 months. The main difference between mice and humans is the presence of mature ovulatory follicles in aged mice which is not present in humans where complete ovarian failure is the main hallmark. The gold standard for evaluating the effects of gonadal hormones is OVX, which is the bilateral surgical removal of the ovaries. Following OVX, recovery usually occurs within one week and leaves a blank slate of gonadal hormones in mice, allowing administration of oestradiol or other ovarian hormones as needed for the study.

Serum oestradiol concentrations can be restored in mice to human levels by oestradiol administration. Oestradiol levels can be modelled using an oestradiol silastic implant that is surgically implanted subcutaneously and restores oestradiol levels. Studies have shown that these implants can restore oestradiol levels to stable serum levels within two weeks (Mosquera et al., 2015). However, the implants have been shown to interfere with tumour metastasis and unpublished observations from our group show tumour cells metastasising to the site of implant (Holen et al., 2016). Because of the issues with oestradiol pellets I modeled human concentrations of oestradiol in mice by adding this back via the drinking water of mice, a technique that was used in our group on a mouse model in the absence of tumour cells first (Canuas-Landero et al., 2021). Replacement in drinking water is a non-invasive technique that successfully models serum oestradiol to menopausal levels.

Zol is a third-generation nitrogen containing bisphosphonate that is used for the treatment of osteoporosis, Paget's disease and metastatic and osteolytic bone disease (Russell and Rogers, 1999). Zol rapidly targets the bone at sites of exposed hydroxyapatite, here it exerts cytotoxic effects on osteoclasts. Like the other nitrogen containing bisphosphonates, Zol is a potent inhibitor of the mevalonate pathway by inhibiting FFP and GGPP, therefore reducing prenylation of small GTPases Ras, RHO and RAC which are important for osteoclast function (Figure 1.4) (Luckman et al., 1998). This classical mechanism of Zol action leads to reduced osteoclast activity and osteoclast cell death, therefore preventing bone loss associated with osteoporosis and bone metastasis. However, since the mevalonate pathway is ubiquitous throughout the body, Zol has been suggested to have action on a number of cells, including immune cells, tumour cells themselves and other bone resident cells (George et al., 2020). Understanding the wider role of Zol in the context of treating breast cancer

metastasis first requires a robust model of breast cancer metastasis, menopausal status and Zol treatment, which is the main objective of this chapter.

3.1.2 Hypothesis

Delivering pre- peri- and post-menopausal concentrations of oestradiol to ovariectomised mice in the drinking water will mimic human menopausal concentrations of oestradiol, stimulate osteoclast induced bone loss and provide a suitable model for determining the effects of oestradiol on the anti-tumour properties of Zol in breast cancer metastasis.

Aims

The overall aim of this chapter is to create a mouse model that mimics pre- peri- and post-menopausal concentrations of oestradiol found in humans and use this to determine the effects of oestradiol +/- Zol on tumour growth in bone and soft tissue. Specifically, I will:

1. Determine the effects of supplementing oestradiol in the drinking water of OVX mice on circulating concentrations of oestradiol, bone volume and osteoclast/osteoblast number and activity in the presence/absence of Zol.
2. Establish the effects of pre- peri- and post- menopausal concentrations of oestradiol +/- Zol on metastatic outgrowth of breast cancer cells in soft tissue and bone.

3.2 Results

3.2.1 Effect of ovariectomy and Zol treatment on serum oestradiol levels in BALBc and C57BL/6 mice.

To model the differential effects of Zol under high and low oestradiol conditions seen in the AZURE trial, I first established immune competent mouse models (Figure 3.1) to allow downstream analysis of immune regulation (see chapter 5). Two immunocompetent mouse models and murine breast cancer cell lines were used: C57BL/6 mice with E0771-LUC cells (n=15 per group) and BALBc mice with 4T1-LUC cells (n=12per group). Since mice have low circulating oestradiol concentrations when compared to humans and do not undergo menopause, 10-12 week old female C57BL/6 mice or BALBc mice were ovariectomised to mimic menopause. Oestradiol was then replaced via drinking water at concentrations of 0 mg/l, 1.375 mg/l and 12.5mg/l, to mimic post, peri and pre-menopausal human concentrations of this hormone, while daily goserelin injection was administered. This allowed me to focus specifically on the effects of oestradiol on the pharmacological effects of Zol without the influence of the steroid hormone FSH. Mice were subsequently randomised to receive PBS (control) or a single dose of Zol 11 days after ovariectomy (Figure 2.2). 5 days (BALBc) or 7 days (C57BL/6) following OVX, mice were injected with 50,000 4T1-LUC or 100,000 E0771-LUC cells via intra cardiac injection (Figure 3.1).

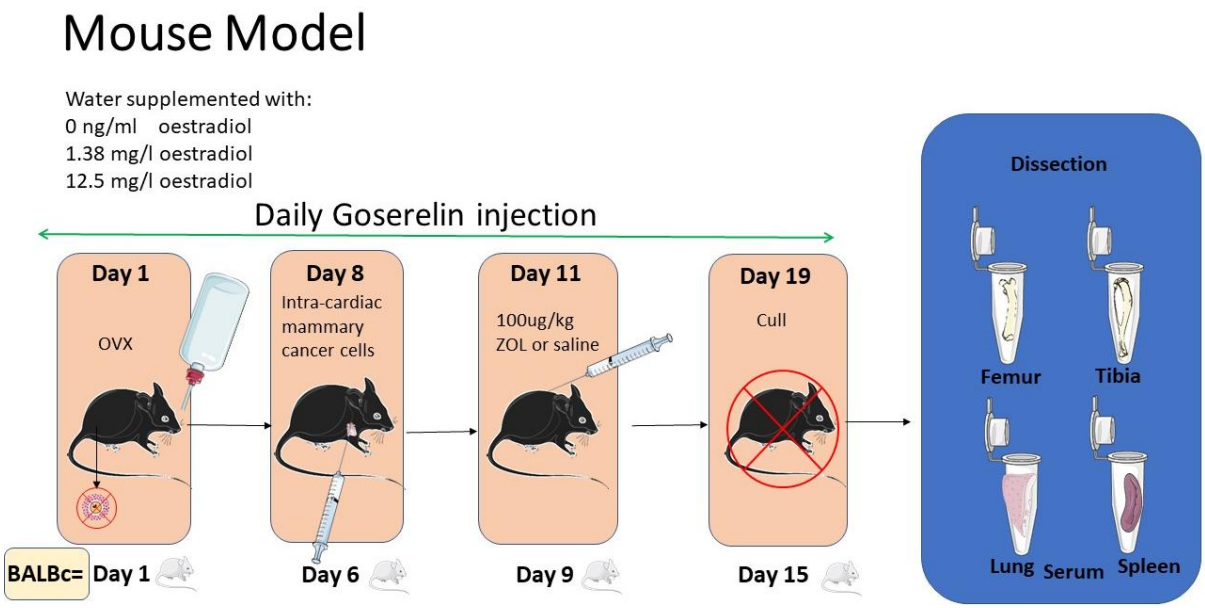

Figure 3.1: In vivo mouse model method for C57BL/6 and BALBc mice

Mice underwent OVX and oestradiol was replaced via drinking water to recreate post, peri and pre-menopausal serum levels. Mice were treated with daily goserelin following OVX. E0771-LUC (100,000 cells) or 4T1-LUC (50,000 cells) murine breast cancer cells were administered via intra cardiac injection before treatment with 100µg/kg of Zol. Mice were culled at day 15 (BALBc) or 19 (C57BL/6) before collection of organs and serum for downstream analysis.

To assess the effect of oestradiol replacement on accuracy to mimic human menopausal concentrations of this hormone, serum oestradiol levels were quantified after 19 days and were found to be comparable to those found in pre-, peri- and post-menopausal women, which normally range from 200-500 pg/ml in the pre-ovulatory phase in pre-menopausal women, and are typically around 20 pg/ml in post-menopausal women (Rodger, 2005). The resulting levels of oestradiol in Zol untreated mice were 59, 144 and 400 pg/ml in the post-, peri- and pre-menopausal groups respectively (Figure 3.2). Zol treated mice had oestradiol levels at 16, 278 and 391 pg/ml in the post-, peri-, and pre-menopausal groups respectively (Figure 3.2). There was a significant difference between the pre- and post-menopausal groups in both Zol treated (P= 0.0109) and untreated mice (P= 0.0029) (n=20) (Figure 3.2). Furthermore, in untreated mice, there was a significant increase in oestradiol concentrations in mice with pre-menopausal serum oestradiol concentrations when compared to peri-menopausal oestradiol concentrations (p=0.0374). There was no significant difference observed between peri-menopausal oestradiol levels compared to pre and post in Zol treated mice. Interestingly, under post-menopausal concentrations of oestradiol, Zol leads to a trend towards reduced serum oestradiol concentrations, however this result was not significant. This data shows that menopausal groups in tumour bearing mice have been modelled effectively.

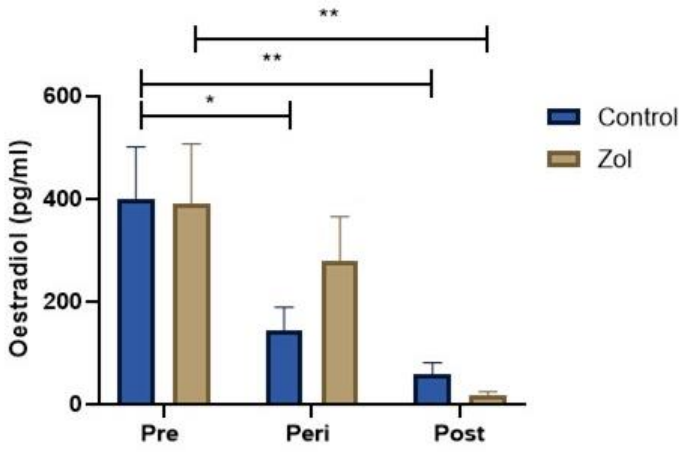

Figure 3.2: Serum oestradiol concentration following ovariectomy and oestradiol replacement.

Serum oestradiol in ovariectomised C57BL/6 mice (n= 10 per group) taken at experimental endpoint. Mice supplemented with post peri and pre menopausal concentrations of oestradiol and treated with 100 µg/kg Zol or saline. Oestradiol measured in serum by ELISA.

Mean ± SEM Statistical analysis by one way ANOVA

*< 0.05, ** < 0.01, *** < 0.001, **** < 0.0001

3.2.2 Effect of Zol on bone microenvironment under post-, peri- and pre-menopausal concentrations of oestradiol in tumour bearing mice

The bone is a dynamic tissue, constantly undergoing remodelling with degradation of old worn-out tissue by osteoclasts and deposition of new bone matrix by osteoblasts (Raggatt and Partridge, 2010). These cells are sensitive to subtle physiological changes leading to an imbalance in the osteoblast, osteoclast ratio, therefore changing the physiological and mechanical structure of the bone. During the menopause, there is a transition towards an osteoclastic bone phenotype, whereby the decrease in circulating oestradiol and the increase in FSH leads to osteoclast survival and stimulation, causing a decrease in bone volume (Manolagas, 2000). The bone microenvironment is favourable for breast cancer metastasis due to high turnover and the release of bone embedded

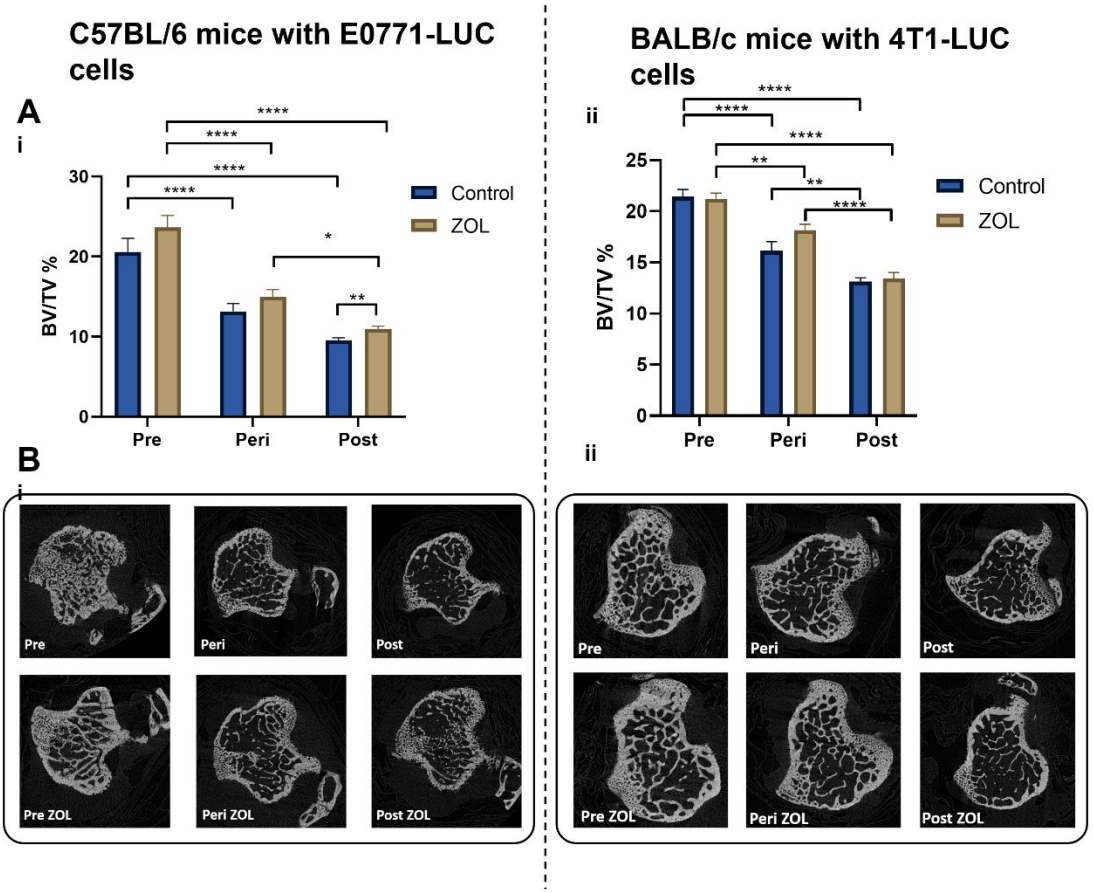

Figure 3.3: Effect of Zol and oestradiol on bone morphology

(A) Tibiae from C57BL/6 with E0771 tumours (i) and BALB/c mice with 4T1-LUC tumours(ii) treated with 100 µg/kg Zol or saline in combination with post, peri and pre-menopausal concentrations of oestradiol. Percentage trabecular bone volume/tissue volume (BV/TV%) determined by µCT analysis after experimental endpoint.

(B) Representative cross-sectional images from C57BL/6 (n=30 per group) (i) and BALB/c (n=12 per group) (ii) mouse tibia

Statistical analysis by one way ANOVA and Tukeys post hock analysis and Students T test. N= 10 per group

*< 0.05, ** < 0.01, *** < 0.001, **** < 0.0001

growth factors, stimulating growth and survival and in turn increasing bone turnover (Roodman, 2004). Zol can disrupt this process and protect the bone by inducing osteoclast apoptosis (Luckman et al., 1998) and downregulating RANK signalling (Kimachi et al., 2011) in the bone to decrease osteoclast mediated bone resorption. Therefore, the bone microenvironment was characterised in mouse models with post-, peri- and pre-menopausal concentrations of oestradiol in the absence and presence of Zol to determine whether oestradiol affected the ability of Zol to exert its bone anabolic effects through inhibiting osteoclastic bone resorption.

3.3 Trabecular bone structure

3.3.1 C57BL/6 mice exposed to pre- peri- or post-menopausal concentrations of oestradiol +/- Zol

Both tibia from each mouse were scanned using µCT to analyse the bone architecture (Figure 3.3) and the percent volume of the trabecular bone fraction (BV/TV%) was calculated (n=30 per group). The mice in the pre-menopausal group had significantly higher trabecular bone volume (BV) when compared to mice with peri-menopausal and post-menopausal concentrations of oestradiol ($p<0.0001$ and $p<0.0001$ respectively) in Zol untreated groups (Figure 3.3 Ai). This suggests that oestradiol administration is effective at modelling pre, peri and post-menopausal concentrations of oestradiol in tumour bearing mice. In the subgroups treated with Zol, pre-menopausal mice also had significantly higher BV than peri-menopausal and post-menopausal mice ($p<0.0001$ and $p<0.0001$ respectively) and peri-menopausal mice had higher BV than post-menopausal mice ($p=0.0281$) (Figure 3.3 Ai). There was a significant corelation between oestradiol concentration and trabecular bone volume ($p=0.0001$) (figure not shown). Interestingly, in mice with post-menopausal concentrations of oestradiol, Zol significantly increased BV ($p=0.0034$), but did not restore it to pre-menopausal levels. However, at other concentrations of oestradiol, trabecular BV followed a similar incremental increase in both Zol treated and untreated groups (Figure 3.3 Ai). This provides evidence that oestradiol replacement in mice was able to model menopausal conditions seen in the bone. Furthermore, Zol has more profound effects on bone in the post-menopausal groups.

3.3.2 BALBc mice exposed to pre- peri- and post-menopausal concentrations of oestradiol +/- Zol

One tibia from each BALBc mouse was scanned by µCT to analyse bone morphology via a second *in vivo* model (n=12 per group). Mice in the pre-menopausal group without Zol had significantly higher bone volume than mice with peri and post-menopausal concentrations of oestradiol ($p<0.0001$

for both), and mice with peri-menopausal concentrations of oestradiol had significantly higher BV than those with post-menopausal concentrations of this hormone (p=0.0044) (Figure 3.3 Aii). In the Zol treated group, the pre-menopausal group also had a significantly higher BV when compared to peri and post-menopausal Zol treated mice (p=0.0021 and p<0.0001 respectively) (Figure 3.3 Aii). Furthermore, peri-menopausal Zol treated mice had significantly higher BV than Post-menopausal Zol treated mice (P<0.0001). This data shows that each oestradiol concentration representing the different stages of the human menopause modelled via oestradiol supplementation in the drinking water was significantly different to each other leading to clear and distinct groups. Unlike in C57BL/6 mice, Zol had no significant effect on trabecular bone volume under any menopausal condition, showing only a trend towards increase with Zol in the peri-menopausal group (p=0.073) (Figure 3.3 Aii). These data show that oestradiol has similar effects on bone volume in C57BL/6 mice and BALBc mice, with increased bone volume being associated with high concentrations of oestradiol, mimicking changes in bone volume observed in women at different stages of the menopause. Interestingly, Zol appeared to be more physiologically active in C57BL/6 mice compared with BALBc mice with significantly increased bone volume observed under post-menopausal concentrations of oestradiol suggesting that differences in the bone microenvironment between the two mouse strains may affect the anti-resorptive properties of this drug especially under low oestradiol conditions.

3.4 Osteoclast activity via TRAcP-5b

3.4.1 C57BL/6 mice exposed to pre- peri- or post-menopausal concentrations of oestradiol +/- Zol

Following investigation into the changes in bone structure following administration of Zol +/- oestradiol in C57BL/6 mice, the effects on bone turnover were investigated at a biochemical level using serum markers that indicate the changes in bone cell activity (n=10) (Figure 3.4). This was important because the relatively short treatment period of Zol may not be sufficient to produce significant physiological changes in bone architecture compared to untreated mice.

The serum biomarker TRAcP-5b, predominantly derived from osteoclasts and commonly used as a biomarker of osteoclast activity, was quantified in the serum of mice at the experimental endpoint. Zol treatment significantly reduced serum TRAcP-5b when compared to untreated mice under pre-, peri- and post-menopausal oestradiol concentrations (p<0.0001 for all) (Figure 3.4 A). Interestingly, circulating oestradiol concentrations had no significant effect on TRAcP-5b levels in serum (Figure 3.4 A).

3.4.2 BALBc mice exposed to pre- peri- or post-menopausal concentrations of oestradiol +/- Zol

Interestingly, Zol was less potent at reducing osteoclast activity in BALB/c mice with pre-menopausal mice showing no significant difference in TRAcP-5b concentrations following treatment with Zol (n=12) (Figure 3.4 B). Furthermore, activities of Zol under different oestradiol concentrations differed in BALB/c mice compared with C57BL/6 mice: In BALB/c mice Zol reduced osteoclast activity under peri- and post-menopausal concentrations of oestradiol but not under pre-menopausal concentrations of this hormone (p=0.012 and p>0.001 respectively) (Figure 3.4 B). Also in this mouse strain oestradiol, modelled by oestradiol replacement, had a significant impact on osteoclast activity in the absence of Zol with post-menopausal concentrations of oestradiol leading to significantly higher TRAcP-5b concentrations than pre-menopausal concentrations of oestradiol (p=0.002).

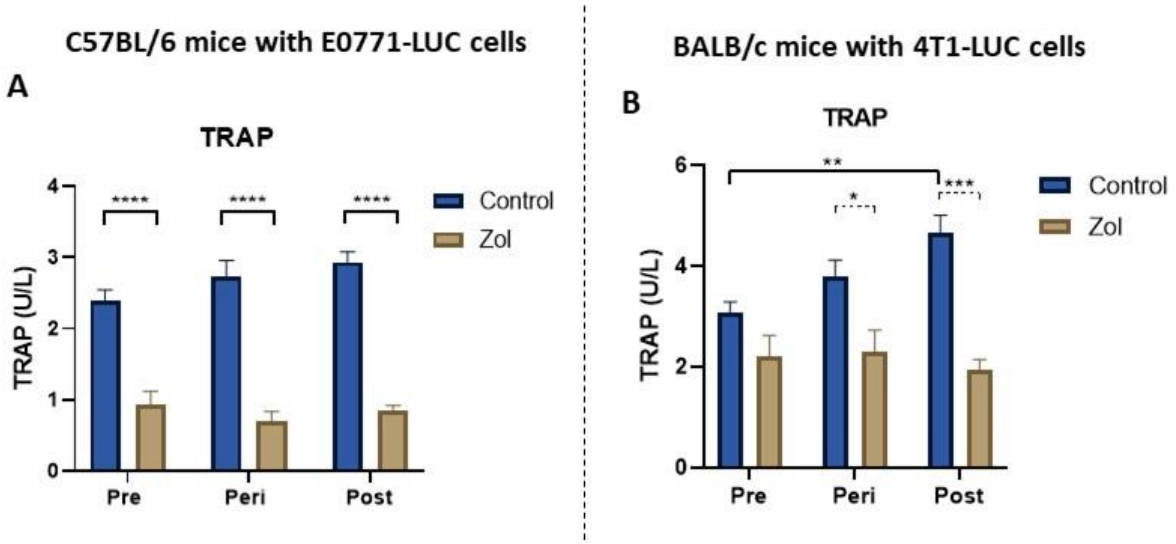

Figure 3.4: Effect of Zol and oestradiol on biochemical markers of osteoclast activity

Serum TRAP concentrations, representative of osteoclast activity, taken from **(A)** C57BL/6 with E0771 tumours (n=10) and **(B)** BALB/c (n=12) mice with 4T1-LUC tumours underwent OVX before treatment with 100 µg/kg Zol or saline in combination with post, peri or pre-menopausal concentrations of oestradiol in drinking water. ELISA analysis for TRAP performed on mouse serum taken at experimental endpoint.

Mean ± SEM Statistical analysis by one way ANOVA with Tukeys post analysis and students T test (n=10-12)

*< 0.05, ** < 0.01, *** < 0.001, **** < 0.0001

3.5 Osteoblast activity via P1NP

3.5.1 C57BL/6 mice exposed to pre- peri- or post-menopausal concentrations of oestradiol +/- Zol

The serum marker P1NP was used to quantify representative osteoblast activity since it is a marker of bone formation from the cleaved N-terminal of collagen (n=10) (Figure 3.5). The study of osteoblast activity via P1NP found that treatment with Zol significantly reduced osteoblast activity in the post- and peri-menopausal groups (p=0.0005, p=0.0004 respectively) (Figure 3.5 A). However, Zol had no significant effect on P1NP in the pre-menopausal group (p=0.2212). When analysing the effect of oestradiol on serum P1NP, no significant difference was found between oestradiol concentration and serum P1NP (Figure 3.5 A).

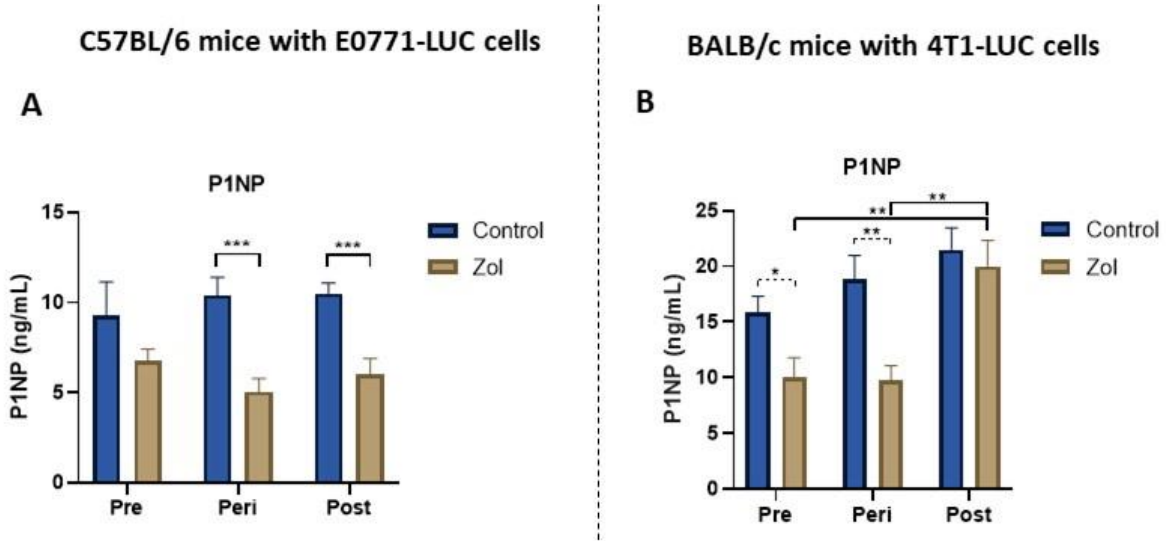

Figure 3.5: Effect of Zol and oestradiol on biochemical markers of osteoblast activity

Serum P1NP concentrations from (A) C57BL/6 and (B) BALB/c mice underwent OVX before treatment with 100 µg/kg Zol or saline in combination with post, peri or pre-menopausal concentrations of oestradiol in drinking water. ELISA analysis for P1NP performed on mouse serum taken at experimental endpoint. Mean ± SEM Statistical analysis by one way ANOVA with Tukeys post analysis and students T test (n=10-12)

*< 0.05, ** < 0.01, *** < 0.001, **** < 0.0001

3.5.2 BALBc mice exposed to pre- peri- or post-menopausal concentrations of oestradiol +/- Zol

Serum P1NP was analysed in the BALB/c mouse model following the experimental end point to assess osteoblast activity (n=12). Interestingly, in this model treatment with Zol significantly decreased osteoblast activity in mice with pre- and peri-menopausal concentrations of oestradiol compared to their untreated counter parts (p=0.021 and p=0.002 respectively) but did not affect

osteoblast activity under post-menopausal concentrations of this hormone, in Zol treated and untreated mice activity remained high (Figure 3.5 B). This contrasts results observed in the C57BL/6 model, where mice with pre-menopausal concentrations of oestradiol were unaffected by Zol. Indeed, mice with post-menopausal concentrations of this hormone treated with Zol had significantly higher osteoblast activity than pre- and peri-menopausal mice treated with Zol ($p=0.002$ and $p=0.001$ respectively) showing the potential role of oestradiol in bone turnover, perhaps as a physiological increase to counter the increased osteoclast activity associated with menopause (Figure 3.5 B).

3.6 Live Imaging of metastatic outgrowth of disseminated tumours in bone and soft tissue

To analyse the effects of menopausal oestradiol concentrations with or without Zol on tumour dissemination and metastatic outgrowth, live tumour imaging was performed (Figure 3.6). Clinical trials have shown that adjuvant treatment with Zol can reduce development of bone metastasis independent of menopausal status, but that high oestradiol can drive increased recurrence of metastasis in soft tissues (Coleman et al., 2018b). Following intracardiac injection of mouse mammary tumour cell lines transfected with luciferase, mice were injected with the substrate luciferin and imaged using the IVIS system to monitor tumour growth and metastatic location.

3.6.1 C57BL/6 mice exposed to pre- peri- or post-menopausal concentrations of oestradiol +/- Zol

In the C57BL/6 mouse model injected with E0771-LUC cells, circulating concentration of oestradiol corelated positively with increased number and size of bone tumours. Supplementation of a pre-menopausal concentration of oestradiol to mice following OVX led to significantly more bone metastases developing when compared to post-menopausal mice ($P < 0.01$) (Figure 3.6 D). In this model, Zol had no significant effect bone metastasis in pre- or peri-menopausal groups, but interestingly it did lead to significantly increased numbers of bone metastases in the post-menopausal group (Figure 3.6 D). Tumour luminescent intensity, a measurement used to determine tumour growth and size, was not significantly changed between any of the treatment groups in the C57BL/6 model, however it could be argued that there is a trend towards increased bone tumour size in the pre-menopausal group (Figure 3.6 F).

In vivo soft tissue was characterising as visible metastasis outside of the hind limb or spine, while *ex vivo* analysis of soft tissue tumour number analysed lung, liver, spleen, and any solid tumours found in dissection. Treatments with oestradiol or Zol led to no significant changes in numbers of soft

tissue metastases in the C57BL/6 group, showing a very minor, insignificant trend towards increase in mice with pre-menopausal circulating concentrations of oestradiol (Figure 3.7 B). However, tumour volume was significantly affected by Zol and oestradiol (Figure 3.7 D). Oestradiol concentration inversely corelated with tumour growth in soft tissue, with post-menopausal mice (-Zol) having significantly larger soft tissue metastases when compared to pre-menopausal mice. Treatment with Zol significantly reduced this soft tissue metastasis in mice supplemented with post-menopausal concentrations of oestradiol but did the opposite and increased metastases volume under pre-menopausal concentrations of oestradiol (Figure 3.7 D). This mirrors the clinic, suggesting that Zol can be beneficial in reducing soft tissue metastasis, but only in the absence of oestradiol. When oestradiol is present, Zol has adverse effects on soft tissue metastasis leading to more tumour growth.

3.6.2 BALBc mice exposed to pre- peri- or post-menopausal concentrations of oestradiol +/- Zol

In the BALBc mouse model, treatment with Zol led to a trend towards a decreased in bone tumours following injection of the 4T1-Luc cell line (Figure 3.6 C). This trend never reached statistical significance; however, it was conserved for all treatment groups. Interestingly, oestradiol had no effect on bone tumour number in the BALBc model, but it did affect bone tumour growth. Oestradiol supplementation inversely corelated with tumour volume as calculated by luminescence intensity *in vivo* with post-menopausal mice (-Zol) having significantly higher bone tumour volume than both peri and pre ($P < 0.1$) (Figure 3.6 E). Interestingly, treatment with Zol reduced the tumour burden in these post-menopausal bones, but only had these effects in the absence of oestradiol.

In the soft tissue, neither oestradiol nor Zol had significant effects on tumour numbers, except perhaps a small trend towards decrease in the pre-menopausal group (Figure 3.7 A). On the other hand, tumour volume in the soft tissue inversely corelated with oestradiol administration, with post-menopausal concentrations of oestradiol leading to significantly increased soft tissue tumour burden when compared to pre-menopausal concentrations ($P < 0.1$) (Figure 3.7 C). Treatment with Zol had no effect on tumour growth in soft tissue under pre- or peri-menopausal oestradiol concentrations, but under post-menopausal concentrations, Zol significantly reduced tumour burden in soft tissue ($p < 0.01$), an effect also observed in the C57BL/6 model (Figure 3.7 C & D). Taken together, this data suggests that Zol is only able to have beneficial effects on soft tissue metastasis in the absence of oestradiol (under post-menopausal conditions), mirroring that seen in the clinic.

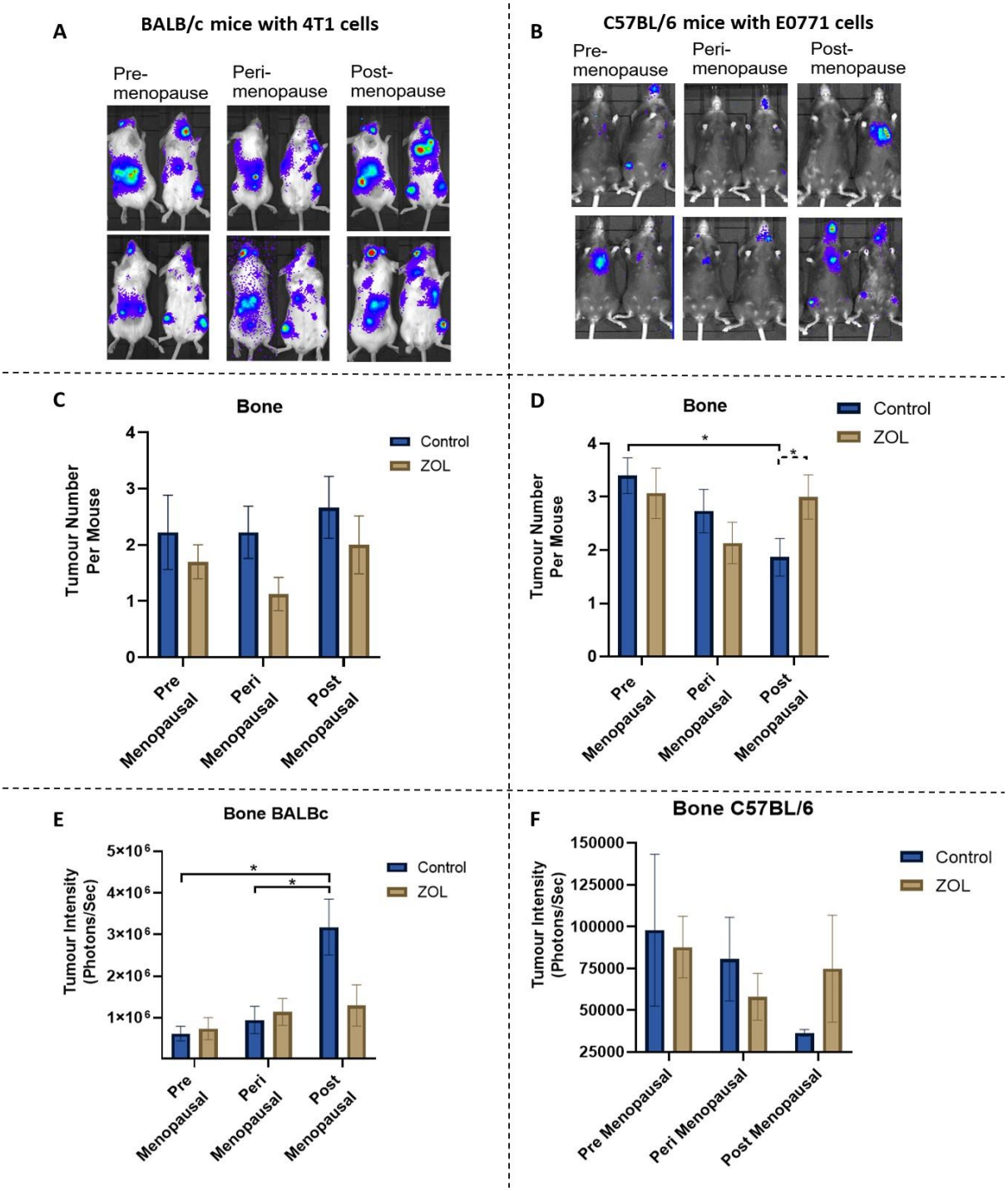

Figure 3.6: The effect of post, peri and pre-menopausal concentrations of oestradiol +/- Zol on bone metastasis

BALBc or C57BL/6 mice underwent OVX before oestradiol replacement in drinking water to model Pre, Peri and Post-menopausal concentrations. Mice were IC injected with 50,000 4T1-LUC cells (BALBc) or 100,000 E0771 cells (C57BL/6) and treated with Zol (100µg/kg). (A) Representative images from BALBc mice (B) Representative images from C57BL/6 mice (C) Mean number of bones with tumour per mouse in BALBc mice and (D) C57BL/6, analysed ex vivo. (E) Mean luminescent intensity (P/S) in bones of BALBc mice, imaged in vivo, representing tumour size. (F) Mean luminescent intensity (P/S) of bones in C57BL/6 mice images in vivo.

Mean ± SEM Statistical analysis by one way ANOVA with Tukeys post analysis and students T test

*< 0.05, ** < 0.01, *** < 0.001, **** < 0.0001

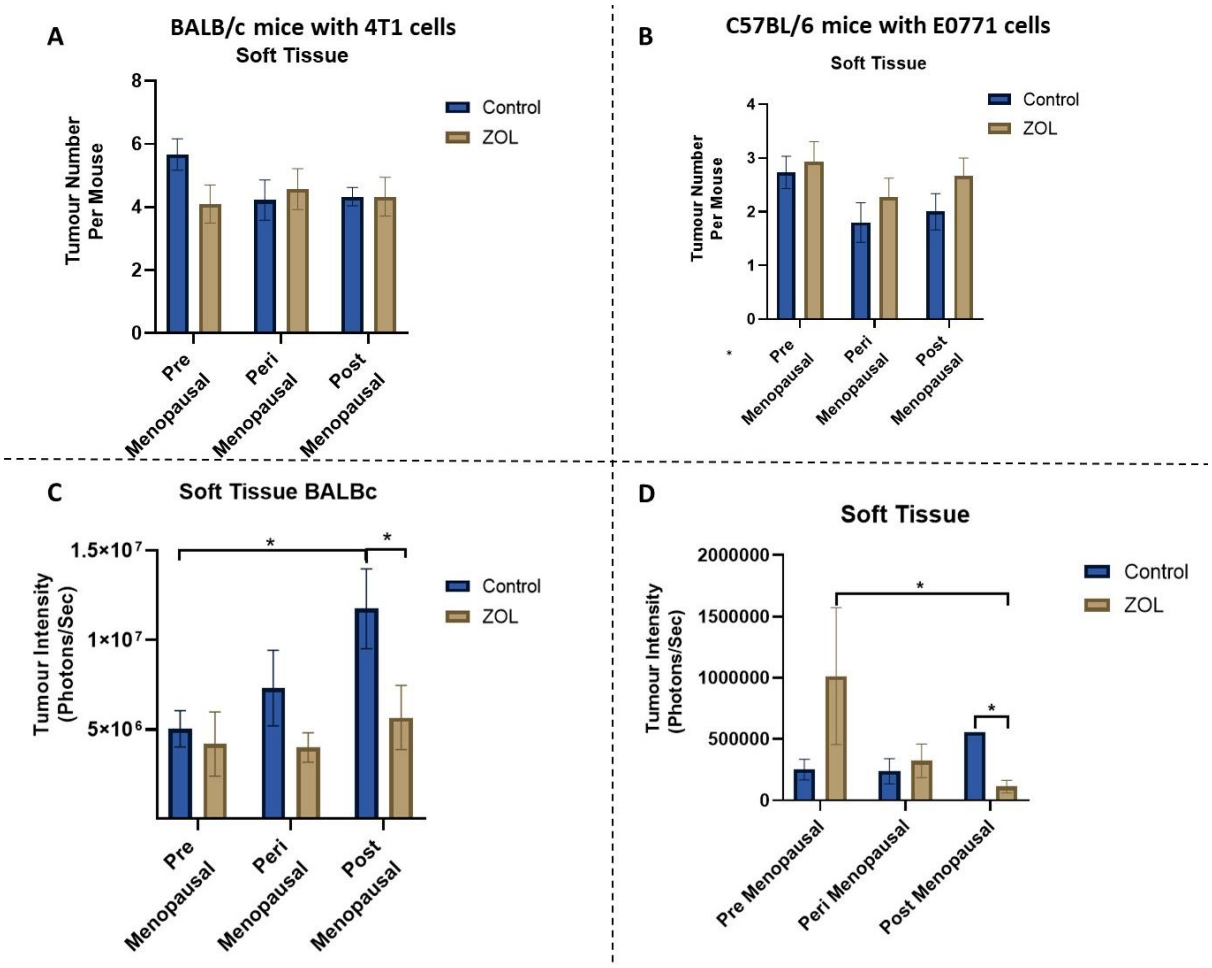

Figure 3.7: The effect of pre-, peri- and post-menopausal concentrations of oestradiol +/- Zol on soft tissue metastasis

BALBc or C57BL/6 mice underwent OVX before oestradiol replacement in drinking water to model Pre-, Peri- and Post-menopausal concentrations. Mice were IC injected with 50,000 4T1-LUC cells (BALBc) or 100,000 E0771 cells (C57BL/6) and treated with Zol (100µg/kg). (A) Mean number of soft tissue with tumour per mouse in BALBc mice and (B) C57BL/6, analysed ex vivo. (C) Mean luminescent intensity (P/S) in soft tissue of BALBc mice, imaged in vivo, representing tumour size. (D) Mean luminescent intensity (P/S) of soft tissue in C57BL/6 mice images in vivo.

Mean ± SEM Statistical analysis by one way ANOVA and students T test

*< 0.05, ** < 0.01, *** < 0.001, **** < 0.0001

3.7 Discussion

3.7.1 Modelling menopausal oestradiol concentrations

Human trials to evaluate the efficacy of Zol to prevent breast cancer metastasis to bone showed that bone metastasis was significantly decreased for both post- and pre-menopausal women. However, only post-menopausal women had a an improved iDFS, with pre-menopausal women displaying increased soft tissue metastasis and a decreased iDFS (Coleman et al., 2018b). The exact reason or mechanism behind this menopause dependent difference in treatment outcome is unknown, with a number of mechanisms proposed (Wilson et al., 2016a) (George et al., 2020). To study the mechanisms behind this change, the first aim of this study was to create an *in vivo* mouse model to replicate the conditions observed in the AZURE trial.

Firstly, OVX was performed on mice to remove their endogenous oestradiol production and enable oestradiol levels to be under our control. OVX has become the gold standard for establishing menopause in mouse models (Koebele and Bimonte-Nelson, 2016), however there are still criticisms around the use of this technique. One potential problem is the sharp rise in circulating FSH, accompanied by a sharp fall in circulating oestradiol. Furthermore, OVX has been shown to be insufficient alone to reduce circulating oestradiol to concentrations comparable to those found in post-menopausal women (Wright et al., 2008). To study the effects of oestradiol on metastasis, oestradiol needed to be isolated away from the sharp rise observed in FSH during the menopausal transition, which has also been suggested to have some effects on bone metastasis (Wilson et al., 2016b). Indeed, analysis of hormone and protein levels in patients from the AZURE trial found a correlation between FSH serum concentration and patient response to Zol treatment to prevent metastasis. However, since the rise in FSH during menopause occurs in tandem with the sharp drop in oestradiol, it is unclear which molecule may be responsible for this phenomenon. To counter this and further reduce oestradiol levels to appropriate post-menopausal concentrations, mice in the current study, were administered with daily injections of goserelin. Furthermore, the use of goserelin allowed the focus of this study to be on the effects of oestradiol without interference from high systemic FSH.

Mice produce relatively low concentrations of circulating oestradiol when compared to humans, and do not undergo the menopause in the same way. Therefore, mice were supplemented with oestradiol to mimic human menopausal concentrations via their drinking water at concentrations of 0, 1.375mg/l and 12.5mg/l to model post-, peri- and pre-menopausal concentrations respectively. This oestradiol concentration was significantly higher than murine physiological serum oestradiol concentrations, suggesting that the human oestradiol levels modelled may not accurately reflect the effects seen in the clinic. However, modelling human oestradiol concentrations in mice has become a

standard modelling technique for the study of menopausal oestradiol effects, with a plethora of publications setting a president for its biological relevance (Canuas-Landero et al., 2021) (Diaz Brinton, 2012).

Mice were also treated with goserelin alongside oestradiol administration to stop endogenous FSH production. This method for modelling serum oestradiol has been independently peer reviewed in the BALB/c model both with and without tumour cells (Canuas-Landero et al., 2021). Therefore, for the BALB/c model, trabecular bone volume was used as an indicator of oestradiol concentration. Measured serum oestradiol concentrations fell at an average of 59, 144 and 400 pg/ml for Zol untreated in C57BL/6b mice and 16, 278 and 391 pg/ml for Zol treatment. This concentration mirrors oestradiol concentrations observed in humans, oestradiol concentrations vary dramatically throughout the menstrual cycle, from 20-80 pg/ml during the mid follicular phase, all the way up to 200-500 pg/ml during the pre-ovulatory phase (Rodger, 2005). Therefore, it could be argued that the pre-menopausal oestradiol state is not effectively modelled in this study. On the other hand, maintaining high levels of oestradiol allows a detailed study of its role in the cancer process, while reducing variation that could be present from cyclical changes in oestradiol concentrations.

Although systemic oestradiol production was controlled in this study, local oestradiol production was not. Aromatase inhibitors were not used to inhibit local production of oestradiol from circulating androgens. Aromatase is most active in adipose tissue where it is considered main source of circulating oestradiol after the gonadal tissue (Nelson and Bulun, 2001), providing local oestradiol to sensitive organs in an autocrine manner. Therefore, it could be argued that the larger, dominant mice in the post-menopausal group would have more local oestradiol production from aromatase due to their increased adipose tissue. Aromatase has also been found expressed in the bone in osteoblasts, chondrocytes and fibroblasts supplying local oestradiol to the organ and influencing bone turnover (Eastell et al., 2006). Aromatase inhibitors were not used in this study because pre-menopausal women are rarely treated with them, unless used in combination with GnRH inhibitors (Pistelli et al., 2018). Furthermore, we initially tested the effects of adding aromatase inhibitors to the model, but this did not affect circulating oestradiol concentrations, so this treatment was not pursued (data not shown). Furthermore, preliminary results from this laboratory showed that adding letrozole to mice following OVX did not alter concentrations of circulating oestradiol.

Taken together, these data show that the model of menopausal transition in these mice is suitable for studying the effect of oestradiol on Zol treatment. Furthermore, this model allowed the study of the effects of oestradiol in the absence of interference from other reproductive hormones such as FSH.

3.7.2 Bone turnover

The bone is dramatically affected by both oestradiol and Zol, with oestradiol stimulating bone turnover by inhibiting the activity of osteoclasts while stimulating osteoblasts, and Zoledronic acid also preventing bone loss by leading to cytotoxic cell death of osteoclasts.

The next aim was to determine if modelling menopausal oestradiol concentrations in the presence or absence of Zol in tumour bearing mice affected bone turnover. The bone is a dynamic tissue that is susceptible to change from external signalling or drug intervention. Zol and oestradiol have both been shown to have profound effects on bone morphology and turnover. Breast cancer cells preferentially metastasise to bone and affect normal bone turnover through reciprocal communications leading to the vicious cycle (Roodman, 2004). Therefore, this study investigated the interactions of these different bone modulatory stimuli. Investigation into the effect of oestradiol on trabecular bone structure found a significant correlation between high oestradiol concentrations and higher bone volume. These data correlate with the observed phenotypic changes in the bone microenvironment of women during the menopausal transition (Neer and Investigators, 2010). There is a large body of evidence showing that under pre-menopausal concentrations of circulating oestradiol, bone remodelling is balanced, with osteoclastic bone resorption and osteoblastic deposition of new bone matrix resulting in no net increase in bone volume (Manolagas, 2000). Peri-menopausal women display an increase in bone resorption, in correlation to the decrease in systemic oestradiol concentrations, since there is an increase in activity of osteoclasts, leading to reduced bone volume. Whereas post-menopausal women experience a rapid loss in bone volume as a consequence of circulating oestradiol being low to undetectable. It has been shown that oestradiol acts on osteoclasts to cause apoptosis and reduce osteoclastogenesis, therefore protecting the bone from excess degradation. During the menopause, this protection is lost, leading to increased bone resorption and osteoporosis (Vaananen and Harkonen, 1996).

The data from the current study reflects this and what is seen in women during the menopause, with oestradiol significantly increasing trabecular bone volume both in the presence and absence of zoledronic acid. When analysing the effect of Zol in the C57BL/6 model, it was only able to increase bone volume in the post-menopausal group, trabecular bone also never reached that of mice treated with pre-menopausal levels of oestradiol. On the other hand, in the BALBc model Zol had no significant effect on trabecular bone volume of tumour bearing mice. Many other studies have described the bone sparing properties of Zol in mice, and shown its ability to prevent osteolytic bone

disease (Croucher et al., 2003) (Jeong et al., 2011), suggesting that the discrepancies seen in this study are due to a short treatment time, as opposed to lack of effect of Zol.

3.7.3 Biomarkers of bone turnover

To understand the actions of Zol in the bone microenvironment further, molecular biomarkers for osteoclast and osteoblast activity were analysed. Osteoblast activity was reduced by Zol under post and peri-menopausal concentrations of oestradiol. However, under pre-menopausal concentrations of oestradiol, osteoblast activity was not significantly different between mice treated with zol and those that received PBS control. Firstly, these data show that Zol reduced osteoblast activity in the bone micro-environment, therefore leading to a change in bone remodelling since osteoblast activity is reduced. This phenomenon of a reduced osteoblast activity in response to Zol has been observed by a number of other groups (Brown et al., 2012) (Haider et al., 2014), but the mechanism is unclear. The data also shows that oestradiol has a protective effect on osteoblast activity in response to Zol, with high concentrations of oestradiol restoring osteoblast activity when compared to post-menopausal treated mice. This conclusion is supported by experiments showing that oestradiol acts on osteoblasts via the β1 receptor to supress apoptotic gene expression encoding InsP3R, a pro-apoptotic calcium channel (Bradford et al., 2010). Therefore, low systemic oestradiol leads to increased expression of InsP3R making cells more susceptible to apoptotic stimuli. Interestingly, expression of caspase-3/7 has also been shown to be inhibited by oestradiol in osteoblasts, providing a mechanism by which oestradiol promotes survival of these cells (Bradford et al., 2010).

Osteoclast activity, as determined by serum TRAcP-5b, was significantly decreased by Zol irrespective of serum oestradiol concentration in the C57BL/6 model. This data is in agreement with literature supporting this mechanism of Zol. In the BALBc model, Zol only significantly reduced TRAcP-5b in peri- and post-menopausal groups, with pre-menopausal mice showing only a trend towards decrease. However, in the BALBc model, oestradiol significantly decreased TRAcP-5b in serum, in line with literature showing oestradiol reducing activity and promoting apoptosis of osteoclasts. One mechanism by which Zol reduces osteoclast activity is by targeting farnesyl pyrophosphate synthase, a prominent enzyme in the mevalonate pathway, leading to reduced isoprenylation of small GTPs and ultimately apoptosis of mature osteoclasts (Luckman et al., 1998). Zol has also been shown to inhibit RANK expression on osteoclast precursors, acting to inhibit RANKL induced upregulation of RANK and inhibiting differentiation and migration of osteoclast precursors, therefore decreasing the number of mature osteoclasts in the bone microenvironment. (Kimachi et al., 2011).

The results from this current study are in agreement with the documented role of Zol on the bone microenvironment. Zol reduced osteoclast activity, as determined by TRAP. Osteoblast activity was also reduced, except in pre-menopausal mice under the protection of oestradiol. This decrease in the number of osteoclasts led to an increased bone volume in C57BL/6 mice treated with post-menopausal concentrations of oestradiol. However, the anabolic effect of higher oestradiol concentrations, alongside the relatively short Zol treatment time, could be the reason that the reductions in osteoclast activity in peri- and pre-menopausal mice did not translate into an increased bone volume compared to untreated mice.

3.7.4 Tumour growth

To study the effect of Zol on the sites of breast cancer dissemination and metastatic outgrowth, C57BL/6 mice were injected with E0771-LUC cells or BALBc mice were injected with 4T1-LUC cells via intracardiac injection. Intracardiac injection, a widely used model for bone metastasis, was utilised as the tumour delivery method in this study since the focus is on later stages of breast cancer metastasis; the ability for cells to arrest, survive and proliferate in the metastatic site (Campbell et al., 2012). The model used in this study to investigate the effect of menopausal concentrations of oestradiol and Zol on breast cancer dissemination and outgrowth is similar to one used in a diverse array of other publications and studies (Canuas-Landero et al., 2021) (Ottewell et al., 2014a) (Brown et al., 2012) (Haider et al., 2014). Stable pre-, peri- and post-menopausal concentrations of oestradiol were established one week prior to injection of breast cancer cells in order to establish the relevant bone phenotype and allow future observations into the changes to the immune landscape caused by oestradiol. As shown in previous data, this modelling of oestradiol concentration, bone volume and osteoclast and osteoblast activity successfully mirrored that seen in the clinic.

In the AZURE trial, where breast cancer patients were treated with Zol alongside standard of care, Zol reduced development of bone metastasis irrespective of menopausal status. However, Zol treatment was only able to improve iDFS in women who were over 5 years since menopause at the beginning of the trial (Coleman et al., 2014a). Indeed, in younger, pre-menopausal women treatment with Zol was associated with increased extra-skeletal tumour relapse and worse overall survival (Coleman et al., 2018a). In our mouse models, Zol did not significantly reduce bone metastasis in any treatment group except in BALBc mice with post-menopausal concentrations of oestradiol, where the Zol significantly reduced the increase in bone metastasis observed in untreated mice from this group. This outcome may be due to the short time span of the experiment due to the aggressive nature of the breast cancer cell lines used for these experiments. On the other hand, soft tissue metastasis was

increased in pre-menopausal mice following treatment with Zol, mirroring the AZURE trial data. In both mouse models, Zol treatment of post-menopausal mice resulted in a significant decrease in soft tissue metastasis size. This suggests that serum oestradiol concentration can affect both bone metastasis and also affect the efficacy of Zol, with Zol being more effective at preventing bone metastasis in the absence of oestradiol.

Indeed, oestradiol inversely corelated with metastatic outgrowth of tumours outside the bone with lower oestradiol concentrations leading to larger extra-skeletal metastasis. The effect was observed in both the BALBc and C57BL/6 tumour models. Furthermore, previous papers from this group have shown that this inverse corelation of soft tissue metastasis and serum oestradiol is only observed in mouse models with intact immune systems (Canuas-Landero et al., 2021). When analysing the same treatments in BALB/$c^{fox/-}$ nude mice, oestrogen did not corelate with soft tissue metastasis, suggesting that the immune system plays a major role in the effects of oestradiol and Zol on soft tissue recurrence. Indeed, in a series of *in vivo* experiments using fluorescently labelled bisphosphonates, it has been suggested that TAMs can act as a mediator of bisphosphonate activity outside of the bone by engulfing small granular macrocalcifications containing bound bisphosphonate and transport it into the tumour microenvironment (Junankar et al., 2015). Furthermore, Zol and oestradiol both have profound, and often opposing effects on the immune system both systemically and in the tumour microenvironment (George et al., 2020), a topic that will be discussed in detail in future chapters.

3.8 Summary

It has been well documented in the clinic that menopausal status is important in predicting patient outcome following adjuvant administration of Zol in combination with standard of care to breast cancer patients to prevent bone metastasis. Previous studies have investigated the role of menopausal hormones in the dissemination of tumour cells following treatment with Zol and identified both oestradiol and FSH as the likely mediators of this phenomenon (Wilson et al., 2016b). Due to its profound immune regulatory effects and its dramatic decrease during menopause, we hypothesised that oestradiol was the main mediator of the menopausal differences in treatment outcome. Therefore, the aim of this chapter was to create a model of the AZURE trial, to effectively replicate menopausal status, Zol treatment, bone morphology, tumour dissemination and immune regulation (future chapters).

Menopausal status was successfully modelled by OVX and oestradiol replacement in drinking water, bringing serum oestradiol levels into the range of human oestradiol at the different

menopausal stages. This modelling of oestradiol concentrations was reflected in the bone microenvironment, with trabecular bone volume significantly increasing following pre-menopausal levels of oestradiol replacement in both models. Interestingly, Zol had a protective effect on bone volume but was only able to increase trabecular bone in the post-menopausal group of C57BL/6 mice. On the other hand, treatment with Zol had significant effects on bone turnover at a cellular level. Zol significantly decreased osteoclast activity, determined by serum TRAcP levels, while also decreasing osteoblast activity, determined by serum P1NP concentration. This shows that Zol is reaching the bone microenvironment and is targeting osteoclast and osteoblast activity, as expected. Finally, the effects of treatment on tumour dissemination were investigated, finding that treatment with Zol in the pre-menopausal group led to increased tumour burden in soft tissue. Furthermore, Zol was only able to significantly affect bone metastasis in the absence of oestradiol. Overall, the two mouse models used to recreate conditions observed in the AZURE trial have proved to be robust models of menopausal oestradiol concentrations, bone turnover and tumour growth. These models will be further used to understand the involvement of the immune system and its interactions with oestradiol and Zol.

Chapter 4: Investigating the direct effect of oestradiol and Zol on breast cancer progression

4.1 Introduction

Zoledronic acid, in combination with standard of care, has been shown to have differential effects on breast cancer DFS and metastasis depending on the menopausal status of the patient. The clinical benefit of utilising adjuvant Zol alongside standard of care has been studied in a number of clinical trials. In the ABCSG-12 trial 1803 pre-menopausal women received Goserelin alongside endocrine treatment with or without Zol (4mg each month). This treatment reduced systemic oestrogen concentrations, to post-menopausal levels. A medial follow up after 94.4 months found that relative risk of disease was reduced in the Zol arm of the study (Gnant et al., 2015b). The ZO-FAST assessed the protective role of Zol in post-menopausal women with early breast cancer and found less recurrences in the Zol group (Bundred et al., 2008). In the AZURE trial, where 3360 women received standard treatment with or without Zol, Zol was shown to decrease bone metastasis and increase DFS for post-menopausal breast cancer patients, regardless of ER status (Coleman et al., 2018a). Women who were deemed clinically postmenopausal at the initiation of adjuvant bisphosphonate treatment had reduced tumour recurrence at all sites. On the other hand, pre-menopausal women had a reduced DFS, although they did have reduced bone metastasis suggesting a role for reproductive hormones within the HPG axis. To determine whether one particular hormone could be affecting the ability of Zol to elicit anti-tumour effects outside of the bone microenvironment, serum from early breast cancer patients in the AZURE trial was retrospectively analysed for concentrations of FSH, oestradiol and inhibin A (Wilson et al., 2016b). Inhibin-A whose concentration inversely corelates with bone turnover, was a promising candidate because of its effects on bone remodelling. However, analysis of patient serum found no significant differences in disease outcome between patients with post-menopausal and non-post-menopausal concentrations of inhibin A (Wilson et al., 2016b). Furthermore, when studied in a preclinical mouse model, osmotic delivery of 10/60/120 ng/day of inhibin A did not significantly affect homing of DiD labelled breast cancer cells to the bone marrow following intracardiac injection, despite changes in osteoclast activity observed. This suggests that the effects seen in the AZURE trial are either mediated by FSH or oestradiol.

There is emerging evidence that oestradiol is a key hormone which can influence sites of dissemination of breast cancer cells. As part of the AZURE trial a large number of baseline serum samples were collected enabling evaluation of baseline hormone levels (oestradiol, follicle stimulating hormone and inhibin). This study demonstrated that an oestradiol level of <50pmol/l (postmenopausal range) was associated with a significantly shorter iDFS compared to an oestradiol level of ≥50pmol/l (HR=1.36; 95% CI 1.05-1.78 p=0.022). This was driven by more distant recurrences (outside of bone), irrespective of whether the primary tumour was ER+ or ER- (Wilson et al., 2016b). These data indicated that very low levels of oestradiol may make the bone a less permissive

environment for dissemination of tumour cells and lead to metastases in other organs. Evidence from pre-clinical models have shown apposing roles for oestradiol, showing that low levels of oestradiol caused by ovariectomy promote tumour outgrowth of tumour cells already disseminated in bone (Ottewell, et al. 2015, Wright, et al 2017), whereas, supplementing mice with oestradiol enhances spontaneous metastasis of ER+ cells to bone (Holen et al 2016). Bone metastases were inhibited in both these models by zoledronic acid in the absence of chemotherapy. Taking the clinical and pre-clinical data together, data suggest that high oestradiol may attract tumour cells to bone and influence their survival and dormancy in the bone microenvironment or cause them to disseminate to other organs. However, the mechanism for this remains unknown.

Oestradiol can excerpt effects on a plethora of different tissues and cell types throughout the body by binding to ERs, which are classified into subtypes. ERα and ERβ are both nuclear hormone receptors acting as transcription regulators that mediate direct genomic signalling by dimerising once activated and binding to oestradiol response elements on DNA and promoting transcription (Bourdeau et al., 2004) (Fuentes and Silveyra, 2019). These receptors can also act by indirect genomic signalling, by acting through protein-protein interactions with other transcription factors. The third ER is a membrane G-protein coupled receptor named GPER1 which signals via activation of intra-cellular signalling cascades following oestrogen binding (Carmeci et al., 1997) (Filardo and Thomas, 2012). Oestrogen signalling can act directly on ER-positive breast cancer cells and stimulate cell proliferation, providing a selective advantage to these cells and increasing tumour growth. However, a number of studies have shown the ability of oestrogen to promote growth and metastasis of breast cancers lacking the ER (ER-negative breast cancer) (Treeck et al., 2020). Due to the ubiquitous nature of ERs, it has been shown that oestrogen signalling can promote breast cancer development via actions on the stromal cells in the host compartment rather than acting directly on tumour cells themselves. Indeed, in an experiment on ovariectomised mice injected with the 4T1- triple negative cell line and supplemented with oestrogen or control, oestrogen was found to accelerate tumour metastasis and enhance tumour colony formation (Yang et al., 2013). Studies using xenograft mouse models of breast cancer formation highlight the importance of estrogens in ER-negative breast cancer development and progression, suggesting an involvement of bone-marrow -derived stromal cell recruitment (Gupta et al., 2007). Conversely, *in vitro* experiments treating the triple negative 4T1 mouse mammary cancer cell line with oestrogen found that treatment increased motility and invasion of the 4T1 cell line. Furthermore, treatment of cells with the ER antagonist ICI 182,780 (1 μM) did not block this phenomenon suggesting a direct, ER independent action of estrogen on these cells (Yang et al., 2013). It has been shown that oestrogen can increase the migration, invasion and viability of the triple negative breast cancer cell line MDA-MB-231 by acting on the GPER1 receptor and upregulating

expression of cyclin A, cyclin D1, Bcl-2, and c-fos (Yu et al., 2014). This shows that oestrogen can still influence breast cancer cells even in the absence or ERα and poses the question of whether the differences in treatment outcome observed in the AZURE trial and EBCTCG meta-analysis are through direct effects on tumour cells or via changes to the microenvironment including T cell driven immune modulatory mechanisms. Therefore, for the experiments in this project, ER α negative breast cancer cell lines were used to enable the effects of oestrogen on the microenvironment to be isolated away from the well documented effects of ER α signalling.

Zoledronic acid is a powerful bone modulatory agent, quickly binding to the bone matrix where it is ingested by osteoclasts, inducing apoptosis by inhibiting the activity of farnesyl diphosphate synthase, thereby reducing bone turnover (Kavanagh et al., 2006). It is believed that the main anti-tumour effects of Zol in the bone are through its effects on osteoclasts and the bone microenvironment, breaking the vicious cycle to make the bone a less conducive environment for tumour dissemination (Ottewell and Wilson, 2019). However, Zol has been shown to have direct cytotoxic effects on breast cancer cell lines, with concentrations between 1-100μM leading to significant decreases in cell number via increased apoptosis, confirmed by fluorescence in situ nick translation assay, when treated *in vitro* (Jagdev et al., 2001). Similar results have been observed across a number of breast cancer cell lines (Ibrahim et al., 2012) (Almubarak et al., 2011). Furthermore, this induction of apoptosis was due to inhibition of enzymes in the mevalonate pathway, as determined by addition of geranylgeraniol alongside Zol which reduced apoptosis to control levels. However, studies show that local concentrations of Zol in the bone following administration have been calculated to be between 0.4 μM and 4.6 μM following administration of a 2-4 mg dose (Scheper et al., 2009). Clinical trials have shown that Zol reduces bone metastasis in both pre- and post-menopausal women, with the differences in treatment outcome presenting outside of the bone. Concentrations of Zol outside of the bone are much lower as Zol rapidly binds to the bone matrix (Weiss et al., 2008). Because of this lower systemic concentration of Zol, it is possible that the effects observed in clinical trials are mediated by indirect actions of Zol, acting through signalling pathways in bone remodelling cells or by stimulating an anti-tumour immune response (a hypothesis which will be explored in later chapters).

4.1.2 Hypothesis

Treating murine breast cancer cell lines 4T1-LUC and E0771 with pre-, peri- and post-menopausal concentrations of oestradiol does not directly affect the anti-tumour actions of Zol *in vitro*.

Aims

The overall aim of this chapter is to determine whether the direct anti-tumour effects of Zol on murine breast cancer cell lines are altered in the presence of pre- or post-menopausal concentrations of oestradiol.

1. Determine the cytotoxic effects of Zol on E0771 and 4T1-LUC cells, and calculate appropriate drug concentrations to utilise for cell culture experiments.

2. Establish the direct effects of Zol on tumour cell proliferation, viability, migration and invasion under pre- and post-menopausal concentrations of oestradiol.

4.2 Results

4.2.1 Growth dynamics of E0771 and 4T1-Luc cells

Understanding the characteristics of the 4T1 and E0771 breast cancer cell lines was very important to inform the experimental design of future in vitro experiments. Therefore, growth curves were performed to determine at what time point the cells were in their exponential growth phase and at what time point cells reached a plateau phase (n=3 performed in triplicate). E0771 cells were plated at 20,000 cells per well in a 24 well plate and cells were counted every 24 hours (Figure 4.1 B). The cells reached the exponential growth phase 24 hours after seeding and reached a maximum confluence at 96 hours. However, after 120 hours the number of E0771 cells decreased as the high confluence led to cell death and cell detachment (Figure 4.1 B). This shows that E0771 cells never reach the plateau phase of growth as other cancer cell lines do, but instead detach and die before plateau is reached.

4T1-LUC grow in a more traditional pattern resembling the sigmoidal curve expected (Figure 4.1 A). The cells reached the exponential growth phase after 48 hours of growth and reached maximum confluence after 96 hours. The cells then reached a plateau phase of growth following 96 hours and did not detach and die as the E0771 cell line did (Figure 4.1 A). Therefore, after plating cells, assays can be conducted during the growth phase of 4T1-LUC cells from 48 hours up to the 96 hour time point.

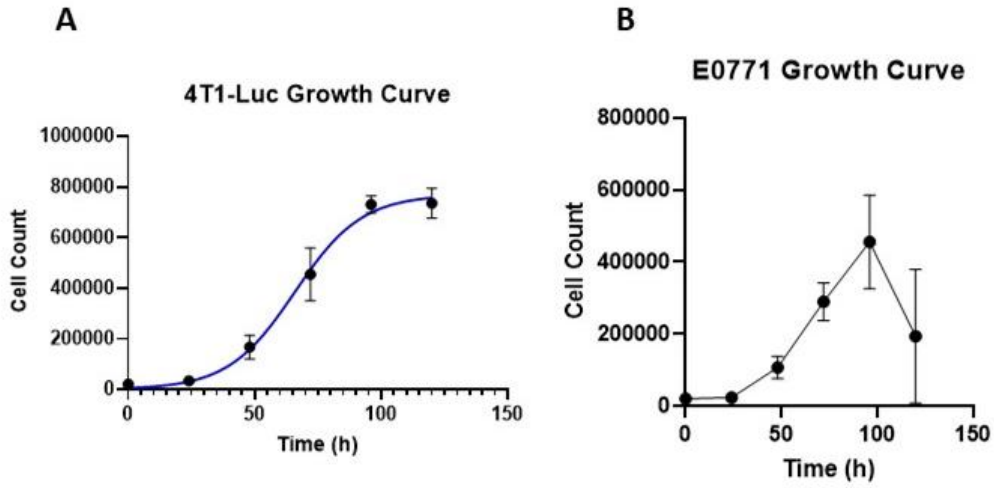

Figure 4.1: Cell growth characteristics of (A) 4T1-LUC cells and (B) E0771 cells, grown in RPMI media supplemented with 10 % FBS in the absence of treatment. Cells counted at 24, 48, 72, 96 and 120h.

Data is mean +/- SEM for n=3 experiments performed in triplicate.

4.2.2 Effect of Zol on murine breast cancer cells lines

As shown in the literature and previously by this laboratory, Zol has direct cytotoxic effects on tumour cells. Therefore, the efficacy of Zol action alone on 2D cell cultures was assessed, to determine the IC50 and most appropriate time frame of treatment. Both tumour cell lines were treated with 5, 10, 25, 50, 100 and 200 μM of Zol and cell viability was assessed by MTT assay (n=3 with 6 technical repeats) (Figure 4.2 B) and proliferation by cell counting (n=3 performed in triplicate) (Figure 4.2 A) at 24 h, 48 h and either 72 h (4T1-LUC) or 96 h (E0771) time points, giving representative cell viability in the presence of Zol. The time point of 48 hours was chosen for the IC50 analysis because IC50 for cell viability was reached when compared to untreated cells in both E0771 (Figure 4.2 Ai-Bi) and 4T1-LUC (Figure 4.2 Aii-Bii). After 24 hours, IC50 was not met at any concentration and after 72 hours total cell death was induced across a wide range of concentrations. E0771 cells were much more sensitive to zoledronic acid than the 4T1-LUC cells with E0771 having an IC50 of 27.82 μM after 48 hours via MTT (Figure 4.2 Bi) and 18.82 via cell count (Figure 4.2 Ai). 4T1-LUC cells were less sensitive to Zol than E0771, with an IC50 of 43.54 μM after 48 hours via MTT assay (Figure 4.2 Bii) and 34.91 μM via cell counting (Figure 4.2 Aii). The same trend of a reduced IC50 in the cell counting experiments compared to MTT assay was observed in both cell lines. There was a significant difference between cell death at IC50 concentrations of Zol between 24h and 48h time points of treatment in 4T1-LUC ($P<0.0001$) (Figure 4.1C) and E0771 ($P=0.043$) (Figure 4.1 A) after cell counting.

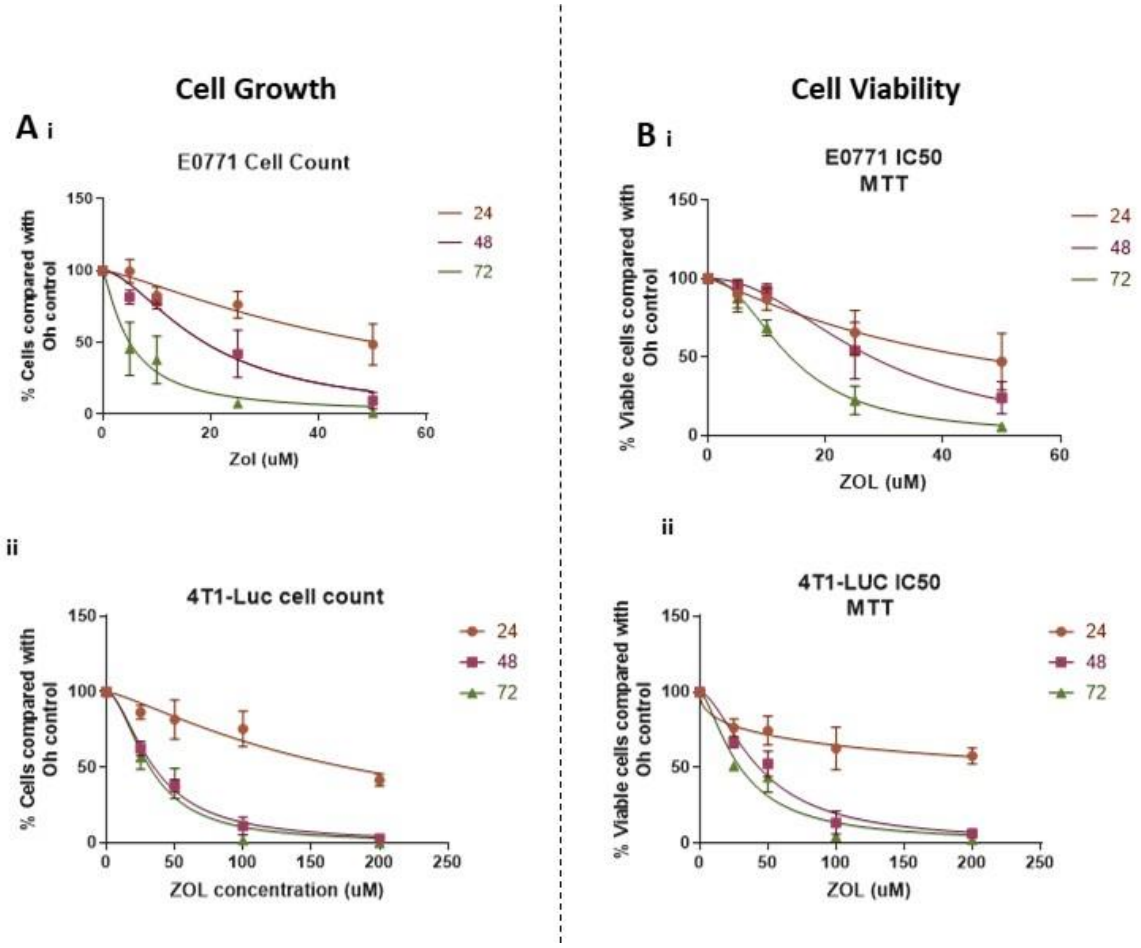

Figure 4.2: Effect of increasing concentrations of Zol on (A) Cell Growth and (B) on Cell Viability in the (i) E0771 and (ii) 4T1-LUC cells following treatment with between 5-200 uM Zol. IC50 was determined at each time point. The time point and concentration for use in future experiments was determined by the shape of the curve and the health of the cells. IC50 concentrations are higher than *in vivo* concentrations found in bone and circulation.

Data are mean +/- SEM for n=3 experiments in triplicate (A) or sextuplet (B)

4.3 Effect of pre- post and peri- menopausal concentrations of oestrogen on anti-tumour activity of Zol *in vitro*.

4.3.1 Tumour cell number

Following the determination of an IC50 for reduced cell number or viability of E0771 and 4T1-LUC cells with Zol, the interaction between oestrogen and Zol on tumours was subsequently assessed (Figure 4.3). Tumour cells were treated with 10 pM/L, 84 pM/L and 300 pM/L of oestradiol (to represent post- peri and pre-menopausal concentrations of oestradiol observed in women) in combination with control or Zol IC50 (25 µM E0771, 40 µM 4T1-LUC) (Figure 4.3). Phenol free RPMI and charcoal stripped FBS were used as growth medium for these experiments. Following treatment, cell growth was quantified by haemocytometer cell counting at three timepoints (n=3 performed in triplicate). Zol significantly reduced cell numbers after 72 hours for both murine breast cancer cell lines following treatment with Zol. In the E0771 cell line, Zol reduced cell numbers at 10 pM/l, 84 pM/l and 300 pM/0 of oestradiol (p= 0.0002, p= 0.0007, p= 0.0047 respectively; Figure 3Ai). Furthermore, Zol had a significant effect on cell number in E0771 cells following 48 hours of treatment. Similarly, in the 4T1-Luc cell line, Zol also significantly reduced cell number after 72 hours at all oestrogen concentrations (p= 0.0308. p=0.0305, p= 0.0307). On the other hand, after 48 hours of treatment, Zol only significantly reduced cell number at 300pM/L of oestradiol, with 84pM/L and 10pM/L showing a strong trend approaching significance (Figure 3Aii). This reflects the IC50 experiments which showed that 4T1-LUC cells are less sensitive to Zol then the E0771 cells, with cell number taking longer to be significantly affected.

4.3.2 Tumour cell viability

This result showing the cytotoxicity of Zol independent of oestradiol concentration was confirmed and quantified by a second method focusing on cell viability. Cells were treated in the same way but quantified by MTT assay (n=3 with 6 technical replicates). Administration of oestradiol to E0771 cells had no significant effect on reduced cell viability following Zol induced at any concentration of oestradiol following 96 hours, assessed by MTT assay (Figure 4.3 Bi). After 48 hours, Zol significantly reduced cell viability at all oestradiol concentrations when compared to their untreated counterparts (P= 0.0143, 0.0039, 0.0064 pre- post and peri menopausal oestradiol concentrations respectively) (Figure 4.3Bi).

4T1-LUC cells treated with Zol and oestradiol reached IC50 after 72 hours treatment, different to that observed in previous IC50 experiments (Figure 4.3Bii). At 72 hours, Zol significantly reduced

cell viability at all oestradiol concentrations when compared with non- Zol treated cells (p=0.0099, p=0.0009, p=0.0093 pre- post and peri menopausal oestradiol concentrations respectively) (Figure 4.3 Bii). Importantly, oestradiol had no effect on the anti-tumour action of Zol or the growth of the tumour cells in the absence of Zol. Oestradiol concentration had no significant effect on the anti-proliferative effects of Zol at any concentration, or any time point, mirroring that seen in the cell growth analysis.

Taken together my data suggests that oestradiol did not significantly affect the direct anti-tumour effect of Zol on the triple negative murine breast cancer cell lines. Therefore, any potential interactions of oestradiol that may inhibit the anti-tumour effects of Zol in patients are likely to be driven by alterations to the tumour microenvironment.

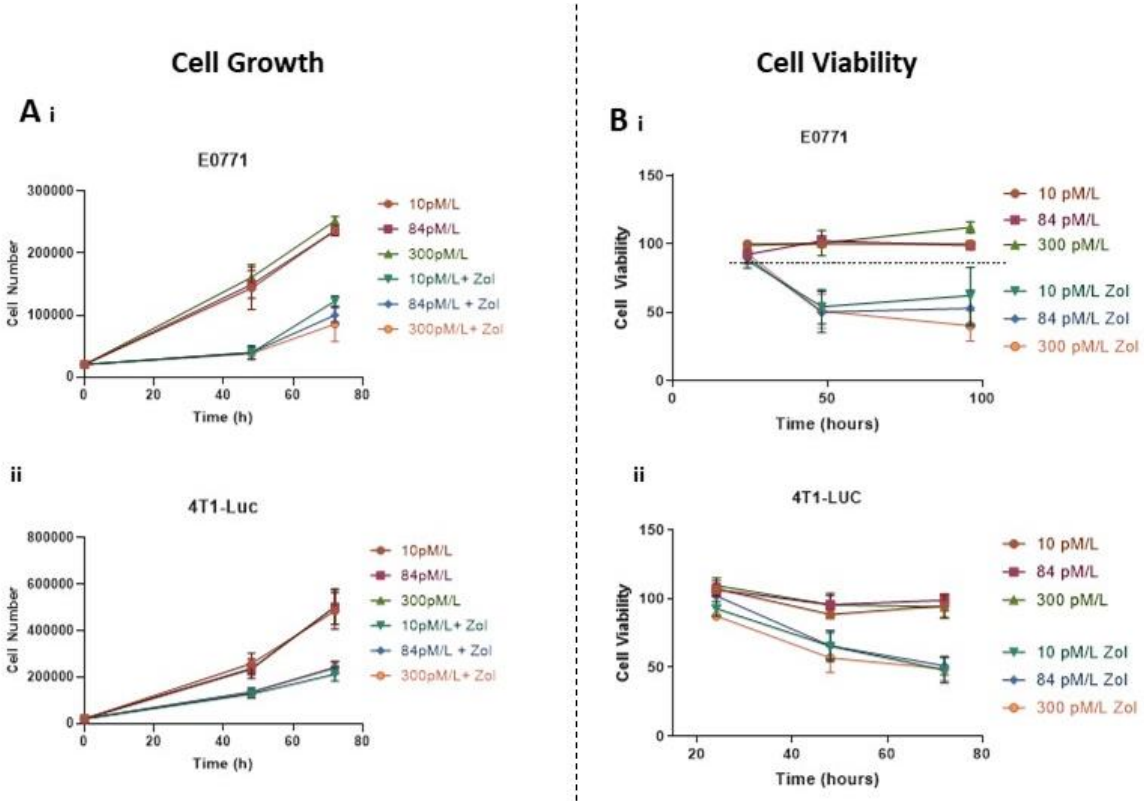

Figure 4.3: Figure 4.3: Effect of oestradiol at post (10 pM), peri (84 pM) and pre-menopausal (300 pM) concentrations on the anti-cancer effects of Zol in vitro.

The effects of the drug combination on (A) Cell Growth determined by cell counting and (B) on Cell Viability determined by MTT assay in the (i) E0771 and (ii) 4T1-LUC cells was analysed. Zol concentration of 15 µM (E0771) and 40 µM (4T1-LUC) was used.

Data are mean +/- SEM for n=3 experiments in triplicate (A) or sextuplet (B)

4.4 Effect of Zol and Oestrogen on migration and invasion of murine breast cancer cell lines

Previous studies have suggested that oestrogen can increase migration and invasion capabilities of oestrogen receptor negative breast cancer cell lines *in vitro,* acting through ER independent mechanisms. Therefore, after determining that oestradiol does not affect the ability of Zol to reduce tumour viability, the effect of oestradiol and Zol on the migratory capabilities of breast cancer cell lines was assessed by scratch assay (Figure 4.4). Tumour cell lines were treated with 10 pM/L, 84 pM/L and 300 pM/L of oestrogen in combination with control (PBS) or low concentration Zol (15 µM 4T1-LUC, 7.5 µM E0771); Lower concentrations were used compared with cell viability experiments to avoid cell death, enabling effects of oestradiol and Zol on migration to be determined. When E0771 cells were treated with Zol and oestradiol, neither treatment led to significant changes in cell migration as determined by scratch assay (Figure 4.4 Ai). However, treatment with Zol led to a trend towards decreased migration when administered along with post- and peri-menopausal concentrations of oestradiol but this decrease was not significant (Figure 4.4 Ai).

Unlike E0771 cells, 4T1 LUC cells appeared to show a trend towards an inverse correlation between oestradiol concentration and migration with post-menopausal concentrations of oestradiol promoting increased migration of cells across the scratch compared with pre-menopausal concentrations of this hormone, although this did not reach significance (Figure 4.4 Bi). Importantly, Zol did not affect migration of cells under pre- peri- or post-menopausal oestradiol concentrations (Figure 4.4 Bi). The lack of significance, either in the presence or absence of Zol, suggests that, even though oestradiol may excerpt effects on ER negative cells, its main action is likely mediated through other mechanisms.

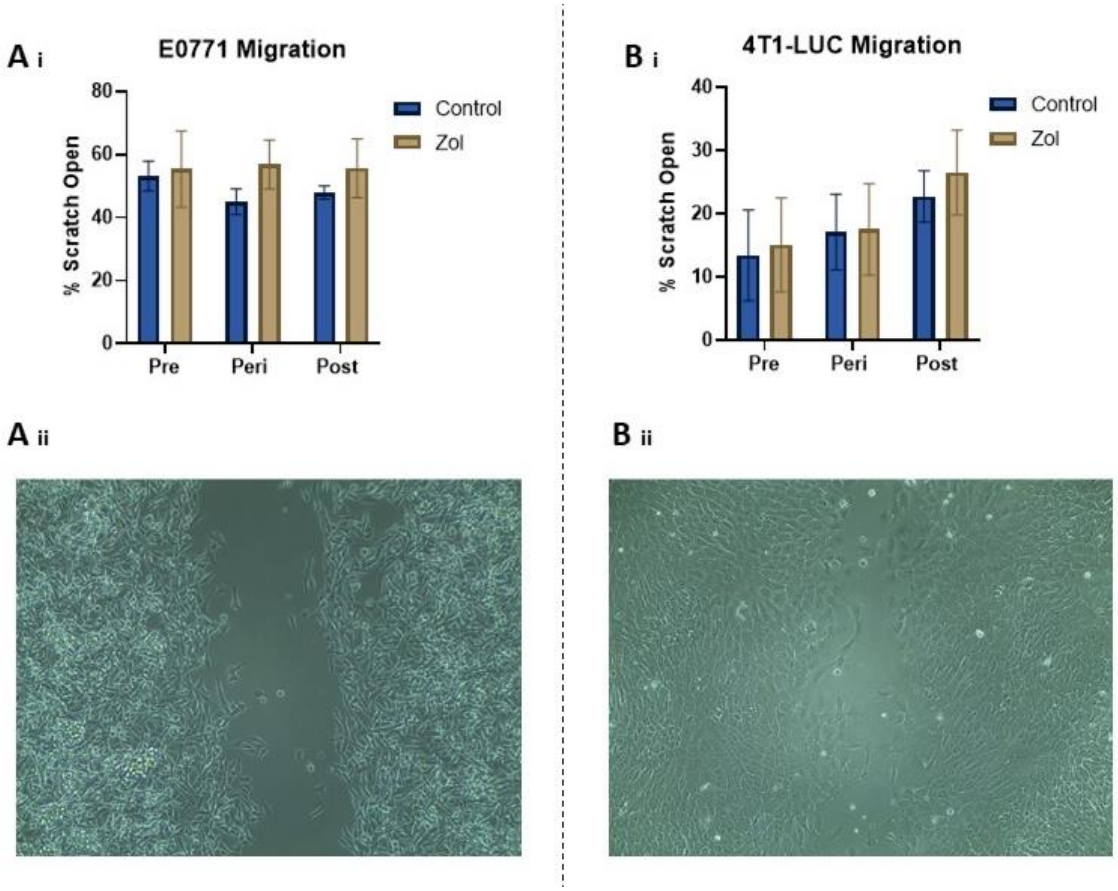

Figure 4.4: Effect of Zol and oestradiol on breast cancer migration at post (10 pM), peri (84 pM) and pre-menopausal (300 pM) concentrations after 24 h of treatment in (A) E0771 and (B) 4T1-LUC. Zol concentrations of 7.5 µM (E0771) and 15 µM (4T1-LUC) were used. (ii) Representative images of scratch assay taken at 24h.

Data are mean +/- SEM for n=3 experiments in duplicate

Statistical analysis performed by students T test and ANOVA with Tukeys post analysis.

Tumour cell invasion was quantified via trans-membrane, matrigel invasion assay following treatment with 10 or 300 pM of oestradiol, representing post- and pre-menopausal oestradiol concentrations respectively, in the presence or absence of Zol (15 µM 4T1-LUC, 7.5 µM E0771) (n=3). Data was normalised to post-menopausal control due to inter-experiment variation, preventing statistical analysis for either E0771 (Figure 4.5 Ai) or for 4T1-LUC (Figure 4.5 Bi) breast cancer cells. Although, both cell lines display a small trend towards decreased invasion following treatment with 300 pM of oestradiol when compared to cells treated with 10 pM, this trend did not come close to significance for either cell line (E0771 p=0.68, 4T1-LUC p=0.88). Taken together my *in-vitro* data supports the idea that differential anti-tumour effects observed between pre- and post-menopausal women treated with adjuvant Zol leading to improved DFS only in post-menopausal women are not due to oestrogen impeding direct anti-tumour effects of Zol against breast cancer cells but instead may be due to wider systemic or micro environmental effects.

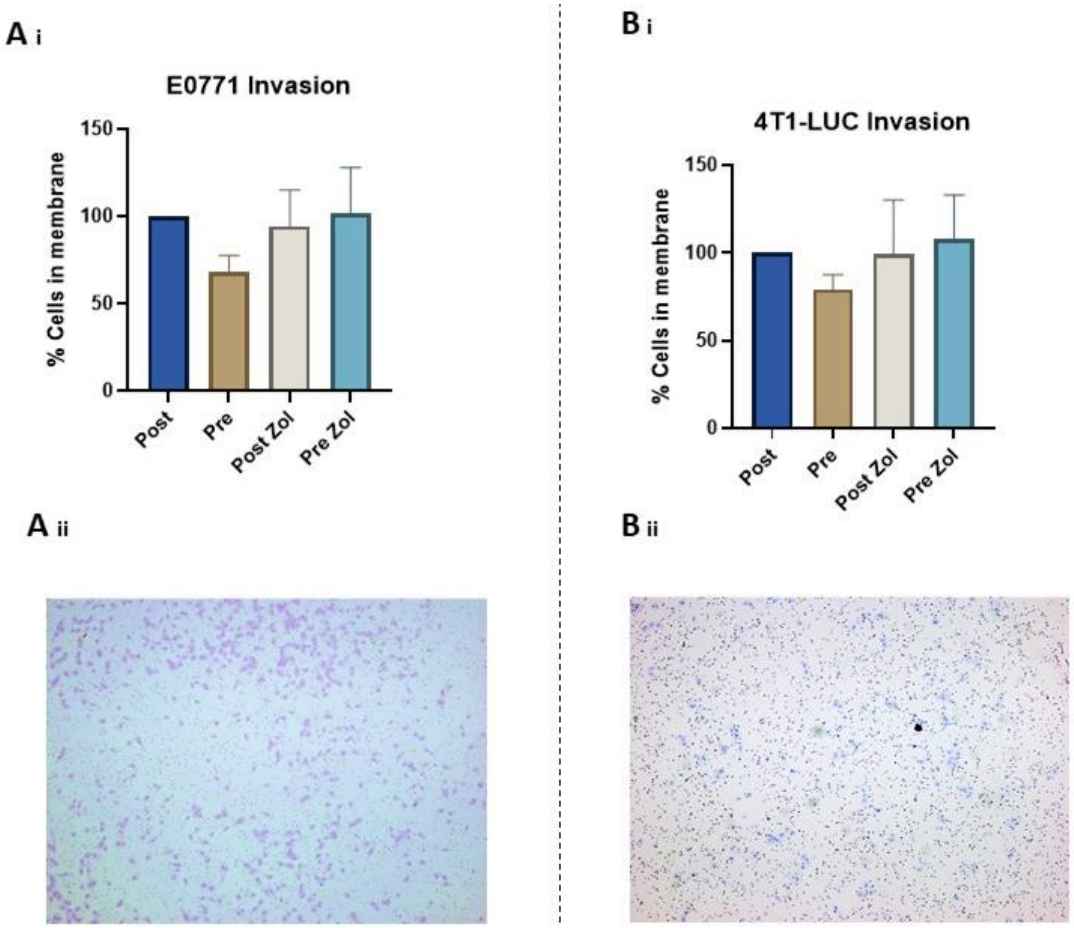

Figure 4.5: Effect of Zol and oestradiol on breast cancer invasion at post (10 pM), peri (84 pM) and pre-menopausal (300 pM) concentrations in (A) E0771 and (B) 4T1-LUCf Zol concentrations of 7.5 µM (E0771) and 15 µM (4T1-LUC) were used. (ii) Representative images of invasion assay. Invasion analysis was normalised to post-menopausal control due to inter-experiment variation, preventing statistical analysis.

Data are mean +/- SEM for n=3 experiments in duplicate

4.5 Discussion

4.5.1 Direct effect of Zol on murine breast cancer cell lines

Zol is used as an antiresorptive agent in the bone, preventing bone loss in osteoporosis and bone metastases. This effect is mediated through inducing apoptosis in osteoclasts (Hughes et al., 1995), caused by inhibiting the mevalonate pathway. The enzyme farnesyl diphosphate synthase is a target of Zol leading to a reduction in the isoprenylation of the small GTPase binding proteins Rho and Ras which are key is cell survival, proliferation and motility (Figure 1.4) (Denoyelle et al., 2003). The mevalonate pathway is ubiquitous across many cell types, including tumour cells, leading to Zol exerting direct anti-tumour effects in multiple cancer cell types *in vitro* (Oades et al., 2003). However, Zol has a short half-life in the circulation, disappearing after 1.87 hours, however this bisphosphonate rapidly targets the bone and remains bound to hydroxyapatite in this organ for many years (Dhillon, 2016). Zol has been shown to have anti-tumour effects within the bone in pre-clinical mouse models, decreasing tumour burden in bones and inducing tumour apoptosis (Zekri et al., 2014). Zol concentration within the bone remains higher than in the soft tissue as osteoclasts break down the bone releasing the bound Zol to the microenvironment. Whether or not Zol has direct anti-cancer effects in soft tissue in vivo remains controversial due to the lower circulating concentrations of Zol. To understand the action of oestradiol and Zol on tumour progression, we must check whether oestradiol has the potential to directly alter the anti-cancer effects of Zol. Firstly, the IC50 concentration for Zol killing tumour cells was determined to allow me to detect any alterations in anti-cancer effects of Zol when given in combination with different menopausal concentrations of oestradiol.

When cultured *in vitro*, using RPMI medium supplemented with 10% FBS, Zol induced anti-tumour effects against both E0771 and 4T1-LUC cell lines. Interestingly, the two methods of quantifying the efficacy of Zol against tumour cells, cell counting (to assess effects on numbers of tumour cells) and MTT assay (to assess tumour cell viability), produced different IC50 values for each cell line. Cell counting led to a lower IC50 than MTT for both E0771 and 4T1 cell lines. The method for cell counting requires detaching cells from their monolayer using trypsin-EDTA, a solution which can cause further cell death in cells and alterations in protein expression (Huang et al., 2010), therefore attenuating the toxic effects caused by Zol treatment. On the other hand, since results are normalised to the control, the effect of trypsin should be negligible. MTT assay and cell counting techniques both quantify different properties of the cells, with cell counting quantifying proliferation of cells and their survival, and MTT assay quantifying cell viability due to the need for the mitochondrial enzymes to create the detectable MTT product, formazan crystals.

IC50 for Zol in E0771 cells was 27.82 µM by MTT, and 43.54 µM for 4T1-LUC cells. These results are in agreement with previous studies showing the direct anti-tumour effect of Zol on the 4T1 cell line (Hiraga et al., 2004). Furthermore, previously published data have confirmed that Zol induced cell death is via the mevalonate pathway, since the addition of mevalonate pathway intermediates, GGOH and FOH, to cells was able to rescue 4T1 cells and reduce apoptosis (Hiraga et al., 2004). E0771 cells were more sensitive to Zol, having a much lower IC50 when compared to 4T1-LUC cells. Although not conclusive, one study suggests that the mevalonate pathway is more active in the E0771 cell line compared to 4T1 because of a required increase in cholesterol synthesis (Fan et al., 2020). However, more research is needed into this difference in response. Having established IC50s for Zol in E0771 and 4T1 breast cancer cell lines, next the possible interactions of oestradiol and Zol was explored. This was to investigate whether or not the negative effects of oestradiol on the anti-tumour effects of Zol seen in clinical trials are due to the direct action of Zol and oestradiol on tumour cells.

4.5.2 Influence of oestradiol on Zol induced tumour cell death in murine breast cancer cell lines

Clinical trials and pre-clinical studies showed that the efficacy of Zol for improving disease free survival in breast cancer patients is restricted to post-menopausal women or women rendered chemically post-menopausal with tamoxifen or goserelin, which suggests an inhibitory role of oestradiol on the anti-tumour effects of Zol (George et al., 2020) (Ottewell and Wilson, 2019) (Coleman et al., 2014b). Therefore, potential direct effects of oestradiol on Zol induced tumour cell death were investigated *in vitro*. Concentrations of oestradiol comparable to those found in post (10 pM/L), peri (84 pM/L) and pre (300 pM/L) menopausal women were added to phenol free growth medium +/- Zol IC50 for each cell line. The effect of oestradiol and Zol was analysed for both cell number by cell counting and cell viability by MTT assay. Interestingly, oestradiol had no significant effect on either tumour cell number or viability at any menopausal concentration, with growth curves in the absence of Zol following similar patterns to the growth curves in the absence of oestradiol. Oestradiol concentrations also had no significant effect on Zol induced cell death, shown by both cell counting and cell viability. However, Zol did not kill all the tumour cells, instead reducing cell number to significantly lower levels than their untreated counterparts.

Since both E0771 and 4T1-LUC are ERα negative breast cancer cell lines, it was expected that oestradiol would not have direct tumour promoting effects, confirming their oestradiol insensitive phenotype. Although the 4T1-LUC cell line is robustly triple negative in phenotype (Schrörs et al., 2020), the E0771 cell line is able to respond to oestradiol via the ERβ receptor, which it has been shown to be expressed at both the transcription and protein levels (Le Naour et al., 2020). Therefore,

this study classified E0771 as a luminal B subtype, one that is often associated with poor prognosis in patients. On the other hand, other studies into the classification of the E0771 cell line have found the cells to be negative for ERα by immunohistochemistry, but reference that there can be a discordance between data analysed by transcriptional profiling and immunohistochemistry, casting uncertainty into the classification of the E0771 cell line (Johnstone et al., 2015). Therefore, understanding the direct effects of oestradiol on the E0771 cell line in regard to cell proliferation and viability are vital in understanding if the effects observed in our *in vivo* experiments are attributed to the microenvironment or to direct actions of oestradiol and Zol on the breast cancer cell lines.

4.5.4 Influence of oestradiol and Zol on tumour cell migration and invasion in murine breast cancer cell lines.

Adjuvant Zol in combination with standard of care treatment reduced recurrence of tumours in soft tissue over a 5-10 year period in post-menopausal women but not pre-menopausal women. I therefore investigated whether Zol could directly affect the ability of tumour cells to migrate and invade (i.e. spread) under pre- and post-menopausal concentrations of oestradiol. Murine breast cancer cell lines were treated with concentrations of Zol that would not affects cell number or cell viability so that effects on migration or invasion could be isolated. Concentrations were taken from the IC50 experiments presented at the start of this chapter using the 48 hour time point as reference with the aim for Zol to be at the highest concentration possible without affecting cell viability. The lower concentrations of Zol used (15 µM 4T1-LUC, 7.5 µM E0771) are still higher than concentrations between 0.4 µM and 4.6 µM measured in the bone marrow following Zol administration of a 2-4 mg dose (Scheper et al., 2009). Scratch assay to determine migration following treatment with Zol at pre-, peri- and post-menopausal concentrations of oestradiol found no significant differences in migration between any treatment group. However, in the 4T1-LUC cell line, there was a strong correlation between oestradiol concentration and cell migration, with higher concentration of oestradiol leading to increased cell migration. This effect was not observed in the E0771 cell line, where oestradiol led to no trend, but Zol led to a small trend towards decreasing cell migration. Interestingly, Zol and oestrogen had no significant effect on cell invasion for either cell line, determined by trans-well matrigel assay.

4T1-LUC does not express the ERα receptor and is considered a triple negative cell line. However, as previously discussed, it has been reported that 4T1 cells can respond to oestradiol via an ER independent mechanism. Following treatment with oestradiol *in vitro*, cells had increased invasive and migratory capability when compared to untreated cells (Yang et al., 2013). Furthermore, Western

blot showed that there was no ER expression in these cells, while ER blockade with the antagonist ICI 182,780 did not significantly affect the increase in migration. The trend from our scratch assays for migration mirror the results observed in these experiments but never reached significance. However, Yang *et al,* (2013) used very high concentrations of oestradiol for their *in vitro* experiments, between 1-100 nM, that are much higher than physiological concentrations normally observed in the menopause and are up to 1000x higher that the oestradiol concentrations used in our *in vitro* experiments. This difference may account for the lack of significance observed in the migration data for the 4T1 cell line.

Since the 4T1 cell line do not express ER, it has been suggested that the effects are mediated through an ER independent mechanism. One such mechanism may be the GPER-1, a G protein coupled receptor able to bind oestradiol via protein-protein interaction on the cell surface and transduce a non-genomic signalling pathway. Indeed, GPER has been found in the MDA-MB-468 cell line where oestradiol mediated signalling via the ERK pathway was found to be involved in cell viability and motility (Yu et al., 2014). This was found to be due to rapid activation of the pERK, increasing the migration and invasion of cells by upregulating expression of cyclin-A, cyclinD1, Bcl-2 and c-fos. On the other hand, signalling through GPER-1 has also been shown to have a tumour supressing effect. When using G1 as a GPER-1 agonist, it was found to inhibit TNBC cell growth via induction of cell cycle arrest in the G2/M phase (Weißenborn et al., 2014). Furthermore, a more recent study found that GPER-1 activation by oestradiol could inhibit invasion, migration, proliferation and angiogenesis of TNBC cell lines by acting on the CD151/miR-199a-3p bio axis (Huang et al., 2020). These conflicting reports lead to confusion about the role of GPER-1 in TNBC development, prompting the need for further study into the complex role of GPER-1 signalling in breast cancer.

4.6 Summary and conclusion

We hypothesised that the differential effects of Zol under pre- and post-menopausal concentrations of oestrogen on breast cancer metastasis, observed in humans and *in vivo* experiments (chapter 3), were likely to be due to their effects on the tumour microenvironment including immune cell regulation, and not down to direct effects on tumour cells. My data show that Zol has direct effects on number and viability of murine breast cancer cell lines, with E0771 cells being more sensitive to Zol than 4T1-LUC cells. Oestradiol had no significant effect on this action of Zol *in vitro* at any concentration, helping to confirm the hypothesis that Zol and oestrogen are active via indirect mechanisms to affect tumour progression and metastasis. On the other hand, higher concentrations of oestradiol led to a trend towards increased migratory capacity of the triple negative 4T1-LUC cell

line, suggesting that oestradiol may have an ER independent mechanism of action for these cells. However, these insignificant effects suggest that another, indirect mechanism of action is likely affecting breast cancer metastasis. Importantly, oestradiol did not alter the effects of Zol under any conditions, in vitro, suggesting that any interactions that may occur between oestradiol and Zol impeding the ability of Zol to promote anti-tumour effects are likely to be driven through regulation of the microenvironment. Future experiments in my thesis therefore focus on systemic investigation into the tumour microenvironment and immune cell regulation.

Chapter 5: Investigating the effect of Zol and oestradiol on anti-cancer immunity

5.1 Introduction

Zol and oestradiol have been shown to effect breast cancer metastasis, and previous chapters have shown that these actions are not down to direct effects of these compounds/hormones on breast cancer cells. In the clinical trials AZURE and ABCSC-12, Zol was shown to decrease breast cancer to bone metastasis irrespective of menopause (Coleman et al., 2014a; Gnant et al., 2011). However, in the AZURE trial whilst post-menopausal patients additionally benefitted from adjuvant Zol with reduced soft tissue metastasis, patients with pre-menopausal serum concentrations of oestradiol were adversely affected displaying increases soft tissue metastasis (Wilson et al., 2016b). *In vitro* experiments in chapter 4 showed that treating murine breast cancer cell lines with oestradiol alongside Zol did not alter the cytotoxic effects of Zol or effects on breast cancer migration. Furthermore, in tumour bearing mice rendered post or pre-menopausal by ovx +/- oestradiol administration, Zol treatment reduced bone metastasis in both BALBc wild type (chapter 3) and BALBc nude mice mimicking outcomes of the AZURE and ABCAC-12 trials (Canuas-Landero et al., 2021). Zol also increased soft tissue metastasis in C57BL6 mice with pre-menopausal concentrations of serum oestradiol, mimicking data from the AZURE trial. Therefore, as oestradiol does not alter the anti-tumour effects of Zol *in vitro,* it is likely that the effects observed in the clinic and in animal models are mediated via microenvironmental action of oestradiol and Zol. Interestingly, administration of Zol to mice with post-menopausal serum oestradiol concentrations did increase bone volume compared to untreated but did not restore bone volume to pre-menopausal levels (Canuas-Landero et al., 2021). This suggests that the anabolic effects of oestradiol are stronger than the anti-resorptive effects of Zol, a differential that may lead to the movement of tumour cells out of bone to circulation. However, it is clear that the effects of oestradiol and Zol on the bone alone does not fully account for the clinical effects seen.

Reducing concentrations of oestradiol to that seen in post-menopausal mice led to an increase in soft tissue metastasis in the immunocompetent mouse models but did not have the same effect in the immunocompromised BALBc Nude. Treatment with Zol followed the same trend, having no significant effects in immune compromised mice, suggesting the involvement of the immune system in the regulation of soft tissue metastasis (Canuas-Landero et al., 2021). In addition, there is amassing evidence showing that Zol and oestradiol have significant and often opposing effects on immune regulation (Introduction section 1.14-1.15) (George et al., 2020). Therefore, I hypothesise that immunological factors are a primary regulator of oestrogen and Zols interaction with metastasising breast cancer cells.

Breast cancer progression and metastasis are profoundly affected by the innate and the adaptive immune systems. Cancer cells undergo genetic and epigenetic alterations leading to changes in cell surface proteins that can be recognised by the immune system, leading to cancer cell death (Pinho and Reis, 2015; Pio et al., 2014). Therefore, cancer cells employ immune modulatory techniques to evade detection, such as upregulation of PD-L1, stimulation of immunosuppressive Treg cells and the polarisation of macrophages into a pro-tumour phenotype (George et al., 2020).

B cells are members of the adaptive immune system responsible for the production of antibodies and have been shown to express ERs. B cells can respond to oestradiol signalling, leading to upregulation of genes cd22, shp-1, bcl-2, and vcam-1, involved in B cell activation and survival (Grimaldi et al., 2002). Furthermore, oestrogen has been shown to have a stimulatory effect on B cells, immunoglobulin (Ig)G and IgM production (Kanda and Tamaki, 1999). IgM represent an important molecule in the suppression of breast cancer progression, leading to direct cytotoxic effects via activation of complement. There is little research into the direct effects of Zol on B cell activity, development, or survival. However, one study, which treated mice with Zol and analysed B cell numbers, found that treatment led to a decrease in B cell number in the bone marrow but did not directly affect differentiation, proliferation and apoptosis (Mansour et al., 2011). These results show the need for more research into the effects of oestradiol and Zol on B cells in cancer.

The overlapping effects of oestradiol and Zol on the immune response to breast cancer, across many cell types, could be one mechanism whereby high oestrogen reduces the survival benefit of Zol treatment. Overall, the literature points to oestradiol promoting a pro-tumour immune cell microenvironment and Zol promoting an antitumour immune cell population. Therefore, investigating the influence of Zol and Oestradiol on the immune populations in different metastatic sites (bone, soft tissue, systemic) could elucidate the cell types responsible for the menopause related differences.

5.1.2 Hypothesis

Zol and oestradiol have opposing effects on anti-cancer immunity in the bone and soft tissue.

Aims

1. To investigate immune cell populations in the bone, lung and spleen following treatment with Zol under post- peri and pre-menopausal oestradiol concentrations.
2. To investigate the effect of Zol and oestradiol on PD-L1 expression on tumour cells and in the tumour microenvironment.

5.2 Results

5.2.1 Context from *in vivo* tumour growth and clinical trials

The effects of oestradiol and Zol on tumour growth in the bone and soft tissue microenvironments differed between C57BL/6 injected with E0771 cells and BALB/c mice injected with 4T1 cells: Following injection of E0771-LUC cells tumour burden was less in the bones of C57BL/6 mice administered pre-menopausal concentrations of oestradiol compared with those given post-menopausal concentrations of this hormone (Figure 3.6). Whereas the opposite was seen in the bones of BALB/c mice following injection of 4T1 cells. Interestingly, administration of Zol to BALB/c mice appeared to mimic clinical findings associated with bone metastasis accurately, resulting in a trend towards reduced metastatic burden in bone independent of circulating oestradiol and significantly reduced bone metastases in mice supplemented with post-menopausal concentrations of oestradiol (Figure 3.6). In contrast Zol did not reduce tumour burden in the bones of C57BL/6 mice and under post-menopausal concentrations of oestradiol Zol increased tumour burden.

In addition to replicating the clinical effects of Zol on tumour growth in bone the 4T1 BALB/c model also replicated data from the ABCSG12 and AZURE trials showing reduced soft tissue metastases following administration of Zol under post-menopausal concentrations of oestradiol (Coleman et al., 2014b; Gnant et al., 2011) (Figure 3.7). Interestingly, in this model Zol induced increased soft tissue metastases under pre-menopausal oestradiol and reduced soft tissue metastases under post-menopausal oestradiol in C57BL/6 mice, accurately replicating the data presented from the AZURE trial. Whereas in BALBc mice with 4T1 derived metastasis soft tissue metastases were not increased following administration of Zol under pre-menopausal concentration of oestradiol, replicating data from the ABCSG-12 trial (Figure 3.7). I hypothesised that differential anti-tumour effects of Zol observed between BALB/c and C57BL/6 mice may be due to different anti-tumour immune responses generated in these mice under pre- peri- and post-menopausal concentrations of oestradiol.

5.3 Effects of Zol +/- post- peri or pre-menopausal concentrations of oestradiol on immune cells in Bone metastases.

5.3.1 C57BL/6 Mice with E0771 derived metastases

C57BL/6 mice underwent OVX followed by oestrogen replacement to model pre, peri and post-menopausal serum oestradiol concentrations before intracardiac injection of 100,000 E0771-LUC cells. Mice were treated with Zol or PBS control and the effects on immune cell populations in

metastatic tumour sites was analysed by flow cytometry, Nanostring, PCR array plate analysis and immunohistochemistry. As shown in chapter 3, oestradiol in the absence of Zol led to a significant increase in the numbers of bone tumours, while showing a trend towards increase in tumour size in bone. Treatment with Zol led to a significant increase in bone tumour number in post-menopausal mice but had no effect on tumour size. I investigated whether changes in tumour growth may be mediated by changes in immune cells within the bone microenvironment.

When mice were treated with high concentrations of oestradiol, it resulted in a strong trend decrease in B cells within the bone when compared to low oestradiol ($P = 0.056$) (Figure 5.1H), alongside a trend towards decreased neutrophils (Figure 5.1B). This decrease in anti-tumour immune cells in the bone under low oestradiol concentrations could account for the reduced tumour burden in the bone observed under low oestradiol concentrations. Administration of Zol to mice with high oestradiol concentration significantly decreased macrophage numbers in the bone ($P=0.035$), mirroring clinical findings showing Zol as less effective in pre-menopausal women. Administration of Zol to mice with low serum oestradiol significantly decreased PD-1 expression on CD8 T cells ($P = 0.0105$) (Figure 5.1L), suggesting a reduced capacity for these cells to be inactivated by PD-L1 signalling. This could help to further promote an anti-tumour phenotype within the bone microenvironment. Under high concentrations of oestradiol, treatment with Zol resulted in a trend towards increased M1 macrophage numbers (Figure 5.1E). Furthermore, administration of Zol to mice supplemented with high oestrogen resulted in a trend towards decreased PD-1 expression on CD8 T cells (Figure 5.1L), altogether promoting an anti-tumour phenotype in the bone following Zol treatment. However, in the presence of Zol, high concentrations of oestradiol led to a trend towards reduced numbers of anti-tumour NK cells (Figure 3.1K), B cells (Figure 5.1H) and dendritic cells (Figure 5.1A) in the bone. This suggests that, even though Zol is acting to increase anti-tumour immune cells in the bone, oestradiol can still exert pro tumour, anti-immune cell effects reducing the capacity of Zol to inhibit bone metastasis in this model.

Analysis of immune cell associated gene expression in bone tumours by qPCR array reviled no significant changes in immune cell types or in markers of immune cell activity (appendix). However, CD274, the gene encoding PD-L1, showed a trend towards increased expression in mice with high oestradiol compared to low when treated with Zol (Figure 5.2), suggesting the increased PD-L1 expression could inhibit anti-tumour immune responses under high oestradiol concentrations.

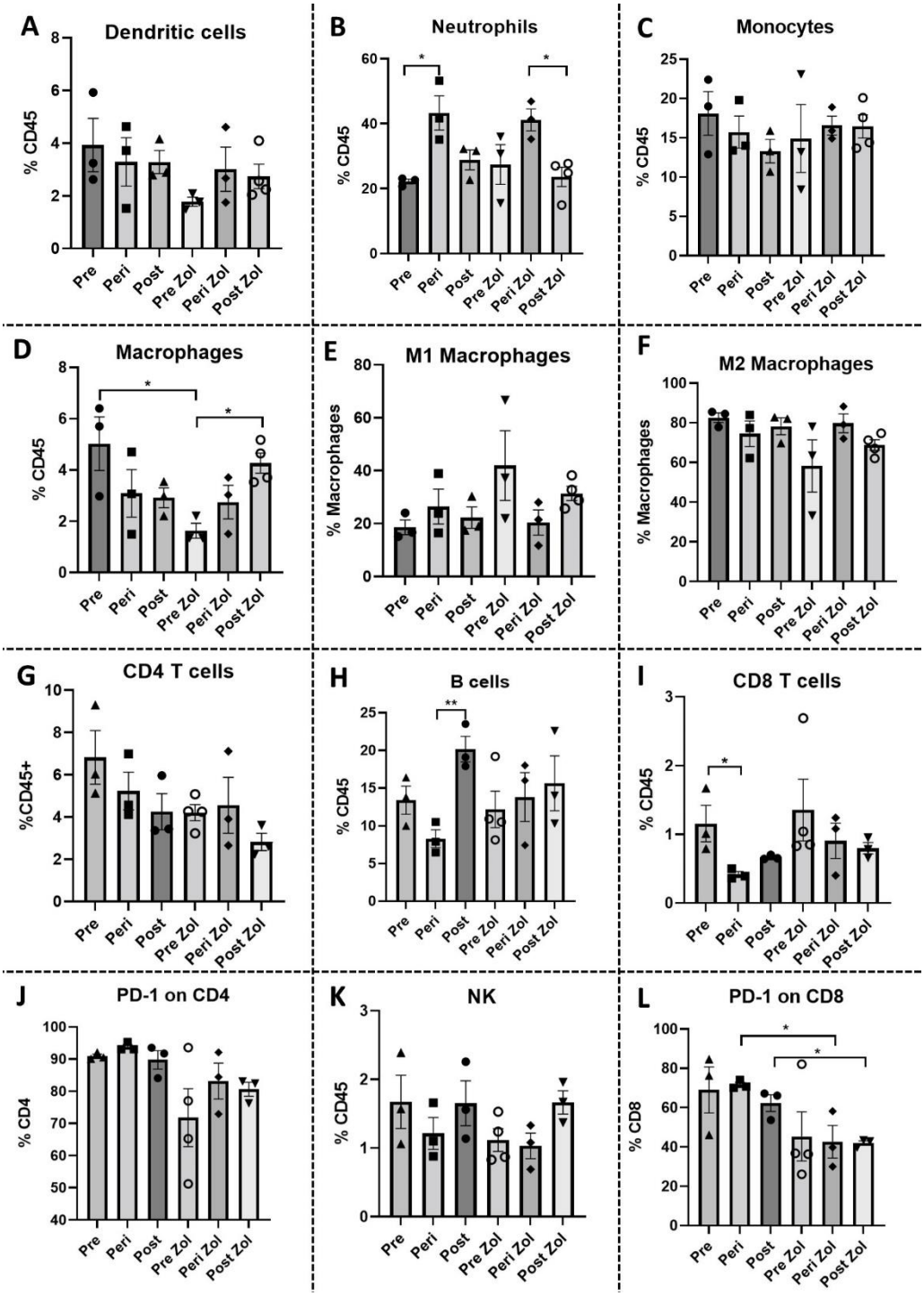

Figure 5.1: Effect of Zol treatment under high and low oestradiol concentrations in C57BL/6 mice with E0771 tumours on immune cell populations in bone.

Mice were treated with Zol under post, peri and pre-menopausal concentrations of oestradiol. Bones were flushed of cells ex vivo before staining with fluorescently labelled antibodies. Cells were analysed by flow cytometry and cell types were separated according to specific markers present. (A) Dendritic cells (CD45+,CD11b+,CD11c+,MHCII+) (B) Neutrophils (CD45+,CD11b+,Ly6G+), (C) Monocytes (CD45+,CD11b+,LY6G-,LY6C+,F480 High,) (D) Macrophages (CD45+,CD11b+,LY6G-,LY6C Low, F480 High), (E) M1 Macrophages (Macrophage, MRC1-), (F) M2 Macrophages (Macrophage, MRC1+), (G) CD4+ T cells (CD45+,CD19-,CD3+,CD4+), (H) B Cells (CD45+,CD19+,CD3-), (I) CD8+ T cells (CD45+,CD19-,CD3+,CD8+) (J) PD-1 on CD4+ T cells (CD4 T cells, PD-1+), (K) NK cells (CD45+,CD19-,CD3-, NK1.1+), (L) PD-1 on CD8+ T cells (CD8 T cells, PD-1+).
Mean ± SEM Statistical analysis by one way ANOVA and students T test
*< 0.05, ** < 0.01, *** < 0.001, **** < 0.0001

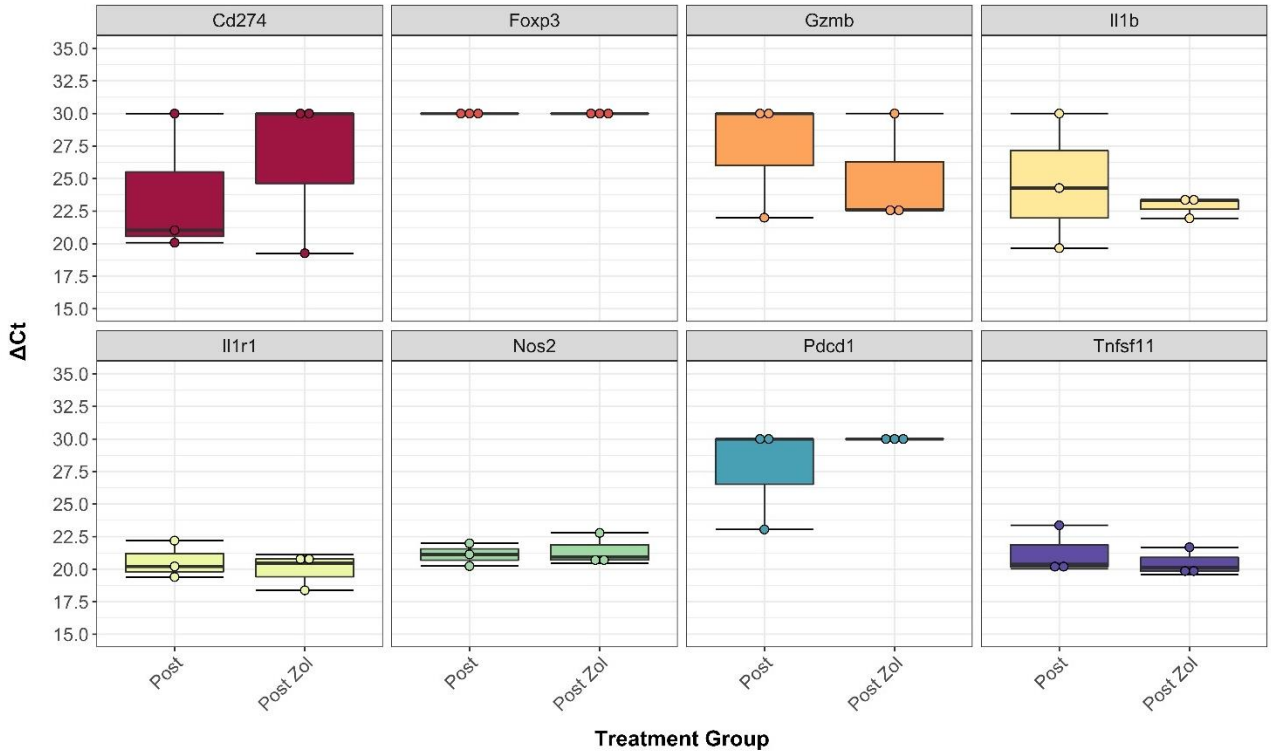

Figure 5.2: Effect of Zol treatment under high and low oestradiol concentrations in C57BL/6 mice with E0771 tumours on immune related genes in bone.

Mice were treated with Zol under post, peri and pre-menopausal concentrations of oestradiol. Bones were lysed and RNA extracted before reverse transcription was performed. cDNA analysis was performed by qPCR array card for immune cell activity markers.
n=3 per group

Mean ± SEM Statistical analysis by one way ANOVA and students T test
*< 0.05, ** < 0.01, *** < 0.001, **** < 0.0001

5.3.2 BALBc mice with 4T1 derived bone metastases

Tumour number and tumour growth followed a different pattern in the BALBc mouse model compared to the C57BL/6 model, as shown in chapter 1. Mice with low oestradiol concentrations had significantly higher bone tumour size compared to low oestrogen mice. Treatment of mice with Zol led to a trend towards decreased tumour number in irrespective of oestradiol concentration. Furthermore, administration of Zol to mice with low oestradiol led to a decrease in tumour size in the bone, a differential response that could be reflected in the immune cell profiling. Interestingly, under high levels of oestradiol when compared to low levels, there was a trend towards increased anti-tumour CD4+ T cells (Figure 5.3 G) and CD8+ T cells (Figure 5.3 I) in the absence of Zol. Nanostring analysis of gene expression showed a significant decrease in mast cells (P = 0.0406) (Figure 5.4) but significant increase in anti-tumour CD8+ T cells (P = 0.00715) (Figure 5.4) and macrophages (P =

0.00154) (Figure 5.4) under high concentrations of oestradiol. This could contribute to the higher tumour volume observed in mice with low circulating oestradiol. Flow cytometry analysis showed that high oestradiol concentrations compared to low oestradiol concentrations in Zol treated mice led to significantly higher CD4+ T cells (P=0.0066) (Figure 5.3 G) and CD8+ T cells in the bone (P = 0.0027) (Figure 5.3 I). However, high oestradiol also led to a trend towards decreased B cells (Figure 5.3 H) in the bone of non Zol treated mice and a significant decrease in B cells (P = 0.0201) in the bone of Zol treated mice.

Zol treatment significantly increased anti- tumour CD8+ T cells in bone under high oestradiol concentrations (P=0.037) (Figure 5.3 I). Nanostring analysis of bones bearing metastatic tumours isolated from mice that had been supplemented with high concentrations of oestradiol showed that Zol treatment led to a decrease in anti-tumour Th1 cells (P = 0.0193) (Figure 5.5) and an increase in pro-tumour Treg cells (P = 0.0467) compared with non-Zol treated mice (Figure 5.5), which would promote a pro-tumour environment in the bones of mice with high oestradiol when treated with Zol. Administration of Zol in the absence of oestradiol led to decreased bone tumour volume as assessed by live imaging. Flow cytometry revealed no significant differences in immune cell populations following Zol treatment under low oestradiol in these mice, however, Nanostring analysis found that Zol treatment led to a significant increase in macrophages (P = 0.00493) (Figure 5.5) and a trend towards an increase in B cells (Figure 5.5) in the bone. This increase in anti-tumour immune cells in bone following Zol may contribute to the reduced metastasis observed in mice with low oestradiol.

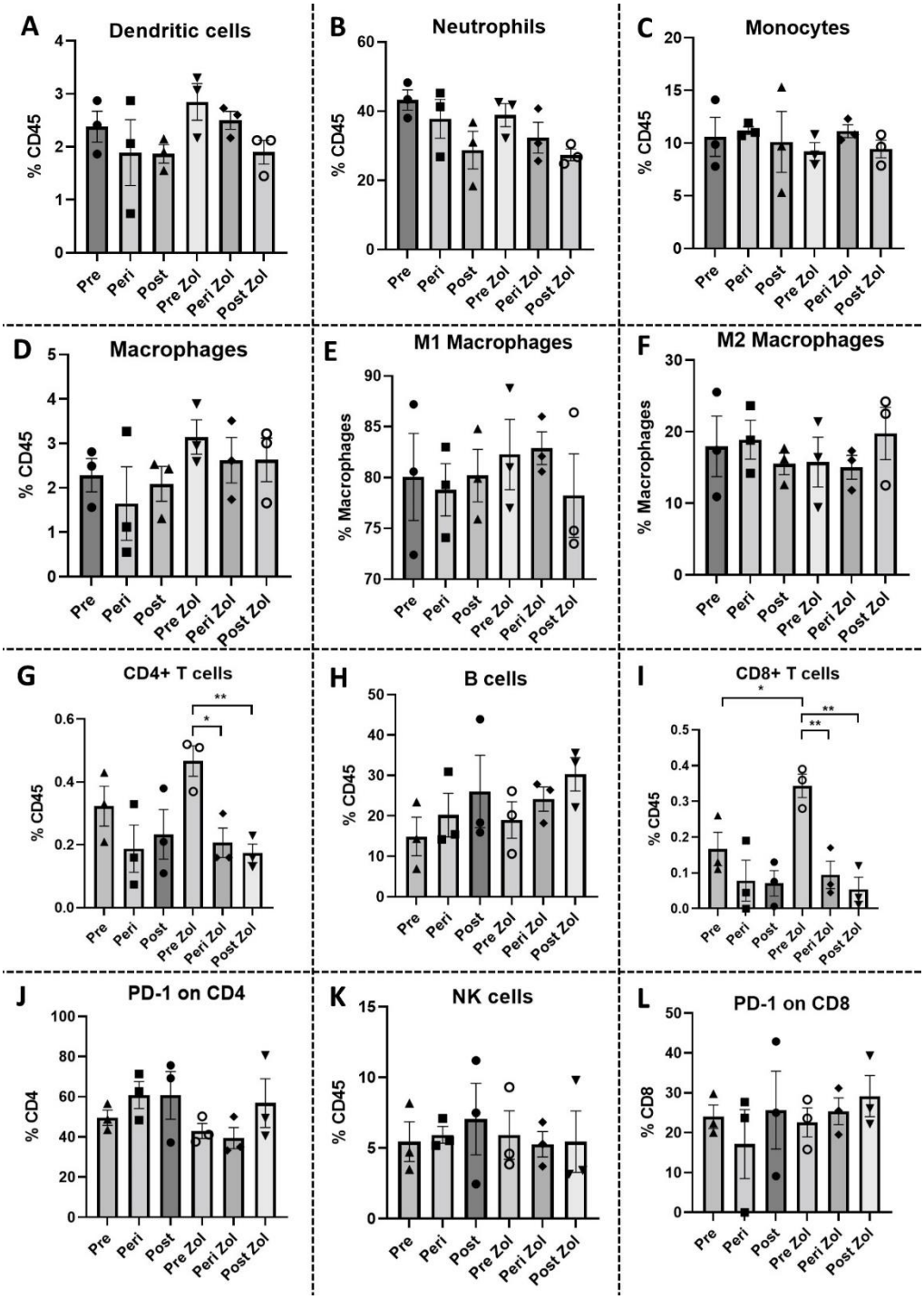

Figure 5.3: Effect of Zol treatment under high and low oestradiol concentrations in BALBc mice with 4T1-LUC tumours on immune cell populations in bone.

Mice were treated with Zol under post-, peri- and pre-menopausal concentrations of oestradiol. Bones were flushed of cells ex vivo before staining with fluorescently labelled antibodies. Cells were analysed by flow cytometry and cell types were separated according to specific markers present. (A) Dendritic cells (CD45+,CD11b+,CD11c+,MHCII+) (B) Neutrophils (CD45+,CD11b+,Ly6G+), (C) Monocytes (CD45+,CD11b+,LY6G-,LY6C+,F480 High,) (D) Macrophages (CD45+,CD11b+,LY6G-,LY6C Low, F480 High), (E) M1 Macrophages (Macrophage, MRC1-), (F) M2 Macrophages (Macrophage, MRC1+), (G) CD4+ T cells (CD45+,CD19-,CD3+,CD4+), (H) B Cells (CD45+,CD19+,CD3-), (I) CD8+ T cells (CD45+,CD19-,CD3+,CD8+) (J) PD-1 on CD4+ T cells (CD4 T cells, PD-1+), (K) NK cells (CD45+,CD19-,CD3-, NK1.1+), (L) PD-1 on CD8+ T cells (CD8 T cells, PD-1+).
Mean ± SEM Statistical analysis by one way ANOVA and students T test
*< 0.05, ** < 0.01, *** < 0.001, **** < 0.0001

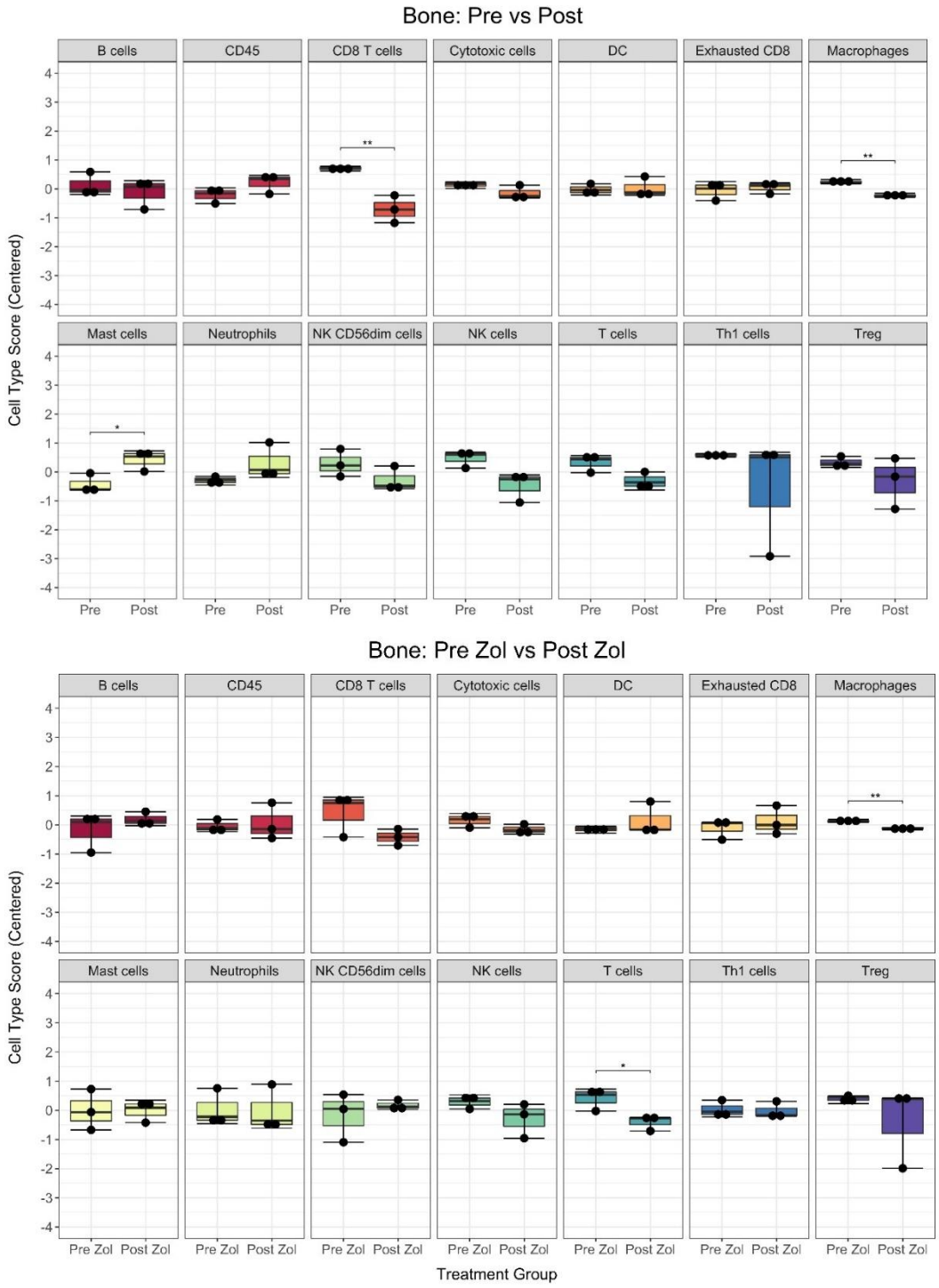

Figure 5.4: Effect of high or low oestradiol concentrations on immune cell populations +/- Zol in tumour bearing bones from BALBc with 4T1-LUC tumours.

Mice were treated with post- and pre-menopausal concentrations of oestradiol +/- Zol. Nanostring analysis was performed on RNA extracted from bones for immune cell markers. B Cells: Blk, Cd19, Ms4a1, Tnfrsf17, CD8 T cells: Cd8a, Cd8b1, Cytotoxic cells: Ctsw, Gzma, Gzmb, Klrb1, ,Klrd1, Klrk1, Prf1, Dendritic Cells: Ccl2, Cd209e, Hsd11b1, Exhausted CD8: Cd244, Eomes, Lag3, Macrophages: Cd163, Cd68, Cd84, Mast cells: Ms4a2, Neutrophils: Csf3r, Fcgr4, NK cells: Il21r, Ncr1, Xcl1, T cells: Cd3d, Cd3e, Cd3g, Cd6, Sh2d1a, TH1: Tbx21, Treg: Foxp3, CD25.

Mean ± SEM Statistical analysis by one way ANOVA *< 0.05, ** < 0.01, *** < 0.001, **** < 0.0001

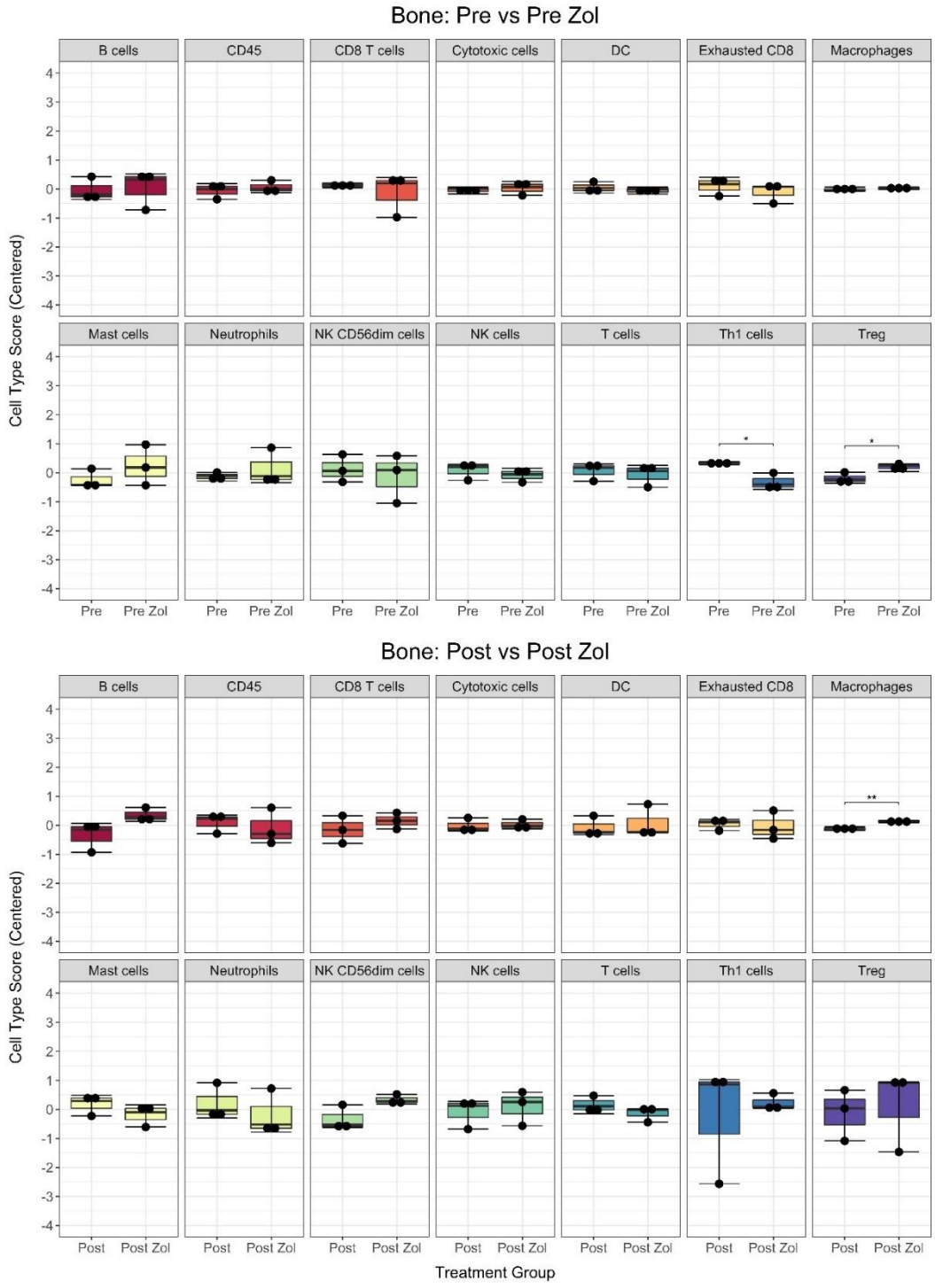

Figure 5.5: Effect of Zol under high or low oestradiol concentrations on immune cell populations in tumour bearing bones from BALBc with 4T1-LUC tumours.

Mice were treated with post- and pre-menopausal concentrations of oestradiol +/- Zol. Nanostring analysis was performed on RNA extracted from bones for immune cell markers. B Cells: Blk, Cd19, Ms4a1, Tnfrsf17, CD8 T cells: Cd8a, Cd8b1, Cytotoxic cells: Ctsw, Gzma, Gzmb, Klrb1, ,Klrd1, Klrk1, Prf1, Dendritic Cells: Ccl2, Cd209e, Hsd11b1, Exhausted CD8: Cd244, Eomes, Lag3, Macrophages: Cd163, Cd68, Cd84, Mast cells: Ms4a2, Neutrophils: Csf3r, Fcgr4, NK cells: Il21r, Ncr1, Xcl1, T cells: Cd3d, Cd3e, Cd3g, Cd6, Sh2d1a, TH1: Tbx21, Treg: Foxp3, CD25.

Mean ± SEM Statistical analysis by one way ANOVA *< 0.05, ** < 0.01, *** < 0.001, **** < 0.0001

5.4 Effects of Zol +/- post- peri- or pre-menopausal concentrations of oestradiol on immune cells in lung metastases.

5.4.1 C57BL/6 Mice with E0771 derived lung metastases

Soft tissue metastasis has been shown to be increased by Zol in pre-menopausal women in the AZURE trial, and is the site where menopausal differences in treatment outcome manifest. In the C57BL/6 mouse model with E0771-LUC cells, numbers of soft tissue metastasis did not change at any oestradiol concentration, irrespective of Zol treatment. On the other hand, tumour volume was significantly affected by oestradiol and Zol, with low concentrations of oestradiol resulting in increased soft tissue metastases in control mice. This increased metastasis in mice with low oestradiol was significantly reduced by Zol treatment. Furthermore, soft tissue metastasis in Zol treated mice with high oestradiol concentrations was significantly increased when compared to control mice with high oestradiol, accurately mimicking clinical data from the AZURE trial, as discussed in chapter 1. When comparing changes in the immune cell populations in tumour bearing lungs of C57BL/6 mice by flow cytometry, there were only minor, insignificant changes following treatment with oestradiol and Zol. High oestradiol concentrations in control mice resulted in a trend towards increased neutrophils (Figure 5.6 B). Zol treatment led to no significant changes in immune cell population in the lung at either high or low oestradiol concentrations in C57BL/6 mice, displaying a minor trend towards increased monocytes (Figure 5.6 C) in pre-menopausal mice, suggesting a minor increase in anti-tumour immune cells in the lung following Zol treatment. Analysis of the transcriptome of tumour bearing lungs by qPCR array following treatment reviled no significant changes in immune cell activity markers or cell type analysis. However, high concentrations of oestradiol in the absence of Zol led to a trend towards increased Foxp3 expression, a marker of Treg cell infiltration and activity.

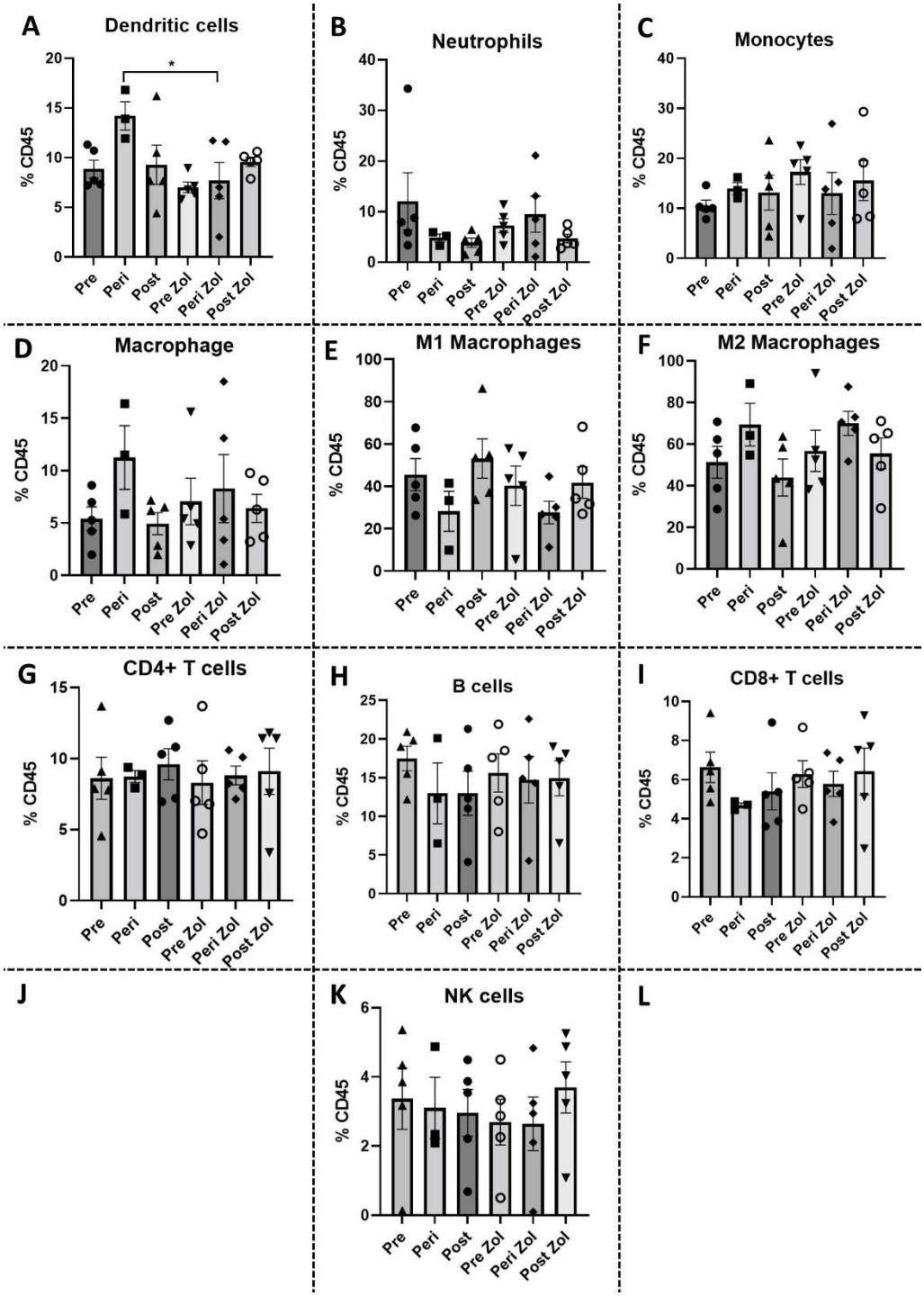

Figure 5.6: Effect of Zol treatment under high and low oestradiol concentrations in C57BL/6 mice with E0771 tumours on immune cell populations in lung.

Mice were treated with Zol under post, peri and pre-menopausal concentrations of oestradiol. Lungs were dissociated before ex vivo before staining with fluorescently labelled antibodies. Cells were analysed by flow cytometry and cell types were separated according to specific markers present. (A) Dendritic cells (CD45+,CD11b+,CD11c+,MHCII+) (B) Neutrophils (CD45+,CD11b+,Ly6G+), (C) Monocytes (CD45+,CD11b+,LY6G-,LY6C+,F480 High,) (D) Macrophages (CD45+,CD11b+,LY6G-,LY6C Low, F480 High), (E) M1 Macrophages (Macrophage, MRC1-), (F) M2 Macrophages (Macrophage, MRC1+), (G) CD4+ T cells (CD45+,CD19-,CD3+,CD4+), (H) B Cells (CD45+,CD19+,CD3-), (I) CD8+ T cells (CD45+,CD19-,CD3+,CD8+) (J) NK cells (CD45+,CD19-,CD3-,NK1.1+),
Mean ± SEM Statistical analysis by one way ANOVA and students T test
*< 0.05, ** < 0.01, *** < 0.001, **** < 0.0001

5.4.2 BALBc mice with 4T1 derived lung metastases

In contrast to the C57BL/6 E0771 model, in the BALBc mice injected with 4T1 cells, a low oestradiol concentration significantly increased soft tissue tumour volume when compared to high oestradiol, in the absence of Zol, in a dose dependent manner. Interestingly, treatment with Zol significantly reduced tumour volume in the low oestradiol group but did not alter tumour volume in the high oestradiol group closely mimicking data from the ABCSG-12 trial. Analysis of immune cell populations by flow cytometry and Nanostring were performed to help to explain these tumour growth results.

Oestradiol concentration in Zol untreated mice as analysed by flow cytometry, significantly increased anti-tumour dendritic cells (Figure 5.7 A) and led to a trend towards increased macrophages (Figure 5.7 D) under high oestradiol concentrations, perhaps contributing to the lower tumour volume in high oestradiol mice. However high oestradiol lead to a trend towards decreased M1 (Figure 5.7 E) macrophages and increased M2 macrophages (Figure 5.7 F) both in the presence and absence of Zol, suggesting the increased macrophage number observed may support tumour progression under high oestradiol. Treatment with Zol had a more pronounced effect on anti-tumour immune cells, with the majority of anti-tumour effects being observed in the low oestradiol group. Treatment of low oestradiol mice with Zol led to a significant increase in CD4+ T cells (P=0.014) (Figure 5.7 G) and CD8+ T cells (P=0.045) (Figure 5.7 I) alongside a trend towards increased anti-tumour B cells (P = 0.0372) (Figure 5.7 H). Interestingly, this effect was not observed under high oestradiol concentrations. Nanostring analysis showed no significant differences in immune cells in mice with low concentrations of oestradiol following Zol but did show a trend towards decreased pro tumour Treg cells (Figure 5.9) following Zol treatment. Taken together, Zol treatment in low oestradiol mice leads to an anti-tumour immune cell infiltrate, perhaps explaining the decrease in tumour volume observed in lungs under low oestradiol conditions, following Zol treatment.

Treatment of mice supplemented with high oestradiol with Zol led to a trend towards decreases in neutrophils (Figure 5.7 B), monocytes (Figure 5.7 C) and NK cells (Figure 5.7 K), suggesting that, under high oestradiol, Zol promotes a pro-tumour phenotype. To explore this further, the effects of oestradiol concentration on immune cell populations in Zol treated mice was explored. High oestradiol when compared to low oestradiol in Zol treated mice reduced B cell numbers, observed as a trend in both cytometry (Figure 4.7 H) and a significant decrease in Nanostring gene expression analysis (P = 0.0201) (Figure 5.8), while showing a trend towards reduced NK cell numbers by Nanostring analysis (Figure 5.8). Furthermore, oestradiol supplementation significantly reduced CD8 T cell numbers (P = 0.025) (Figure 5.7 I) and led to a strong trend towards reduced CD4 T cell numbers

(P=0.095)(Figure 5.7 G). Interestingly, this reduction in T cell activity at high oestradiol concentrations in the presence of Zol occurs in a dose dependent manner. High oestradiol in mice treated with Zol also led to a significant increase in PD-1 expression on CD4+ T cells (P = 0.0277) (Figure 5.7 J) and a trend towards increase on CD8+ T cell (Figure 5.7 L), suggesting these cells are more susceptible to inactivation via PD-L1 signalling. This result suggests that under high oestrogen concentrations, Zol promotes a pro-tumour phenotype, whereas under low oestradiol concentrations Zol promotes an anti-tumour phenotype. This data reflects that seen in tumour growth analysis, were Zol is effective at reducing soft tissue metastasis only under the influence of low oestradiol concentrations.

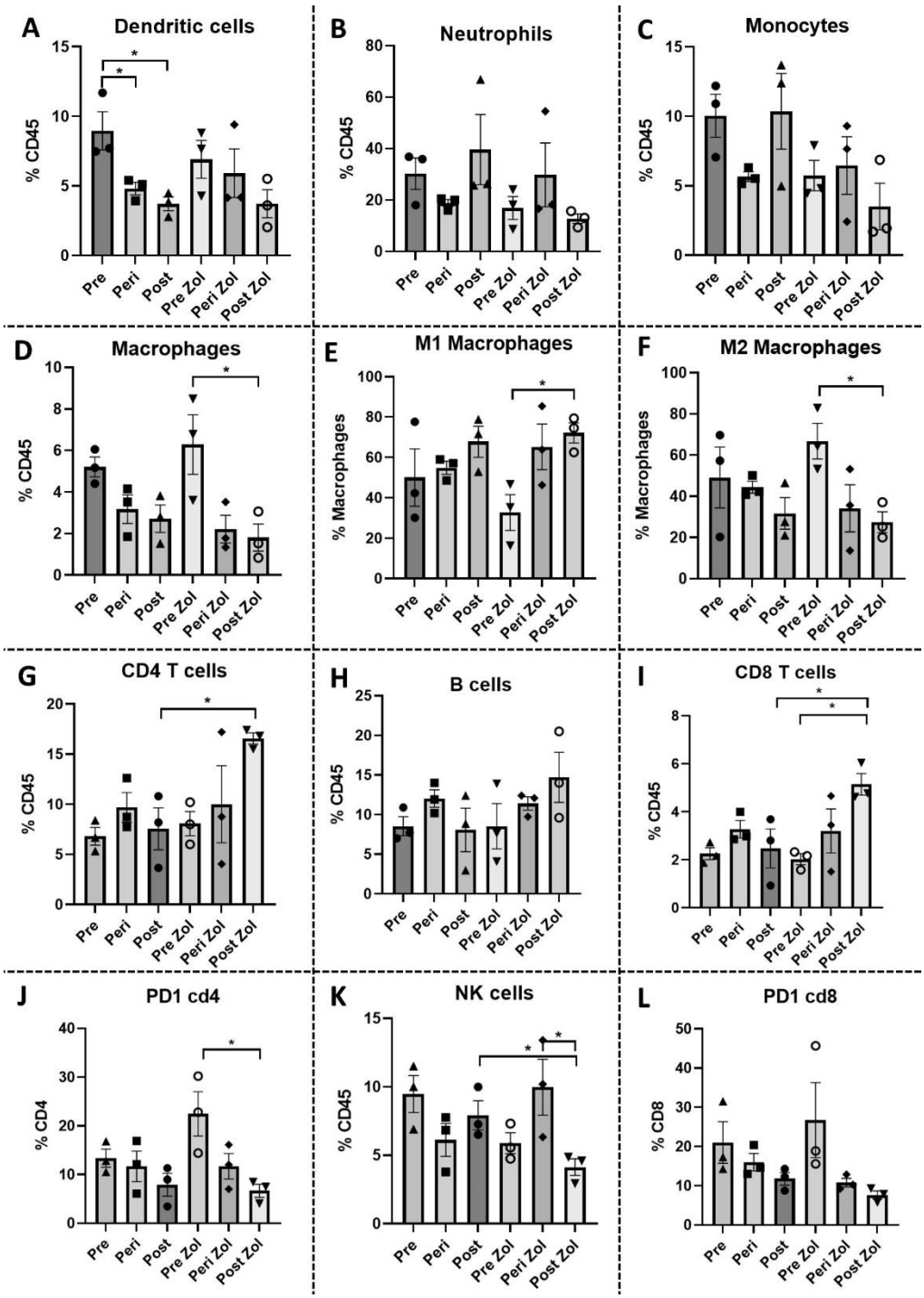

Figure 5.7: Effect of Zol treatment under high and low oestradiol concentrations in BALBc mice with 4T1-LUC tumours on immune cell populations in lung.

Mice were treated with Zol under post, peri and pre-menopausal concentrations of oestradiol. Lungs were dissociated before ex vivo before staining with fluorescently labelled antibodies. Cells were analysed by flow cytometry and cell types were separated according to specific markers present. (A) Dendritic cells (CD45+,CD11b+,CD11c+,MHCII+) (B) Neutrophils (CD45+,CD11b+,Ly6G+), (C) Monocytes (CD45+,CD11b+,LY6G-,LY6C+,F480 High,) (D) Macrophages (CD45+,CD11b+,LY6G-,LY6C Low, F480 High), (E) M1 Macrophages (Macrophage, MRC1-), (F) M2 Macrophages (Macrophage, MRC1+), (G) CD4+ T cells (CD45+,CD19-,CD3+,CD4+), (H) B Cells (CD45+,CD19+,CD3-), (I) CD8+ T cells (CD45+,CD19-,CD3+,CD8+) (J) PD-1 on CD4+ T cells (CD4 T cells, PD-1+), (K) NK cells (CD45+,CD19-,CD3-, NK1.1+), (L) PD-1 on CD8+ T cells (CD8 T cells, PD-1+).
Mean ± SEM Statistical analysis by one way ANOVA and students T test
*< 0.05, ** < 0.01, *** < 0.001, **** < 0.0001

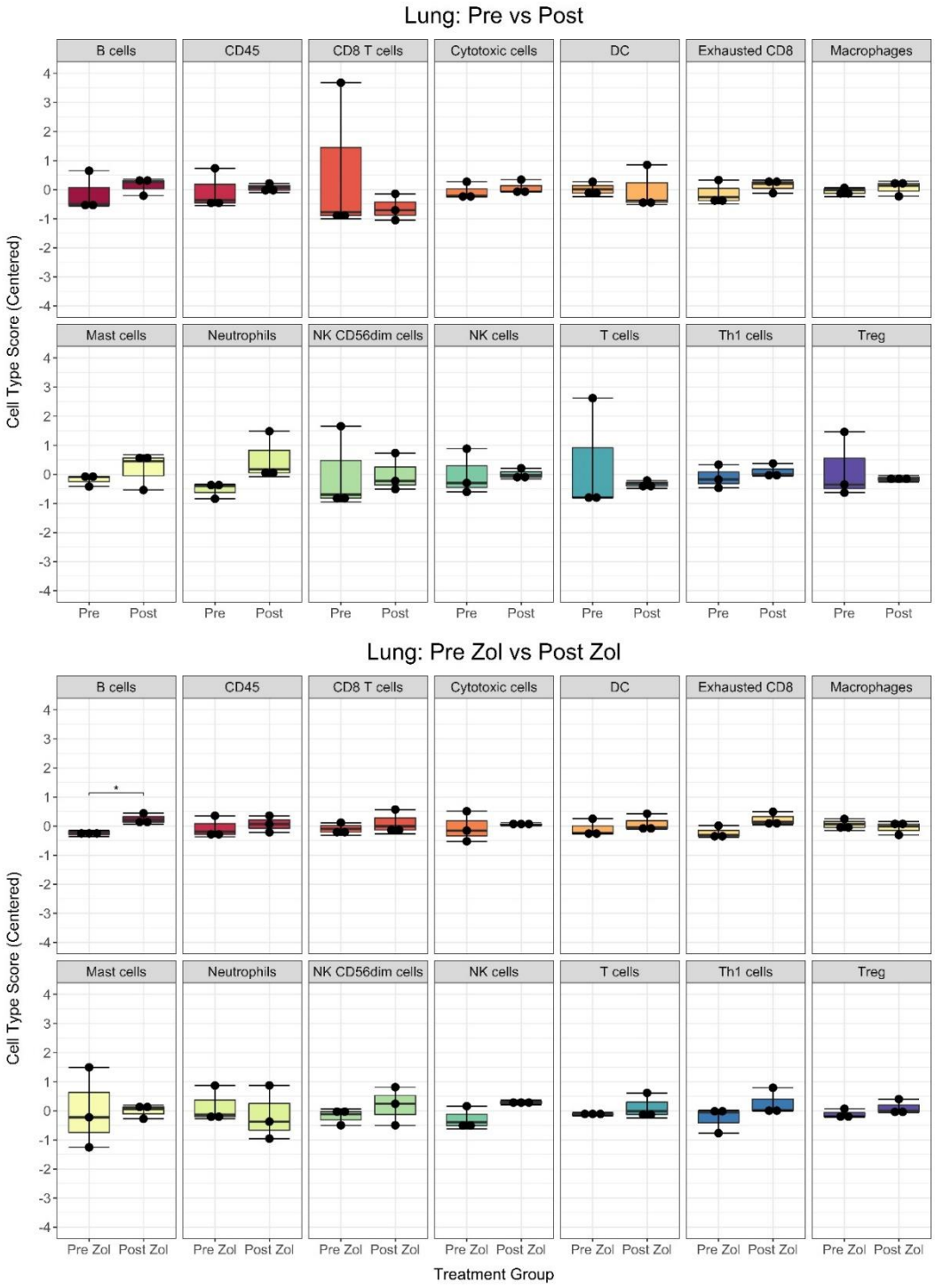

Figure 5.8: Effect of high or low oestradiol concentrations on immune cell populations +/- Zol in tumour bearing lungs on BALBc with 4T1-LUC tumours.

Mice were treated with post and pre-menopausal concentrations of oestradiol +/- Zol. Nanostring analysis was performed on RNA extracted from lungs for immune cell markers. B Cells: Blk, Cd19, Ms4a1, Tnfrsf17, CD8 T cells: Cd8a, Cd8b1, Cytotoxic cells: Ctsw, Gzma, Gzmb, Klrb1, ,Klrd1, Klrk1, Prf1, Dendritic Cells: Ccl2, Cd209e, Hsd11b1, Exhausted CD8: Cd244, Eomes, Lag3, Macrophages: Cd163, Cd68, Cd84, Mast cells: Ms4a2, Neutrophils: Csf3r, Fcgr4, NK cells: Il21r, Ncr1, Xcl1, T cells: Cd3d, Cd3e, Cd3g, Cd6, Sh2d1a, TH1: Tbx21, Treg: Foxp3, CD25.

Mean ± SEM Statistical analysis by one way ANOVA *< 0.05, ** < 0.01, *** < 0.001, **** < 0.0001

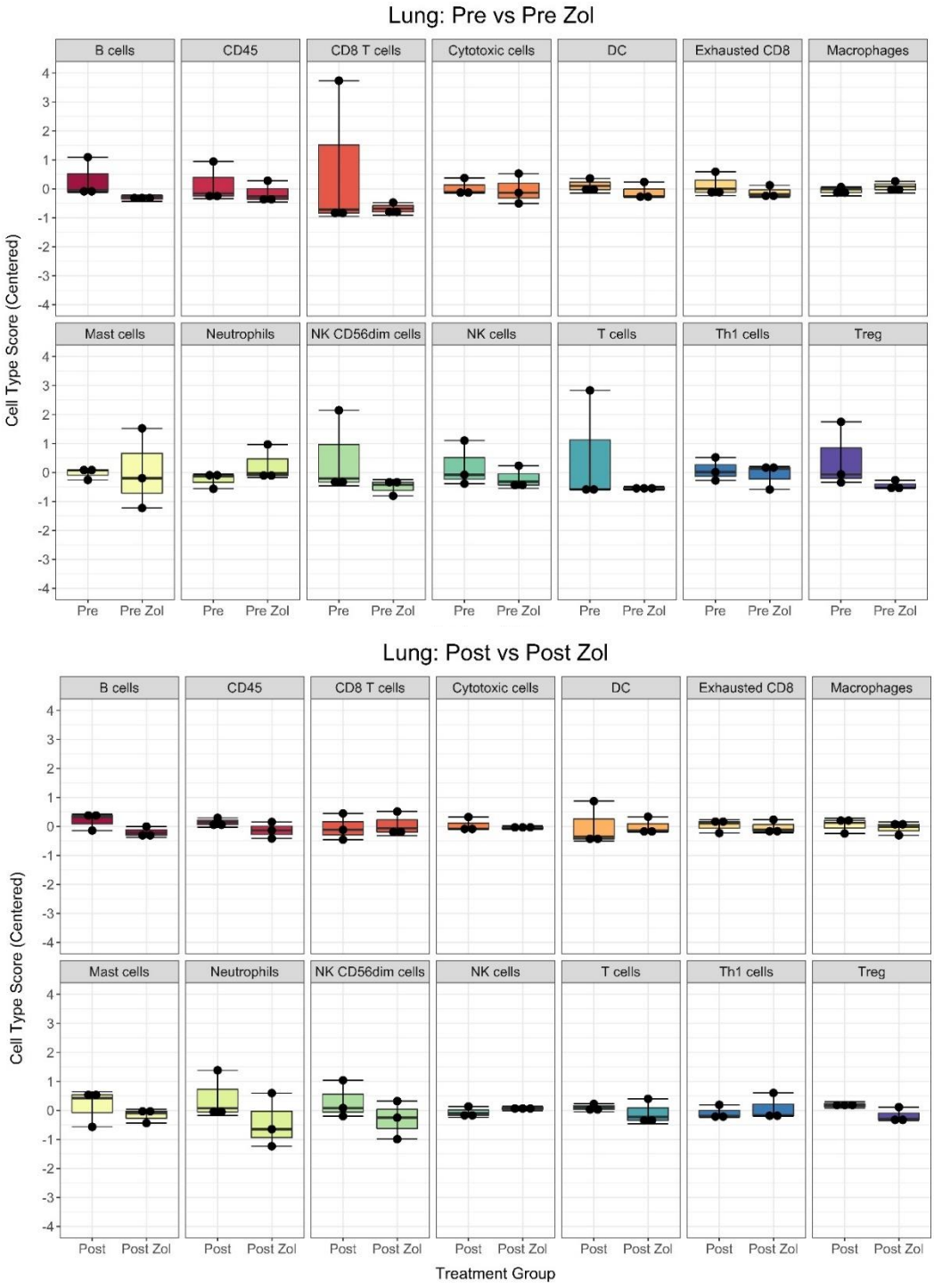

Figure 5.9: Effect of Zol under high or low oestradiol concentrations on immune cell populations in tumour bearing lungs from BALBc mice with 4T1-LUC tumours.

Mice were treated with post and pre-menopausal concentrations of oestradiol +/- Zol. Nanostring analysis was performed on RNA extracted from lungs for immune cell markers. B Cells: Blk, Cd19, Ms4a1, Tnfrsf17, CD8 T cells: Cd8a, Cd8b1, Cytotoxic cells: Ctsw, Gzma, Gzmb, Klrb1, ,Klrd1, Klrk1, Prf1, Dendritic Cells: Ccl2, Cd209e, Hsd11b1, Exhausted CD8: Cd244, Eomes, Lag3, Macrophages: Cd163, Cd68, Cd84, Mast cells: Ms4a2, Neutrophils: Csf3r, Fcgr4, NK cells: Il21r, Ncr1, Xcl1, T cells: Cd3d, Cd3e, Cd3g, Cd6, Sh2d1a, TH1: Tbx21, Treg: Foxp3, CD25.

Mean ± SEM Statistical analysis by one way ANOVA *< 0.05, ** < 0.01, *** < 0.001, **** < 0.0001

5.5 Effects of Zol +/- post- peri or pre-menopausal concentrations of oestradiol on immune cells in the Spleen

In the clinical trials AZURE and ABCSG-12 Zol was administered as an adjuvant treatment to patients with early breast cancer (before evidence of metastasis). It is therefore possible that differences in future metastatic development in soft tissues observed between pre- and post-menopausal women treated with Zol may be due to changes in systemic immunity as opposed to or in addition to changes in immune cells in the metastatic environment/tumour. I, therefore, investigated the systemic effects of oestradiol on immune cell populations in spleen to establish how immune cell populations were altered following administration of Zol under high (pre-menopausal) and low (post-menopausal) concentrations of oestradiol in C57BL/6 and BALB/c mice.

5.5.1 C57BL/6 mice with E0771 derived metastases

Analysis of immune cells in the spleen following supplementation with low and high concentrations of oestradiol was performed by flow cytometry. Administration of high concentrations of oestradiol resulted in a significant decrease in the anti-tumour NK cells (P = 0.017) (Figure 5.10 J) when compared to mice with low oestradiol concentrations. Furthermore, high oestradiol concentrations correlated with a trend towards decreased macrophages (Figure 5.10 D) and monocytes (Figure 5.10 C). This decrease in circulating immune cells under high oestradiol concentrations is indicative of a pro tumour environment in mice. Administration of Zol induced differential effects on immune cells depending on oestradiol concentrations: Under low oestradiol concentrations Zol significantly reduced macrophage numbers (P = 0.024) (Figure 5.10 D), suggesting a reduced anti-tumour immune response in the absence of oestradiol. In contrast, under high concentrations of oestradiol, Zol significantly increased CD4+ T cells (P = 0.024) (Figure 5.10 G) and CD8+ T cells (P = 0.04) (Figure 5.10 I), which could facilitate an anti-tumour phenotype. On the other hand, Dendritic cells were significantly decreased by Zol treatment under high oestradiol (P=0.033). Therefore, it could be argued that Zol treatment under low oestradiol concentrations confers a pro tumour environment via actions on myeloid cells. Whereas under high oestradiol concentrations, Zol confers an anti-tumour environment via upregulation of circulating anti-tumour lymphoid cells.

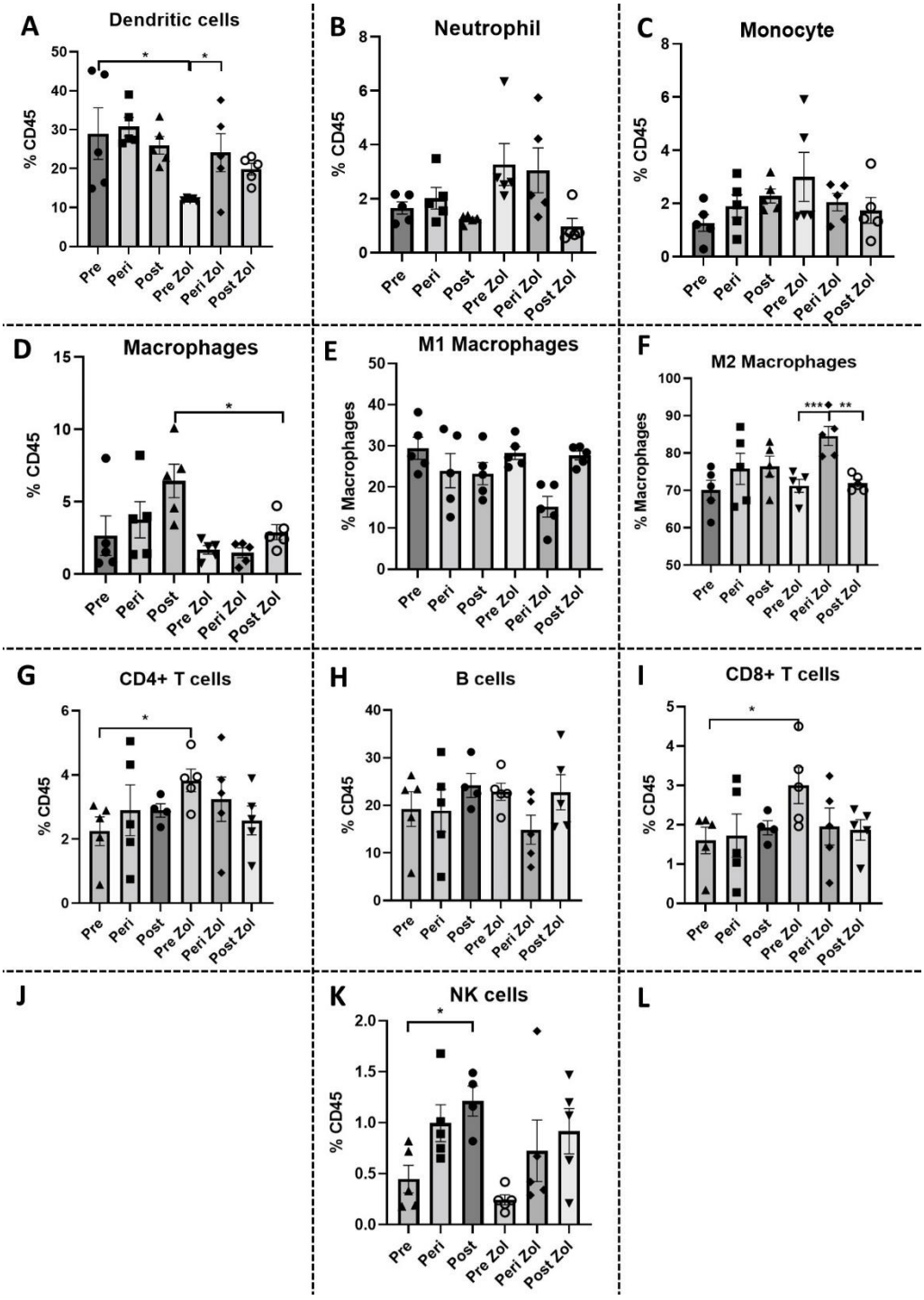

Figure 5.10: Effect of Zol treatment under high and low oestradiol concentrations in C57BL/6 mice with E0771 tumours on immune cell populations in spleen.

Mice were treated with Zol under post, peri and pre-menopausal concentrations of oestradiol. Spleens were dissociated before ex vivo before staining with fluorescently labelled antibodies. Cells were analysed by flow cytometry and cell types were separated according to specific markers present. (A) Dendritic cells (CD45+,CD11b+,CD11c+,MHCII+) (B) Neutrophils (CD45+,CD11b+,Ly6G+), (C) Monocytes (CD45+,CD11b+,LY6G-,LY6C+,F480 High,) (D) Macrophages (CD45+,CD11b+,LY6G-,LY6C Low, F480 High), (E) M1 Macrophages (Macrophage, MRC1-), (F) M2 Macrophages (Macrophage, MRC1+), (G) CD4+ T cells (CD45+,CD19-,CD3+,CD4+), (H) B Cells (CD45+,CD19+,CD3-), (I) CD8+ T cells (CD45+,CD19-,CD3+,CD8+) (J) NK cells (CD45+,CD19-,CD3-, NK1.1+),

Mean ± SEM Statistical analysis by one way ANOVA and students T test

*< 0.05, ** < 0.01, *** < 0.001, **** < 0.0001

5.5.2 BALBc mice with 4T1 derived metastasis

Numbers of circulating immune cells in the spleen following treatment with Zol and oestradiol follow a different pattern in the BALBc mouse model, reflecting that seen in other organs. Treatment of mice with high concentrations of oestradiol led to a significant increase in CD8+ T cells (P=0.03) (Figure 5.11 I) and a trend towards increased CD4+ T cells. On the other high oestradiol led to a trend towards reduction in B cells and neutrophils (Figure 5.11 H). These changes in response to oestradiol stimulation confer both an anti-tumour phenotype (increased CD8 and CD4) and a pro-tumour phenotype (decrease in B cells and neutrophils), suggesting that there may be more complex interactions mediating metastasis or that recruitment of immune cells/subsets into metastatic tumours have impacted on the makeup of systemic immune cells. Zol treatment under low concentrations of oestradiol also led to both pro and anti-tumour immune cell responses. Macrophages were significantly increased (P = 0.0023) (Figure 5.11 D) and Dendritic cells were significantly increased (P=0.004) (Figure 5.11 A) in spleen following Zol treatment under low oestradiol, facilitating an anti-tumour environment. However, B cells (Figure 5.11 H) showed a trend towards decreased following Zol treatment (P = 0.0383), conferring a pro-tumour phenotype.

Treatment with Zol under high concentrations of oestradiol resulted in a significant increase in dendritic cell number (P = 0.014) (Figure 5.11 A) and a significant increase in macrophage number (P = 0.0089) (Figure 5.11 D), which would suggest an anti-tumour phenotype. However, when macrophage polarisation was analysed, it was found that Zol increased the proportion of circulating pro-tumour M2 macrophages (P = <0.0001) (Figure 5.11 F). This could suggest that the increase in macrophages observed following Zol treatment is a consequence of increased M2 macrophage polarisation, resulting in a pro tumour phenotype in circulating immune cells.

Taken together, these data suggest that for the C57BL/6 model Zol induced changes to systemic immunity may be important regulators of metastatic outgrowth and this can be impeded by the presence of high concentrations of oestradiol. In contrast in the BALB/c model Zol induced changes to tumour immune cell infiltrate appears to be the primary regulator of metastases and oestradiol concentrations can impact the number and type of immune cell infiltrate, promoting or reducing growth of metastases in soft tissue.

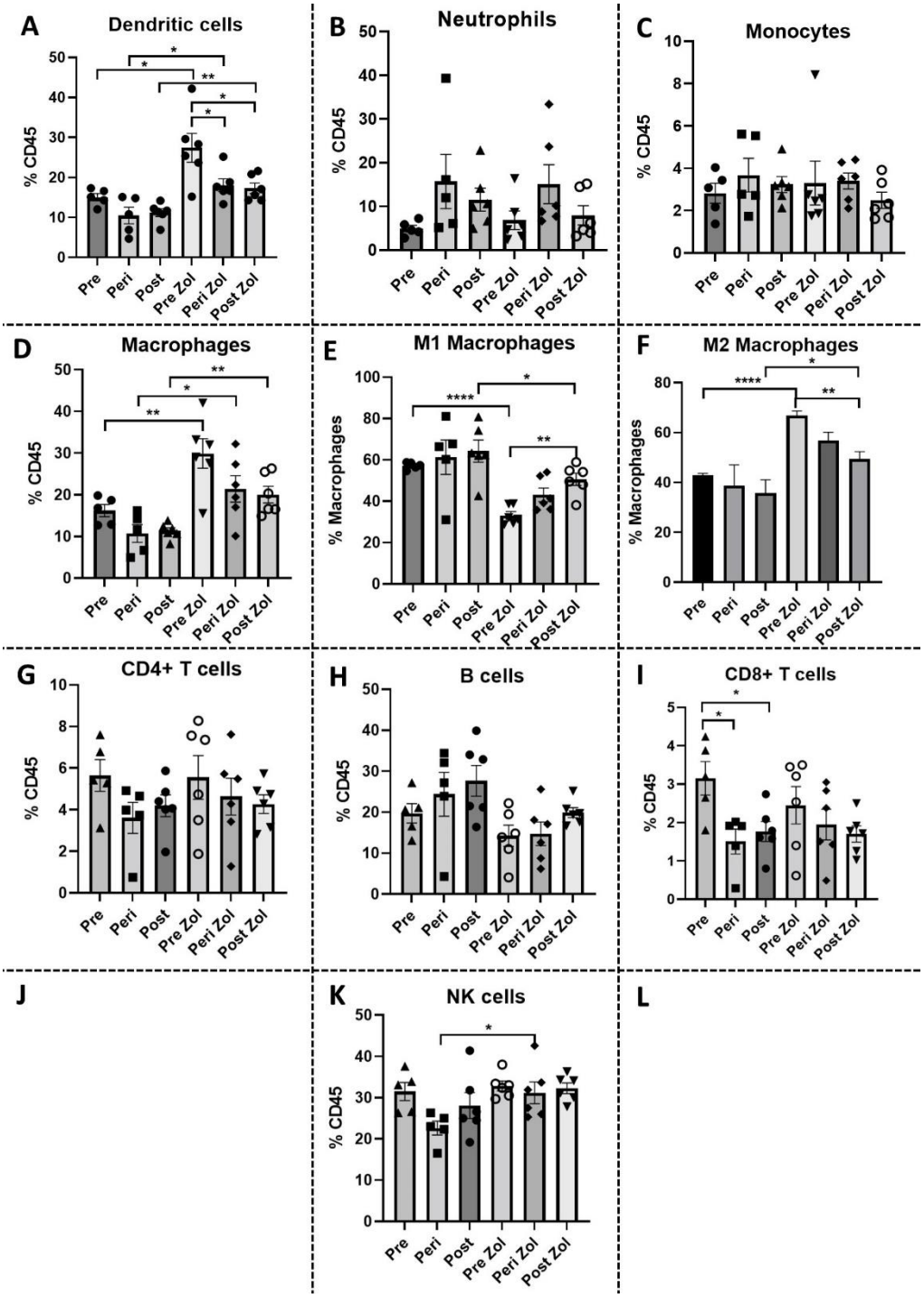

Figure 5.11: Effect of Zol treatment under high and low oestradiol concentrations in BALBc mice with 4T1-LUC tumours on immune cell populations in spleen.

Mice were treated with Zol under post, peri and pre-menopausal concentrations of oestradiol. Spleens were dissociated before ex vivo before staining with fluorescently labelled antibodies. Cells were analysed by flow cytometry and cell types were separated according to specific markers present. (A) Dendritic cells (CD45+,CD11b+,CD11c+,MHCII+) (B) Neutrophils (CD45+,CD11b+,Ly6G+), (C) Monocytes (CD45+,CD11b+,LY6G-,LY6C+,F480 High,) (D) Macrophages (CD45+,CD11b+,LY6G-,LY6C Low, F480 High), (E) M1 Macrophages (Macrophage, MRC1-), (F) M2 Macrophages (Macrophage, MRC1+), (G) CD4+ T cells (CD45+,CD19-,CD3+,CD4+), (H) B Cells (CD45+,CD19+,CD3-), (I) CD8+ T cells (CD45+,CD19-,CD3+,CD8+) (J) NK cells (CD45+,CD19-,CD3-, NK1.1+),
Mean ± SEM Statistical analysis by one way ANOVA and students T test
*< 0.05, ** < 0.01, *** < 0.001, **** < 0.0001

5.6 Effects of Zol under high and low oestradiol concentrations on immune cell infiltration into bone metastatic and soft tissue tumour microenvironments

To determine if Zol altered immune cell infiltrate into metastatic organs in BALB/c and C57BL/6 mice, and if this could be influenced by oestradiol, I analysed immune cell infiltration into metastatic tumours by immunohistochemical staining (IHC) of tumour bearing lungs and bone. IHC analysis of immune cell populations within bone tumours revealed no significant differences for any treatment group, with wide variation between data. Treatment with Zol led to a small trend towards increased macrophage numbers within the bone (Figure 5.13 A). Zol treatment also led to a small trend towards increased M2 macrophage populations within bone (Figure 5.13 C), however this trend was minor and did not approach significance in post, peri or pre-menopausal groups (p=0.68, 0.28 and 0.25 respectively). Insignificant trends in LY6G positive cells (Figure 5.13 D), a marker of neutrophil infiltration, showed that Zol decreased neutrophil infiltration under low oestradiol concentrations (P=0.37), perhaps promoting a pro tumour phenotype. However, none of the analysis for the IHC experiments approached statistical significance, highlighting the need for further research to increase n numbers and analyse markers of immune cell activity.

IHC staining of tumour bearing lungs from BALBc mice revealed no significant differences in immune cell populations for any treatment group (Figure 5.12). However, high concentrations of oestradiol did lead to a trend towards reduction in granzyme B (P = 0.1556) (Figure 5.12 B), a marker for T cell activity, in the absence of Zol. This would confer an anti-tumour phenotype under low oestradiol compared to high oestradiol. On the other hand, CD163 (Figure 5.12 C)**,** a marker of M2 macrophages shows a trend towards increase in low oestradiol mice compared to high oestradiol mice in the presence of Zol. This suggests an opposing pro-tumour immune cell increase under low oestradiol concentrations in the presence of Zol. Interesting, this trend is not present in the absence of Zol. These data only show early trends of immune cell populations within lung tumours, with more research needed into the populations present by increasing n numbers and analysing more markers of immune cell activity.

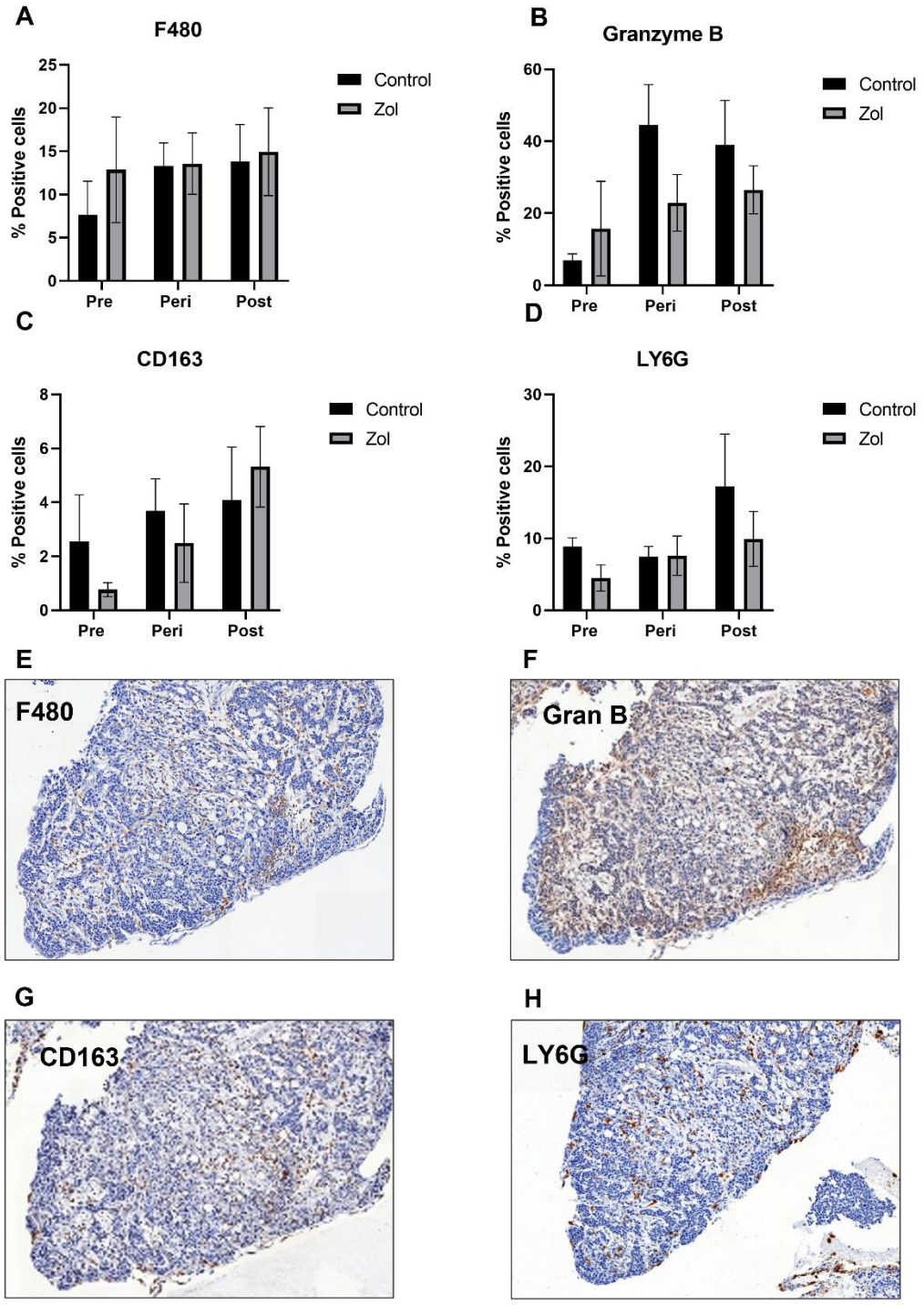

Figure 5.12: Effect of Zol treatment under high and low oestradiol concentrations in BALBc mice with 4T1-LUC tumours on immune cell populations in lung tumours.

Mice were treated with 100 µg/kg Zol under post, peri and pre-menopausal concentrations of oestradiol. Lungs were fixed, cut then stained by immunohistochemistry for immune cell markers**. (A&E)** F480 staining quantification and representative image, **(B&F)** Granzyme B staining quantification and representative image, **(C&G)** CD163 staining quantification and representative image **(D&H)** LY6G staining quantification and representative image

Mean ± SEM Statistical analysis by one way ANOVA and students T test n=2-5

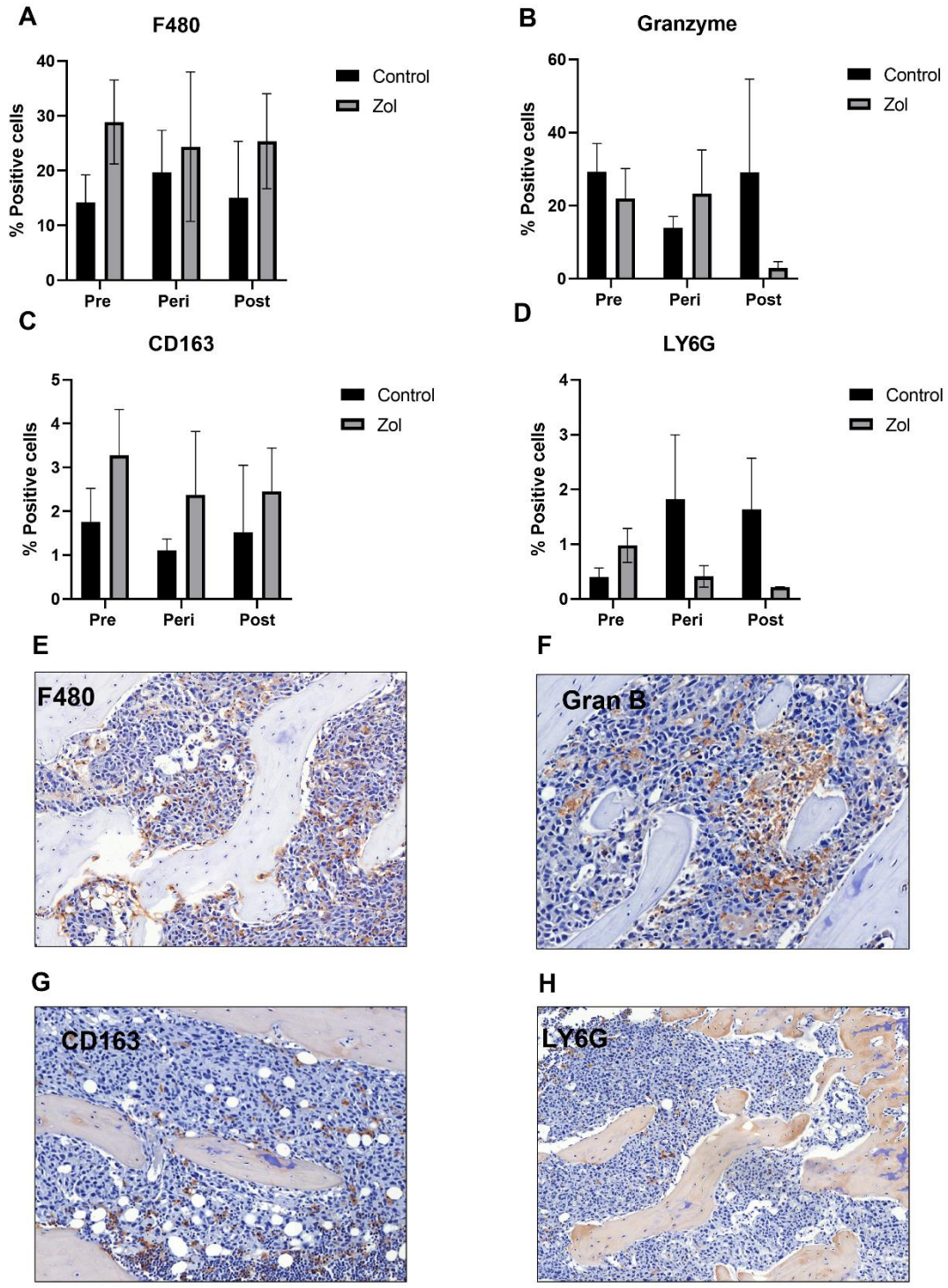

Figure 5.13: Effect of Zol treatment under high and low oestradiol concentrations in C57BL/6 mice with E0771 tumours on immune cell populations in bone tumours.

Mice were treated with 100 µg/kg Zol under post-, peri- and pre-menopausal concentrations of oestradiol. Bones were fixed, decalcified, cut then stained by immunohistochemistry for immune cell markers. **(E)** F480 staining representative image, **(F)** Granzyme B staining representative image, **(G)** CD163 staining representative image **(H)** LY6G staining representative image

Mean ± SEM Statistical analysis by one way ANOVA and students T test, n=2-5

5.7 Effects of Zol under high and low oestradiol conditions on PD-L1 expression.

PD-L1 is an immune checkpoint marker normally important in maintaining peripheral tolerance and the prevention of "self" recognition by immune cells. PD-L1 is expressed on tumour cells and immune cells and has been shown to be important for cancer progression. Binding of PD-L1 to its receptor PD-1 on T cells and NK cells silences immune responses and allows cancer cells to avoid immune recognition. Therefore, the direct effect of oestradiol and Zol on PD-L1 expression in murine breast cancer cell lines was assessed *in vitro*, with the aim of understanding if effects on PD-L1 are due to direct effects on cancer cells or the microenvironment. Therefore, E0771 and 4T1-LUC breast cancer cell lines were incubated with post-, peri- or pre-menopausal concentrations of oestradiol in the presence or absence of Zol, before qPCR analysis was performed to determine PD-L1 relative expression. PD-L1 was found to be expressed in these cells, however, treatment with Zol or oestradiol led to no significant differences in PD-L1 expression for either cell line (Figure 5.14). The 4T1-Luc cell line expressed PD-L1 at a higher concentration, with amplification appearing at around 26 cycles (Figure 5.14 A) compared to E0771 cells where amplification started at around 29 cycles (Figure 5.14 B).

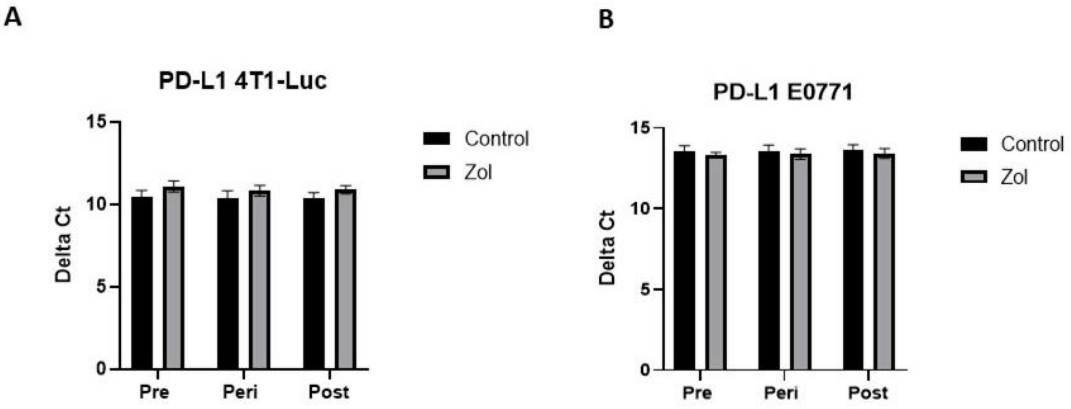

Figure 5.14: Effect of Zol treatment under high and low oestradiol concentrations on PD-L1 expression in 4T1-Luc and E0771 cells *in vitro*

Effect of oestradiol at post (10 pM), peri (84 pM) and pre-menopausal (300 pM) concentrations on PD-L1 mRNA expression in vitro. Zol concentrations of 7.5 µM (E0771) and 15 µM (4T1-LUC) were used. Mean ± SEM Statistical analysis by one way ANOVA and students T test, data normalised to GAPDh expression

5.8 Discussion

Clinical trials investigating the efficacy of Zol and other bisphosphonates at preventing bone metastasis found that post-menopausal women benefit from decreased bone metastasis, decreased soft tissue metastasis and increased iDFS (Gnant et al., 2011) (J. Bergh *et al.*, 2015). However, the AZURE clinical trial found that patients with pre-menopausal serum concentrations of oestradiol had increased soft tissue metastasis and reduced iDFS (Coleman et al., 2014a). The mechanism behind this differential response remains unknown. A study into the effects of treatment on bone resident cells set up mouse models to model menopausal oestradiol concentrations and Zol treatment in mice with disseminated breast cancer cells to study the effects on bone metastasis (Canuas-Landero et al., 2021). Interestingly, Zol treatment was shown to reduce soft tissue metastasis in the immunocompetent BALBc and C57BL/6 models but had no significant effect on the immunocompromised BALBc Nude mice, suggesting immunological factors likely contribute to this differential response. Therefore, I investigated the effects of Zol treatment under post, peri and pre-menopausal concentrations of oestradiol on immune populations in the bone, lung and spleen.

		High oestradiol	**Zol in Low oestradiol**	**Zol in High oestradiol**
Bone Marrow	**+**	Monocytes, Macrophages, CD4 T, CD8 T,	Macrophages	
C57BL/6	-	B cells	PD-1 on CD4, PD-1 on CD8	Macrophages,
Bone Marrow	**+**	CD4 T, CD8 T, Neutrophils		CD8 T
BALBc	-	B cells,		
Lung	**+**			
C57BL/6	-			
Lung	**+**	Dendritic, Macrophages, M2, PD-1 on CD4 & CD8	CD4, CD8,	PD1 on CD4,
BALBc	-	M1	NK cells, Monocytes	
Spleen	**+**			CD4, CD8,
C57BL/6	-	Macrophages, CD4	Macrophages	Dendritic
Spleen	**+**	CD8, CD4	Dendritic, Macrophages, M2	Dendritic, M2
BALBc	-	B cells	M1	M1

Table 5.1: Summery of immune cell characterisation by flow cytometry , showing the effect of high oestradiol, Zol under low oestradiol and Zol under low oestradiol concentrations on immune cell numbers in the bone marrow, lung and spleen in C57BL/6 with E0771-LUC tumours and BALBc mice with 4T1-LUC tumours.

Flow cytometry was on of the most important techniques used in this project to investigate and characterise the immune response following treatments Zol and oestradiol. However, there were some experimental drawbacks when utilising this technique that must be addressed when interpreting this data. As shown in Figure 2.4 and 2.5, the stain used for cell viability had some problems staining the dead cells, showing the majority of cells gated from forward and side scatter as viable. Therefore, later gating could include a small population of dead cells that did not stain. A second issue identified in the flow cytometry experiments was the staining of MRC1, used to differentiate between M1 like macrophages and M2 like macrophages. Although MRC1 is expressed

on the plasma membrane, it also has expression in the cytoplasm of macrophages (Feinberg et al., 2021). Our flow cytometry experiments focused only on cell surface antigens since the cells were not permeabilised, meaning that the macrophage polarisation marker may not paint a complete picture.

5.8.1 Effect of oestradiol on immune cell populations

Analysis of immune populations in C57BL/6 mice showed that high oestradiol reduced numbers of anti-tumour immune cells. However, in the lung oestradiol did not have a significant effect on immune cells. Overall, the data suggests a decrease in anti-tumour immune cell numbers under high oestradiol concentrations in the absence of Zol in the spleen and bone. The decrease in immune cell infiltration into the bone with high oestrogen could help explain the increase in bone metastasis observed in the bone under high concentrations of oestradiol. In the lung, tumour growth was higher under post-menopausal oestradiol concentrations. Oestradiol did not significantly affect immune cell populations in the absence of Zol, which could explain the reduced metastasis in the lung under high oestradiol concentrations.

The effects of oestradiol on immune cells in the BALBc mouse model with 4T1-LUC tumour followed a different pattern to that seen in the C57BL/6 model, reflecting the differences observed in tumour growth experiments. High oestradiol in the bone led to a trend towards reduced anti-tumour B cells in the absence of Zol. Interestingly, studies investigating the effect of oestradiol on B cells has reported that high oestradiol led to an increase in B cell activation alongside an increase in immunoglobulin (Ig)G and IgM production (Grimaldi et al., 2002), contradicting my findings of reduced B cell numbers with high oestradiol. On the other hand, high oestradiol led to an increase in anti-tumour immune cells in bone, reflecting tumour growth experiments where bone metastasis was significantly lower in pre-menopausal mice compared to post-menopausal mice. However, this data also goes against previous literature, showing that high oestradiol concentrations reduce numbers and activity of T cells by reducing early T cell development in the thymus (Okasha et al., 2001) and increasing Treg cell activity and number (Polanczyk et al., 2004). Importantly, these studies do not analyse populations of T cells within the bone, with the focus on *in vitro, in vivo* soft tissue and circulating levels. Therefore, this discrepancy could be explained by organ specific differences in immune cell infiltrate. Indeed, clinically, it is in the soft tissue, not the bone, where differences in treatment outcome following Zol treatment at different menopausal oestradiol concentrations are observed (Coleman et al., 2014a). Although not statistically significant, anti-tumour immune cell populations in the lung and spleen of BALBc mice also showed trends towards increase, which reflects tumour growth analysis where mice with pre-menopausal oestradiol had significantly lower tumour volume compared to mice with post-menopausal oestradiol concentrations. Overall, in the BALBc

model, high oestradiol concentrations seem to promote an anti-cancer phenotype in the bone and lung.

The immune response following oestradiol treatment in the BALBc and the C57BL/6 mouse models differed, with oestrogen promoting an anti-cancer immune profile in BALBc mice while promoting a pro-cancer immune profile in C57BL/6 mice. It has been shown that both the C57BL/6 and BALBc mouse strains respond differently across a number of settings, with their immune response being a main contributor. Indeed, under physiological conditions, BALBc mice have a high volume density of the T zone in the spleen and an increased production of IL-2, IL-3, IL-4, IL-10 and TNF-α compared to C57BL/6 mice (Trunova et al., 2011). C57BL/6 mice have been shown to have higher cytostatic activity of NK cells in the spleen when compared to BALBc (Trunova et al., 2011). Further to immune populations present within the spleen, NK cells have been shown to respond differently to stimuli in the mouse models due to differences in the genetic encoding of these cell responses (Higuchi et al., 2010). The response of NK cells to interaction with its target cell is dependent on signalling from numerous receptors, either inhibitory or activating. Genes for these NK cell receptors are encoded in gene complexes, such as the natural killer gene complex, and genes in these complexes manifest strain specific polymorphisms. For example, the number Ly49 receptor genes in C57BL/6, a family of receptors binding MHC-1 molecules to distinguish "self", consists of 15 genes for inhibitory and activating receptors. On the other hand, BALBc mice have a much smaller Ly49 haplotype, containing just 7 genes, with only a single inhibitory gene (Kane et al., 2004). These differences in NK cells depending on mouse strain could go some way to explaining the differential NK cell responses observed under different oestradiol concentrations.

Interestingly, the BALBc model with 4T1-LUC tumours had a higher neutrophil infiltration when compared to the C57BL/6 model with E0771 cells. High neutrophil infiltration is characteristic of a poor prognosis for breast cancer patients, being associated with worse disease free survival and overall survival, suggesting the 4T1 mouse model is representative of a more aggressive subset of breast cancer.

The immune suppressive Treg cells are a vital cell type in supporting tumour growth and maintaining an immunosuppressive microenvironment in tumours. Mouse strain specific differences have also been observed in these cells and their ability to supress effector T cell activity. Interestingly, there was a higher frequency of CD4+CD25+ Treg cells in the thymus and peripheral lymphoid tissues of BALBc mice when compared to C57BL/6 mice. Furthermore, Treg cells from C57BL/6 mice were less effective at supressing CD4+ T cells when compared to BALBc derived Treg (Chen et al., 2005). These differences in Treg cell number and response between the two mouse models may also contribute to

the lack of lymphocyte cell response to oestradiol and Zol observed in the C57BL/6 mouse model. Oestradiol has been shown to increase Treg cell populations, whereas Zol has been shown to supress T cell activity in pre-clinical studies. Therefore, in the C57BL/6 mouse model, the reduced Treg cell population could contribute to the lack of effect of Zol or high oestradiol on lymphocyte populations. On the other hand, in the BALBc model, Zol increases T cell numbers in lungs of mice with low oestradiol, but high oestradiol supresses this, possibly by acting on Treg cell populations absent in the C57BL/6 model.

5.8.2 Effect of Zol on immune cell populations

Zol has also been shown to be a highly immunogenic drug, affecting immune cell populations in cancer (George et al., 2020). Therefore, I investigated the effect of Zol, under high and low oestradiol concentrations, on immune cell populations within bone and soft tissue sites in mouse models. The aim was to understand if Zol and oestradiol induced changes to immune populations affect breast cancer metastasis.

In the C57BL/6 mouse model, treatment with Zol under low oestradiol concentrations has no significant effect on immune cell populations in the bone. This counters studies observed in the literature, whereby Zol increased M1 macrophage infiltration (Coscia et al., 2010). When these results are viewed in the context of tumour growth experiments, the results observed by flow cytometry not reflected in bone tumour frequency where Zol significantly increased bone tumour numbers under low oestradiol concentrations. Under high oestradiol concentrations in the bone, Zol also did not have a significant effect on immune cell populations.

In the lung of C57BL/6 mice, Zol had no significant effect on immune cell populations, irrespective of oestradiol concentration, showing only a trend towards increased monocytes and macrophages under high-oestradiol concentrations. Interestingly, tumour growth in the lung was shown to be significantly decreased by Zol under low oestradiol concentrations, and significantly increased by Zol under high oestradiol concentrations. This change in tumour growth is not reflected in the immune cell profiling for C57BL/6 mice. Therefore, I investigated the effect of Zol on systemic immune cell populations by analysing splenic populations. Interestingly, under low oestradiol concentrations, Zol significantly decreased myeloid immune cell populations. However, under high oestradiol concentrations Zol significantly increased lymphocyte populations.

The effect of Zol on immune cell populations was also analysed in the BALBc mouse model. Nanostring analysis suggested that treatment with Zol under high oestradiol concentrations confers a

pro-tumour phenotype in the bone, whereas Zol treatment under low oestradiol confers an anti-tumour phenotype. In the lung, results suggest that Zol treatment under low oestradiol concentrations stimulates an anti-tumour immune response, whereas under high oestradiol stimulates a pro-tumour immune response. This result is reflected in tumour growth, where Zol significantly reduces tumour growth in the lung, but only under low oestradiol concentrations, having no significant effect under high oestradiol concentrations. This anti-tumour effect on lymphocytes under low oestradiol could be mediated through the previously discussed effect of Zol on Treg cell populations. Zol excerpts an inhibitory effect on Treg cells, reducing migration, recruitment into the tumour microenvironment and inhibitory activities of these cells (George et al., 2020). However, oestradiol can stimulate Treg conversion and activity, while increasing PD-L1 expression, creating an immune suppressive microenvironment (George et al., 2020). These differences could contribute to the differences in Zol treatment outcome under high and low oestradiol concentrations. The responses of the immune system to Zol also show strain specific differences as explored in the previous section.

5.8.3 Effect of oestradiol and Zol on the immune response

Overall, in BALBc mice, Zol seems to have an anti-tumour effect on the immune population in the presence of low oestradiol concentrations but has a pro-tumour effect under the influence of high oestradiol. This result reflects that seen in tumour growth analysis experiments from chapter 1. Furthermore, these results reflect that seen in the AZURE trial, where pre-menopausal women have increased soft tissue metastasis following treatment with Zol. This modulation of Zols effect on immune cell populations by high oestradiol concentration could be due to overlapping and often opposing actions of oestradiol and Zol on immune cell subsets. For example, Zol and oestradiol have opposing effects on macrophage populations, with oestradiol increasing MMP-9 expression in macrophages (Hwang et al., 2006) and Zol decreasing MMP-9 expression (Melani et al., 2007). MMP-9 is an important enzyme for macrophage infiltration and tumour invasion (Foda and Zucker, 2001). Therefore, Zol treatment could reduce the ability of tumour associated macrophages to infiltrate the tumour microenvironment, whereas oestradiol could do the opposite, increasing the metastatic potential of breast cancer cells.

As previously described, oestradiol and Zol have opposing effects on Treg cells. Oestradiol can regulate Treg cell development, and suppressive activity by regulating PD-1 expression (Polanczyk et al., 2007). Oestradiol signalling upregulated PD-1 expression, vital for the suppressive activity of Treg cells. On the other hand, Zol has been shown to down regulate PD-1 expression on Treg cells, therefore

reducing their ability to supress T effector cells whilst reducing Treg conversion from naive cells (Liu et al., 2019). These overlapping effects on T cell regulation could reduce the anti-tumour immune response elicited by Zol in high oestradiol mice compared to low oestradiol mice, contributing to the differences observed in clinical trials of bisphosphonates for early breast cancer treatment (Coleman et al., 2018a).

One interesting immune modulatory effect of oestradiol is on PD-L1 expression. PD-L1 is an immune checkpoint signalling molecule used by cells to identify self and is upregulated in cancer cells allowing them to evade immune detection and elimination. I evaluated the effect of Zol treatment under post-, peri- and pre-menopausal concentrations of oestradiol on PD-L1 gene expression *in vitro*. My data showed that treatment with oestradiol or Zol had no significant effect on PD-L1 gene expression. Both the 4T1-LUC and E0771 cell lines used are ERα negative, with E0771 expressing ERβ and 4T1 having a triple negative phenotype. Therefore, it is unsurprising that oestradiol has no significant effects on PD-L1 gene expression. Interestingly, oestradiol has been shown to increase PD-L1 protein expression in the ER^+ human breast cancer cell line MCF-7 via Akt/PI3K activation, resulting in reduced T cell function and T cell exhaustion (Yang et al., 2017). Interestingly, this was found to be mediated by an increase in mRNA stability, with oestrogen having no effect on PD-L1 mRNA expression. This reflects my data on PD-L1 expression, prompting the need to assess the effects of oestradiol and Zol on PD-L1 protein expression. Oestradiol's ability to increase PD-L1 expression (Yang et al., 2017) could help to explain the decrease in lymphocyte cell numbers in mice treated with Zol under high oestradiol concentrations compared to low oestradiol concentrations.

PD-L1 is a powerful immunosuppressive agent, silencing immune cell targeting of cancer cells in the tumour microenvironment. Furthermore, Zol has been shown to stimulate immune responses and create an anti-tumour phenotype. Therefore, the blockade of PD-L1 in combination with Zol treatment could be a beneficial treatment to sensitize tumour cells to immune cell destruction.

5.9 Conclusions

The effect of oestradiol and Zol on the immune response to cancer in the bone and the soft tissue show mouse strain and organ specific differences, representing the heterogeneity of the patient population. However, treatment with Zol has been shown to be significantly affected by oestradiol concentration. In the lung, Zol significantly increases anti-tumour lymphocyte numbers, but only in the presence of low oestradiol concentrations. This shows that high oestradiol can inhibit the immune stimulatory effects of Zol, perhaps through its own immune modulatory effects. Indeed, oestradiol was shown to significantly decrease B cell population within the bone, while also increasing expression of PD-1, creating a pro-tumour immune environment. Both my results showing increased PD-1

expression with oestradiol and the literature suggest that oestradiol increases checkpoint inhibition, which would increase immune cell exhaustion in the tumour microenvironment. Therefore, blockade of immune checkpoint molecules in combination with Zol could improve treatment outcome in pre-menopausal patients.

Chapter 6: Investigating the effect of combination therapy with Avelumab and Zol under post- and pre-menopausal oestradiol concentrations on breast cancer metastasis

6.1 Introduction

Avelumab is a human anti-PD-L1 IgG1 monoclonal antibody that inhibits the interaction of PD-1 with its ligand PD-L1 (Collins and Gulley, 2019). The PD-1, PD-L1 proteins are members of the immune checkpoint family which are vital in T-cell tolerance and maintaining immune homeostasis under physiological conditions (Jung and Choi, 2013). Tumour cells can upregulate this pathway, the binding of PD-L1 to PD-1, its receptor on immune cells, inhibits the adaptive immune response within the tumour microenvironment, allowing tumours to escape from immune cells. The presence of tumour infiltrating lymphocytes has been shown to be a predictor of improved disease progression, alongside an improved response to standard of care treatments such as neoadjuvant chemotherapy for TNBC (Ono et al., 2012).

PD-L1 is a type 1 transmembrane glycoprotein and is a member of the B7 superfamily (Han et al., 2020). It has been found to be overexpressed on breast cancer cells as an adaptive immune mechanism facilitating immune escape, mediated via aberrant signalling pathways and chromosomal alterations (Topalian et al., 2016). Indeed, PI3K-AKT pathway activation via PTEN mutations has been shown to result in extensive PD-L1 expression in cancer cells (Topalian et al., 2016), with 30-40% of primary breast tumours exhibiting PTEN loss (Gonzalez-Angulo et al., 2011). Interestingly, PD-L1 expression has been found to be higher in ERα negative breast cancer subtypes, with qPCR and Western blot analysis showing the ERα positive cell lines MCF7 and T47D with significantly lower PD-L1 expression than the ERα negative MDA-MB-231 and BT549 (Liu et al., 2018). PD-L1 expression in solid tumours is associated with high proliferation, large tumour size, high grade (Sabatier et al., 2015) and is inversely corelated with survival in breast cancer (Muenst et al., 2013).

PD-1 is a transmembrane protein receptor that acts as an inhibitor of both the adaptive and innate immune responses. It has been shown to be expressed on activated T cells, B lymphocytes, NK cells, macrophages, monocytes and dendritic cells (Han et al., 2020). PD-1 is also highly expressed on tumour specific T cells, in line with its role in promoting a pro tumour immune microenvironment (Ahmadzadeh et al., 2009). Interestingly, cancer leakage has been shown to upregulate expression of PD-1 by increasing expression of the c-FOS subunit of AP1 (Xiao et al., 2012). Activation of PD-1 by binding of PD-L1 reduces T cell activity, cytokine production, induces T cell lysis and induces tolerance to antigens (Schütz et al., 2017). Therefore, blockade of the PD-1, PD-L1 axis, by drugs such as Avelumab, represents an exciting new treatment for cancer patients.

Avelumab disrupts the PD-1/PD-L1 interaction and is a promising new cancer treatment. Further to this disruption, and unlike other immune checkpoint inhibitors, Avelumab has been shown to display some antibody-dependent cell-mediated cytotoxicity *in vitro*, adding an additional

mechanism of action to this drug (Julia et al., 2018). Indeed, treatment with avelumab has been shown to significantly increase NK cell mediated cytotoxicity against multiple TNBC cells (Julia et al., 2018). Unfortunately, this effect cannot be studied in mice as Avelumab does not mediate antibody mediated cell cytotoxicity in mouse models, which instead are dependent on CD4+ T cell and CD8+ T cell populations (Vandeveer et al., 2016). The JAVELIN clinical study investigated Avelumab across more than 15 different tumour types as a monotherapy or as a combination therapy. In the phase 1 JAVELIN study, Avelumab treatment was assessed in 168 patients with breast cancer, covering a number of different subtypes (Dirix et al., 2018b). The overall response rate (ORR) was disappointingly low at 3% overall (95% CI 1.0–6.8), and at 5.2% for triple negative breast cancer. Interestingly, there was a trend towards increased ORR in patients with PD-L1+ tumour-associated immune cells compared to PD-L1- in the overall population (16.7% vs 1.6%) and in the triple negative breast cancer group (22.2% vs. 2.6%). The responses to Avelumab were found to be durable during the trial, and the drug had a tolerable safety profile (Dirix et al., 2018b). Breast cancer treatments with Avelumab could, therefore, benefit from combined therapies with new or standard treatment drugs to improve immunotherapeutic efficacy in a wider group of patients.

Zoledronic acid, the third-generation nitrogen containing bisphosphonate, has shown promise in the treatment of early breast cancer to reduce the risk of bone metastasis. However, Zol has only shown efficacy in the post-menopausal cohort, with pre-menopausal patients presenting with increased soft tissue metastasis and a reduced iDFS (Coleman et al., 2018a). Aside from its well documented bone sparing properties, mediated through an inhibition of osteoclast activity via inhibition of the mevalonate pathway, Zol can directly target tumour cells, target immune cells and increase anti-tumour immune surveillance (George et al., 2020). Indeed, Zol has been shown to modulate macrophage polarisation towards an anti-tumour phenotype, decrease Treg cell infiltration and activity and increase effector T cell infiltration. However, high concentrations of oestradiol, such as that seen in pre-menopausal patients, can have opposing effects on anti-tumour immunity by increasing Treg activity (Luo et al., 2011), increasing tumour associated macrophage polarisation (Svensson et al., 2015) and increasing PD-L1 expression (Shuai et al., 2020) to create a pro-tumour immune environment. Combining Zol with an anti PD-L1 therapy, such as Avelumab, could increase the efficacy of both drugs by increasing populations of anti-tumour immune cells (Zol) while removing immune checkpoint blockade to improve immune cell targeting of cancer cells.

The blockade of the PD-1/PD-L1 interaction alongside Zol treatment has been investigated in a pre-clinical study aiming to enhance the breast cancer treatment benefit (Li et al., 2018). BALBc mice were subcutaneously implanted with 4T1-LUC cells in their right flank before treatment with Zol (100µg/kg every two days) and/or anti-PD-1 antibody (200µg/kg every 2 days) via IP injection. Analysis

of tumour growth by bioluminescent intensity showed that the combined therapy of Zol and anti PD-1 Ab significantly reduced primary tumour growth when compared to both control and single Zol or Ab treatment. This is the first evidence showing that combined treatment of PD-1/PD-L1 blockade alongside Zol treatment is effective at reducing tumour growth at the primary site. However, this study did not analyse the effect of the combined treatment on breast cancer metastasis, instead focusing on a subcutaneous tumour growth model, more representative of primary tumour growth. They then analysed the effect of treatments on immune cell populations within the tumour, finding a significant increase in CD8+ T cells with combined therapy, alongside a significant decrease in myeloid derived suppressor cells following treatment with Zol (Li et al., 2018). This data shows the first evidence that the combined therapy of PD-1/PD-L1 blockade alongside Zol treatment effectively reduces primary tumour growth, while increasing numbers of anti-tumour immune cells in the primary tumour. Interestingly, the immune profiling data seems to suggest two different mechanisms of action of the drugs, with PD-1 blockade effective at increasing CD8+ T cell infiltration and Zol effective at reducing the immune suppressive myeloid derived suppressor cell infiltration.

Data from chapter 5 show that CD4+ T cells and CD8+ T cells isolated from mice under pre-menopausal oestradiol concentrations had increased PD-1 protein expression compared to those isolated from mice with post-menopausal oestradiol concentrations. This increase would render these cells more susceptible to silencing by PD-L1 binding in the tumour microenvironment and suggests that PD-L1 blockade could improve Zol treatment for pre-menopausal patients. The study by (Li et al., 2018) forms an excellent base to show the efficacy of combination therapy for primary triple negative breast cancer treatment. However, the effects of combination therapy on breast cancer metastasis to bone and soft tissue were not analysed. Furthermore, the differential effects of treatment under post and pre-menopausal concentrations of oestradiol were also not analysed. The effects of combination treatment under post and pre-menopausal oestradiol concentrations could help to determine if Zol treatment could be made effective at reducing bone metastasis and soft tissue metastasis when combined with avelumab in the pre-menopausal cohort.

6.1.2 Hypothesis

Combination treatment with Avelumab and Zol could reduce bone and soft tissue metastasis under pre-menopausal oestradiol concentrations by increasing immune cell infiltrate and activity in tumours.

Aims

1. Establish the effects of combining Avelumab with Zol on metastatic outgrowth of TNBC in pre- and post-menopausal mouse models.
2. Analyse the effects of combination treatment on bone morphology and remodelling
3. Investigate the effect of combination treatment on immune cell populations and activity in different metastatic sites.

6.2 Results

6.2.1 Effects of Avelumab and Zol alone and in combination on the metastatic outgrowth of 4T1 cells.

The effect of Zol and Avelumab combined treatment on breast cancer metastasis and location was analysed by IVIS live imaging. BALBc mice injected IC with 50,000 4T1-LUC cells were treated with subcutaneous Zol (100μg/kg/week), intraperitoneal Avelumab (400μg/kg every 2-days), Avelumab+Zol or control under high or low oestradiol concentrations (n=10 per group). Soft tissue metastases and bone metastases were analysed to see how the treatments affected breast cancer metastatic dissemination and growth at the secondary sites (Figure 6.1). When soft tissue metastases were analysed under high oestradiol concentrations, Zol and Avelumab combination therapy resulted in a significant decrease in the size of metastatic deposits when compared to control (P=0.0004) (Figure 6.1 A). Furthermore, treatment with single agent Zol also resulted in a significant decrease in the size of soft tissue metastases under pre-menopausal oestradiol concentrations (P=0.0032), but this decrease was less than that observed for combination treatment. Soft tissue metastases under post-menopausal oestradiol concentrations did not show any significant differences, however treatment with combined Zol and Avelumab therapy did lead to a strong trend towards reduced soft tissue metastasis when compared to control (Figure 6.1 A). Interestingly, under post-menopausal concentrations of oestradiol, Zol did not significantly decrease soft tissue metastasis as seen under pre-menopausal oestradiol concentrations. This data shows the first evidence of combined Zol and Avelumab therapy reducing soft tissue breast cancer metastasis.

Following the exciting results observed in soft tissue metastases, the effects of combination therapy on metastasis were analysed in the bone (Figure 6.1 B). Under pre-menopausal oestradiol concentrations there were no significant differences in bone metastasis for any treatment group. However, there was a minor trend towards decreased metastasis for combination therapy and for single Zol treatment when compared to control. Interestingly, in mice with post-menopausal oestradiol concentrations, treatment with Single agent Zol (P=0.0016), single agent Avelumab (P=0.022), and combination therapy with Zol and Avelumab (P=0.0011) all significantly decreased bone metastasis when compared to control mice (Figure 6.1 B). Furthermore, treatment with combination therapy resulted in the lowest bone metastasis when compared to other treatment groups. The data suggests that combination therapy with Avelumab and Zol is effective at preventing

bone metastasis under post-menopausal concentrations of oestradiol, while it is effective at reducing soft tissue metastasis under pre- and post-menopausal oestradiol concentrations.

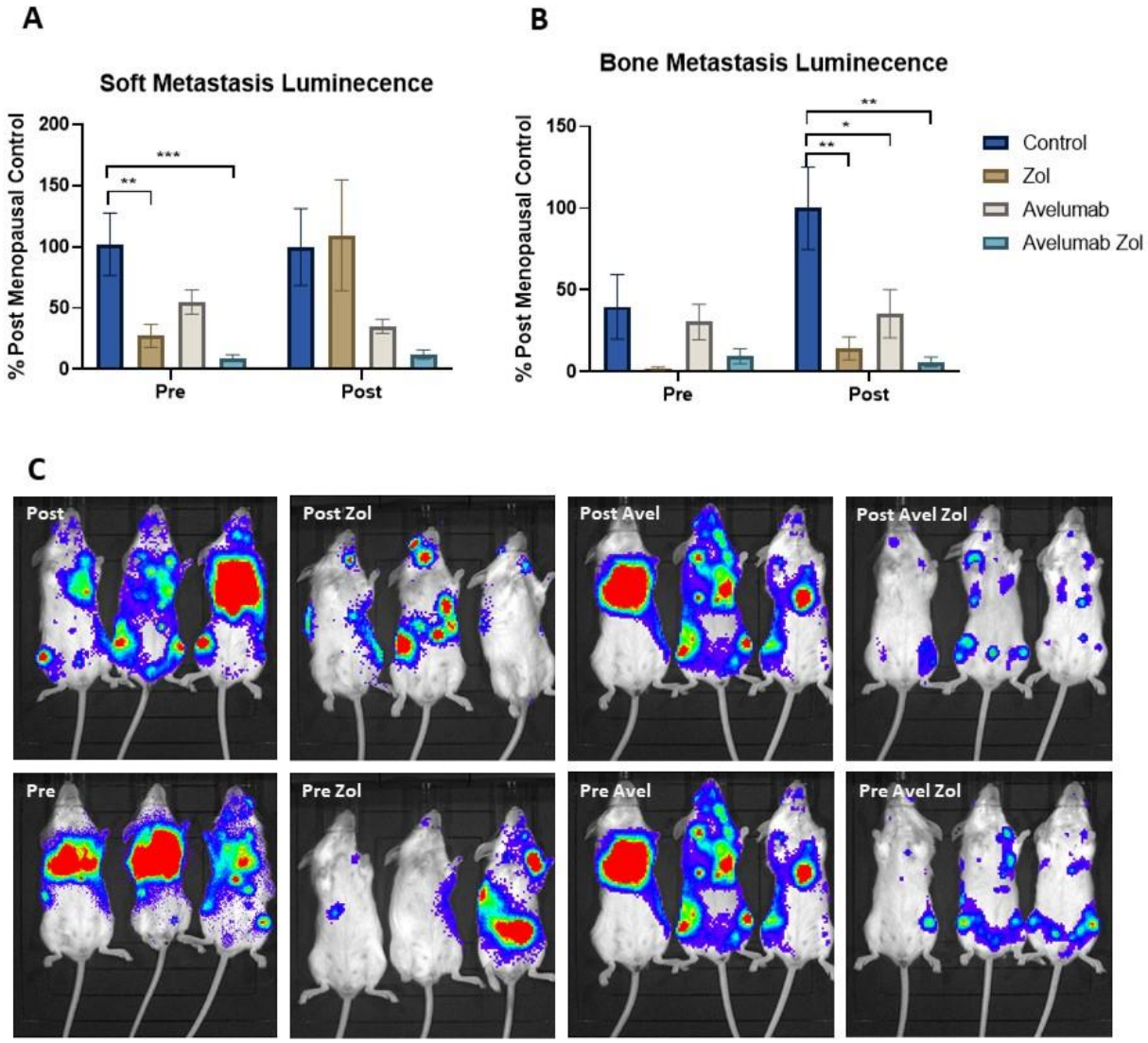

Figure 6.1: The effect of combination therapy with Avelumab and Zol on tumour growth

BALBc mice underwent OVX before oestradiol replacement in drinking water to model Post and Pre-menopausal concentrations. Mice were injected IC with 50,000 4T1-LUC cells and treated with Zol (100µg/kg), Avelumab (400µg every 2 days) or combined Avelumab & Zol. Mice were injected with luciferin before imaging by the IVIS system. **(A)** In vivo luminescent analysis of tumour growth in soft tissue showing photons/sec (n=10 per group) **(B)** In vivo luminescent analysis of tumour growth in bone tissue showing photons/sec (n=10 per group) **(C)** Representative images showing tumour growth in live mice following treatments.

Data shown are mean ± SEM and statistical analysis was by one way ANOVA with Tukeys post test and students T test

*< 0.05, ** < 0.01, *** < 0.001, **** < 0.0001

6.2.2 The of combination therapy with Avelumab and Zol on immune cell populations

6.2.2.1 effect Immune cell populations in the bone

The immune response plays a pivotal role in breast cancer progression and metastasis, and the use of immune modulatory drugs in this study aims to stimulate anti-tumour immune responses to prevent metastasis. Following on from the encouraging tumour growth analysis showing combined treatment significantly reducing both bone and soft tissue metastasis, I next analysed the effect of combination treatment on immune cell populations in tumour bearing bones, lungs and in the spleen representing systemic effects. The infiltrating immune cells could provide a mechanism whereby combined treatment excerpts its anti-tumour effects.

Within tumour bearing bones, oestradiol concentrations significantly decreased B cell numbers under high oestradiol concentrations in single treatment Avelumab groups (P=0.0015) and a trend in the Avelumab/Zol group (Figure 6.2 H). Oestradiol has limited effects on other cell types within the bone, showing effects only in the single treatment Avelumab group where high oestradiol significantly increased NK cell number(P=0.0532) (Figure 6.2 K) and neutrophil numbers (P=0.3) (Figure 6.2 B). Interestingly, under low oestradiol, combination therapy with Avelumab and Zol significantly increased numbers of the anti-cancer B cells (P=0.02) (Figure 6.2 H), CD4+ T cells (P=0.009) (Figure 6.2 G) and CD8+ T cells (P=0.033) (Figure 6.2 I), suggesting that combination therapy may reduce T cell exhaustion and increase infiltration. On the other hand, combination therapy also significantly decreased the infiltration of some immune cell subsets. NK cells were significantly decreased by Avelumab and Zol under low oestradiol concentrations (P=0.0004) (Figure 6.2 K), alongside a significant decrease in neutrophils (P=0.017) (Figure 6.2 B) and monocytes (P=0.046) (Figure 6.2 C). These results show both an anti-tumour immune profile in T cells and B cells and a pro-tumour immune profile for NK cells and neutrophils following combination therapy with Avelumab and Zol. However, tumour growth experiments showed combination therapy significantly decreases bone metastasis, suggesting that the anti-tumour immune effects may outweigh the decreases seen in NK cells, and that there may be effects mediated by non-immune bone resident cells.

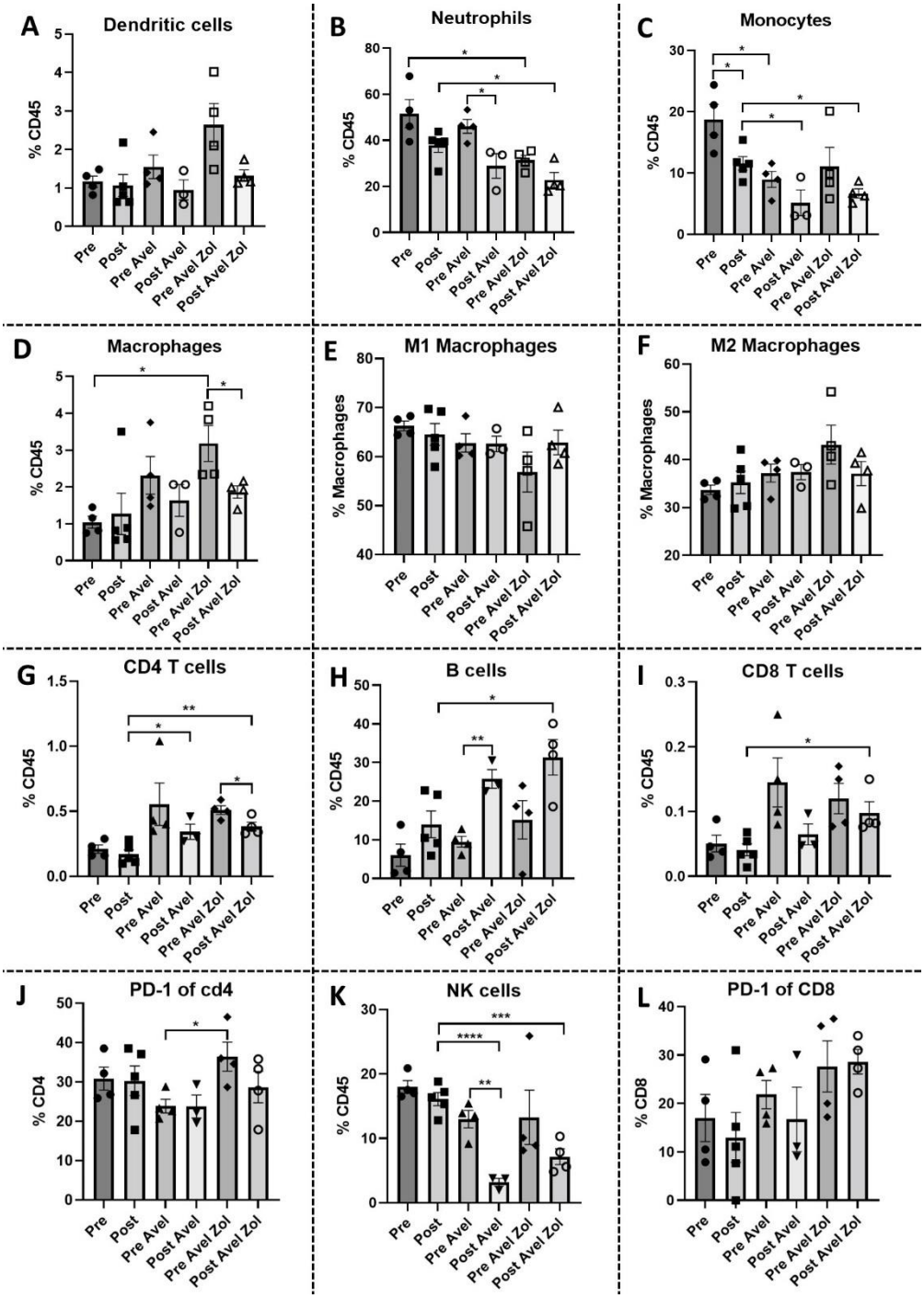

Figure 6.2: The effect of combination therapy with Avelumab and Zol on immune cells in bone

BALBc mice with 4T1-LUC tumours underwent OVX before oestradiol replacement in drinking water to model Post and Pre-menopausal concentrations. Mice were IC injected with 50,000 4T1-LUC cells and treated with Zol (100µg/kg), Avelumab (400µg every 2 days) or combined Avelumab & Zol. Flow cytometry analysis for immune cell populations.

(A) Dendritic cells (CD45+,CD11b+,CD11c+,MHCII+) **(B) Neutrophils** (CD45+,CD11b+,Ly6G+), **(C) Monocytes** (CD45+,CD11b+,LY6G-,LY6C+,F480) **High, (D) Macrophages** (CD45+,CD11b+,LY6G-,LY6C Low, F480 High), **(E) M1 Macrophages** (Macrophage, MRC1-), **(F) M2 Macrophages** (Macrophage, MRC1+), **(G) CD4+ T cells** (CD45+,CD19-,CD3+,CD4+), **(H) B Cells** (CD45+,CD19+,CD3-), **(I) CD8+ T cells** (CD45+,CD19-,CD3+,CD8+) **(J) PD-1 on CD4+ T cells** (CD4 T cells, PD-1+), **(K) NK cells** (CD45+,CD19-,CD3-, NK1.1+), **(L) PD-1 on CD8+ T cells** (CD8 T cells, PD-1+).Data shown are mean ± SEM and statistical analysis by one way ANOVA with Tukeys post test and students T test

*< 0.05, ** < 0.01, *** < 0.001, **** < 0.0001

6.2.2.2 Immune cell populations in the lung

Tumour bearing lungs were analysed by flow cytometry and qPCR array for immune cell populations following treatment as described above (Figure 6.3 & 6.4). Flow cytometry analysis showed that combination therapy with Avelumab and Zol significantly increased CD4 T cells in the lung under high oestradiol concentrations (P=0.048) (Figure 6.3 G). Moreover, qPCR array analysis showed that combination therapy significantly increased *granzyme B* gene expression in lungs under low oestradiol concentrations (P=0.0378) (Figure 6.4), suggesting an increase in lymphocyte activity and CD4+ lymphocyte cell number following combined Avelumab and Zol treatment. On the other hand, combined therapy under high oestradiol concentrations significantly reduced anti-tumour NK cell numbers in the lung, opposing the effects observed in CD4 T cells (P=0.048) (Figure 6.3 K). In CD8 T cells, combination therapy had no significant effect, however, under low oestradiol concentrations, single treatment Avelumab significantly reduced CD8 T cell number (P=0.013). Interestingly, combined therapy under low oestradiol concentrations significantly increased *Nos2* gene expression when compared to control in mice (Figure 6.4). *Nos2* is a marker of M2 macrophage activity, and expression in cancer cells and can be a predictor of poor prognosis. Interestingly, under the influence of low oestradiol concentrations, combined therapy significantly increased *cd274* gene expression when compared to single agent Zol (encoding PD-L1 protein) (Figure 6.4). Furthermore, combination treatment when compared to single treatment Zol significantly increased *IL1b* gene expression, a pro-inflammatory molecule (Figure 6.4).

Combined therapy with Avelumab and Zol has significant effects on neutrophils of the myeloid lineage (Figure 6.3 B). qPCR array analysis showed that combination therapy significantly reduces neutrophil expression in the lung when compared to single treatment Zol (P=0.0139) (Figure 6.4). Flow cytometry analysis showed that combination therapy significantly reduced neutrophils compared to control under high oestradiol concentrations (P=0.0101) (Figure 6.3 B). However, single Avelumab treatment had no significant effect on neutrophil numbers compared to control and the reduction in neutrophil numbers in combination therapy. qPCR array card analysis showed no significant changes to immune cell populations in the combination therapy group when compared to control (appendix). Furthermore, oestradiol concentration had no significant effect on either immune cells or immune cell activity markers analysed by qPCR array card (appendix). The immune cell analysis is complex; however, overall combination therapy increases only CD4 T cell numbers, while significantly increase markers of lymphocyte activity, perhaps explaining the significant decrease in tumour growth in the lung following combination treatment with Avelumab and Zol.

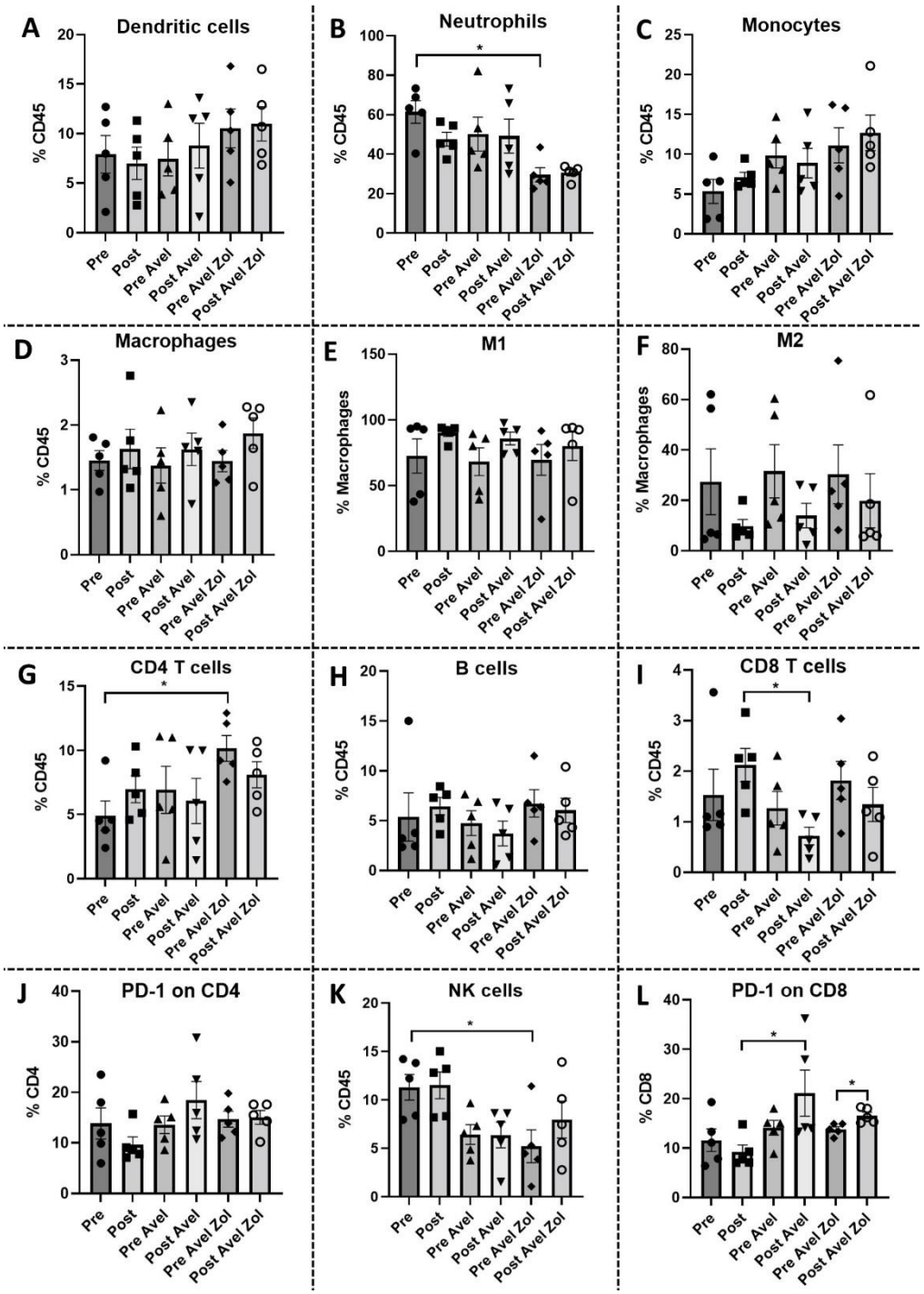

Figure 6.3: The effect of combination therapy with Avelumab and Zol on immune cells in lung

BALBc with 4T1-LUC tumours mice underwent OVX before oestradiol replacement in drinking water to model Post and Pre-menopausal concentrations. Mice were IC injected with 50,000 4T1-LUC cells and treated with Zol (100µg/kg), Avelumab (400µg every 2 days) or combined Avelumab & Zol. Flow cytometry analysis for immune cell populations.

(A) Dendritic cells (CD45+,CD11b+,CD11c+,MHCII+) **(B) Neutrophils** (CD45+,CD11b+,Ly6G+), **(C) Monocytes** (CD45+,CD11b+,LY6G-,LY6C+,F480) **High, (D) Macrophages** (CD45+,CD11b+,LY6G-,LY6C Low, F480 High), **(E) M1 Macrophages** (Macrophage, MRC1-), **(F) M2 Macrophages** (Macrophage, MRC1+), **(G) CD4+ T cells** (CD45+,CD19-,CD3+,CD4+), **(H) B Cells** (CD45+,CD19+,CD3-), **(I) CD8+ T cells** (CD45+,CD19-,CD3+,CD8+) **(J) PD-1 on CD4+ T cells** (CD4 T cells, PD-1+), **(K) NK cells** (CD45+,CD19-,CD3-, NK1.1+), **(L) PD-1 on CD8+ T cells** (CD8 T cells, PD-1+).Data shown are mean ± SEM and statistical analysis by one way ANOVA with Tukeys post test and students T test

*< 0.05, ** < 0.01, *** < 0.001, **** < 0.0001

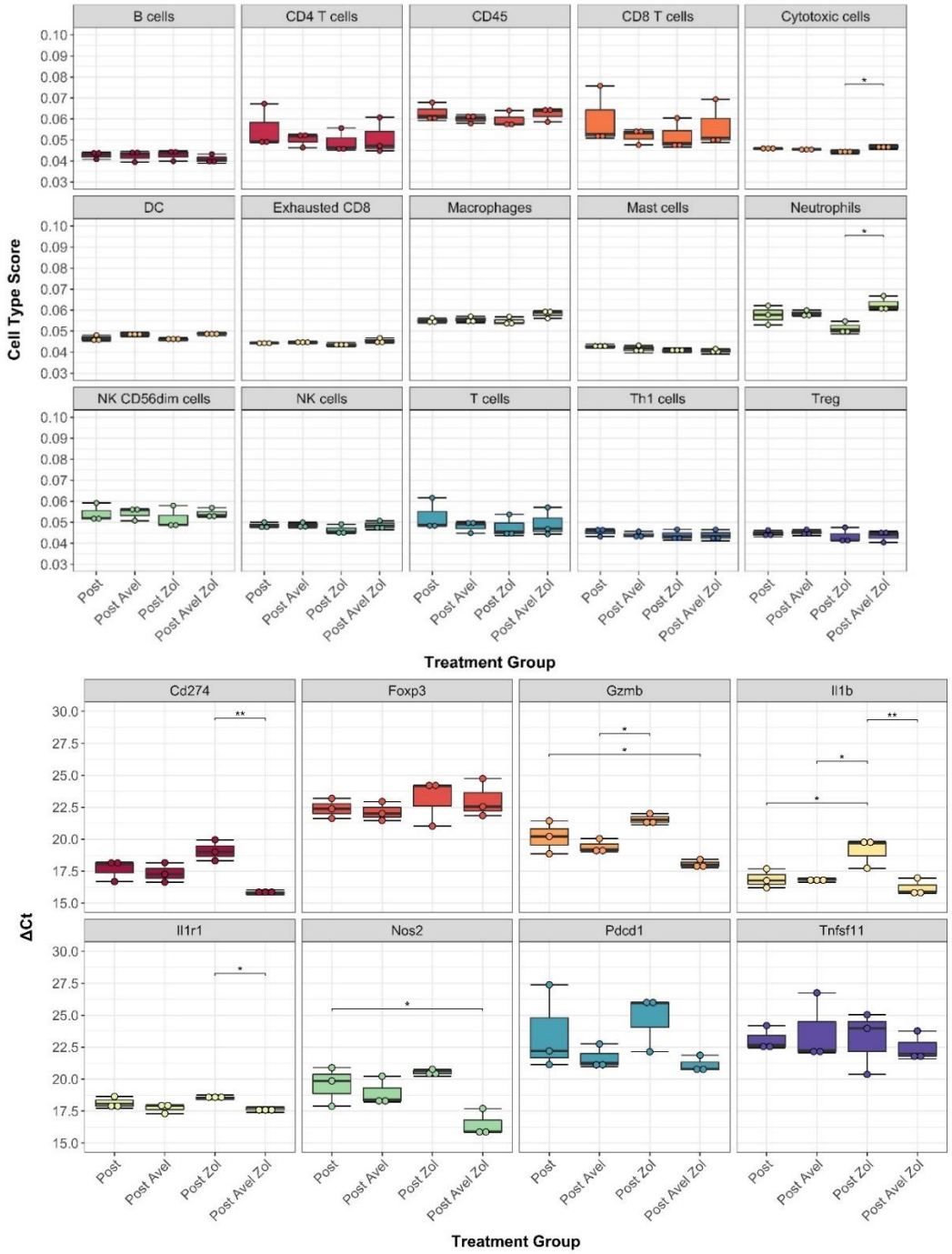

Figure 6.4: The effect of combination therapy with Avelumab and Zol on immune cells in bone

BALBc mice with 4T1 LUC tumours underwent OVX before oestradiol replacement in drinking water to model Post and Pre-menopausal concentrations. Mice were IC injected with 50,000 4T1-LUC cells and treated with Zol (100µg/kg), Avelumab (400µg every 2 days) or combined Avelumab & Zol. RNA was extracted from lung using before reverse transcription followed by Taqman qPCR array. For immune cell typing, delta CT was calculated from Raw CT values and formatted into an expression matrix. Immune cell type signatures were taken from Nanostring and expression matrix was sub-setted into columns and rows corresponding to cell type gene signatures. A cell type signature score was calculated as inverse geometric mean resulting in a single value for a cell type for each replicate.
Cell type markers in section 2.7.2
Data shown are mean ± SEM and statistical analysis performed by one way ANOVA with Tukeys post test and students T test
*< 0.05, ** < 0.01, *** < 0.001, **** < 0.0001

6.2.2.3 Immune cell population in the spleen

In both the AZURE and the ABCSG-12 trials, adjuvant Zol was administered prior to evidence of metastasis in breast cancer patients. Differences in metastasis development may be mediated by changes in systemic immunity alongside changes at specific metastatic sites. Therefore, I investigated the effect of combination therapy with Avelumab and Zol on immune cell populations in the spleen (Figure 6.5). Combination therapy under low oestradiol concentrations significantly increased Dendritic cell numbers in the spleen (P=0.015) (Figure 6.5 A), and increased macrophage numbers in the spleen (P=0.0016) (Figure 6.5 D). However, under high oestradiol, combination therapy significantly decreased macrophage numbers in the spleen (P=0.029). Interestingly, combination therapy also altered macrophage polarisation under low oestradiol concentrations, increasing polarisation towards an M2 macrophage phenotype. Overall, this data suggests a decrease in systemic anti-tumour immune cells following combination therapy. Interestingly, under low oestradiol concentrations, combined treatment with Avelumab and Zol significantly increased PD-1 expression on circulating CD4+ T cells (P=0.0006)(Figure 6.5 J) and CD8+ T cells (P=0.0094)(Figure 6.5 L). This increase in PD-1+ cells may be due to a decrease in PD-L1 binding because of Avelumab treatment, leading to a decrease in exhausted T cells and an increase in PD-1 positive lymphocytes.

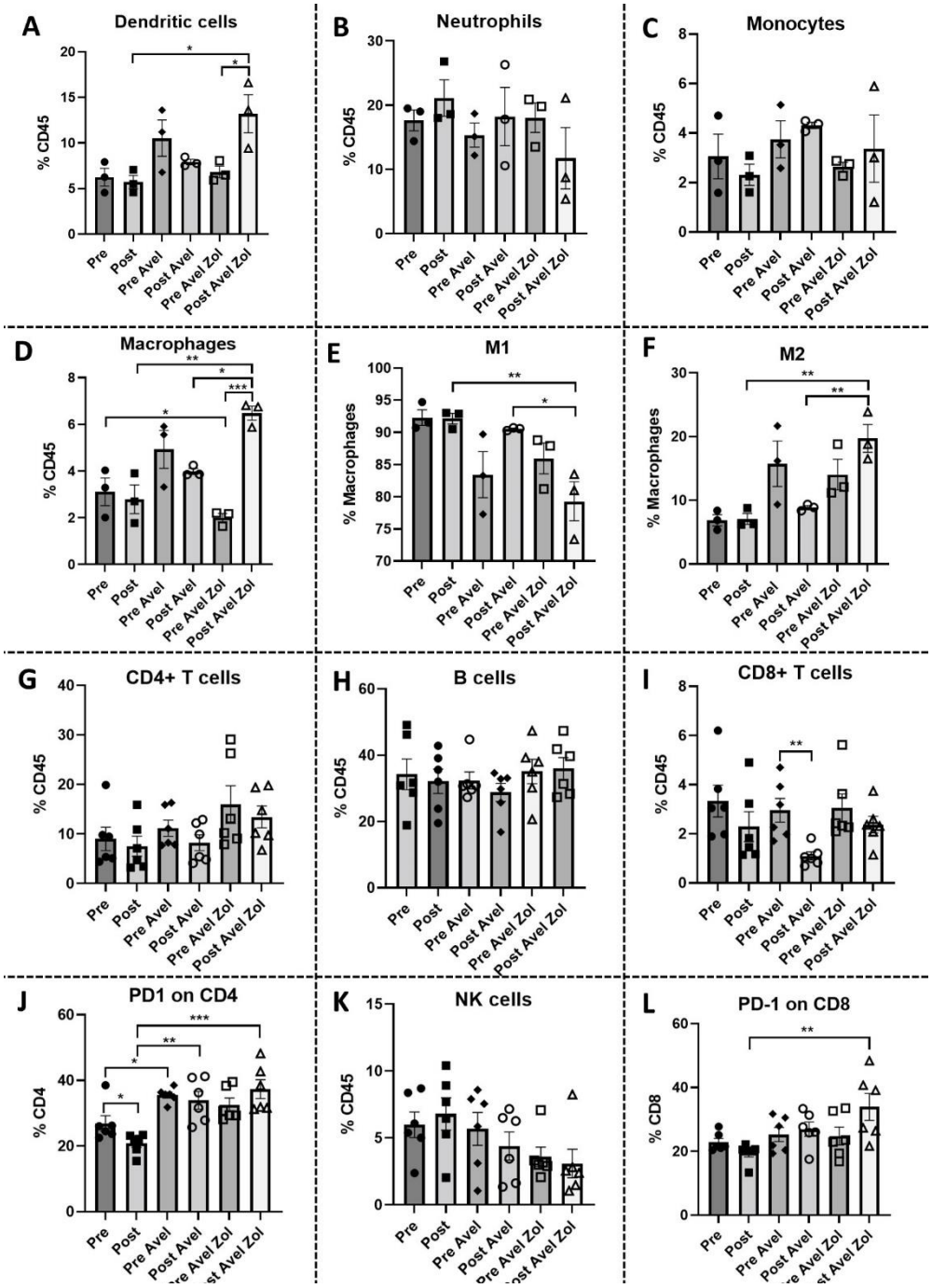

Figure 6.5: The effect of combination therapy with Avelumab and Zol on immune cells in spleen

BALBc mice with 4T1-LUC tumours underwent OVX before oestradiol replacement in drinking water to model Post and Pre-menopausal concentrations. Mice were IC injected with 50,000 4T1-LUC cells and treated with Zol (100µg/kg), Avelumab (400µg every 2 days) or combined Avelumab & Zol. Flow cytometry analysis for immune cell populations.
(A) Dendritic cells (CD45+,CD11b+,CD11c+,MHCII+) **(B) Neutrophils** (CD45+,CD11b+,Ly6G+), **(C) Monocytes** (CD45+,CD11b+,LY6G-,LY6C+,F480) **High, (D) Macrophages** (CD45+,CD11b+,LY6G-,LY6C Low, F480 High), **(E) M1 Macrophages** (Macrophage, MRC1-), **(F) M2 Macrophages** (Macrophage, MRC1+), **(G) CD4+ T cells** (CD45+,CD19-,CD3+,CD4+), **(H) B Cells** (CD45+,CD19+,CD3-), **(I) CD8+ T cells** (CD45+,CD19-,CD3+,CD8+) **(J) PD-1 on CD4+ T cells** (CD4 T cells, PD-1+), **(K) NK cells** (CD45+,CD19-,CD3-, NK1.1+), **(L) PD-1 on CD8+ T cells** (CD8 T cells, PD-1+).Data shown are mean ± SEM and statistical analysis by one way ANOVA with Tukeys post test and students T test

*< 0.05, ** < 0.01, *** < 0.001, **** < 0.0001

6.2.3 Effect of Avelumab and Zol on trabecular bone volume

Following immune cell analysis in the bone showing a pro-tumour phenotype following combination treatment with Avelumab and Zol, I investigated the effects of treatment on the bone microenvironment to elucidate if changes in bone turnover contribute to the reduced metastasis observed in Figure 6.1. The effects of combined treatment on bone volume and bone resident cell activity was evaluated by µCT and ELISA analysis. Analysis of trabecular bone volume in tumour bearing bones following treatment with high and low oestradiol concentrations following OVX (representing pre- and post-menopausal oestradiol) displayed a similar pattern to previous models (Figure 6.6 A) with high oestradiol concentrations significantly increasing trabecular bone volume when compared to low oestradiol mice irrespective of Zol or Avelumab treatment ($p<0.0001$ control, Zol, Avel, $P=0.0001$ Avel Zol). Interestingly, single agent therapy with Zol or Avelumab resulted in no significant change to trabecular bone volume under high or low oestradiol concentrations. However, combined treatment with Avelumab + Zol resulted in a significant increase in trabecular bone volume under both high and low oestradiol concentrations (Figure 6.6 A)($P= 0.0132$ & 0.0464 respectively). Furthermore, combined treatment with Avelumab and Zol significantly increased bone volume when compared to single treatment Zol under high oestradiol concentrations. This suggests that treatment with Avelumab alongside Zol improves the anti-resorptive properties of Zol.

6.2.4 Effect of Avelumab and Zol on bone remodelling markers

Serum analysis for TRAPcP-5b concentration, a marker of osteoclast activity, was performed by ELISA analysis of serum following the experimental endpoint (Figure 6.6 B). Interestingly, oestradiol concentration had no significant effect on TRAPcP-5b concentrations under any treatment group in this BALBc model. This result is different to that seen in the previous BALBc model, where oestrogen significantly decreased TRAPcP-5b in the control arm. Zol treatment under high and low oestradiol concentrations did significantly decrease TRAPcP-5b concentrations ($P=0.001$ & $P=0.0007$ respectively), indicating a decrease in osteoclast activity following Zol treatment (Figure 6.6 B). Furthermore, combined treatment with Avelumab and Zol also significantly decreased TRAPcP-5b concentration to similar levels to that seen in Zol single treatment under high and low oestradiol concentrations ($P=0.0035$ & $P=0.014$ respectively). Interestingly, under low oestradiol concentration, Avelumab single treatment significantly decreased TRAPcP-5b concentration ($P=0.0424$), indicating that Avelumab treatment alone is able to affect osteoclast activity in bone.

Serum analysis for P1NP concentrations, a marker of osteoblast activity, was also performed by ELISA analysis at the experimental endpoint (Figure 6.6 C). Low concentrations of oestradiol compared to high concentrations significantly decreased P1NP concentration in the combined treatment group, but significantly increased P1NP concentration in the Zol treatment group. Treatment with Zol significantly decreased P1NP concentration in the high oestradiol group. However, combined treatment with avelumab and Zol significantly increased P1NP concentrations compared to single Zol treatment to levels similar to control levels (Figure 6.6 C). This data could go some way to explaining results seen in the µCT analysis where combination therapy resulted in significantly higher trabecular bone volume, possibly because combination treatment stimulates an increase in osteoblast activity while inhibiting osteoclast activity.

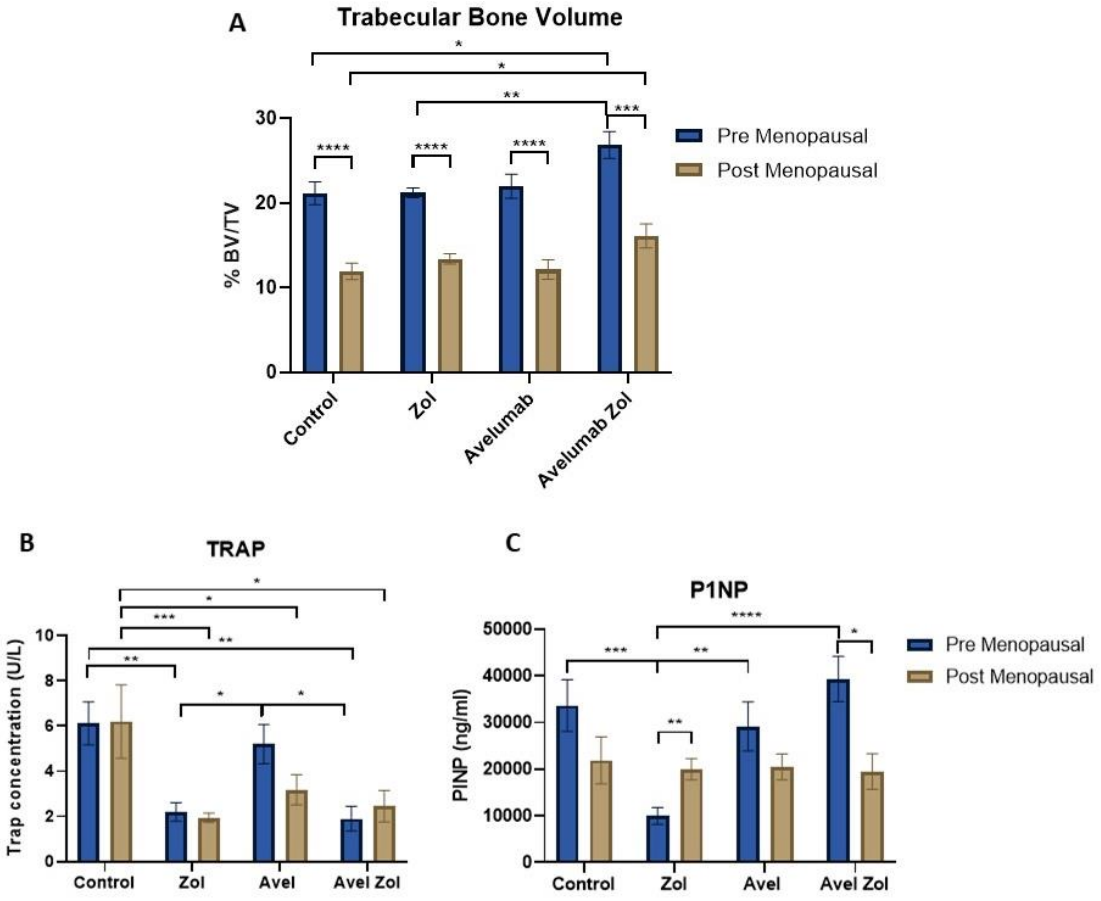

Figure 6.6: The effect of combination therapy with Avelumab and Zol on bone turnover

BALBc mice underwent OVX before oestradiol replacement in drinking water to model Post and Pre-menopausal concentrations. Mice were injected IC with 50,000 4T1-LUC cells and treated with Zol (100µg/kg/week), Avelumab (400µg every 2 days) or combined Avelumab & Zol. **(A)** Tibia from mice analysed by µCT showing trabecular bone volume/ tissue volume (%BV/TV) (n=10 per group) **(B)** Serum from mice at experimental endpoint analysed by ELISA for TRAcP5b concentrations (n=5) **(C)** Serum from mice at experimental endpoint analysed by ELISA for P1NP concentrations (n=5)

Data shown are mean ± SEM and statistical analysis by one way ANOVA with Tukeys post test and students T test

*< 0.05, ** < 0.01, *** < 0.001, **** < 0.0001

6.3 Discussion

Combination therapy represents an important cornerstone of cancer treatment, often allowing the amalgamation of drugs efficacy. Furthermore, improving the efficacy of drugs that have already gone through clinical trial and approval represents a cost effective and efficient way to bring drugs to the clinic. Researching combination treatment, compared to mono-therapy, could help to improve the efficacy of a drug in a demographic of patients where there was previously little benefit. The ABCSG-12 trial showed that adjuvant treatment with Zol after primary tumour resection is effective at preventing bone metastasis. However, the AZURE trial showed that women with pre-menopausal oestradiol concentrations had increased soft tissue metastasis and reduced iDFS following adjuvant Zol. Interestingly, Zol and oestradiol have been shown to have effects on the immune system, with Zol increasing anti-tumour immune cells and oestradiol decreasing anti-tumour immunity while increasing PD-L1 expression (George et al., 2020). Therefore, I hypothesised that combination treatment with Zol alongside the anti-PD-L1 antibody Avelumab could improve the efficacy of Zol and allow its use in the pre-menopausal cohort.

The effect of combination therapy with Avelumab and Zol on tumour growth within the bone and soft tissue was analysed to elucidate the anti-tumour efficacy of treatments. Interestingly, combination therapy led to a significant decrease in bone metastasis under low oestradiol concentrations and a significant decrease in soft tissue metastasis under high oestradiol concentrations, while leading to strong trends towards decreased metastasis in other oestradiol groups. Although combination therapy with PD-1 blockade alongside Zol has previously been shown to reduce primary tumour growth (Li et al., 2018), this data provides the first evidence of the anti-tumour efficacy of combination therapy on breast cancer metastasis to both the bone and the soft tissue. Interestingly, combination therapy was shown to reduce soft tissue metastasis in the presence of high oestradiol concentrations. In the AZURE trial, in women with pre-menopausal oestradiol concentrations, adjuvant therapy with Zol was shown to increase soft tissue metastasis incidence while decreasing iDFS, meaning that preventative Zol treatment is not used in these patients. Therefore, this data shows that combining Zol treatment with Avelumab could facilitate the use of this preventative treatment in the pre-menopausal cohort of patients.

A previous study has shown that combining Zol and anti-PD-1 therapies significantly reduces primary tumour growth of breast cancer in immune competent mouse models (Li et al., 2018). However, the drug used differed from Avelumab used in the present study, binding to the PD-1 receptor instead of its ligand PD-L1. The use of Avelumab instead of an anti-PD-1 antibody could be more efficacious in the patient population, since Avelumab has been shown to have a secondary mode

of action in humans, eliciting antibody mediated cell cytotoxicity (Julia et al., 2018). Therefore, if used in the clinic alongside Zol, the combination therapy could be more effective than seen in the mouse models by directly inducing cancer cell death alongside its effects on the microenvironment.

To understand the mechanism behind the observed decreases in tumour volume following combined treatment with oestradiol and Zol, I next analysed immune cell populations within tumour bearing bones, tumour bearing lungs and the spleen following experimental endpoint. Overall, in all organs, combination therapy with Avelumab and Zol led to a trend towards reduced numbers of anti-tumour immune cells when compared to controls. For example, in bone, combination therapy significantly reduced numbers of monocytes, neutrophils and NK cells, while in lung combination therapy also significantly reduced neutrophil numbers. On the other hand, in lung combination therapy resulted in a significant increase in *granzyme B* gene expression, suggesting an increased activity of immune cells following treatment. Interestingly, *PD-L1* gene expression was significantly increased following combination therapy under low oestradiol concentrations, suggesting an increased immune evasive ability of cells following treatment. However, Avelumab treatment should block the downstream effects of this increase in PD-L1 expression by binding to the resulting protein and preventing signalling with PD-1 receptor. These immune population results are unexpected, as treatment with Avelumab would be expected to increase immune cell infiltration into tumour bearing organs by reducing checkpoint inhibition, reducing Treg cell activation and promoting tumour cell cytotoxicity. Inversely, the blocking of checkpoint inhibition means that fewer immune cells in the tumour can excerpt a greater response as cells do not become exhausted. This theory is reflected in *Granzyme B* expression analysis, suggesting increased immune cell activity following Avelumab and Zol combination therapy. Li *et al. (*2018) analysed tumour infiltrating immune lymphocytes following Zol and anti-PD-1 treatments and found a significant increase in CD8+ T cells alongside a significant decrease in myeloid derived suppresser cells following combination treatment. Although this significant increase in lymphocyte populations was not observed in the current study, there was a trend towards increased CD4+ T cell numbers in bone following combination therapy, and a significant increase in CD4+ T cells in bone following single agent Avelumab. Furthermore, regulatory immune cells, immune supressing cells and markers of immune cell activity were not analysed in these experiments, cells that could be responsible for the changes in tumour growth and metastasis observed. The flow cytometry experiments have relatively low n numbers per group (n=3-5) and display a reasonable level of variation as expected from *in vivo* experiments. Therefore, future experiments could be performed to increase n numbers for these experiments to help better elucidate changes in immune cell populations.

The results from immune cell analysis in the bone following combination therapy with Avelumab and Zol showed a pro-tumour effect, suggesting that another mechanism may be responsible for the observed decrease in bone metastases. Therefore, the effect of Avelumab and Zol on bone volume and bone turnover was investigated to determine if Avelumab as a single treatment or in combination with Zol can alter bone resident cell activity. Interestingly, combination therapy with Avelumab and Zol significantly increased trabecular bone volume, significantly decreased TRAPcP-5b serum concentration (a marker of osteoclast activity) and led to a trend towards increased P1NP concentration (a marker of osteoblast activity). Furthermore, for trabecular bone volume and P1NP concentration, the increases observed were significantly higher when compared to single treatment Zol. This suggests that Avelumab in the presence of Zol increases trabecular bone volume by decreasing osteoclast activity and increasing osteoblast activity. This result may be an artifact of the reduced tumour volume in bones following combination therapy, reducing tumour mediated osteolysis. However, single treatment Zol under high oestradiol concentrations also exhibited low tumour volume, but did not have increased bone volume, suggesting another mechanism at play. It has been shown that PD-L1 binding PD-1, in the presence of RANKL, induced osteoclastogenesis (Wang et al., 2020). Induction of osteoclasts from bone marrow cells with MCSF and RANKL, alongside PD-L1 found that PD-L1 increased osteoclast differentiation, an effect that was blocked by treatment with the anti-PD-1 antibody nivolumab. Furthermore, following treatment of tumour bearing mice with nivolumab, serum CTX-I levels, a marker of bone resorption, were significantly decreased, suggesting reduced osteoclast activity. Interestingly, this was found to be an effect mediated during the differentiation stage of osteoclasts, with osteoclasts loosing PD-1 expression as they mature *in vitro* (Wang et al., 2020). This paper could help to explain the increase in bone volume observed following combination therapy with Zol, a potent anti-resorptive drug, and Avelumab.

Reducing bone resorption and osteoclast activity is highly beneficial for the treatment of bone metastasis. In tumour bearing bones, osteoclasts form part of a vicious cycle of bone degradation and tumour growth, with tumour cells promoting osteoclastogenesis and osteoclast activity, thereby increasing bone resorption which releases bone derived growth factors that promote tumour growth. Inhibiting osteoclast action breaks the vicious cycle, making the bone a less hospitable place for tumour growth. However, osteoclasts can also regulate the immune system, with osteoclasts and T cells having reciprocal communication. Indeed, *in vitro* experiments have shown that osteoclasts can supress T cell proliferation (Grassi et al., 2011), while T cells have been shown to inhibit osteoclast proliferation and differentiation (Takayanagi, 2009). Therefore, inhibiting osteoclasts with Zol alongside removing checkpoint inhibition could help to improve T cell infiltrate into tumour bearing bones, while making the bone a less hospitable environment for tumour growth.

6.4 Summary and conclusion

Combination therapy is an effective clinical tool to improve the treatment outcome over single agent therapies alone. Avelumab and Zol combined treatment significantly decreased tumour volume in the bone and in the soft tissue of mice, having the most potent effects under high oestradiol concentration in soft tissue and under low oestradiol concentrations in bone. Analysis of immune cell populations in metastatic sites and circulating tissues gave inconclusive results, with some immune cells decreasing following combined therapy, but some markers of immune cell activity increasing following combination therapy, highlighting the need for further analysis. Interestingly, combination therapy using Zol and Avelumab significantly increased trabecular bone volume while increasing osteoblast activity *in vivo*, suggesting that combination therapy promotes an anti-tumour microenvironment in the bone. This data is the first evidence of combination therapy with Avelumab and Zol effectively reducing breast cancer metastasis. Furthermore, this exciting data suggests that utilising Avelumab alongside Zol in the clinic could allow the preventative treatment to be effective in the pre-menopausal cohort of patients for the first time.

Chapter 7: Discussion

Zol is a third-generation nitrogen containing bisphosphonate that quickly binds hydroxyapatite in the bone and prevents bone loss by inhibiting enzymes of the mevalonate pathway, therefore inhibiting osteoclast activity and promoting osteoclast apoptosis. However, Zol also has anticancer properties and a number of clinical trials have evaluated its efficacy at preventing bone metastasis in breast cancer patients following primary tumour resection. The first reported benefits from adjuvant Zol for breast cancer recurrence were described by the ABCSG12 and AZURE clinical trials. These two studies differed in treatment regime, the ABCSG-12 trial treated 1803 pre-menopausal patients with Zol, alongside Goserelin and endocrine therapy which rendered patients chemically post-menopausal (Gnant et al., 2011). This trial saw a significant decrease in relative risk of disease for all patients. The AZURE trial on 3360 pre- and post-menopausal women receiving standard treatment alongside adjuvant Zol following primary tumour resection found that OS and DFS were not affected by Zol (Coleman et al., 2018a). However, subgroup analysis found that patients who were more than 5-years post-menopausal benefited from treatment and had an improved iDFS and OS, while pre-menopausal patients did not benefit, displaying increased soft tissue metastasis. The mechanism behind this differential result is still to be elucidated, however, I hypothesized that oestradiol driven changes to the immune microenvironment and PD-L1 expression in breast cancer metastasis effects the efficacy of Zol treatment. Therefore, I set up two distinct immunocompetent mouse models in which breast cancer cells were disseminated into metastatic organs (primarily bone and lung) in the presence of Post-, Peri- or Pre-menopausal concentrations of oestradiol to evaluate the effect of Zol on metastatic outgrowth and immune cell composition.

7.1 Effect of Zol treatment under post-, peri- or pre-menopausal oestradiol concentrations on breast cancer metastasis

The selected mouse models, C57BL/6 with E0771-LUC cells and BALBc with 4T1-LUC cells, responded differently to Zol treatment under different oestradiol concentrations. In the C57BL/6 model, IC injected with E0771-LUC cells, high oestradiol concentrations significantly increased numbers of bone metastases, while Zol treatment under low (post-menopausal) concentrations of oestradiol significantly increased numbers of bone metastases. A similar trend was observed for tumour volume analysis. On the other hand, in the BALBc model, post-menopausal oestradiol concentrations significantly increased volume of bone metastases, while Zol treatment led to a trend towards decreased bone metastasis under post-menopausal oestradiol concentrations. Incidence of bone metastases in the absence of Zol in the C57BL/6 model more closely resembles the clinical setting. A clinical study of 3553 breast cancer patients found that increased age at the time of breast

cancer diagnosis corelated with a reduced risk of distant bone metastasis (Purushotham et al., 2014). On the other hand, the effect of Zol treatment on bone metastasis reflected the clinical setting best in the BALBc model, with Zol leading to trends towards decreased bone metastases number across all oestrogen concentrations, and a reduction in tumour volume under post-menopausal oestradiol concentrations.

Soft tissue metastasis also differed between the two models used for this study. In the C57BL/6 model, Zol treatment under pre-menopausal concentrations of oestradiol significantly increased soft tissue metastasis when compared to Zol treated mice under post-menopausal oestradiol concentrations. This reflects that seen in the clinic, where pre-menopausal patients treated with Zol exhibited higher soft tissue metastasis and had reduced OS. Interestingly, in BALBc mice, Zol treatment had no effect on soft tissue metastasis under pre-menopausal concentrations of oestradiol but did significantly decrease metastasis under post-menopausal concentrations. This data also reflects elements seen in the AZURE trial, showing that Zol treatment decreases soft tissue metastasis in the absence of oestradiol, but in the presence of oestradiol, it does not exert any beneficial effects (Coleman et al., 2018a). Taken together, the two models show different trends of tumour growth following Zol treatments, but together each model contains elements relating to isolated effects observed in clinical findings. The data highlights how genetic and physiological background of patients/mice can affect treatment outcome. Indeed, patient genetic background and tumour genetic makeup can affect the pattern of metastasis from breast cancers and response to treatment. An analysis of the genetic expression profiles of 92 breast cancer patients, 46 with bone metastasis and 46 without, found 22 significantly differentially expressed genes between the two groups and found that these could be used to better predict bone metastasis risk (Cosphiadi et al., 2018). The genetic differences present between both the mouse strains and the murine breast cancer cell lines used could help to explain the differences in tumour metastasis and response to treatment observed in this study. Interestingly, a previous publication from our research team found that high concentrations of oestradiol increased soft tissue metastasis in the immunocompetent mouse models but did not affect metastasis to the soft tissues of immunocompromised mice, suggesting the immune response is important for the anti-tumour effect of Zol in soft tissue (Canuas-Landero et al., 2021).

7.2 Effect of Zol treatment under post-, peri- or pre-menopausal oestradiol concentrations on metastatic microenvironments.

Following *in vitro* experiments showing that the effects of Zol and oestradiol *in vivo* are not mediated via direct actions on breast cancer cells (Chapter 3), I analysed effects on the

microenvironments of the metastatic sites. I hypothesize that the effects observed in the ABCSG-12 and AZURE trials are due to Zol and oestradiol altering the immune response to breast cancer. To differentiate between immune regulated and bone cell regulated effects of Zol and oestradiol, I first assessed to what extent changes to the bone microenvironment following treatment could contribute to differential metastatic patterns. High oestradiol concentrations significantly increased trabecular bone volume in both mouse models, with Zol having little effect on bone volume. This supports the well documented role of oestradiol promoting healthy bone turnover by reducing osteoclast activity, inducing osteoclast apoptosis alongside promoting osteoblast activity (Emmanuelle et al., 2021). Zol treatment significantly decreased osteoclast activity and osteoblast activity. Depending on the oestradiol concentration, the models showed strain specific differences in results, with Zol treatment less effective at reducing osteoclast activity under the presence of pre-menopausal oestradiol concentrations in BALBc mice compared with C57BL/6. Moreover, Zol led to no significant change in P1NP in the post-menopausal BALBc model, but significantly decreased P1NP in the C57BL/6 model. Overall, this shows another strain specific difference in treatment, highlighting the importance of utilising multiple mouse models to reflect the heterogeneity of patients.

Overall, these reductions in bone cell activity are indicative of a decrease in bone turnover, reducing bone resorption and formation. Mouse models of both breast and prostate cancer show that tumour cells home to areas in the bone with high osteoblast numbers, known as the endosteal niche (Shiozawa et al., 2011). Treatment with Zol has been shown to alter this niche, alongside closely linked osteoclast activity, and result in tumour cell relocation to other areas of bone (Haider et al., 2014). This reduction in bone turnover creates a less hospitable environment for established tumour growth by breaking the vicious cycle of bone degradation feeding tumour growth in bone metastasis (Chen et al., 2010). Both the ABCSG-12 and the AZURE trial showed that treatment with Zol reduced bone metastasis incidence with the AZURE trial showing that this effect was independent of oestradiol concentration. Therefore, this reduction in bone metastasis could, in part, be mediated by a Zol induced decrease in bone turnover creating a less hospitable environment for breast cancer growth. However, treatment with Zol at different oestradiol concentrations also has significant effects on soft tissue metastasis, suggesting that the microenvironmental effects are not limited to bone resident cells.

The immune system plays a crucial role in the progression of both primary and metastatic breast cancer. I hypothesise that it is Zol and oestradiol induced changes to the immune response that drive the differences in treatment outcome observed in pre and post-menopausal patients. Following treatment with Zol and different oestradiol concentrations, I analysed immune cell populations in the bone, soft tissue and circulation to elucidate how changes in immune cells affect tumour growth in

different metastatic sites. In the literature, Zol and oestrogen have both profound and often opposing effects on the immune response to breast cancer. Zol has been shown to increase γδ T cell activation (Kondo et al., 2011), influence macrophage polarisation towards an anti-tumour phenotype (Coscia et al., 2010) and decrease Treg activation (Liu et al., 2016), expansion and activity in the tumour microenvironment. On the other hand, high oestradiol concentrations have been shown to have an immune suppressive effects, often supporting tumour growth by increasing Treg cell expansion and activity (Polanczyk et al., 2007), decreasing NK cell cytotoxicity (Baral et al., 1995), decreasing T cell development (Okasha et al., 2001) and influencing macrophage polarisation towards a pro-tumour phenotype (Svensson et al., 2015). This would support the findings of the AZURE trial, where treatment with Zol in patients with post-menopausal oestradiol concentrations resulted in an improved iDFS and reduced bone and soft tissue metastasis. Whereas in pre-menopausal patients, there was an increased soft tissue metastasis and no improvement in iDFS. This could be mediated by an increase in anti-tumour immune cell infiltration under the influence of Zol in the absence of oestradiol, an effect that could be reversed by high oestradiol concentrations reducing these immune mediated benefits.

Immune results from my current study are complex and differ depending on mouse strain and cancer cell line used, as has been observed in both tumour growth and bone turnover analysis. In agreement with the hypothesis and reflecting that seen in the literature, high oestradiol concentrations in the bone of both models significantly decreased B cell numbers when compared to control. Furthermore, in the lung of the BALBc mouse model, high oestradiol concentrations significantly decrease B cells, CD4+ T cells and CD8+ T cells in the presence of Zol, showing that oestradiol can inhibit the immune stimulatory effects of Zol treatment in the lung. Indeed, treatment with Zol under low oestradiol concentrations in the lung of BALBc mice increased numbers of cells of the lymphoid lineage: B cells, CD4 and CD8+ T cells, but has no effect under high oestradiol concentrations. While in lungs of C57BL/6 mice high oestradiol decreased numbers of cells of the myeloid lineage, including dendritic cells, monocytes and macrophages. These results help explain the data obtained from tumour growth experiments, where Zol treatment had no effect under high oestradiol concentrations but significantly reduced lung metastasis under low oestradiol concentrations. Moreover, results reflect that seen in the AZURE trial, where under high oestradiol concentrations there is increased lung metastasis following treatment with Zol (Coleman et al., 2014b), perhaps because oestradiol treatment opposes the pro-immunogenic benefits of Zol treatment.

In contrast, and in disagreement with the hypothesis, high oestradiol concentrations were shown increased numbers of some anti-tumour immune cells. In the bone of BALBc mice, oestradiol

increased numbers of CD4+ T cells and CD8+ T in Zol treated groups, whereas in the bone of C57BL/6, oestradiol did not significantly affect these cells, and instead resulted in a reduction in NK cells and dendritic cells. Although these results do not fit the hypothesis, they do reflect the heterogeneity of the clinical population, and further highlight the importance of utilising multiple models in pre-clinical studies.

Immune checkpoints represent an important mechanism whereby tumour cells evade detection and destruction by immune cells. PD-L1 is often expressed on tumour cells, and binding of PD-L1 to its receptor PD-1 on immune effector cells inhibits immune cell function and allows tumour cells to escape immune recognition (Han et al., 2020). Interestingly, when analysing PD-1 expression on CD4 and CD8+ T cells, I found that Zol significantly decreased PD-1 expression on T cells within the bone, suggesting these cells may have a reduced capacity for silencing by PD-L1. Furthermore, in the lungs of BALBc mice, high oestradiol concentrations significantly increased PD-1 expression on T cells. This result fits the hypothesis, with Zol increasing anti-tumour immunity and oestradiol leading to a decrease in anti-tumour immunity. This increase in immune checkpoint expression with oestradiol could contribute to the differential effects of Zol on breast cancer metastasis under different menopausal oestradiol concentrations. Indeed, oestradiol has been shown effect the PD-L1/PD-1 axis in breast cancer. High concentrations of oestradiol increase PD-L1 expression on ER+ breast cancer cells via a post-translational activation of the PI3K pathway, both *in vitro* and *in vivo* (Yang et al., 2017). Therefore, combined treatment with an immune checkpoint inhibitor alongside Zol could improve treatment outcome in premenopausal patients by increasing anti-tumour immune cell activity induced by Zol.

7.3 Effect of combination therapy with Avelumab and Zol

To test this hypothesis that combination therapy with Avelumab and Zol will increase the anti-metastatic efficacy of Zol in pre-menopausal women, I utilised the pre- and post-menopausal BALBc, 4T1 LUC mouse models of breast cancer metastasis. Combination therapy led to a significant decrease in tumour growth in both soft tissue and bone of BALBc mice, showing the first evidence of combination therapy with Avelumab and Zol effectively reducing breast cancer metastasis incidence. A previous pre-clinical study has reported the efficacy of combining an anti PD-1 antibody with Zol in a primary breast cancer model, showing significant reductions in primary tumour volume following combination treatment (Li et al., 2018). Put together, these studies show the first evidence of the efficacy of Zol treatment on tumours outside the bone when combined with immune checkpoint inhibitors. This result has an important clinical significance in the prevention of breast cancer

metastasis. Meta analysis of 26 randomised clinical trials of adjuvant bisphosphonates for early breast cancer showed that while bisphosphonates benefit bone recurrence irrespective of menopausal status, subgroup analysis showed that post-menopausal patients had a clear benefit in overall recurrence, distant recurrence and mortality (J. Bergh *et al.*, 2015). Pre-menopausal patients did not have the same benefits from treatment, with the AZURE trial showing that these patients had a worse clinical outcome with increased soft tissue metastasis (Coleman et al., 2014b). The results from my tumour growth experiments following combination therapy show evidence that combining Zol with Avelumab could be used in the clinic to prevent breast cancer metastasis in pre-menopausal patients. Indeed, results showed that combination therapy significantly reduced soft tissue metastasis in mice with pre-menopausal concentrations of oestradiol, representing exciting translational prospects to a clinical subgroup of patients who previously did not benefit from Zol treatment.

To understand the mechanism behind the reduction in metastasis observed with combination therapy, I analysed changes in the tumour microenvironments of different metastatic sites. Combination therapy significantly increased trabecular bone volume compared to control and single treatment Zol, while significantly decreasing osteoclast activity. These changes in bone turnover help create a less hospitable environment for breast cancer metastasis to bone, alongside reducing tumour growth of previously established tumour cells by breaking the vicious cycle of bone degradation and tumour growth (Chen et al., 2010). This data presents further evidence that combining Zol with Avelumab can increase its efficacy, while also showing evidence of Avelumab activity within the bone microenvironment. PD-1 blockade has been previously shown to effect bone resident cells, with Nivolumab treatment significantly decreasing osteoclastogenesis in WT mice. Moreover, in a multiple myeloma model, signalling through the PD-1/PD-L1 pathway has been associated with hyper-active osteoclast activity. Therefore, this anti-osteoclast activity of PD-L1 inhibition in the bone represents a secondary anti-tumour activity of this drug in the bone microenvironment. However, tumour growth experiments show that combination treatment has significant effects outside the bone, reducing soft tissue metastasis. To investigate this, I analysed infiltrating immune cell numbers and activity in the bone, soft tissue and circulation of tumour bearing mice following treatment under high and low oestradiol concentrations.

Blockade of the PD-L1/PD-1 signalling pathway with Avelumab aims to block immune checkpoint signalling in the tumour microenvironment and enable immune mediated tumour cytotoxicity. Moreover, Zol has been shown to have immune modulatory effects, stimulating anti-tumour immune cells by increasing M1 macrophage polarisation, reducing Treg cell infiltration and differentiation and increasing T cell activation (George et al., 2020). Therefore, I hypothesised that combining Avelumab and Zol could increase immune cell populations in the tumour

microenvironment while stimulating immune mediated tumour cell cytotoxicity. Interestingly, flow cytometry analysis showed that following combination treatment, a number of anti-tumour immune cells did not respond as predicted. In bone, there were significant reductions in neutrophils, monocytes and NK cells in mice that received combination treatment, while in the lung, combination therapy had no significant effect on immune cell numbers except for a decrease in neutrophil number. These decreases in immune cell number in the lung and bone seem to contradict the expected effect of combination treatment and that seen in tumour growth experiments where combination therapy significantly decreased lung and bone tumour burden. Interestingly, (Li et al., 2018) combined Zol with a PD-1 inhibitor in a primary breast cancer mouse model and analysed tumour infiltrating immune cells. They found a significant increase in CD8+ T cells and a significant decrease in myeloid derived suppressor cells. Furthermore, they observed an increase in IFN-γ and IL-18 signifying an increase in immune activity. However, these experiments differ from the current study where bone, lung and spleen were analysed, instead utilising a primary subcutaneous tumour model. The bone represents a unique immune microenvironment that is significantly immunocompromised providing an immune privileged niche for disseminated tumour cells, containing a high number of immature and inhibitory immune cell types (Baschuk et al., 2015). Furthermore, the bone has a significantly lower population of NK cells, CD4+ T cells and CD8+ T cells when compared to peripheral blood and other metastatic sites. This low immune cell base population could account for differences in treatment outcome between bone, soft tissue and primary tumour. Moreover, it could suggest that the anti-tumour effects of Avelumab and Zol in the bone are not solely mediated via an immune cell dependent mechanism, perhaps acting through bone turnover cells.

After observing no significant increase in immune cell population in tumour bearing organs following combination treatment, I next analysed markers of immune cell activity by qPCR array. Interestingly, combination therapy significantly increased Granzyme B expression under low oestradiol concentrations in the lung, suggesting an increase in immune cell function. Granzyme B is a serine protease found in granules from NK cells and cytotoxic T cells and is a marker of lymphocyte activity, suggesting that while treatment did not affect lymphocyte number, it did significantly increase activity. Granzyme B serum levels in cancer patients following PD-1 blockade have been corelated with improved clinical outcome (Hurkmans et al., 2020), so combination with Zol could help to further improve the beneficial lymphocyte activity associated with granzyme B. An investigation into the effects of Avelumab treatment on immune cell subsets in the peripheral blood of 28 cancer patients found that there was no significant change to any immune cell subsets observed. However, the study found an increase in ratio of CD27:CD40L which is indicative of immune activation. This reflects my data, where Avelumab and Zol increase immune cell activity but seem to decrease number

of immune cells. Overall, further work is needed to understand the effects of combination therapy with Avelumab and Zol on the immune response. Taken together, combination therapy with Avelumab and Zol significantly reduces both soft tissue and bone metastasis, showing the first evidence that combining these two drugs could be an exciting new treatment option for breast cancer patients, regardless of menopausal status.

7.4 Future directions

This study has elucidated some exciting results with translational potential for the preventative treatment of breast cancer metastasis. However, there are still a number of unanswered questions and unclear results that could be addressed in future studies. The analysis of the immune cells following treatments for both models could benefit from further analysis. Although some interesting results have come to light from these experiments, a wide variation in results coupled with relatively low n numbers (n=3-5) make teasing out the changes a challenge. Future flow cytometry experiments should focus on characterising infiltrating immune cells from metastatic sites while standardising tumour size and increasing n numbers to reduce variation between mice. Furthermore, analysis of markers of immune cell activity and PD-L1 and PD-1 should take focus in future experiments to complement the analysis of immune cell numbers. This analysis should be performed using a number of different methods. Firstly, analysing immune cell activity by *in vitro* assays to determine how different menopausal conditions with and without Zol affect immune cell activity would help elucidate the important regulators of the immune effects. Moreover, analysis should include determination of specific immune cells in the tumour microenvironment by immunohistochemistry alongside flow cytometry for immune cell characterisation and qPCR/Nanostring analysis for gene expression profiles. Moreover, RNAseq analysis from patient samples from the AZURE trial would provide important clinical data to strengthen the results. This more comprehensive analysis should help to elucidate the mechanism behind the anti-metastatic effect of combination therapy.

This study found that combination therapy with Avelumab and Zol significantly reduces breast cancer metastasis. However, only one mouse model was used in the analysis of this combination treatment. Considering the mouse strain specific differences I observed in previous experiments, future work should utilise multiple different mouse models to confirm this novel finding.

7.5 Concluding remarks

Zoledronic acid is currently used in the clinic for the prevention of early breast cancer metastasis in post-menopausal women. However, clinical trials show that pre-menopausal women do not benefit from this treatment, instead suffering increased soft tissue metastasis and a decreased iDFS, showing the need to find effective treatments that can prevent future relapse in these young women. This project aimed to understand the mechanism behind this differential effect of Zol and hypothesised that oestradiol driven changes to the immune microenvironment altered the anti-metastatic effects of Zol. Therefore, mouse models were set up, successfully modelling menopausal oestradiol concentrations, breast cancer dissemination and Zol treatment. Zol was found to be more effective at reducing soft tissue metastasis under low oestradiol concentrations in both models, a change that was found to be, in part, mediated by Zol induced changes to immune cell infiltration and activity. Therefore, Zol treatment was combined with the anti PD-L1 antibody Avelumab to try to improve their anti-metastatic properties. Avelumab and Zol combination treatment significantly reduced both bone and soft tissue metastasis under high and low oestradiol, showing potential for clinical translation for the treatment of both pre- and post-menopausal women.

Bibliography

Abe, O., Abe, R., Enomoto, K., Kikuchi, K., Koyama, H., Masuda, H., Nomura, Y., Sakai, K., Sugimachi, K., Tominaga, T., Uchino, J., Yoshida, M., Haybittle, J. L., Davies, C., Harvey, V. J., Holdaway, T. M., Kay, R. G., Mason, B. H., Forbes, J. F., Wilcken, N., Gnant, M., Jakesz, R., Ploner, M., Yosef, H. M. A., Focan, C., Lobelle, J. P., Peek, U., Oates, G. D., Powell, J., Durand, M., Mauriac, L., Di Leo, A., Dolci, S., Piccart, M. J., Masood, M. B., Parker, D., Price, J. J., Hupperets, P., Jackson, S., Ragaz, J., Berry, D., Broadwater, G., Cirrincione, C., Muss, H., Norton, L., Weiss, R. B., Abu-Zahra, H. T., Portnoj, S. M., Baum, M., Cuzick, J., Houghton, J., Riley, D., Gordon, N. H., Davis, H. L., Beatrice, A., Mihura, J., Naja, A., Lehingue, Y., Romestaing, P., Dubois, J. B., Delozier, T., Mace-Lesec'h, J., Rambert, P., Andrysek, O., Barkmanova, J., Owen, J. R., Meier, P., Howell, A., Ribeiro, G. C., Swindell, R., Alison, R., Boreham, J., Clarke, M., Collins, R., Darby, S., Elphinstone, P., Evans, V., Godwin, J., Gray, R., Harwood, C., Hicks, C., James, S., MacKinnon, E., McGale, P., McHugh, T., Mead, G., Peto, R., Wang, Y., Albano, J., de Oliveira, C. F., Gervasio, H., Gordilho, J., Johansen, H., Mouridsen, H. T., Gelman, R. S., Harris, J. R., Henderson, I. C., Shapiro, C. L., Andersen, K. W., Axelsson, C. K., et al. (2005) Effects of chemotherapy and hormonal therapy for early breast cancer on recurrence and 15-year survival: an overview of the randomised trials. *Lancet,* 365(9472)**,** 1687-1717.

Ahmadzadeh, M., Johnson, L. A., Heemskerk, B., Wunderlich, J. R., Dudley, M. E., White, D. E. & Rosenberg, S. A. (2009) Tumor antigen-specific CD8 T cells infiltrating the tumor express high levels of PD-1 and are functionally impaired. *Blood,* 114(8)**,** 1537-44. 10.1182/blood-2008-12-195792.

Albrecht, A. E., Hartmann, B. W., Scholten, C., Huber, J. C., Kalinowska, W. & Zielinski, C. C. (1996) Effect of estrogen replacement therapy on natural killer cell activity in postmenopausal women. *Maturitas,* 25(3)**,** 217-22. 10.1016/s0378-5122(96)01063-8.

Ali, H. R., Provenzano, E., Dawson, S. J., Blows, F. M., Liu, B., Shah, M., Earl, H. M., Poole, C. J., Hiller, L., Dunn, J. A., Bowden, S. J., Twelves, C., Bartlett, J. M., Mahmoud, S. M., Rakha, E., Ellis, I. O., Liu, S., Gao, D., Nielsen, T. O., Pharoah, P. D. & Caldas, C. (2014) Association between CD8+ T-cell infiltration and breast cancer survival in 12,439 patients. *Ann Oncol,* 25(8)**,** 1536-43. 10.1093/annonc/mdu191.

Almubarak, H., Jones, A., Chaisuparat, R., Zhang, M., Meiller, T. F. & Scheper, M. A. (2011) Zoledronic acid directly suppresses cell proliferation and induces apoptosis in highly tumorigenic prostate and breast cancers. *Journal of carcinogenesis,* 10**,** 2-2. 10.4103/1477-3163.75723.

Baral, E., Nagy, E. & Berczi, I. (1995) Modulation of natural killer cell-mediated cytotoxicity by tamoxifen and estradiol. *Cancer,* 75(2)**,** 591-9. 10.1002/1097-0142(19950115)75:2<591::aid-cncr2820750224>3.0.co;2-u.

Baschuk, N., Rautela, J. & Parker, B. S. (2015) Bone specific immunity and its impact on metastasis. *BoneKEy reports,* 4**,** 665-665. 10.1038/bonekey.2015.32.

Bates, G. J., Fox, S. B., Han, C., Leek, R. D., Garcia, J. F., Harris, A. L. & Banham, A. H. (2006) Quantification of regulatory T cells enables the identification of high-risk breast cancer patients and those at risk of late relapse. *J Clin Oncol,* 24(34)**,** 5373-80. 10.1200/jco.2006.05.9584.

Bergh, J. Pritchard, K. I., Albain, K., (2015) Adjuvant bisphosphonate treatment in early breast cancer: meta-analyses of individual patient data from randomised trials. *The Lancet,* 386(10001)**,** 1353-1361. 10.1016/S0140-6736(15)60908-4.

Bhattarai, H. K., Shrestha, S., Rokka, K. & Shakya, R. (2020) Vitamin D, Calcium, Parathyroid Hormone, and Sex Steroids in Bone Health and Effects of Aging. *Journal of osteoporosis,* 2020**,** 9324505-9324505. 10.1155/2020/9324505.

Bidwell, B. N., Slaney, C. Y., Withana, N. P., Forster, S., Cao, Y., Loi, S., Andrews, D., Mikeska, T., Mangan, N. E., Samarajiwa, S. A., de Weerd, N. A., Gould, J., Argani, P., Moller, A., Smyth, M. J., Anderson, R. L., Hertzog, P. J. & Parker, B. S. (2012) Silencing of Irf7 pathways in breast cancer cells promotes bone metastasis through immune escape. *Nature Medicine,* 18(8)**,** 1224-1231. 10.1038/nm.2830.

Biswas, S. K. & Mantovani, A. (2010a) Macrophage plasticity and interaction with lymphocyte subsets: cancer as a paradigm. *Nature Immunology,* 11(10)**,** 889-896. 10.1038/ni.1937.

Biswas, S. K. & Mantovani, A. (2010b) Macrophage plasticity and interaction with lymphocyte subsets: cancer as a paradigm. *Nat Immunol,* 11(10)**,** 889-96. 10.1038/ni.1937.

Bourdeau, V., Deschênes, J., Métivier, R., Nagai, Y., Nguyen, D., Bretschneider, N., Gannon, F., White, J. H. & Mader, S. (2004) Genome-wide identification of high-affinity estrogen response elements in human and mouse. *Mol Endocrinol,* 18(6)**,** 1411-27. 10.1210/me.2003-0441.

Bradford, P. G., Gerace, K. V., Roland, R. L. & Chrzan, B. G. (2010) Estrogen regulation of apoptosis in osteoblasts. *Physiology & Behavior,* 99(2)**,** 181-185. 10.1016/j.physbeh.2009.04.025.

Braun, S., Vogl, F. D., Naume, B., Janni, W., Osborne, M. P., Coombes, R. C., Schlimok, G., Diel, I. J., Gerber, B., Gebauer, G., Pierga, J. Y., Marth, C., Oruzio, D., Wiedswang, G., Solomayer, E. F., Kundt, G., Strobl, B., Fehm, T., Wong, G. Y., Bliss, J., Vincent-Salomon, A. & Pantel, K. (2005) A pooled analysis of bone marrow micrometastasis in breast cancer. *N Engl J Med,* 353(8)**,** 793-802. 10.1056/NEJMoa050434.

Braunstein, L. Z., Niemierko, A., Shenouda, M. N., Truong, L., Sadek, B. T., Abi Raad, R., Wong, J. S., Punglia, R. S., Taghian, A. G. & Bellon, J. R. (2015) Outcome Following Local-Regional Recurrence in Women with Early-Stage Breast Cancer: Impact of Biologic Subtype. *Breast Journal,* 21(2)**,** 161-167. 10.1111/tbj.12371.

Brown, H. K., Ottewell, P. D., Evans, C. A., Coleman, R. E. & Holen, I. (2012) A single administration of combination therapy inhibits breast tumour progression in bone and modifies both osteoblasts and osteoclasts. *Journal of Bone Oncology,* 1(2)**,** 47-56. 10.1016/j.jbo.2012.05.001.

Bui, K. T., Willson, M. L., Goel, S., Beith, J. & Goodwin, A. (2020) Ovarian suppression for adjuvant treatment of hormone receptor-positive early breast cancer. Cochrane Database Syst Rev, 3(3), Cd013538. 10.1002/14651858.cd013538.

Bulun, S. E., Chen, D., Lu, M., Zhao, H., Cheng, Y., Demura, M., Yilmaz, B., Martin, R., Utsunomiya, H., Thung, S., Su, E., Marsh, E., Hakim, A., Yin, P., Ishikawa, H., Amin, S., Imir, G., Gurates, B., Attar, E., Reierstad, S., Innes, J. & Lin, Z. (2007) Aromatase excess in cancers of breast, endometrium and ovary. *Journal of Steroid Biochemistry and Molecular Biology,* 106(1-5)**,** 81-96. 10.1016/j.jsbmb.2007.05.027.

Bundred, N. J., Campbell, I. D., Davidson, N., DeBoer, R. H., Eidtmann, H., Monnier, A., Neven, P., von Minckwitz, G., Miller, J. C., Schenk, N. L. & Coleman, R. E. (2008) Effective inhibition of aromatase inhibitor-associated bone loss by zoledronic acid in postmenopausal women with early breast cancer receiving adjuvant letrozole: ZO-FAST Study results. *Cancer,* 112(5)**,** 1001-10. 10.1002/cncr.23259.

Burger, H. G., Dudley, E. C., Hopper, J. L., Groome, N., Guthrie, J. R., Green, A. & Dennerstein, L. (1999) Prospectively measured levels of serum follicle-stimulating hormone, estradiol, and the dimeric inhibins during the menopausal transition in a population-based cohort of women. *J Clin Endocrinol Metab,* 84(11)**,** 4025-30. 10.1210/jcem.84.11.6158.

Bussard, K. M., Venzon, D. J. & Mastro, A. M. (2010) Osteoblasts are a major source of inflammatory cytokines in the tumor microenvironment of bone metastatic breast cancer. *Journal of cellular biochemistry,* 111(5)**,** 1138-1148. 10.1002/jcb.22799.

Cai, J., Wang, D., Zhang, G. & Guo, X. (2019) The Role Of PD-1/PD-L1 Axis In Treg Development And Function: Implications For Cancer Immunotherapy. *OncoTargets and therapy,* 12**,** 8437-8445. 10.2147/OTT.S221340.

Caligioni, C. S. (2009) Assessing reproductive status/stages in mice. *Current protocols in neuroscience,* Appendix 4**,** Appendix-4I. 10.1002/0471142301.nsa04is48.

Campbell, J. P., Merkel, A. R., Masood-Campbell, S. K., Elefteriou, F. & Sterling, J. A. (2012) Models of Bone Metastasis. *Jove-Journal of Visualized Experiments*(67). 10.3791/4260.

Canuas-Landero, V. G., George, C. N., Lefley, D. V., Corness, H., Muthana, M., Wilson, C. & Ottewell, P. D. (2021) Oestradiol Contributes to Differential Antitumour Effects of Adjuvant Zoledronic Acid Observed Between Pre- and Post-Menopausal Women. *Frontiers in Endocrinology,* 12**,** 1287.

Capulli, M., Angelucci, A., Driouch, K., Garcia, T., Clement-Lacroix, P., Martella, F., Ventura, L., Bologna, M., Flamini, S., Moreschini, O., Lidereau, R., Ricevuto, E., Muraca, M., Teti, A. & Rucci, N. (2012) Increased expression of a set of genes enriched in oxygen binding function discloses a predisposition of breast cancer bone metastases to generate metastasis spread in multiple organs. *Journal of Bone and Mineral Research,* 27(11)**,** 2387-2398. 10.1002/jbmr.1686.

Carbonell, W. S., Ansorge, O., Sibson, N. & Muschel, R. (2009) The Vascular Basement Membrane as "Soil" in Brain Metastasis. *PLOS ONE,* 4(6)**,** e5857. 10.1371/journal.pone.0005857.

Carmeci, C., Thompson, D. A., Ring, H. Z., Francke, U. & Weigel, R. J. (1997) Identification of a gene (GPR30) with homology to the G-protein-coupled receptor superfamily associated with estrogen receptor expression in breast cancer. *Genomics,* 45(3)**,** 607-17. 10.1006/geno.1997.4972.

Chen, X., Oppenheim, J. J. & Howard, O. M. (2005) BALB/c mice have more CD4+CD25+ T regulatory cells and show greater susceptibility to suppression of their CD4+CD25- responder T cells than C57BL/6 mice. *J Leukoc Biol,* 78(1)**,** 114-21. 10.1189/jlb.0604341.

Chen, Y.-C., Sosnoski, D. M. & Mastro, A. M. (2010) Breast cancer metastasis to the bone: mechanisms of bone loss. *Breast Cancer Research,* 12(6)**,** 215. 10.1186/bcr2781.

Coleman, R., Cameron, D., Dodwell, D., Bell, R., Wilson, C., Rathbone, E., Keane, M., Gil, M., Burkinshaw, R., Grieve, R., Barrett-Lee, P., Ritchie, D., Liversedge, V., Hinsley, S. & Marshall, H.

(2014a) Adjuvant zoledronic acid in patients with early breast cancer: final efficacy analysis of the AZURE (BIG 01/04) randomised open-label phase 3 trial. *Lancet Oncol,* 15(9)**,** 997-1006. 10.1016/s1470-2045(14)70302-x.

Coleman, R., Cameron, D., Dodwell, D., Bell, R., Wilson, C., Rathbone, E., Keane, M., Gil, M., Burkinshaw, R., Grieve, R., Barrett-Lee, P., Ritchie, D., Liversedge, V., Hinsley, S., Marshall, H. & Investigators, A. (2014b) Adjuvant zoledronic acid in patients with early breast cancer: final efficacy analysis of the AZURE (BIG 01/04) randomised open-label phase 3 trial. *Lancet Oncology,* 15(9)**,** 997-1006. 10.1016/s1470-2045(14)70302-x.

Coleman, R. E., Collinson, M., Gregory, W., Marshall, H., Bell, R., Dodwell, D., Keane, M., Gil, M., Barrett-Lee, P., Ritchie, D., Bowman, A., Liversedge, V., De Boer, R. H., Passos-Coelho, J. L., O'Reilly, S., Bertelli, G., Joffe, J., Brown, J. E., Wilson, C., Tercero, J. C., Jean-Mairet, J., Gomis, R. & Cameron, D. (2018a) Benefits and risks of adjuvant treatment with zoledronic acid in stage II/III breast cancer. 10 years follow-up of the AZURE randomized clinical trial (BIG 01/04). *Journal of bone oncology,* 13**,** 123-135. 10.1016/j.jbo.2018.09.008.

Coleman, R. E., Finkelstein, D., Barrios, C. H., Martin, M., Iwata, H., Glaspy, J. A., Zhou, Y., Jandial, D. & Chan, A. (2018b) Adjuvant denosumab in early breast cancer: First results from the international multicenter randomized phase III placebo controlled D-CARE study. *Journal of Clinical Oncology,* 36(15). 10.1200/JCO.2018.36.15_suppl.501.

Coleman, R. E., Marshall, H., Cameron, D., Dodwell, D., Burkinshaw, R., Keane, M., Gil, M., Houston, S. J., Grieve, R. J., Barrett-Lee, P. J., Ritchie, D., Pugh, J., Gaunt, C., Rea, U., Peterson, J., Davies, C., Hiley, V., Gregory, W. & Bell, R. (2011) Breast-cancer adjuvant therapy with zoledronic acid. *N Engl J Med,* 365(15)**,** 1396-405. 10.1056/NEJMoa1105195.

Collins, J. M. & Gulley, J. L. (2019) Product review: avelumab, an anti-PD-L1 antibody. *Human vaccines & immunotherapeutics,* 15(4)**,** 891-908. 10.1080/21645515.2018.1551671.

Colzani, E., Johansson, A. L. V., Liljegren, A., Foukakis, T., Clements, M., Adolfsson, J., Hall, P. & Czene, K. (2014) Time-dependent risk of developing distant metastasis in breast cancer patients according to treatment, age and tumour characteristics. *British Journal of Cancer,* 110(5)**,** 1378-1384. 10.1038/bjc.2014.5.

Coscia, M., Quaglino, E., Iezzi, M., Curcio, C., Pantaleoni, F., Riganti, C., Holen, I., Monkkonen, H., Boccadoro, M., Forni, G., Musiani, P., Bosia, A., Cavallo, F. & Massaia, M. (2010) Zoledronic acid repolarizes tumour-associated macrophages and inhibits mammary carcinogenesis by targeting the mevalonate pathway. *Journal of Cellular and Molecular Medicine,* 14(12)**,** 2803-2815. 10.1111/j.1582-4934.2009.00926.x.

Cosphiadi, I., Atmakusumah, T. D., Siregar, N. C., Muthalib, A., Harahap, A. & Mansyur, M. (2018) Bone Metastasis in Advanced Breast Cancer: Analysis of Gene Expression Microarray. *Clinical Breast Cancer,* 18(5)**,** e1117-e1122. 10.1016/j.clbc.2018.03.001.

Creighton, H., Beach, B. & Bamford, S.-M. (2015) Rethinking cancer the big c quantifying the social and economic impact. https://www.bl.uk/collection-items/rethinking-cancer-the-big-c-quantifying-the-social-and-economic-impact.

Criscitiello, C., Azim, H. A., Schouten, P. C., Linn, S. C. & Sotiriou, C. (2012) Understanding the biology of triple-negative breast cancer. *Annals of Oncology,* 23**,** 13-18. 10.1093/annonc/mds188.

Croucher, P. I., De Raeve, H., Perry, M. J., Hijzen, A., Shipman, C. M., Lippitt, J., Green, J., Van Marck, E., Van Camp, B. & Vanderkerken, K. (2003) Zoledronic acid treatment of 5T2MM-bearing mice inhibits the development of myeloma bone disease: Evidence for decreased osteolysis, tumor burden and angiogenesis, and increased survival. *Journal of Bone and Mineral Research,* 18(3)**,** 482-492. 10.1359/jbmr.2003.18.3.482.

Curran, E. M., Berghaus, L. J., Vernetti, N. J., Saporita, A. J., Lubahn, D. B. & Estes, D. M. (2001) Natural killer cells express estrogen receptor-alpha and estrogen receptor-beta and can respond to estrogen via a non-estrogen receptor-alpha-mediated pathway. *Cellular Immunology,* 214(1)**,** 12-20. 10.1006/cimm.2002.1886.

Curran, E. M., Judy, B. M., Duru, N. A., Wang, H. Q., Vergara, L. A., Lubahn, D. B. & Estes, D. M. (2006) Estrogenic regulation of host immunity against an estrogen receptor - Negative human breast cancer. *Clinical Cancer Research,* 12(19)**,** 5641-5647. 10.1158/1078-0432.ccr-05-1117.

Demicheli, R., Abbattista, A., Miceli, R., Valagussa, P. & Bonadonna, G. (1996) Time distribution of the recurrence risk for breast cancer patients undergoing mastectomy: Further support about the concept of tumor dormancy. *Breast Cancer Research and Treatment,* 41(2)**,** 177-185. 10.1007/BF01807163.

Denoyelle, C., Hong, L., Vannier, J. P., Soria, J. & Soria, C. (2003) New insights into the actions of bisphosphonate zoledronic acid in breast cancer cells by dual RhoA-dependent and -independent effects. *British Journal of Cancer,* 88(10)**,** 1631-1640. 10.1038/sj.bjc.6600925.

Dent, R., Trudeau, M., Pritchard, K. I., Hanna, W. M., Kahn, H. K., Sawka, C. A., Lickley, L. A., Rawlinson, E., Sun, P. & Narod, S. A. (2007) Triple-negative breast cancer: Clinical features and patterns of recurrence. *Clinical Cancer Research,* 13(15)**,** 4429-4434. 10.1158/1078-0432.ccr-06-3045.

Dethlefsen, C., Hojfeldt, G. & Hojman, P. (2013) The role of intratumoral and systemic IL-6 in breast cancer. *Breast Cancer Res Treat,* 138(3)**,** 657-64. 10.1007/s10549-013-2488-z.

Dhillon, S. (2016) Zoledronic Acid (Reclast (R), Aclasta (R)): A Review in Osteoporosis. *Drugs,* 76(17)**,** 1683-1697. 10.1007/s40265-016-0662-4.

Di Gregorio, G. B., Yamamoto, M., Ali, A. A., Abe, E., Roberson, P., Manolagas, S. C. & Jilka, R. L. (2001) Attenuation of the self-renewal of transit-amplifying osteoblast progenitors in the murine bone marrow by 17 beta-estradiol. *J Clin Invest,* 107(7)**,** 803-12. 10.1172/jci11653.

Diaz Brinton, R. (2012) Minireview: translational animal models of human menopause: challenges and emerging opportunities. Endocrinology, 153(8), 3571-8. 10.1210/en.2012-1340.

Diefenbach, A., Jensen, E. R., Jamieson, A. M. & Raulet, D. H. (2001) Rae1 and H60 ligands of the NKG2D receptor stimulate tumour immunity. *Nature,* 413(6852)**,** 165-171. 10.1038/35093109.

Dirix, L. Y., Takacs, I., Jerusalem, G., Nikolinakos, P., Arkenau, H.-T., Forero-Torres, A., Boccia, R., Lippman, M. E., Somer, R., Smakal, M., Emens, L. A., Hrinczenko, B., Edenfield, W., Gurtler, J., von Heydebreck, A., Grote, H. J., Chin, K. & Hamilton, E. P. (2018a) Avelumab, an anti-PD-L1 antibody, in patients with locally advanced or metastatic breast cancer: a phase 1b JAVELIN Solid Tumor study. *Breast cancer research and treatment,* 167(3)**,** 671-686. 10.1007/s10549-017-4537-5.

Dirix, L. Y., Takacs, I., Jerusalem, G., Nikolinakos, P., Arkenau, H. T., Forero-Torres, A., Boccia, R., Lippman, M. E., Somer, R., Smakal, M., Emens, L. A., Hrinczenko, B., Edenfield, W., Gurtler, J.,

von Heydebreck, A., Grote, H. J., Chin, K. & Hamilton, E. P. (2018b) Avelumab, an anti-PD-L1 antibody, in patients with locally advanced or metastatic breast cancer: a phase 1b JAVELIN Solid Tumor study. *Breast Cancer Res Treat,* 167(3)**,** 671-686. 10.1007/s10549-017-4537-5.

Eastell, R., Hannon, R. A., Cuzick, J., Dowsett, M., Clack, G., Adams, J. E. & Grp, A. T. (2006) Effect of an aromatase inhibitor on BMD and bone turnover markers: 2-year results of the Anastrozole, Tamoxifen, Alone or in Combination (ATAC) trial (18233230). *Journal of Bone and Mineral Research,* 21(8)**,** 1215-1223. 10.1359/jbmr.060508.

Elston, C. W. & Ellis, I. O. (1991) Pathological prognostic factors in breast cancer. I. The value of histological grade in breast cancer: experience from a large study with long-term follow-up. *Histopathology,* 19(5)**,** 403-10. 10.1111/j.1365-2559.1991.tb00229.x.

Emmanuelle, N.-E., Marie-Cécile, V., Florence, T., Jean-François, A., Françoise, L., Coralie, F. & Alexia, V. (2021) Critical Role of Estrogens on Bone Homeostasis in Both Male and Female: From Physiology to Medical Implications. *International journal of molecular sciences,* 22(4)**,** 1568. 10.3390/ijms22041568.

Esposito, M., Mondal, N., Greco, T. M., Wei, Y., Spadazzi, C., Lin, S.-C., Zheng, H., Cheung, C., Magnani, J. L., Lin, S.-H., Cristea, I. M., Sackstein, R. & Kang, Y. (2019) Bone vascular niche E-selectin induces mesenchymal–epithelial transition and Wnt activation in cancer cells to promote bone metastasis. *Nature Cell Biology,* 21(5)**,** 627-639. 10.1038/s41556-019-0309-2.

Fan, Y., Jalali, A., Chen, A., Zhao, X., Liu, S., Teli, M., Guo, Y., Li, F., Li, J., Siegel, A., Yang, L., Liu, J., Na, S., Agarwal, M., Robling, A. G., Nakshatri, H., Li, B.-Y. & Yokota, H. (2020) Skeletal loading regulates breast cancer-associated osteolysis in a loading intensity-dependent fashion. *Bone Research,* 8(1)**,** 9. 10.1038/s41413-020-0083-6.

Feinberg, H., Jégouzo, S. A. F., Lasanajak, Y., Smith, D. F., Drickamer, K., Weis, W. I. & Taylor, M. E. (2021) Structural analysis of carbohydrate binding by the macrophage mannose receptor CD206. J Biol Chem, 296, 100368. 10.1016/j.jbc.2021.100368.

Fidler, I. J. (1970) Metastasis: quantitative analysis of distribution and fate of tumor emboli labeled with 125 I-5-iodo-2'-deoxyuridine. *J Natl Cancer Inst,* 45(4)**,** 773-82.

Filardo, E. J. & Thomas, P. (2012) Minireview: G protein-coupled estrogen receptor-1, GPER-1: its mechanism of action and role in female reproductive cancer, renal and vascular physiology. *Endocrinology,* 153(7)**,** 2953-62. 10.1210/en.2012-1061.

Fleming, C., Morrissey, S., Cai, Y. H. & Yan, J. (2017) gamma delta T Cells: Unexpected Regulators of Cancer Development and Progression. *Trends in Cancer,* 3(8)**,** 561-570. 10.1016/j.trecan.2017.06.003.

Foda, H. D. & Zucker, S. (2001) Matrix metalloproteinases in cancer invasion, metastasis and angiogenesis. *Drug Discov Today,* 6(9)**,** 478-482. 10.1016/s1359-6446(01)01752-4.

Fowler, D. W., Copier, J., Dalgleish, A. G. & Bodman-Smith, M. D. (2014) Zoledronic acid causes gamma delta T cells to target monocytes and down-modulate inflammatory homing. *Immunology,* 143(4)**,** 539-549. 10.1111/imm.12331.

Fowler, D. W., Copier, J., Dalgleish, A. G. & Bodman-Smith, M. D. (2017) Zoledronic acid renders human M1 and M2 macrophages susceptible to V delta 2(+) gamma delta T cell cytotoxicity in a

perforin-dependent manner. *Cancer Immunology Immunotherapy,* 66(9)**,** 1205-1215. 10.1007/s00262-017-2011-1.

Francisco, L. M., Salinas, V. H., Brown, K. E., Vanguri, V. K., Freeman, G. J., Kuchroo, V. K. & Sharpe, A. H. (2009) PD-L1 regulates the development, maintenance, and function of induced regulatory T cells. *Journal of Experimental Medicine,* 206(13)**,** 3015-3029. 10.1084/jem.20090847.

Fuentes, N. & Silveyra, P. (2019) Estrogen receptor signaling mechanisms. *Advances in protein chemistry and structural biology,* 116**,** 135-170. 10.1016/bs.apcsb.2019.01.001.

Garrido, F., Cabrera, T. & Aptsiauri, N. (2010) "Hard" and "soft" lesions underlying the HLA Class I alterations in cancer cells: implications for immunotherapy. *International Journal of Cancer,* 127(2)**,** 249-256. 10.1002/ijc.25270.

George, C. N., Canuas-Landero, V., Theodoulou, E., Muthana, M., Wilson, C. & Ottewell, P. (2020) Oestrogen and zoledronic acid driven changes to the bone and immune environments: Potential mechanisms underlying the differential anti-tumour effects of zoledronic acid in pre- and post-menopausal conditions. *Journal of Bone Oncology,* 25**,** 100317. https://doi.org/10.1016/j.jbo.2020.100317.

Gnant, M., Mlineritsch, B., Stoeger, H., Luschin-Ebengreuth, G., Heck, D., Menzel, C., Jakesz, R., Seifert, M., Hubalek, M., Pristauz, G., Bauernhofer, T., Eidtmann, H., Eiermann, W., Steger, G., Kwasny, W., Dubsky, P., Hochreiner, G., Forsthuber, E. P., Fesl, C., Greil, R., Austrian, B. & Colorectal Cancer Study Group, V. A. (2011) Adjuvant endocrine therapy plus zoledronic acid in premenopausal women with early-stage breast cancer: 62-month follow-up from the ABCSG-12 randomised trial. *Lancet Oncol,* 12(7)**,** 631-41. 10.1016/S1470-2045(11)70122-X.

Gnant, M., Mlineritsch, B., Stoeger, H., Luschin-Ebengreuth, G., Knauer, M., Moik, M., Jakesz, R., Seifert, M., Taucher, S., Bjelic-Radisic, V., Balic, M., Eidtmann, H., Eiermann, W., Steger, G., Kwasny, W., Dubsky, P., Selim, U., Fitzal, F., Hochreiner, G., Wette, V., Sevelda, P., Ploner, F., Bartsch, R., Fesl, C., Greil, R., Austrian, B. & Colorectal, C. (2015a) Zoledronic acid combined with adjuvant endocrine therapy of tamoxifen versus anastrozol plus ovarian function suppression in premenopausal early breast cancer: final analysis of the Austrian Breast and Colorectal Cancer Study Group Trial 12. *Annals of Oncology,* 26(2)**,** 313-320. 10.1093/annonc/mdu544.

Gnant, M., Pfeiler, G., Dubsky, P. C., Hubalek, M., Greil, R., Jakesz, R., Wette, V., Balic, M., Haslbauer, F., Melbinger, E., Bjelic-Radisic, V., Artner-Matuschek, S., Fitzal, F., Marth, C., Sevelda, P., Mlineritsch, B., Steger, G. G., Manfreda, D., Exner, R., Egle, D., Bergh, J., Kainberger, F., Talbot, S., Warner, D., Fesl, C. & Singer, C. F. (2015b) Adjuvant denosumab in breast cancer (ABCSG-18): a multicentre, randomised, double-blind, placebo-controlled trial. *Lancet,* 386(9992)**,** 433-43. 10.1016/s0140-6736(15)60995-3.

Gonzalez-Angulo, A. M., Ferrer-Lozano, J., Stemke-Hale, K., Sahin, A., Liu, S., Barrera, J. A., Burgues, O., Lluch, A. M., Chen, H., Hortobagyi, G. N., Mills, G. B. & Meric-Bernstam, F. (2011) PI3K Pathway Mutations and PTEN Levels in Primary and Metastatic Breast Cancer. *Molecular Cancer Therapeutics,* 10(6)**,** 1093. 10.1158/1535-7163.MCT-10-1089.

Grassi, F., Manferdini, C., Cattini, L., Piacentini, A., Gabusi, E., Facchini, A. & Lisignoli, G. (2011) T cell suppression by osteoclasts in vitro. *J Cell Physiol,* 226(4)**,** 982-90. 10.1002/jcp.22411.

Grimaldi, C. M., Cleary, J., Dagtas, A. S., Moussai, D. & Diamond, B. (2002) Estrogen alters thresholds for B cell apoptosis and activation. *The Journal of clinical investigation,* 109(12)**,** 1625-1633. 10.1172/JCI14873.

Gupta, P. B., Proia, D., Cingoz, O., Weremowicz, J., Naber, S. P., Weinberg, R. A. & Kuperwasser, C. (2007) Systemic stromal effects of estrogen promote the growth of estrogen receptor-negative cancers. *Cancer Res,* 67(5)**,** 2062-71. 10.1158/0008-5472.can-06-3895.

Haider, M. T., Holen, I., Dear, T. N., Hunter, K. & Brown, H. K. (2014) Modifying the osteoblastic niche with zoledronic acid in vivo-Potential implications for breast cancer bone metastasis. *Bone,* 66**,** 240-250. 10.1016/j.bone.2014.06.023.

Hamilton, K. J., Arao, Y. & Korach, K. S. (2014) Estrogen hormone physiology: reproductive findings from estrogen receptor mutant mice. *Reproductive biology,* 14(1)**,** 3-8. 10.1016/j.repbio.2013.12.002.

Han, Y., Liu, D. & Li, L. (2020) PD-1/PD-L1 pathway: current researches in cancer. *American journal of cancer research,* 10(3)**,** 727-742.

Hartkopf, A. D., Taran, F. A., Wallwiener, M., Hahn, M., Becker, S., Solomayer, E. F., Brucker, S. Y., Fehm, T. N. & Wallwiener, D. (2014) Prognostic relevance of disseminated tumour cells from the bone marrow of early stage breast cancer patients - results from a large single-centre analysis. *Eur J Cancer,* 50(15)**,** 2550-9. 10.1016/j.ejca.2014.06.025.

Heil, J., Fuchs, V., Golatta, M., Schott, S., Wallwiener, M., Domschke, C., Sinn, P., Lux, M. P., Sohn, C. & Schutz, F. (2012) Extent of Primary Breast Cancer Surgery: Standards and Individualized Concepts. *Breast Care,* 7(5)**,** 364-369. 10.1159/000343976.

Higuchi, D. A., Cahan, P., Gao, J., Ferris, S. T., Poursine-Laurent, J., Graubert, T. A. & Yokoyama, W. M. (2010) Structural variation of the mouse natural killer gene complex. *Genes & Immunity,* 11(8)**,** 637-648. 10.1038/gene.2010.48.

Hiraga, T., Williams, P. J., Ueda, A., Tamura, D. & Yoneda, T. (2004) Zoledronic acid inhibits visceral metastases in the 4T1/luc mouse breast cancer model. *Clinical Cancer Research,* 10(13)**,** 4559-4567. 10.1158/1078-0432.ccr-03-0325.

Holen, I. & Coleman, R. E. (2010) Anti-tumour activity of bisphosphonates in preclinical models of breast cancer. *Breast Cancer Research,* 12(6). 10.1186/bcr2769.

Holen, I., Walker, M., Nutter, F., Fowles, A., Evans, C. A., Eaton, C. L. & Ottewell, P. D. (2016) Oestrogen receptor positive breast cancer metastasis to bone: inhibition by targeting the bone microenvironment in vivo. *Clin Exp Metastasis,* 33(3)**,** 211-24. 10.1007/s10585-015-9770-x.

Huang, H. L., Hsing, H. W., Lai, T. C., Chen, Y. W., Lee, T. R., Chan, H. T., Lyu, P. C., Wu, C. L., Lu, Y. C., Lin, S. T., Lin, C. W., Lai, C. H., Chang, H. T., Chou, H. C. & Chan, H. L. (2010) Trypsin-induced proteome alteration during cell subculture in mammalian cells. *Journal of Biomedical Science,* 17. 10.1186/1423-0127-17-36.

Huang, R., Li, J., Pan, F., Zhang, B. & Yao, Y. (2020) The activation of GPER inhibits cells proliferation, invasion and EMT of triple-negative breast cancer via CD151/miR-199a-3p bio-axis. *American journal of translational research,* 12(1)**,** 32-44.

Hughes, D. E., Wright, K. R., Uy, H. L., Sasaki, A., Yoneda, T., Roodman, G. D., Mundy, G. R. & Boyce, B. F. (1995) Bisphosphonates promote apoptosis in murine osteoclasts in-vitro and in-vivo. *Journal of Bone and Mineral Research,* 10(10)**,** 1478-1487.

Hughes, R., Chen, X., Hunter, K. D., Hobbs, J. K., Holen, I. & Brown, N. J. (2019) Bone marrow osteoprogenitors are depleted whereas osteoblasts are expanded independent of the osteogenic vasculature in response to zoledronic acid. *Faseb j,* 33(11)**,** 12768-12779. 10.1096/fj.201900553RR.

Hurkmans, D. P., Basak, E. A., Schepers, N., Oomen-De Hoop, E., Van der Leest, C. H., El Bouazzaoui, S., Bins, S., Koolen, S. L. W., Sleijfer, S., Van der Veldt, A. A. M., Debets, R., Van Schaik, R. H. N., Aerts, J. G. J. V. & Mathijssen, R. H. J. (2020) Granzyme B is correlated with clinical outcome after PD-1 blockade in patients with stage IV non-small-cell lung cancer. *Journal for ImmunoTherapy of Cancer,* 8(1)**,** e000586. 10.1136/jitc-2020-000586.

Hwang, J., Hodis, H. N., Hsiai, T. K., Asatryan, L. & Sevaniana, A. (2006) Role of annexin II in estrogen-induced macrophage matrix metalloproteinase-9 activity: The modulating effect of statins. *Atherosclerosis,* 189(1)**,** 76-82. 10.1016/j.atherosclerosis.2005.11.026.

Ibrahim, T., Mercatali, L., Sacanna, E., Tesei, A., Carloni, S., Ulivi, P., Liverani, C., Fabbri, F., Zanoni, M., Zoli, W. & Amadori, D. (2012) Inhibition of breast cancer cell proliferation in repeated and non-repeated treatment with zoledronic acid. *Cancer Cell International,* 12(1)**,** 48. 10.1186/1475-2867-12-48.

Irelli, A., Sirufo, M. M., D'Ugo, C., Ginaldi, L. & De Martinis, M. (2020) Sex and Gender Influences on Cancer Immunotherapy Response. *Biomedicines,* 8(7)**,** 232. 10.3390/biomedicines8070232.

Isakoff, S. J., Mayer, E. L., He, L., Traina, T. A., Carey, L. A., Krag, K. J., Rugo, H. S., Liu, M. C., Stearns, V., Come, S. E., Timms, K. M., Hartman, A. R., Borger, D. R., Finkelstein, D. M., Garber, J. E., Ryan, P. D., Winer, E. P., Goss, P. E. & Ellisen, L. W. (2015) TBCRC009: A Multicenter Phase II Clinical Trial of Platinum Monotherapy With Biomarker Assessment in Metastatic Triple-Negative Breast Cancer. *Journal of Clinical Oncology,* 33(17)**,** 1902-U67. 10.1200/jco.2014.57.6660.

Iwasaki, M., Tanaka, Y., Kobayashi, H., Murata-Hirai, K., Miyabe, H., Sugie, T., Toi, M. & Minato, N. (2011) Expression and function of PD-1 in human gamma delta T cells that recognize phosphoantigens. *European Journal of Immunology,* 41(2)**,** 345-355. 10.1002/eji.201040959.

Jacobs, J. F. M., Idema, A. J., Bol, K. F., Nierkens, S., Grauer, O. M., Wesseling, P., Grotenhuis, J. A., Hoogerbrugge, P. M., de Vries, I. J. M. & Adema, G. J. (2009) Regulatory T cells and the PD-L1/PD-1 pathway mediate immune suppression in malignant human brain tumors. *Neuro-Oncology,* 11(4)**,** 394-402. 10.1215/15228517-2008-104.

Jagdev, S. P., Coleman, R. E., Shipman, C. M., Rostami-H, A. & Croucher, P. I. (2001) The bisphosphonate, zoledronic acid, induces apoptosis of breast cancer cells: evidence for synergy with paclitaxel. *British Journal of Cancer,* 84(8)**,** 1126-1134. 10.1054/bjoc.2001.1727.

Jakacka, M., Ito, M., Weiss, J., Chien, P. Y., Gehm, B. D. & Jameson, J. L. (2001) Estrogen receptor binding to DNA is not required for its activity through the nonclassical AP1 pathway. *J Biol Chem,* 276(17)**,** 13615-21. 10.1074/jbc.M008384200.

Jakesz, R., Hausmaninger, H., Kubista, E., Gnant, M., Menzel, C., Bauernhofer, T., Seifert, M., Haider, K., Mlineritsch, B., Steindorfer, P., Kwasny, W., Fridrik, M., Steger, G., Wette, V. & Samonigg, H. (2002) Randomized adjuvant trial of tamoxifen and goserelin versus cyclophosphamide,

methotrexate, and fluorouracil: Evidence for the superiority of treatment with endocrine blockade in premenopausal patients with hormone-responsive breast cancer - Austrian Breast and Colorectal Cancer Study Group Trial 5. *Journal of Clinical Oncology,* 20(24)**,** 4621-4627. 10.1200/jco.2002.09.112.

Jeong, J., Lee, K. S., Choi, Y. K., Oh, Y. J. & Lee, H. D. (2011) Preventive Effects of Zoledronic Acid on Bone Metastasis in Mice Injected with Human Breast Cancer Cells. *Journal of Korean Medical Science,* 26(12)**,** 1569-1575. 10.3346/jkms.2011.26.12.1569.

Ji, M.-X. & Yu, Q. (2015) Primary osteoporosis in postmenopausal women. *Chronic diseases and translational medicine,* 1(1)**,** 9-13. 10.1016/j.cdtm.2015.02.006.

Jiang, X., Ellison, S. J., Alarid, E. T. & Shapiro, D. J. (2007) Interplay between the levels of estrogen and estrogen receptor controls the level of the granzyme inhibitor, proteinase inhibitor 9 and susceptibility to immune surveillance by natural killer cells. *Oncogene,* 26(28)**,** 4106-14. 10.1038/sj.onc.1210197.

Jin, X. & Mu, P. (2015) Targeting Breast Cancer Metastasis. *Breast Cancer-Basic and Clinical Research,* 9**,** 23-34. 10.4137/bcbcr.s25460.

Johnstone, C. N., Smith, Y. E., Cao, Y., Burrows, A. D., Cross, R. S. N., Ling, X., Redvers, R. P., Doherty, J. P., Eckhardt, B. L., Natoli, A. L., Restall, C. M., Lucas, E., Pearson, H. B., Deb, S., Britt, K. L., Rizzitelli, A., Li, J., Harmey, J. H., Pouliot, N. & Anderson, R. L. (2015) Functional and molecular characterisation of EO771.LMB tumours, a new C57BL/6-mouse-derived model of spontaneously metastatic mammary cancer. *Disease models & mechanisms,* 8(3)**,** 237-251. 10.1242/dmm.017830.

Julia, E. P., Amante, A., Pampena, M. B., Mordoh, J. & Levy, E. M. (2018) Avelumab, an IgG1 anti-PD-L1 Immune Checkpoint Inhibitor, Triggers NK Cell-Mediated Cytotoxicity and Cytokine Production Against Triple Negative Breast Cancer Cells. *Frontiers in Immunology,* 9. 10.3389/fimmu.2018.02140.

Junankar, S., Shay, G., Jurczyluk, J., Ali, N., Down, J., Pocock, N., Parker, A., Nguyen, A., Sun, S., Kashemirov, B., McKenna, C. E., Croucher, P. I., Swarbrick, A., Weilbaecher, K., Phan, T. G. & Rogers, M. J. (2015) Real-time intravital imaging establishes tumor-associated macrophages as the extraskeletal target of bisphosphonate action in cancer. *Cancer Discov,* 5(1)**,** 35-42. 10.1158/2159-8290.cd-14-0621.

Jung, K. & Choi, I. (2013) Emerging Co-signaling Networks in T Cell Immune Regulation. *Immune network,* 13(5)**,** 184-193. 10.4110/in.2013.13.5.184.

Kanda, N. & Tamaki, K. (1999) Estrogen enhances immunoglobulin production by human PBMCs. *Journal of Allergy and Clinical Immunology,* 103(2)**,** 282-288. https://doi.org/10.1016/S0091-6749(99)70503-8.

Kane, K. P., Lavender, K. J. & Ma, B. J. (2004) Ly-49 receptors and their functions. *Crit Rev Immunol,* 24(5)**,** 321-48. 10.1615/critrevimmunol.v24.i5.20.

Kang, Y. B., Siegel, P. M., Shu, W. P., Drobnjak, M., Kakonen, S. M., Cordon-Cardo, C., Guise, T. A. & Massague, J. (2003) A multigenic program mediating breast cancer metastasis to bone. *Cancer Cell,* 3(6)**,** 537-549. 10.1016/s1535-6108(03)00132-6.

Katzenellenbogen, B. S., Montano, M. M., Ediger, T. R., Sun, J., Ekena, K., Lazennec, G., Martini, P. G., McInerney, E. M., Delage-Mourroux, R., Weis, K. & Katzenellenbogen, J. A. (2000) Estrogen receptors: selective ligands, partners, and distinctive pharmacology. *Recent Prog Horm Res,* 55**,** 163-93; discussion 194-5.

Kaufmann, M., Jonat, W., Blamey, R., Cuzick, J., Namer, M., Fogelman, I., de Haes, J. C., Schumacher, M., Sauerbrei, W. & Zoladex Early Breast Canc Res, A. (2003) Survival analyses from the ZEBRA study: goserelin (Zoladex (TM)) versus CMF in premenopausal women with node-positive breast cancer. *European Journal of Cancer,* 39(12)**,** 1711-1717. 10.1016/s0959-8049(03)00392-7.

Kavanagh, K. L., Guo, K., Dunford, J. E., Wu, X., Knapp, S., Ebetino, F. H., Rogers, M. J., Russell, R. G. & Oppermann, U. (2006) The molecular mechanism of nitrogen-containing bisphosphonates as antiosteoporosis drugs. *Proc Natl Acad Sci U S A,* 103(20)**,** 7829-34. 10.1073/pnas.0601643103.

Keselman, A., Fang, X., White, P. B. & Heller, N. M. (2017) Estrogen Signaling Contributes to Sex Differences in Macrophage Polarization during Asthma. *Journal of Immunology,* 199(5)**,** 1573-1583. 10.4049/jimmunol.1601975.

Kikuiri, T., Kim, L., Yamaza, T., Akiyama, K., Zhang, Q. Z., Li, Y. S., Chen, C. D., Chen, W. J., Wang, S. L., Le, A. D. & Shi, S. T. (2010) Cell-Based Immunotherapy With Mesenchymal Stem Cells Cures Bisphosphonate-Related Osteonecrosis of the Jaw-like Disease in Mice. *Journal of Bone and Mineral Research,* 25(7)**,** 1668-1679. 10.1002/jbmr.37.

Kim, E. S. & Scott, L. J. (2017) Palbociclib: A Review in HR-Positive, HER2-Negative, Advanced or Metastatic Breast Cancer. *Targeted Oncology,* 12(3)**,** 373-383. 10.1007/s11523-017-0492-7.

Kimachi, K., Kajiya, H., Nakayama, S., Ikebe, T. & Okabe, K. (2011) Zoledronic acid inhibits RANK expression and migration of osteoclast precursors during osteoclastogenesis. *Naunyn-Schmiedebergs Archives of Pharmacology,* 383(3)**,** 297-308. 10.1007/s00210-010-0596-4.

Koebele, S. V. & Bimonte-Nelson, H. A. (2016) Modeling menopause: The utility of rodents in translational behavioral endocrinology research. *Maturitas,* 87**,** 5-17. 10.1016/j.maturitas.2016.01.015.

Kondo, M., Izumi, T., Fujieda, N., Kondo, A., Morishita, T., Matsushita, H. & Kakimi, K. (2011) Expansion of Human Peripheral Blood gamma delta T Cells using Zoledronate. *Jove-Journal of Visualized Experiments*(55). 10.3791/3182.

Kovats, S. (2015) Estrogen receptors regulate innate immune cells and signaling pathways. *Cellular immunology,* 294(2)**,** 63-69. 10.1016/j.cellimm.2015.01.018.

Krzeszinski, J. Y. & Wan, Y. (2015) New therapeutic targets for cancer bone metastasis. *Trends in pharmacological sciences,* 36(6)**,** 360-373. 10.1016/j.tips.2015.04.006.

Kusumbe, A. P. (2016) Vascular niches for disseminated tumour cells in bone. *Journal of Bone Oncology,* 5(3)**,** 112-116. https://doi.org/10.1016/j.jbo.2016.04.003.

Lang, M., Zhou, Z., Shi, L., Niu, J., Xu, S., Lin, W., Chen, Z. & Wang, Y. (2016) Influence of zoledronic acid on proliferation, migration, and apoptosis of vascular endothelial cells. *Br J Oral Maxillofac Surg,* 54(8)**,** 889-893. 10.1016/j.bjoms.2016.05.030.

Langley, R. R. & Fidler, I. J. (2007) Tumor cell-organ microenvironment interactions in the pathogenesis of cancer metastasis. *Endocrine Reviews,* 28(3)**,** 297-321. 10.1210/er.2006-0027.

Le Naour, A., Koffi, Y., Diab, M., Le Guennec, D., Rougé, S., Aldekwer, S., Goncalves-Mendes, N., Talvas, J., Farges, M.-C., Caldefie-Chezet, F., Vasson, M.-P. & Rossary, A. (2020) EO771, the first luminal B mammary cancer cell line from C57BL/6 mice. *Cancer cell international,* 20**,** 328-328. 10.1186/s12935-020-01418-1.

Lee, J. C., Lee, K. M., Kim, D. W. & Heo, D. S. (2004) Elevated TGF-beta1 secretion and down-modulation of NKG2D underlies impaired NK cytotoxicity in cancer patients. *J Immunol,* 172(12)**,** 7335-40. 10.4049/jimmunol.172.12.7335.

Lerner, U. H. (2006) Bone remodeling in post-menopausal osteoporosis. *J Dent Res,* 85(7)**,** 584-95. 10.1177/154405910608500703.

Li, E. C. & Davis, L. E. (2003) Zoledronic acid: A new parenteral bisphosphonate. *Clinical Therapeutics,* 25(11)**,** 2669-2708. https://doi.org/10.1016/S0149-2918(03)80327-2.

Li, Y., Du, Y., Sun, T., Xue, H., Jin, Z. & Tian, J. (2018) PD-1 blockade in combination with zoledronic acid to enhance the antitumor efficacy in the breast cancer mouse model. *BMC cancer,* 18(1)**,** 669-669. 10.1186/s12885-018-4412-8.

Lieberman, J. (2003) The ABCs of granule-mediated cytotoxicity: new weapons in the arsenal. *Nat Rev Immunol,* 3(5)**,** 361-70. 10.1038/nri1083.

Lin, Y. X., Xu, J. X. & Lan, H. Y. (2019) Tumor-associated macrophages in tumor metastasis: biological roles and clinical therapeutic applications. *Journal of Hematology & Oncology,* 12. 10.1186/s13045-019-0760-3.

Lipton, A., Cook, R., Saad, F., Major, P., Garnero, P., Terpos, E., Brown, J. E. & Coleman, R. E. (2008) Normalization of bone markers is associated with improved survival in patients with bone metastases from solid tumors and elevated bone resorption receiving zoledronic acid. *Cancer,* 113(1)**,** 193-201. 10.1002/cncr.23529.

Liu, H., Wang, S. H., Chen, S. C., Chen, C. Y. & Lin, T. M. (2019) Zoledronic acid blocks the interaction between breast cancer cells and regulatory T-cells. *Bmc Cancer,* 19. 10.1186/s12885-019-5379-9.

Liu, H., Wang, S. H., Chen, S. C., Chen, C. Y., Lo, J. L. & Lin, T. M. (2016) Immune modulation of CD4(+)CD25(+) regulatory T cells by zoledronic acid. *Bmc Immunology,* 17. 10.1186/s12865-016-0183-7.

Liu, L., Shen, Y., Zhu, X., Lv, R., Li, S., Zhang, Z., Shi, Y. G. & Tan, L. (2018) ERα is a negative regulator of PD-L1 gene transcription in breast cancer. *Biochem Biophys Res Commun,* 505(1)**,** 157-161. 10.1016/j.bbrc.2018.09.005.

Lo, C. H. & Lynch, C. C. (2018) Multifaceted Roles for Macrophages in Prostate Cancer Skeletal Metastasis. *Frontiers in Endocrinology,* 9. 10.3389/fendo.2018.00247.

Lopez, R. D., Mineishi, S., Lamb, L. S., Kim, H. G. & Beck, B. (2012) PD-1 (CD279) Contributes to the Exhaustion of Gamma/Delta-T Cells in Tumor-Bearing Mice. *Blood,* 120(21).

Lorenzo-Herrero, S., López-Soto, A., Sordo-Bahamonde, C., Gonzalez-Rodriguez, A. P., Vitale, M. & Gonzalez, S. (2018) NK Cell-Based Immunotherapy in Cancer Metastasis. *Cancers,* 11(1)**,** 29. 10.3390/cancers11010029.

Luckman, S. P., Hughes, D. E., Coxon, F. P., Russell, R. G. G. & Rogers, M. J. (1998) Nitrogen-containing bisphosphonates inhibit the mevalonate pathway and prevent post-translational prenylation of GTP-binding proteins, including Ras. *Journal of Bone and Mineral Research,* 13(4)**,** 581-589. 10.1359/jbmr.1998.13.4.581.

Luo, C. Y., Wang, L., Sun, C. & Li, D. J. (2011) Estrogen enhances the functions of CD4(+)CD25(+)Foxp3(+) regulatory T cells that suppress osteoclast differentiation and bone resorption in vitro. *Cellular & Molecular Immunology,* 8(1)**,** 50-58. 10.1038/cmi.2010.54.

Madak-Erdogan, Z., Kieser, K. J., Kim, S. H., Komm, B., Katzenellenbogen, J. A. & Katzenellenbogen, B. S. (2008) Nuclear and extranuclear pathway inputs in the regulation of global gene expression by estrogen receptors. *Mol Endocrinol,* 22(9)**,** 2116-27. 10.1210/me.2008-0059.

Mancino, A. T., Klimberg, V. S., Yamamoto, M., Manolagas, S. C. & Abe, E. (2001) Breast cancer increases osteoclastogenesis by secreting M-CSF and upregulating RANKL in stromal cells. *Journal of Surgical Research,* 100(1)**,** 18-24. 10.1006/jsre.2001.6204.

Manolagas, S. C. (2000) Birth and death of bone cells: Basic regulatory mechanisms and implications for the pathogenesis and treatment of osteoporosis. *Endocrine Reviews,* 21(2)**,** 115-137. 10.1210/er.21.2.115.

Mansour, A., Anginot, A., Mancini, S. J. C., Schiff, C., Carle, G. F., Wakkach, A. & Blin-Wakkach, C. (2011) Osteoclast activity modulates B-cell development in the bone marrow. *Cell Research,* 21(7)**,** 1102-1115. 10.1038/cr.2011.21.

Martin-Millan, M., Almeida, M., Ambrogini, E., Han, L., Zhao, H., Weinstein, R. S., Jilka, R. L., O'Brien, C. A. & Manolagas, S. C. (2010) The Estrogen Receptor-α in Osteoclasts Mediates the Protective Effects of Estrogens on Cancellous But Not Cortical Bone. In: *Mol Endocrinol.*

McKinlay, S. M., Brambilla, D. J. & Posner, J. G. (1992) The normal menopause transition. *Maturitas,* 14(2)**,** 103-15. 10.1016/0378-5122(92)90003-m.

Melani, C., Sangaletti, S., Barazzetta, F. M., Werb, Z. & Colombo, M. P. (2007) Amino-biphosphonate-mediated MMP-9 inhibition breaks the tumor-bone marrow axis responsible for myeloid-derived suppressor cell expansion and macrophage infiltration in tumor stroma. *Cancer Res,* 67(23)**,** 11438-46. 10.1158/0008-5472.can-07-1882.

Miyamoto, K., Yoshida, S., Kawasumi, M., Hashimoto, K., Kimura, T., Sato, Y., Kobayashi, T., Miyauchi, Y., Hoshi, H., Iwasaki, R., Miyamoto, H., Hao, W., Morioka, H., Chiba, K., Yasuda, H., Penninger, J. M., Toyama, Y., Suda, T. & Miyamoto, T. (2011) Osteoclasts are dispensable for hematopoietic stem cell maintenance and mobilization. *J Exp Med,* 208(11)**,** 2175-81. 10.1084/jem.20101890.

Miyamoto, T. (2013) Role of osteoclasts in regulating hematopoietic stem and progenitor cells. *World journal of orthopedics,* 4(4)**,** 198-206. 10.5312/wjo.v4.i4.198.

Mosquera, L., Shepherd, L., Torrado, A. I., Torres-Diaz, Y. M., Miranda, J. D. & Segarra, A. C. (2015) Comparison of Two Methods of Estradiol Replacement: their Physiological and Behavioral

Outcomes. *Journal of veterinary science & technology,* 6(6)**,** 276-276. 10.4172/2157-7579.1000276.

Mueller, S. K., Altvater, B., Chen, C., Kailayangiri, S., Ahlmann, M., Dirksen, U., Juergens, H. & Rossig, C. (2013) Zoledronic acid negatively affects the expansion of in vitro activated human NK cells and their cytolytic interactions with Ewing sarcoma cells. *Oncol Rep,* 29(6)**,** 2348-54. 10.3892/or.2013.2350.

Muenst, S., Soysal, S. D., Gao, F., Obermann, E. C., Oertli, D. & Gillanders, W. E. (2013) The presence of programmed death 1 (PD-1)-positive tumor-infiltrating lymphocytes is associated with poor prognosis in human breast cancer. *Breast Cancer Res Treat,* 139(3)**,** 667-76. 10.1007/s10549-013-2581-3.

Muller, A., Homey, B., Soto, H., Ge, N. F., Catron, D., Buchanan, M. E., McClanahan, T., Murphy, E., Yuan, W., Wagner, S. N., Barrera, J. L., Mohar, A., Verastegui, E. & Zlotnik, A. (2001) Involvement of chemokine receptors in breast cancer metastasis. *Nature,* 410(6824)**,** 50-56. 10.1038/35065016.

Mödder, U. I., Roforth, M. M., Hoey, K., McCready, L. K., Peterson, J. M., Monroe, D. G., Oursler, M. J. & Khosla, S. (2011) Effects of estrogen on osteoprogenitor cells and cytokines/bone-regulatory factors in postmenopausal women. *Bone,* 49(2)**,** 202-207. 10.1016/j.bone.2011.04.015.

Nabholtz, J. M. & Arimidex Study, G. (2003) Advanced breast cancer updates on anastrozole versus tamoxifen. *Journal of Steroid Biochemistry and Molecular Biology,* 86(3-5)**,** 321-325. 10.1016/s0960-0760(03)00374-1.

Narang, P., Chen, M., Sharma, A. A., Anderson, K. S. & Wilson, M. A. (2019) The neoepitope landscape of breast cancer: implications for immunotherapy. BMC Cancer, 19(1), 200. 10.1186/s12885-019-5402-1.

Neer, R. M. & Investigators, S. (2010) Bone loss across the menopausal transition. *Skeletal Biology and Medicine,* 1192**,** 66-71. 10.1111/j.1749-6632.2009.05233.x.

Nelson, L. R. & Bulun, S. E. (2001) Estrogen production and action. *Journal of the American Academy of Dermatology,* 45(3)**,** S116-S124. 10.1067/mjd.2001.117432.

Nilsson, N. & Carlsten, H. (1994) Estrogen induces suppression of natural-killer-cell cytotoxicity and augmentation of polyclonal b-cell activation. *Cellular Immunology,* 158(1)**,** 131-139. 10.1006/cimm.1994.1262.

Nishikawa, H. & Sakaguchi, S. (2010) Regulatory T cells in tumor immunity. *International Journal of Cancer,* 127(4)**,** 759-767. 10.1002/ijc.25429.

Nussbaumer, O., Gruenbacher, G., Gander, H. & Thurnher, M. (2011) DC-like cell-dependent activation of human natural killer cells by the bisphosphonate zoledronic acid is regulated by γδ T lymphocytes. *Blood,* 118(10)**,** 2743-2751. 10.1182/blood-2011-01-328526.

Nutter, F., Holen, I., Brown, H. K., Cross, S. S., Evans, C. A., Walker, M., Coleman, R. E., Westbrook, J. A., Selby, P. J., Brown, J. E. & Ottewell, P. D. (2014) Different molecular profiles are associated with breast cancer cell homing compared with colonisation of bone: evidence using a novel bone-seeking cell line. *Endocrine-Related Cancer,* 21(2)**,** 327-341. 10.1530/erc-13-0158.

Oades, G. M., Senaratne, S. G., Clarke, I. A., Kirby, R. S. & Colston, K. W. (2003) Nitrogen containing bisphosphonates induce apoptosis and inhibit the mevalonate pathway, impairing Ras membrane localization in prostate cancer cells. *Journal of Urology,* 170(1)**,** 246-252. 10.1097/01.ju.0000070685.34760.5f.

Okasha, S. A., Ryu, S., Do, Y., McKallip, R. J., Nagarkatti, M. & Nagarkatti, P. S. (2001) Evidence for estradiol-induced apoptosis and dysregulated T cell maturation in the thymus. *Toxicology,* 163(1)**,** 49-62. https://doi.org/10.1016/S0300-483X(01)00374-2.

Ono, M., Tsuda, H., Shimizu, C., Yamamoto, S., Shibata, T., Yamamoto, H., Hirata, T., Yonemori, K., Ando, M., Tamura, K., Katsumata, N., Kinoshita, T., Takiguchi, Y., Tanzawa, H. & Fujiwara, Y. (2012) Tumor-infiltrating lymphocytes are correlated with response to neoadjuvant chemotherapy in triple-negative breast cancer. *Breast Cancer Research and Treatment,* 132(3)**,** 793-805. 10.1007/s10549-011-1554-7.

Ottewell, P. & Wilson, C. (2019) Bone-Targeted Agents in Breast Cancer: Do We Now Have All the Answers? *Breast Cancer (Auckl),* 13**,** 1178223419843501. 10.1177/1178223419843501.

Ottewell, P. D., Wang, N., Brown, H. K., Fowles, C. A., Croucher, P. I., Eaton, C. L. & Holen, I. (2015) OPG-Fc inhibits ovariectomy-induced growth of disseminated breast cancer cells in bone. *International Journal of Cancer,* 137(4)**,** 968-977. 10.1002/ijc.29439.

Ottewell, P. D., Wang, N., Brown, H. K., Reeves, K. J., Fowles, C. A., Croucher, P. I., Eaton, C. L. & Holen, I. (2014a) Zoledronic acid has differential anti-tumour activity in the pre-and post-menopausal bone microenvironment in vivo. *Clin Cancer Res,* 20(11)**,** 2922-32. 10.1158/1078-0432.ccr-13-1246.

Ottewell, P. D., Wang, N., Brown, H. K., Reeves, K. J., Fowles, C. A., Croucher, P. I., Eaton, C. L. & Holen, I. (2014b) Zoledronic Acid Has Differential Antitumor Activity in the Pre- and Postmenopausal Bone Microenvironment In Vivo. *Clinical Cancer Research,* 20(11)**,** 2922-2932. 10.1158/1078-0432.ccr-13-1246.

Paget, S. (1989) The distribution of secondary growths in cancer of the breast, 1889. *Cancer and Metastasis Reviews,* 8(2)**,** 98-101.

Pedersen, E. A., Shiozawa, Y., Pienta, K. J. & Taichman, R. S. (2012) The prostate cancer bone marrow niche: more than just 'fertile soil'. *Asian journal of andrology,* 14(3)**,** 423-427. 10.1038/aja.2011.164.

Peppercorn, J., Perou, C. M. & Carey, L. A. (2008) Molecular subtypes in breast cancer evaluation and management: divide and conquer. *Cancer Invest,* 26(1)**,** 1-10. 10.1080/07357900701784238.

Pfeilschifter, J. & Mundy, G. R. (1987) Modulation of type-beta transforming growth-factor activity in bone cultures by osteotropic hormones. *Proceedings of the National Academy of Sciences of the United States of America,* 84(7)**,** 2024-2028. 10.1073/pnas.84.7.2024.

Pinho, S. S. & Reis, C. A. (2015) Glycosylation in cancer: mechanisms and clinical implications. *Nat Rev Cancer,* 15(9)**,** 540-55. 10.1038/nrc3982.

Pio, R., Corrales, L. & Lambris, J. D. (2014) The role of complement in tumor growth. *Adv Exp Med Biol,* 772**,** 229-62. 10.1007/978-1-4614-5915-6_11.

Pistelli, M., Della Mora, A., Ballatore, Z. & Berardi, R. (2018) Aromatase inhibitors in premenopausal women with breast cancer: the state of the art and future prospects. *Current Oncology,* 25(2)**,** E168-E175. 10.3747/co.25.3735.

Polanczyk, M. J., Carson, B. D., Subramanian, S., Afentoulis, M., Vandenbark, A. A., Ziegler, S. F. & Offner, H. (2004) Cutting edge: Estrogen drives expansion of the CD4(+) CD25(+) regulatory T cell compartment. *Journal of Immunology,* 173(4)**,** 2227-2230. 10.4049/jimmunol.173.4.2227.

Polanczyk, M. J., Hopke, C., Vandenbark, A. A. & Offner, H. (2007) Treg suppressive activity involves estrogen-dependent expression of programmed death-1 (PD-1). *Int Immunol,* 19(3)**,** 337-43. 10.1093/intimm/dxl151.

Puhalla, S., Bhattacharya, S. & Davidson, N. E. (2012) Hormonal therapy in breast cancer: A model disease for the personalization of cancer care. *Molecular Oncology,* 6(2)**,** 222-236. 10.1016/j.molonc.2012.02.003.

Purushotham, A., Shamil, E., Cariati, M., Agbaje, O., Muhidin, A., Gillett, C., Mera, A., Sivanadiyan, K., Harries, M., Sullivan, R., Pinder, S. E., Garmo, H. & Holmberg, L. (2014) Age at diagnosis and distant metastasis in breast cancer--a surprising inverse relationship. *Eur J Cancer,* 50(10)**,** 1697-1705. 10.1016/j.ejca.2014.04.002.

Rack, B., Juckstock, J., Genss, E. M., Schoberth, A., Schindlbeck, C., Strobl, B., Heinrigs, M., Rammel, G., Zwingers, T., Sommer, H., Friese, K. & Janni, W. (2010) Effect of zoledronate on persisting isolated tumour cells in patients with early breast cancer. *Anticancer Res,* 30(5)**,** 1807-13.

Rakha, E. A., Reis-Filho, J. S., Baehner, F., Dabbs, D. J., Decker, T., Eusebi, V., Fox, S. B., Ichihara, S., Jacquemier, J., Lakhani, S. R., Palacios, J., Richardson, A. L., Schnitt, S. J., Schmitt, F. C., Tan, P.-H., Tse, G. M., Badve, S. & Ellis, I. O. (2010) Breast cancer prognostic classification in the molecular era: the role of histological grade. *Breast cancer research : BCR,* 12(4)**,** 207-207. 10.1186/bcr2607.

Rijhsinghani, A. G., Thompson, K., Bhatia, S. K. & Waldschmidt, T. J. (1996) Estrogen blocks early T cell development in the thymus. *Am J Reprod Immunol,* 36(5)**,** 269-77. 10.1111/j.1600-0897.1996.tb00176.x.

Rodger, F. (2005) Yen and Jaffe's reproductive endocrinology: Physiology, pathophysiology, and clinical management. *Journal of Family Planning and Reproductive Health Care,* 31(3)**,** 192-192. 10.1783/1471189054483843.

Roelofs, A. J., Jauhiainen, M., Monkkonen, H., Rogers, M. J., Monkkonen, J. & Thompson, K. (2009) Peripheral blood monocytes are responsible for gamma delta T cell activation induced by zoledronic acid through accumulation of IPP/DMAPP. *British Journal of Haematology,* 144(2)**,** 245-250. 10.1111/j.1365-2141.2008.07435.x.

Rogers, T. L., Wind, N., Hughes, R., Nutter, F., Brown, H. K., Vasiliadou, I., Ottewell, P. D. & Holen, I. (2013) Macrophages as potential targets for zoledronic acid outside the skeleton-evidence from in vitro and in vivo models. *Cellular Oncology,* 36(6)**,** 505-514. 10.1007/s13402-013-0156-2.

Roodman, G. D. (2004) Mechanisms of bone metastasis. *N Engl J Med,* 350(16)**,** 1655-64. 10.1056/NEJMra030831.

Rooney, Michael S., Shukla, Sachet A., Wu, Catherine J., Getz, G. & Hacohen, N. (2015) Molecular and Genetic Properties of Tumors Associated with Local Immune Cytolytic Activity. *Cell,* 160(1)**,** 48-61. https://doi.org/10.1016/j.cell.2014.12.033.

Rosen, L. S., Gordon, D., Kaminski, M., Howell, A., Belch, A., Mackey, J., Apffelstaedt, J., Hussein, M. A., Coleman, R. E., Reitsma, D. J., Chen, B. L. & Seaman, J. J. (2003) Long-term efficacy and safety of zoledronic acid compared with pamidronate disodium in the treatment of skeletal complications in patients with advanced multiple myeloma or breast carcinoma - A randomized, double-blind, multicenter, comparative trial. *Cancer,* 98(8)**,** 1735-1744. 10.1002/cncr.11701.

Russell, R. G. G. & Rogers, M. J. (1999) Bisphosphonates: From the laboratory to the clinic and back again. *Bone,* 25(1)**,** 97-106. 10.1016/s8756-3282(99)00116-7.

Räkel, A., Boucher, A. & Ste-Marie, L.-G. (2011) Role of zoledronic acid in the prevention and treatment of osteoporosis. *Clinical interventions in aging,* 6**,** 89-99. 10.2147/CIA.S7282.

Sabatier, R., Finetti, P., Mamessier, E., Adelaide, J., Chaffanet, M., Ali, H. R., Viens, P., Caldas, C., Birnbaum, D. & Bertucci, F. (2015) Prognostic and predictive value of PDL1 expression in breast cancer. *Oncotarget,* 6(7)**,** 5449-64. 10.18632/oncotarget.3216.

Salkeni, M. A. & Hall, S. J. (2017) Metastatic breast cancer: Endocrine therapy landscape reshaped. *Avicenna journal of medicine,* 7(4)**,** 144-152. 10.4103/ajm.AJM_20_17.

Sandstrom, A., Peigne, C. M., Leger, A., Crooks, J. E., Konczak, F., Gesnel, M. C., Breathnach, R., Bonneville, M., Scotet, E. & Adams, E. J. (2014) The Intracellular B30.2 Domain of Butyrophilin 3A1 Binds Phosphoantigens to Mediate Activation of Human V gamma 9V delta 2 T Cells. *Immunity,* 40(4)**,** 490-500. 10.1016/j.immuni.2014.03.003.

Santini, D., Vincenzi, B., Dicuonzo, G., Avvisati, G., Massacesi, C., Battistoni, F., Gavasci, M., Rocci, L., Tirindelli, M. C., Altomare, V., Tocchini, M., Bonsignori, M. & Tonini, G. (2003) Zoledronic acid induces significant and long-lasting modifications of circulating angiogenic factors in cancer patients. *Clin Cancer Res,* 9(8)**,** 2893-7.

Sarhan, D., Leijonhufvud, C., Murray, S., Witt, K., Seitz, C., Wallerius, M., Xie, H. J., Ullen, A., Harmenberg, U., Lidbrink, E., Rolny, C., Andersson, J. & Lundqvist, A. (2017) Zoledronic acid inhibits NFAT and IL-2 signaling pathways in regulatory T cells and diminishes their suppressive function in patients with metastatic cancer. *Oncoimmunology,* 6(8). 10.1080/2162402x.2017.1338238.

Schech, A. J., Kazi, A. A., Gilani, R. A. & Brodie, A. H. (2013) Zoledronic acid reverses the epithelial-mesenchymal transition and inhibits self-renewal of breast cancer cells through inactivation of NF-κB. *Mol Cancer Ther,* 12(7)**,** 1356-66. 10.1158/1535-7163.mct-12-0304.

Scheper, M. A., Badros, A., Salama, A. R., Warburton, G., Cullen, K. J., Weikel, D. S. & Meiller, T. F. (2009) A novel bioassay model to determine clinically significant bisphosphonate levels. *Support Care Cancer,* 17(12)**,** 1553-7. 10.1007/s00520-009-0710-7.

Schneider, R., Barakat, A., Pippen, J. & Osborne, C. (2011) Aromatase inhibitors in the treatment of breast cancer in post-menopausal female patients: an update. *Breast cancer (Dove Medical Press),* 3**,** 113-25. 10.2147/bctt.s22905.

Schreiber, R. D., Old, L. J. & Smyth, M. J. (2011) Cancer immunoediting: integrating immunity's roles in cancer suppression and promotion. *Science,* 331(6024)**,** 1565-70. 10.1126/science.1203486.

Schrörs, B., Boegel, S., Albrecht, C., Bukur, T., Bukur, V., Holtsträter, C., Ritzel, C., Manninen, K., Tadmor, A. D., Vormehr, M., Sahin, U. & Löwer, M. (2020) Multi-Omics Characterization of the 4T1 Murine Mammary Gland Tumor Model. *Front Oncol,* 10**,** 1195. 10.3389/fonc.2020.01195.

Schütz, F., Stefanovic, S., Mayer, L., von Au, A., Domschke, C. & Sohn, C. (2017) PD-1/PD-L1 Pathway in Breast Cancer. *Oncology Research and Treatment,* 40(5)**,** 294-297. 10.1159/000464353.

Sethi, N., Dai, X., Winter, C. G. & Kang, Y. (2011) Tumor-derived JAGGED1 promotes osteolytic bone metastasis of breast cancer by engaging notch signaling in bone cells. *Cancer cell,* 19(2)**,** 192-205. 10.1016/j.ccr.2010.12.022.

Shiozawa, Y., Pedersen, E. A., Havens, A. M., Jung, Y., Mishra, A., Joseph, J., Kim, J. K., Patel, L. R., Ying, C., Ziegler, A. M., Pienta, M. J., Song, J., Wang, J., Loberg, R. D., Krebsbach, P. H., Pienta, K. J. & Taichman, R. S. (2011) Human prostate cancer metastases target the hematopoietic stem cell niche to establish footholds in mouse bone marrow. *J Clin Invest,* 121(4)**,** 1298-312. 10.1172/jci43414.

Shuai, C., Yang, X., Pan, H. & Han, W. (2020) Estrogen Receptor Downregulates Expression of PD-1/PD-L1 and Infiltration of CD8(+) T Cells by Inhibiting IL-17 Signaling Transduction in Breast Cancer. *Frontiers in oncology,* 10**,** 582863-582863. 10.3389/fonc.2020.582863.

Siddiqui, J. A. & Partridge, N. C. (2016) Physiological Bone Remodeling: Systemic Regulation and Growth Factor Involvement. *Physiology,* 31(3)**,** 233-245. 10.1152/physiol.00061.2014.

Simpson, E., Rubin, G., Clyne, C., Robertson, K., O'Donnell, L., Jones, M. & Davis, S. (2000) The role of local estrogen biosynthesis in males and females. *Trends in Endocrinology and Metabolism,* 11(5)**,** 184-188. 10.1016/s1043-2760(00)00254-x.

Soki, F. N., Li, X., Berry, J., Koh, A., Sinder, B. P., Qian, X., Kozloff, K. M., Taichman, R. S. & McCauley, L. K. (2013) The effects of zoledronic acid in the bone and vasculature support of hematopoietic stem cell niches. *Journal of cellular biochemistry,* 114(1)**,** 67-78. 10.1002/jcb.24301.

Sorlie, T., Tibshirani, R., Parker, J., Hastie, T., Marron, J. S., Nobel, A., Deng, S., Johnsen, H., Pesich, R., Geisler, S., Demeter, J., Perou, C. M., Lonning, P. E., Brown, P. O., Borresen-Dale, A. L. & Botstein, D. (2003) Repeated observation of breast tumor subtypes in independent gene expression data sets. *Proceedings of the National Academy of Sciences of the United States of America,* 100(14)**,** 8418-8423. 10.1073/pnas.0932692100.

Stopeck, A. T., Lipton, A., Body, J. J., Steger, G. G., Tonkin, K., de Boer, R. H., Lichinitser, M., Fujiwara, Y., Yardley, D. A., Viniegra, M., Fan, M., Jiang, Q., Dansey, R., Jun, S. & Braun, A. (2010) Denosumab compared with zoledronic acid for the treatment of bone metastases in patients with advanced breast cancer: a randomized, double-blind study. *J Clin Oncol,* 28(35)**,** 5132-9. 10.1200/jco.2010.29.7101.

Streicher, C., Heyny, A., Andrukhova, O., Haigl, B., Slavic, S., Schuler, C., Kollmann, K., Kantner, I., Sexl, V., Kleiter, M., Hofbauer, L. C., Kostenuik, P. J. & Erben, R. G. (2017) Estrogen Regulates Bone Turnover by Targeting RANKL Expression in Bone Lining Cells. *Scientific Reports,* 7. 10.1038/s41598-017-06614-0.

Su, H. I. & Freeman, E. W. (2009) Hormone changes associated with the menopausal transition. *Minerva ginecologica,* 61(6)**,** 483-489.

Sundquist, M., Thorstenson, S., Brudin, L. & Nordenskjold, B. (1999) Applying the Nottingham Prognostic Index to a Swedish breast cancer population. South East Swedish Breast Cancer Study Group. *Breast Cancer Res Treat,* 53(1)**,** 1-8. 10.1023/a:1006052115874.

Svensson, E., Christiansen, C. F., Ulrichsen, S. P., Rorth, M. R. & Sorensen, H. T. (2017) Survival after bone metastasis by primary cancer type: a Danish population-based cohort study. *Bmj Open,* 7(9). 10.1136/bmjopen-2017-016022.

Svensson, S., Abrahamsson, A., Rodriguez, G. V., Olsson, A. K., Jensen, L., Cao, Y. H. & Dabrosin, C. (2015) CCL2 and CCL5 Are Novel Therapeutic Targets for Estrogen-Dependent Breast Cancer. *Clinical Cancer Research,* 21(16)**,** 3794-3805. 10.1158/1078-0432.ccr-15-0204.

Swain, S. M., Baselga, J., Kim, S. B., Ro, J., Semiglazov, V., Campone, M., Ciruelos, E., Ferrero, J. M., Schneeweiss, A., Heeson, S., Clark, E., Ross, G., Benyunes, M. C., Cortes, J. & Grp, C. S. (2015) Pertuzumab, Trastuzumab, and Docetaxel in HER2-Positive Metastatic Breast Cancer. *New England Journal of Medicine,* 372(8)**,** 724-734. 10.1056/NEJMoa1413513.

Tai, P., Wang, J. P., Jin, H. L., Song, X. M., Yan, J., Kang, Y. M., Zhao, L., An, X. J., Du, X. G., Chen, X. F., Wang, S. B., Xia, G. & Wang, B. (2008) Induction of regulatory T cells by physiological level estrogen. *Journal of Cellular Physiology,* 214(2)**,** 456-464. 10.1002/jcp.21221.

Takayanagi, H. (2009) Osteoimmunology and the effects of the immune system on bone. *Nature Reviews Rheumatology,* 5(12)**,** 667-676. 10.1038/nrrheum.2009.217.

Tan, W., Zhang, W. Z., Strasner, A., Grivennikov, S., Cheng, J. Q., Hoffman, R. M. & Karin, M. (2011) Tumour-infiltrating regulatory T cells stimulate mammary cancer metastasis through RANKL-RANK signalling. *Nature,* 470(7335)**,** 548-553. 10.1038/nature09707.

Teng, Y. T., Nguyen, H., Gao, X., Kong, Y. Y., Gorczynski, R. M., Singh, B., Ellen, R. P. & Penninger, J. M. (2000) Functional human T-cell immunity and osteoprotegerin ligand control alveolar bone destruction in periodontal infection. *J Clin Invest,* 106(6)**,** R59-67. 10.1172/jci10763.

Thiery, J. P. (2003) Epithelial-mesenchymal transitions in development and pathologies. *Current Opinion in Cell Biology,* 15(6)**,** 740-746. 10.1016/j.ceb.2003.10.006.

Topalian, S. L., Taube, J. M., Anders, R. A. & Pardoll, D. M. (2016) Mechanism-driven biomarkers to guide immune checkpoint blockade in cancer therapy. *Nature Reviews Cancer,* 16(5)**,** 275-287. 10.1038/nrc.2016.36.

Treeck, O., Schüler-Toprak, S. & Ortmann, O. (2020) Estrogen Actions in Triple-Negative Breast Cancer. *Cells,* 9(11)**,** 2358. 10.3390/cells9112358.

Trunova, G. V., Makarova, O. V., Diatroptov, M. E., Bogdanova, I. M., Mikchailova, L. P. & Abdulaeva, S. O. (2011) Morphofunctional Characteristic of the Immune System in BALB/c and C57Bl/6 Mice. *Bulletin of Experimental Biology and Medicine,* 151(1)**,** 99-102. 10.1007/s10517-011-1268-1.

Tsagozis, P., Eriksson, F. & Pisa, P. (2008) Zoledronic acid modulates antitumoral responses of prostate cancer-tumor associated macrophages. *Cancer Immunol Immunother,* 57(10)**,** 1451-9. 10.1007/s00262-008-0482-9.

Tulotta, C. & Ottewell, P. (2018) The role of IL-1B in breast cancer bone metastasis. *Endocrine-Related Cancer,* 25(7)**,** R421-R434. 10.1530/erc-17-0309.

Vaananen, H. K. & Harkonen, P. L. (1996) Estrogen and bone metabolism. *Maturitas,* 23**,** S65-S69.

Vandeveer, A. J., Fallon, J. K., Tighe, R., Sabzevari, H., Schlom, J. & Greiner, J. W. (2016) Systemic Immunotherapy of Non-Muscle Invasive Mouse Bladder Cancer with Avelumab, an Anti-PD-L1 Immune Checkpoint Inhibitor. *Cancer immunology research,* 4(5)**,** 452-462. 10.1158/2326-6066.CIR-15-0176.

Vasiliadou, I. & Holen, I. (2013) The role of macrophages in bone metastasis. *Journal of Bone Oncology,* 2(4)**,** 158-166. 10.1016/j.job.2013.07.002.

Wang, K., Gu, Y., Liao, Y., Bang, S., Donnelly, C. R., Chen, O., Tao, X., Mirando, A. J., Hilton, M. J. & Ji, R.-R. (2020) PD-1 blockade inhibits osteoclast formation and murine bone cancer pain. *The Journal of clinical investigation,* 130(7)**,** 3603-3620. 10.1172/JCI133334.

Wang, N., Docherty, F. E., Brown, H. K., Reeves, K. J., Fowles, A. C. M., Ottewell, P. D., Dear, T. N., Holen, I., Croucher, P. I. & Eaton, C. L. (2014) Prostate Cancer Cells Preferentially Home to Osteoblast-rich Areas in the Early Stages of Bone Metastasis: Evidence From In Vivo Models. *Journal of Bone and Mineral Research,* 29(12)**,** 2688-2696. 10.1002/jbmr.2300.

Watson, N. F., Ramage, J. M., Madjd, Z., Spendlove, I., Ellis, I. O., Scholefield, J. H. & Durrant, L. G. (2006) Immunosurveillance is active in colorectal cancer as downregulation but not complete loss of MHC class I expression correlates with a poor prognosis. *Int J Cancer,* 118(1)**,** 6-10. 10.1002/ijc.21303.

Weiss, H. M., Pfaar, U., Schweitzer, A., Wiegand, H., Skerjanec, A. & Schran, H. (2008) Biodistribution and plasma protein binding of zoledronic acid. *Drug Metab Dispos,* 36(10)**,** 2043-9. 10.1124/dmd.108.021071.

Weitzmann, M. N. & Pacifici, R. (2006) Estrogen deficiency and bone loss: an inflammatory tale. *J Clin Invest,* 116(5)**,** 1186-94. 10.1172/jci28550.

Weißenborn, C., Ignatov, T., Ochel, H. J., Costa, S. D., Zenclussen, A. C., Ignatova, Z. & Ignatov, A. (2014) GPER functions as a tumor suppressor in triple-negative breast cancer cells. *J Cancer Res Clin Oncol,* 140(5)**,** 713-23. 10.1007/s00432-014-1620-8.

Westbrook, J. A., Cairns, D. A., Peng, J. H., Speirs, V., Hanby, A. M., Holen, I., Wood, S. L., Ottewell, P. D., Marshall, H., Banks, R. E., Selby, P. J., Coleman, R. E. & Brown, J. E. (2016) CAPG and GIPC1: Breast Cancer Biomarkers for Bone Metastasis Development and Treatment. *Jnci-Journal of the National Cancer Institute,* 108(4). 10.1093/jnci/djv360.

Wilson, C., Bell, R., Hinsley, S., Marshall, H., Brown, J., Cameron, D., Dodwell, D. & Coleman, R. (2018) Adjuvant zoledronic acid reduces fractures in breast cancer patients; an AZURE (BIG 01/04) study. *European Journal of Cancer,* 94**,** 70-78. 10.1016/j.ejca.2018.02.004.

Wilson, C., Brown, H. & Holen, I. (2016a) The endocrine influence on the bone microenvironment in early breast cancer. *Endocr Relat Cancer,* 23(12)**,** R567-r576. 10.1530/erc-16-0238.

Wilson, C., Hinsley, S., Marshall, H., Cameron, D., Bell, R., Dodwell, D. & Coleman, R. E. (2016b) Reproductive hormone analyses and effects of adjuvant zoledronic acid in early breast cancer

- An AZURE (BIG 01/04) sub-study. *Journal of bone oncology,* 9**,** 48-54. 10.1016/j.jbo.2016.10.005.

Wright, L. E., Christian, P. J., Rivera, Z., Van Alstine, W. G., Funk, J. L., Bouxsein, M. L. & Hoyer, P. B. (2008) Comparison of skeletal effects of ovariectomy versus chemically induced ovarian failure in mice. *Journal of Bone and Mineral Research,* 23(8)**,** 1296-1303. 10.1359/jbmr.080309.

Xiang, L. S. & Gilkes, D. M. (2019) The Contribution of the Immune System in Bone Metastasis Pathogenesis. *International Journal of Molecular Sciences,* 20(4). 10.3390/ijms20040999.

Xiao, G., Deng, A., Liu, H., Ge, G. & Liu, X. (2012) Activator protein 1 suppresses antitumor T-cell function via the induction of programmed death 1. *Proc Natl Acad Sci U S A,* 109(38)**,** 15419-24. 10.1073/pnas.1206370109.

Xu, Z., Hurchla, M. A., Deng, H., Uluckan, O., Bu, F., Berdy, A., Eagleton, M. C., Heller, E. A., Floyd, D. H., Dirksen, W. P., Shu, S., Tanaka, Y., Fernandez, S. A., Rosol, T. J. & Weilbaecher, K. N. (2009) Interferon-gamma targets cancer cells and osteoclasts to prevent tumor-associated bone loss and bone metastases. *J Biol Chem,* 284(7)**,** 4658-66. 10.1074/jbc.M804812200.

Yang, L., DeBusk, L. M., Fukuda, K., Fingleton, B., Green-Jarvis, B., Shyr, Y., Matrisian, L. M., Carbone, D. P. & Lin, P. C. (2004) Expansion of myeloid immune suppressor Gr+CD11b+ cells in tumor-bearing host directly promotes tumor angiogenesis. *Cancer Cell,* 6(4)**,** 409-21. 10.1016/j.ccr.2004.08.031.

Yang, L., Huang, F., Mei, J., Wang, X., Zhang, Q., Wang, H., Xi, M. & You, Z. (2017) Posttranscriptional Control of PD-L1 Expression by 17 beta-Estradiol via PI3K/Akt Signaling Pathway in ER alpha-Positive Cancer Cell Lines. *International Journal of Gynecological Cancer,* 27(2)**,** 196-205. 10.1097/igc.0000000000000875.

Yang, X. J., Belosay, A., Du, M. Y., Fan, T. M., Turner, R. T., Iwaniec, U. T. & Helferich, W. G. (2013) Estradiol increases ER-negative breast cancer metastasis in an experimental model. *Clinical & Experimental Metastasis,* 30(6)**,** 711-721. 10.1007/s10585-012-9559-0.

Yao, G. H. & Hou, Y. Y. (2004) Thymic atrophy via estrogen-induced apoptosis is related to Fas/FasL pathway. *International Immunopharmacology,* 4(2)**,** 213-221. 10.1016/j.intimp.2003.12.005.

Yu, T., Liu, M., Luo, H., Wu, C., Tang, X., Tang, S., Hu, P., Yan, Y., Wang, Z. & Tu, G. (2014) GPER mediates enhanced cell viability and motility via non-genomic signaling induced by 17β-estradiol in triple-negative breast cancer cells. *J Steroid Biochem Mol Biol,* 143**,** 392-403. 10.1016/j.jsbmb.2014.05.003.

Zabuawala, T., Taffany, D. A., Sharma, S. M., Merchant, A., Adair, B., Srinivasan, R., Rosol, T. J., Fernandez, S., Huang, K., Leone, G. & Ostrowski, M. C. (2010) An ets2-driven transcriptional program in tumor-associated macrophages promotes tumor metastasis. *Cancer Res,* 70(4)**,** 1323-33. 10.1158/0008-5472.can-09-1474.

Zekri, J., Mansour, M. & Karim, S. M. (2014) The anti-tumour effects of zoledronic acid. *Journal of bone oncology,* 3(1)**,** 25-35. 10.1016/j.jbo.2013.12.001.

Zeman, M. K. & Cimprich, K. A. (2014) Causes and consequences of replication stress. *Nature Cell Biology,* 16(1)**,** 2-9. 10.1038/ncb2897.

Zhao, E., Wang, L., Dai, J., Kryczek, I., Wei, S., Vatan, L., Altuwaijri, S., Sparwasser, T., Wang, G., Keller, E. T. & Zou, W. (2012) Regulatory T cells in the bone marrow microenvironment in patients with prostate cancer. *Oncoimmunology,* 1(2)**,** 152-161. 10.4161/onci.1.2.18480.

Zoller, A. L. & Kersh, G. J. (2006) Estrogen induces thymic atrophy by eliminating early thymic progenitors and inhibiting proliferation of beta-selected thymocytes. *Journal of Immunology,* 176(12)**,** 7371-7378. 10.4049/jimmunol.176.12.7371.

Zou, L. H., Barnett, B., Safah, H., LaRussa, V. F., Evdemon-Hogan, M., Mottram, P., Wei, S. N., David, O., Curiel, T. J. & Zou, W. P. (2004) Bone marrow is a reservoir for CD4(+)CD25(+) regulatory T cells that traffic through CXCL12/CXCR4 signals. *Cancer Research,* 64(22)**,** 8451-8455. 10.1158/0008-5472.can-04-1987.

Appendix

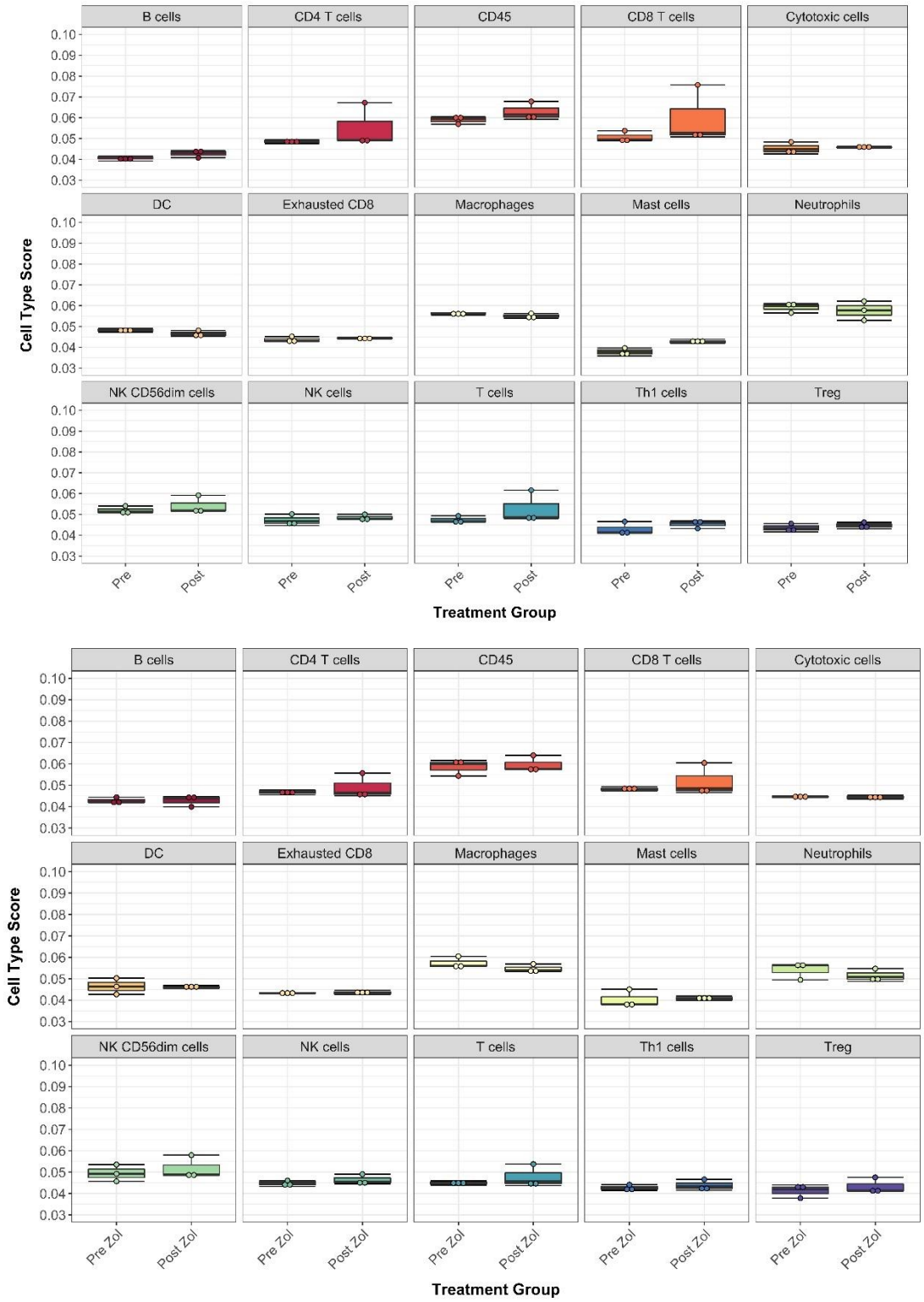

A: The effect of oestradiol +/- Zol on immune cells in bone

BALBc mice underwent OVX before oestradiol replacement in drinking water to model Post and Pre-menopausal concentrations. Mice were IC injected with 50,000 4T1-LUC cells and treated with Zol (100µg/kg), Avelumab (400µg every 2 days) or combined Avelumab & Zol. RNA was extracted from lung using before reverse transcription followed by Taqman qPCR array.

Cell type markers in appendix.

Data shown are mean ± SEM and statistical analysis performed by one way ANOVA and students T test

*< 0.05, ** < 0.01, *** < 0.001, **** < 0.0001

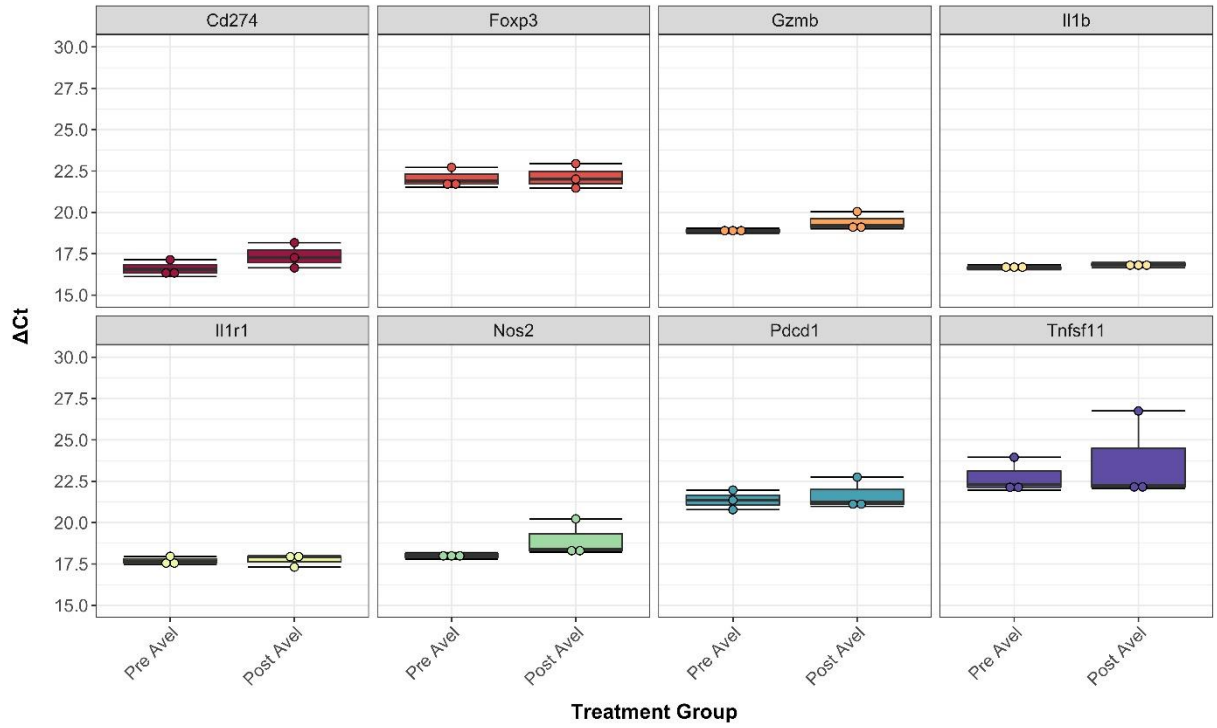

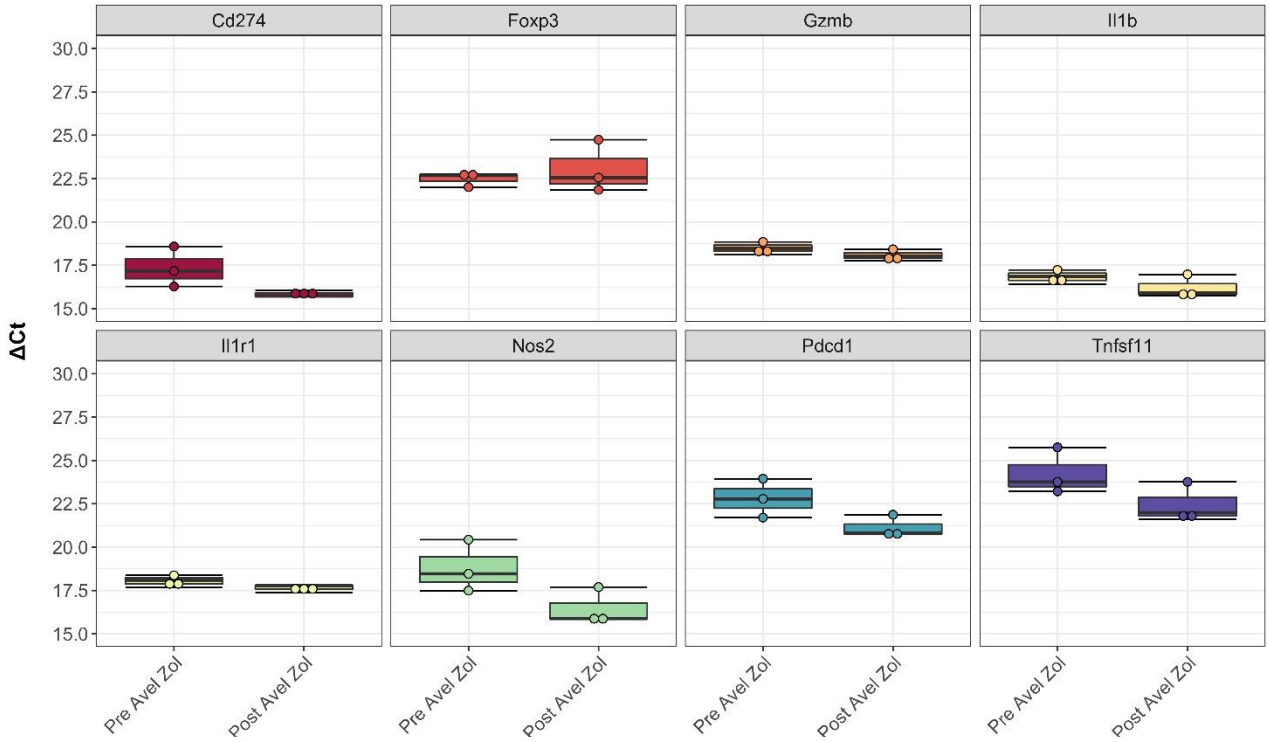

B: The effect of oestradiol +/- Avelumab/Zol on immune cells in bone

BALBc mice underwent OVX before oestradiol replacement in drinking water to model Post and Pre-menopausal concentrations. Mice were IC injected with 50,000 4T1-LUC cells and treated with Zol (100µg/kg), Avelumab (400µg every 2 days) or combined Avelumab & Zol. RNA was extracted from lung using before reverse transcription followed by Taqman qPCR array.

Cell type markers in appendix.

Data shown are mean ± SEM and statistical analysis performed by one way ANOVA and students T test

*< 0.05, ** < 0.01, *** < 0.001, **** < 0.0001

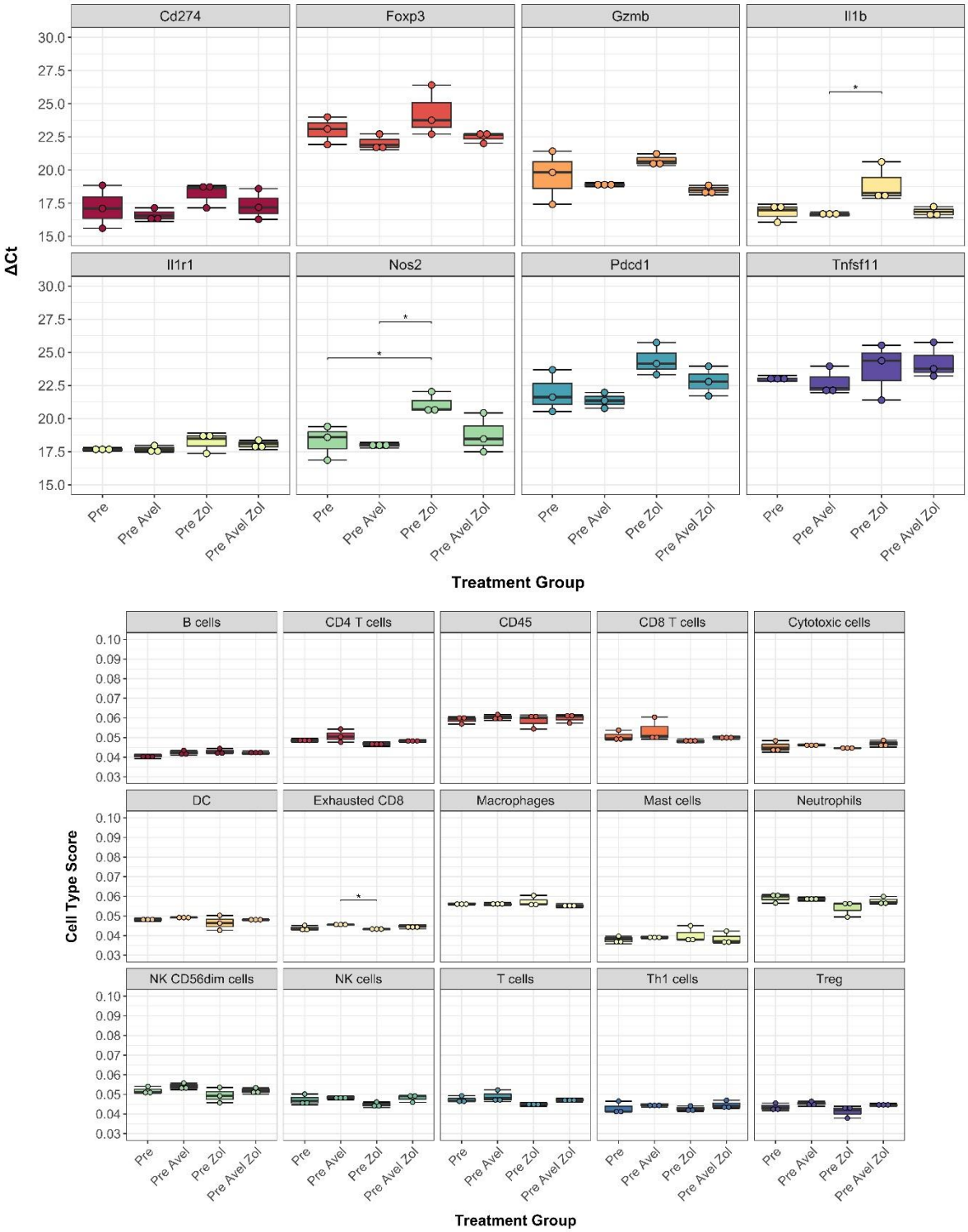

C: The effect of combination therapy with Avelumab/Zol on immune cells in bone

BALBc mice underwent OVX before oestradiol replacement in drinking water to model Post and Pre-menopausal concentrations. Mice were IC injected with 50,000 4T1-LUC cells and treated with Zol (100µg/kg), Avelumab (400µg every 2 days) or combined Avelumab & Zol. RNA was extracted from lung using before reverse transcription followed by Taqman qPCR array.

Cell type markers in appendix.

Data shown are mean ± SEM and statistical analysis performed by one way ANOVA and students T test

*< 0.05, ** < 0.01, *** < 0.001, **** < 0.0001

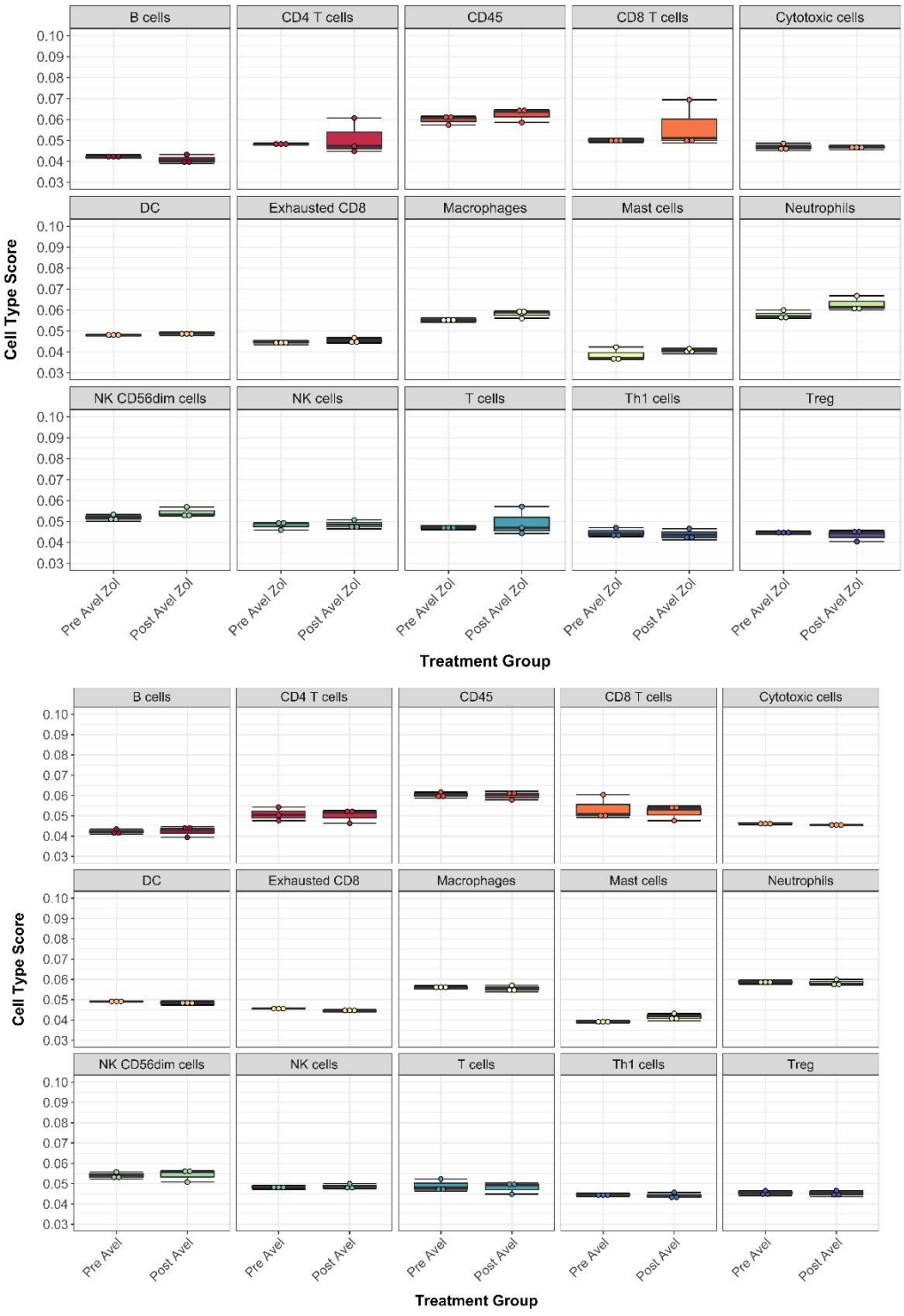

D: The effect of oestradiol +/- Avelumab/Zol on immune cells in bone

BALBc mice underwent OVX before oestradiol replacement in drinking water to model Post and Pre-menopausal concentrations. Mice were IC injected with 50,000 4T1-LUC cells and treated with Zol (100µg/kg), Avelumab (400µg every 2 days) or combined Avelumab & Zol. RNA was extracted from lung using before reverse transcription followed by Taqman qPCR array.

Cell type markers in appendix.

Data shown are mean ± SEM and statistical analysis performed by one way ANOVA and students T test

*< 0.05, ** < 0.01, *** < 0.001, **** < 0.0001

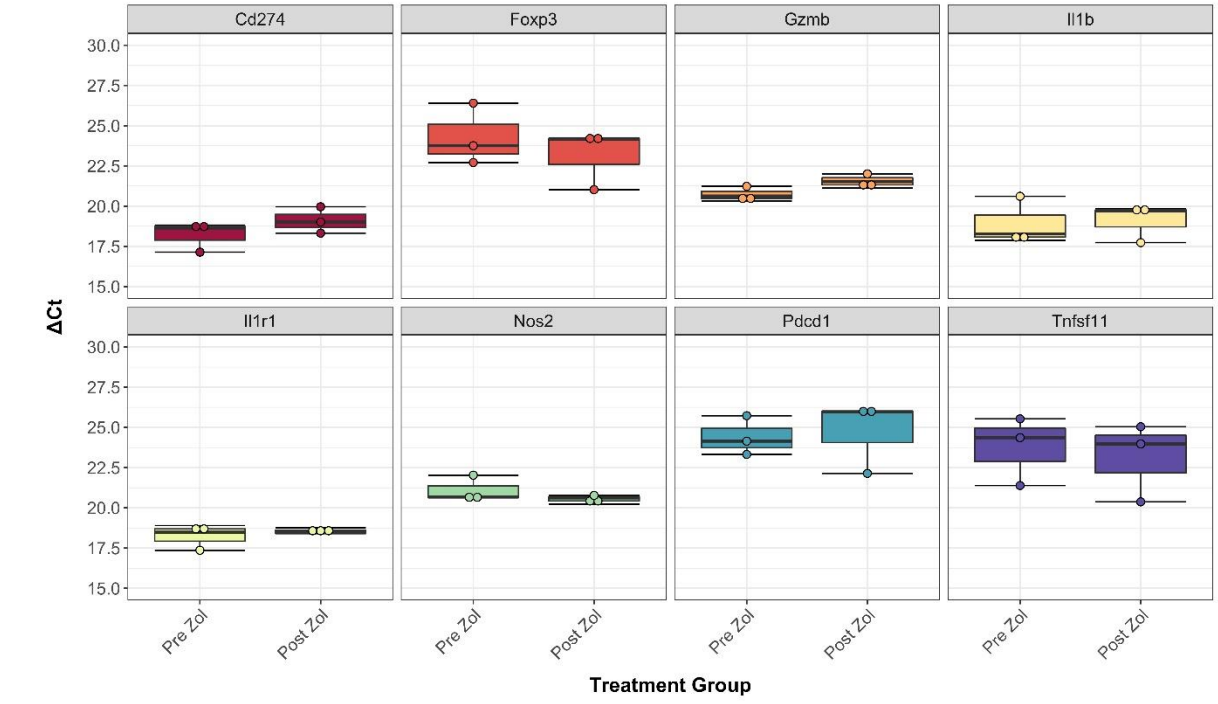

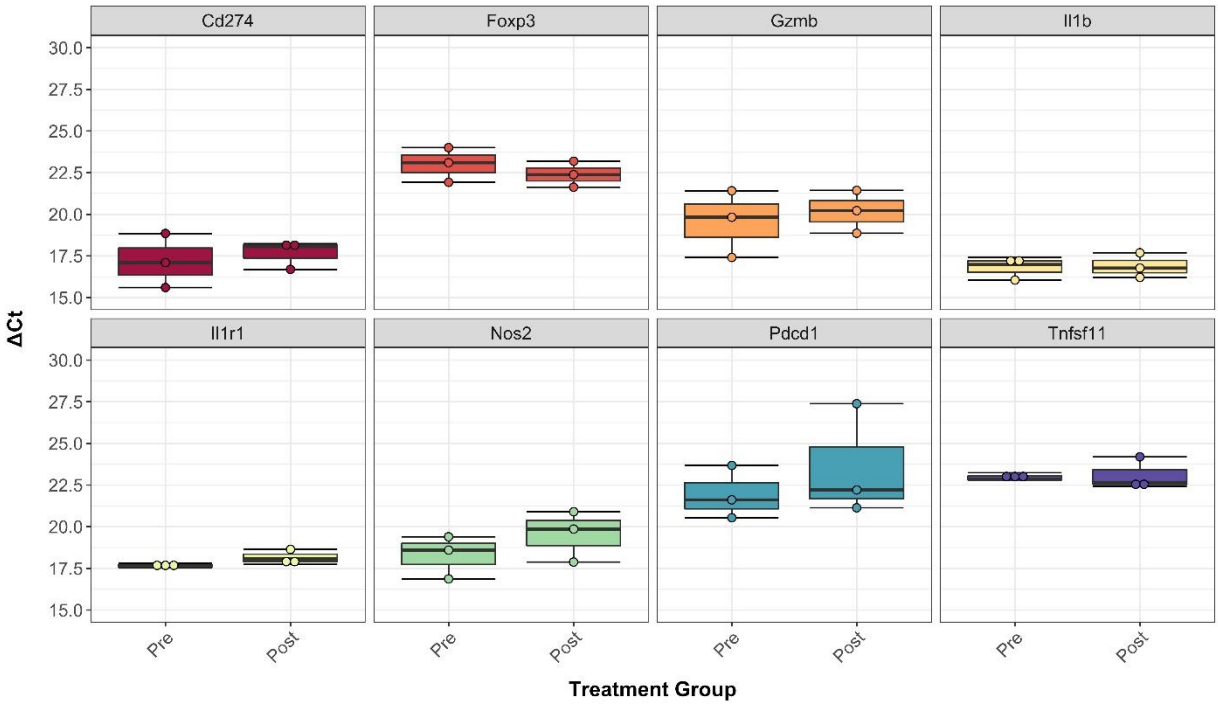

E: The effect of oestradiol +/- Zol on immune cells in bone

BALBc mice underwent OVX before oestradiol replacement in drinking water to model Post and Pre-menopausal concentrations. Mice were IC injected with 50,000 4T1-LUC cells and treated with Zol (100µg/kg), Avelumab (400µg every 2 days) or combined Avelumab & Zol. RNA was extracted from lung using before reverse transcription followed by Taqman qPCR array.

Cell type markers in appendix.

Data shown are mean ± SEM and statistical analysis performed by one way ANOVA and students T test

*< 0.05, ** < 0.01, *** < 0.001, **** < 0.0001

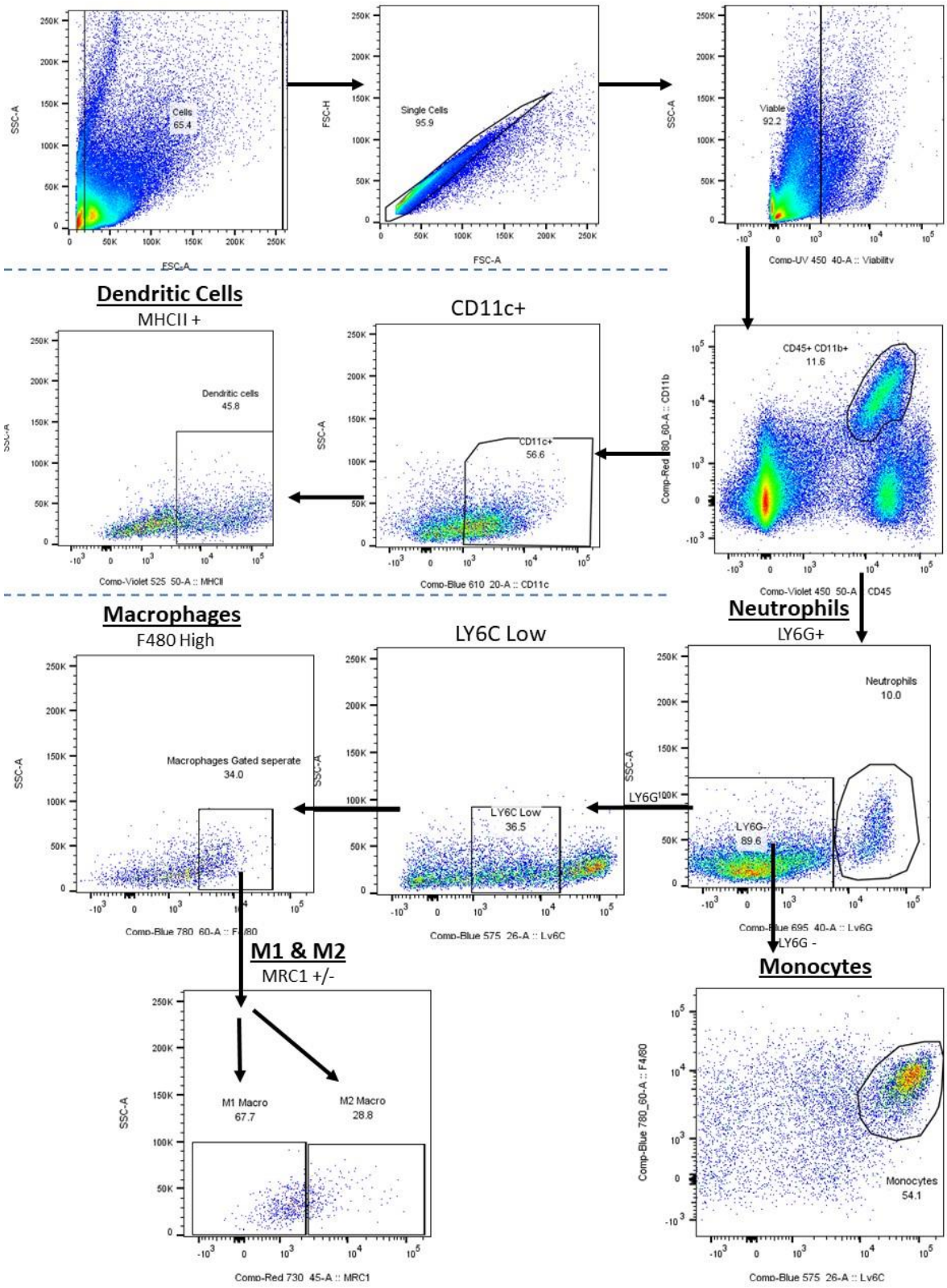

F: Flow cytometry myeloid panel gating strategy for Lung.

Dendritic cells (CD45+,CD11b+,CD11c+,MHCII+), Neutrophils (CD45+,CD11b+,Ly6G+), Monocytes (CD45+,CD11b+,LY6G-,LY6C+,F480) High, Macrophages (CD45+,CD11b+,LY6G-,LY6C Low, F480 High), M1 Macrophages (Macrophage, MRC1-), M2 Macrophages (Macrophage, MRC1+)

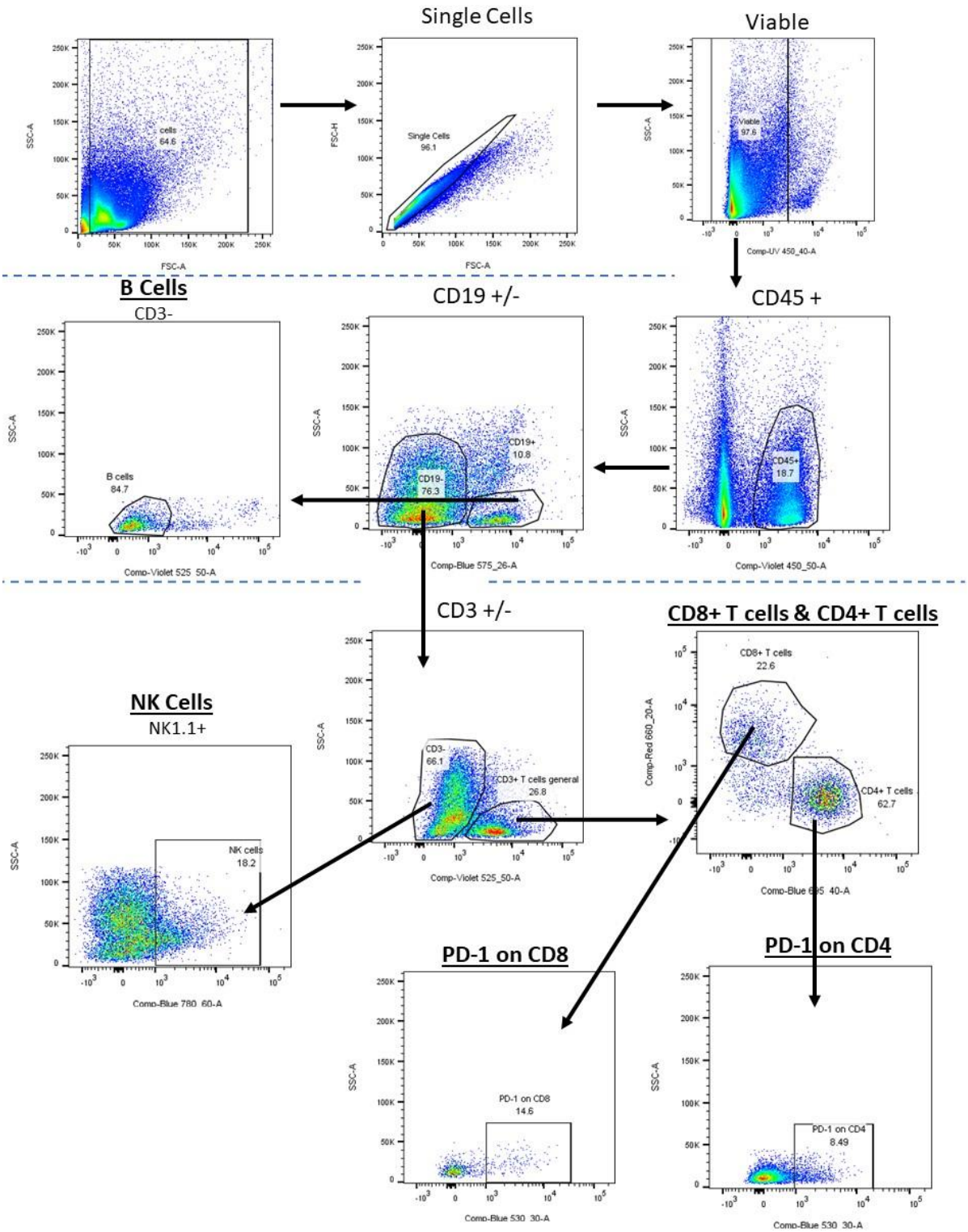

G: Flow cytometry lymphoid panel gating strategy for Lung.

CD4+ T cells (CD45+,CD19-,CD3+,CD4+), B Cells (CD45+,CD19+,CD3-), CD8+ T cells (CD45+,CD19-, CD3+,CD8+), PD-1 on CD4+ T cells (CD4 T cells, PD-1+), PD-1 on CD8+ T cells (CD8 T cells, PD-1+), NK cells (CD45+,CD19-,CD3-, NK1.1+)

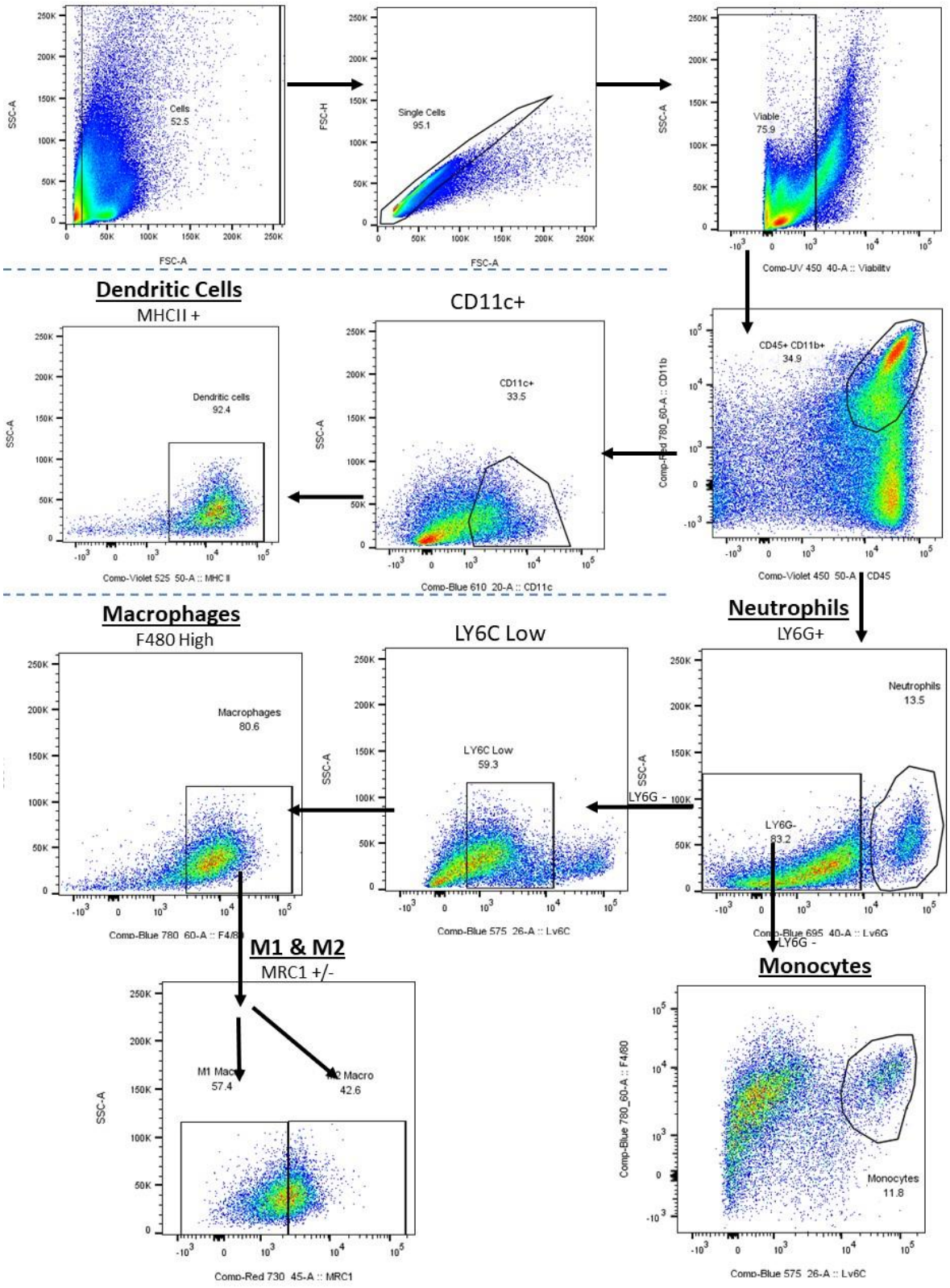

H: Flow cytometry Myeloid panel gating strategy for Spleen

Dendritic cells (CD45+,CD11b+,CD11c+,MHCII+), Neutrophils (CD45+,CD11b+,Ly6G+), Monocytes (CD45+,CD11b+,LY6G-,LY6C+,F480) High, Macrophages (CD45+,CD11b+,LY6G-,LY6C Low, F480 High), M1 Macrophages (Macrophage, MRC1-), M2 Macrophages (Macrophage, MRC1+)

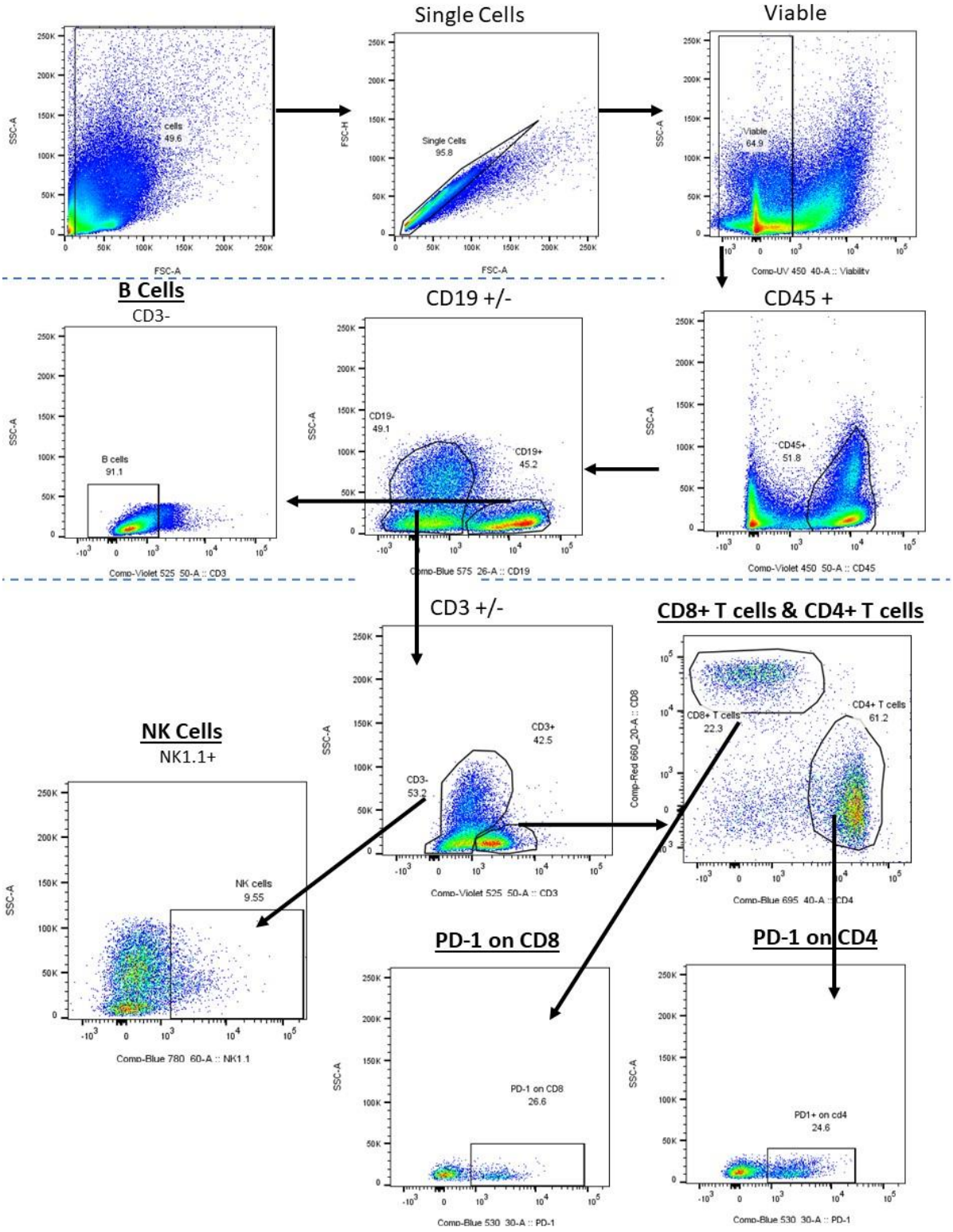

I: Flow cytometry lymphoid panel gating strategy for Spleen.

CD4+ T cells (CD45+,CD19-,CD3+,CD4+), B Cells (CD45+,CD19+,CD3-), CD8+ T cells (CD45+,CD19-, CD3+,CD8+), PD-1 on CD4+ T cells (CD4 T cells, PD-1+), PD-1 on CD8+ T cells (CD8 T cells, PD-1+), NK cells (CD45+,CD19-,CD3-, NK1.1+)